PROBABILISTIC ASPECTS OF FATIGUE

R. A. Heller, Editor

STP 511

75TH ASTM ANNIVERSARY

AMERICAN SOCIETY FOR TESTING AND MATERIALS

PROBABILISTIC ASPECTS OF FATIGUE

A symposium
presented at the
Seventy-fourth Annual Meeting
AMERICAN SOCIETY FOR
TESTING AND MATERIALS

Atlantic City, N. J., 27 June – 2 July 1971

ASTM SPECIAL TECHNICAL PUBLICATION 511
Robert A. Heller, symposium chairman

List price $19.75
04–511000–30

AMERICAN SOCIETY FOR TESTING AND MATERIALS
1916 Race Street, Philadelphia, Pa. 19103

Library of Congress Catalog Card Number: 72–75900

NOTE

The Society is not responsible, as a body,
for the statements and opinions
advanced in this publication.

Printed in Baltimore, Md.
July 1972

Foreword

The Symposium on Probabilistic Aspects of Fatigue was presented at the Seventy-fourth Annual Meeting of ASTM held in Atlantic City, N. J., 27 June-2 July 1971. The sponsor of this symposium was ASTM Committee E-9 on Fatigue. Robert A. Heller, Virginia Polytechnic Institute, presided as symposium chairman.

Related ASTM Publications

Fatigue at High Temperatures, STP 459, (1969), $11.25

Effects of Environment and Complex Load History on Fatigue Life, STP 462, (1970), $22.00

Manual on Low Cycle Fatigue Testing, STP 465, (1970), $12.50

Contents

Introduction

The analysis and design of engineering structures and systems are, in most cases, carried out with the assumption that loads, environmental factors, and material properties are deterministic quantities, though it is generally recognized that most design parameters have statistical variations.

Early experiments have already revealed a much wider scatter in fatigue test results than in most static tests and hence researchers have been concerned with the statistical interpretation of data.

Because extrapolation and interpolation based on limited experimental evidence have been the aim of most tests, attention was initially focused on various suitable methods of data plotting, curve fitting, and determination of distribution functions for fatigue life. Today regression analysis and mathematical techniques of curve fitting, aided by electronic computers, have replaced curve fitting by eye.

The use of the normal and logarithmic normal distributions has been supplemented with the extremal distributions of Weibull and Gumbel and various other transformations which either fit the data better or are based on an underlying physical process. To date proponents of various theories are not in complete agreement on the most suitable distribution functions for the description of the statistical variations of fatigue life.

Response curves and confidence bands for fatigue strength and their relationship to life distributions have also received considerable attention in the past. Methods are still being sought to determine a statistically justifiable fatigue limit based on a minimum number of test results.

The recognition of the effects of variable loads on fatigue life has led to the extensive study of random processes and their application to the description of fatigue loads produced by gusts and aircraft maneuvers, road-surface roughness, and ocean waves. Testing machines have been developed to apply such random loads to specimens, components, and complete structures and cumulative damage concepts, based on deterministic considerations, have been updated with the inclusion of probabilistic techniques concerning both loads and material response.

While in the past safety factors or scatter factors were used to take care of the variability of both strength and loads, in recent years the mathematics of reliability analysis have been adapted to fatigue design for a quantitative determination of levels of safety and reliability. These methods have given rise to the examination of the need for redundancy, establishment of realistic inspection periods, maintenance schedules, and retirement policies.

Computer simulation of the fatigue process and of crack propagation based on probabilistic considerations is a recently developed tool that has been found useful in explaining experimental results.

Though statistical design of experiments and decision theory are well known to statisticians, the use of these techniques in the planning and interpretation of fatigue tests has received wide recognition only during the last few years. These methods point the way towards the most efficient utilization of available specimens.

The probabilistic aspects of fatigue include also the establishment of realistic statistical procedures for small samples, the use of early failures in the estimation of population parameters, and the adaptation of available techniques to new materials and environments.

The 1971 Symposium on Probabilistic Aspects of Fatigue examined the most recent work in several of these areas with the aid of authors whose reputations are international.

The symposium chairman wishes to thank those authors for their valuable contributions. The work of the session chairmen and chairwomen, W. J. Trapp, M. N. Torrey, R. S. Swanson, and A. S. Heller, is also greatly appreciated.

Robert A. Heller

Professor of Engineering Mechanics
Virginia Polytechnic Institute
Blacksburg, Va.
symposium general chairman

F. A. Bastenaire [1]

New Method for the Statistical Evaluation of Constant Stress Amplitude Fatigue-Test Results

REFERENCE: Bastenaire, F. A., "**New Method for the Statistical Evaluation of Constant Stress Amplitude Fatigue-Test Results,**" *Probabilistic Aspects of Fatigue, ASTM STP 511,* American Society for Testing and Materials, 1972, pp. 3-28.

ABSTRACT: Using the experimental and theoretical results of previous research work, the author presents a probabilistic description of constant stress amplitude fatigue-test results. This description includes the *S-N* curves (or equiprobability of fracture curves), *P-S* curves (or stress-response curves), *P-N* curves (cumulative distribution functions of fatigue endurances), and accounts for the occurrence of runouts.

A method of estimation of the model coefficients which uses the information provided by all the specimens tested (broken or unbroken) is also presented. The application of this method is demonstrated through five examples for each of which several hundred test results are available.

KEY WORDS: fatigue(materials), probability theory, stress analysis, statistical analysis, mathematical model, distribution theory, *S-N* diagrams, fatigue tests

A number of theories have been proposed to explain and describe the scatter of fatigue-test results using the concept of probability distribution.

The consistency and applicability of most of these theories has been examined in Ref *1*, and it has been shown in the same study that a model using the familiar concept of a normal distribution gave an adequate representation of all the test data subjected to analysis.

The model was checked using the available data at the time of publication of Ref *1*. In view of the remarkable adequacy of the model to these test results, an extensive program of tests was set up to confirm the conclusions of this research work.

[1] Head, Statistical Applications Department, IRSID, Saint Germain-en-Laye, France.

This program has now been completed, and the purpose of the present paper is to demonstrate the application of a new statistical method of evaluation based on the same underlying mathematical model to the experimental data collected throughout this program.

General Expression for the Probability of Fatigue Failure

It has long been known that the scatter of fatigue lives in constant stress amplitude tests could be represented using a set of equiprobability curves in a *P-S-N* diagram [*2*]. The *P-S-N* diagram is a simple method of representing the following relationship between the probability of fracture P, the stress amplitude S, and the number of load cycles N:

$$P = F(S,N) \tag{1}$$

The two quantities S and N are assumed to be independent variables to which the experimenter can assign any values since he is at liberty to carry out a test that *may* last up to N cycles under stress S and examine whether or not the specimen sustains this number of cycles without fracturing. From this standpoint, P is the probability of fracture regarded as one of two alternatives.

However, $F(S,N)$ is *also* the cumulative distribution function (CDF) of the number of cycles to fracture (NCF) regarded as a random variate. In fact, a CDF is defined as the probability, for a given random variate such as the NCF of being less than or equal to some *preassigned* value, say N. It follows from this definition that $F(S,N)$ is the CDF of the NCF at any stress level S.

The experimenter can also carry out tests in which N (maximum test duration) will be maintained at one and the same value, while S will be set equal to one out of K different values $S_1, S_2, \ldots, S_K$. If a group of specimens is allocated to each stress level, it is possible to estimate the probability of fracture $F(S_i,N)$ from the proportion of specimens broken in the ith group before N cycles are completed. A curve can be drawn which shows the variation of $F(S,N)$ as a function of S for constant N. Such curves known as "stress-response curves" are schematically represented in Fig. 1.

For any given value of S, the value of N which is such that $F(S,N_p) = P$ is the Pth quantile of the distribution of the NCF which can be denoted by N_p.

Similarly, S_p may designate the value of S which verifies the condition

$$F(S_p, N) = P \tag{2}$$

If it is assumed that P increases when either S or N increases then

$$\frac{\partial F}{\partial S} > 0 \text{ and } \frac{\partial F}{\partial N} > 0 \tag{3}$$

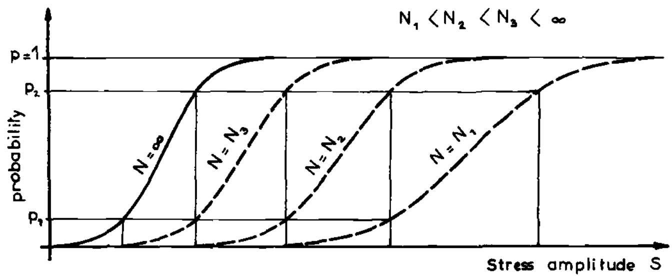

FIG. 1–*Probability of fracture versus values of* N.

Differentiating Eq 1, we obtain

$$dP = \frac{\partial F}{\partial S}dS + \frac{\partial F}{\partial N}dN \tag{4}$$

This equation allows the calculation of the derivative dS/dN along an equiprobability curve which represents the relationship between S and N when P is kept constant.

In this case, $dP = 0$ and, therefore,

$$\frac{dS_p}{dN} = -\frac{\partial F}{\partial N}\Bigg/\frac{\partial F}{\partial S} \tag{5}$$

Using the above inequalities, we find that $dS_p/dN < 0$. For constant P, S_p is, therefore, a decreasing function of N, as shown by the schematic equiprobability curves of Fig. 2.

This decrease of S_p for increasing N has its counterpart in Fig. 1 in which points plotted on the stress-response curves at a constant ordinate value (for example, P_1 or P_2) move from *right* to *left* with increasing values of N.

It can further be noted that, since the probability of fracture increases with N under constant stress amplitude, a parallel to the P-axis in Fig. 1 intersects the stress response curves in the ascending order of their parameter N. It follows that the curves of this family never intersect.

The above remarks are useful for the determination of the limit to the stress-response curves when N tends to infinity.

First, one must remember that S is a stress *amplitude* and, therefore, cannot be negative. Second, a zero stress amplitude can be assumed to produce no fatigue effects in a material. S_p being a bounded decreasing function of N, a limit $E_p \geqslant 0$ to S_p always exists (except, perhaps for $p = 1$, for which S_p may not be defined). It can be concluded that a limiting stress-response curve certainly exists, though it may possess two different shapes. If the limits to the

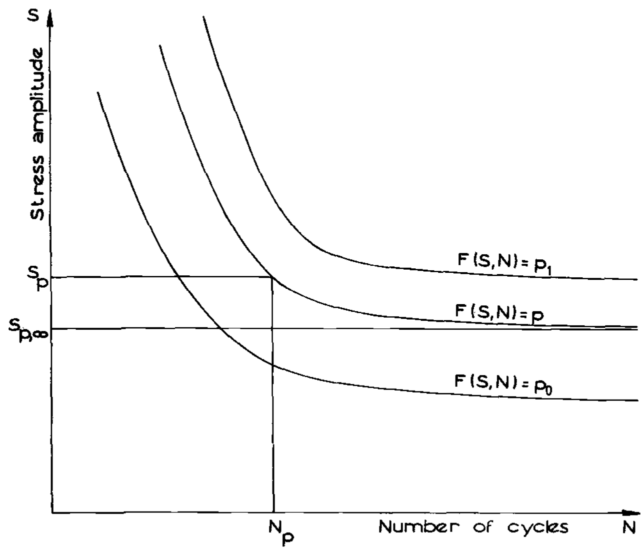

FIG. 2–*Schematic diagram of equiprobability of fracture curves.*

S_p values are different, the limiting curve will be as shown in Fig. 1 for $N = \infty$ but, if the limits are equal, the limiting stress-response curve will be as shown in Fig. 3.

These two different cases correspond to two different patterns of the equiprobability curves: when the S_p's have different limits, the equiprobability curves tend to different asymptotes, whereas when the limit to the S_p's is unique, all these curves have only one asymptote.

Important differences in the distributions of the NCF's can also be noted according to the limiting shape of the stress-response curves. If S is held constant and N increases, this is represented in Fig. 1 by a point moving upwards along a vertical straight line and it can be seen that, within a certain range of stress values, the *probability of fracture will never reach unity* however large N may

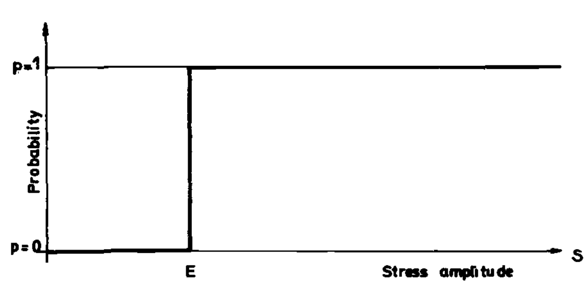

FIG. 3–*Limiting form of the probability of fracture versus stress curve when all the equiprobability curves have the same asymptote.*

become (this occurs all over the range of stress values covered by the limiting curve). In contrast with this, the probability of fracture is either zero (if $S \leqslant E$) or tends to unity when $N \to \infty$ ($S > E$) in the case illustrated by Fig. 3.

As noted at the beginning of this section, stress response curves can be drawn from experimental data. Experience shows that it is advantageous to plot the proportions of specimens failing before N load cycles have been completed on a normal or logistic probability scale. Normal probability paper has been used in the cases illustrated in Figs. 4 and 5. It can be seen from these figures that the experimental points lie near straight lines. A possible explanation of this result is to assume that a threshold stress value causing fracture of the specimen in N load cycles at the most is attached to each specimen. With this assumption, each stress-response curve is the observed or empirical CDF of such threshold values. If a straight line is obtained on probability paper, it can be concluded that the threshold stresses are normally distributed with a standard deviation shown by the slope of the straight line. We are then entirely justified in using the words "scatter in stress" to express the spread of the equiprobability curves along the S-axis.

For the last point in this section, however, the stress-response curves do not

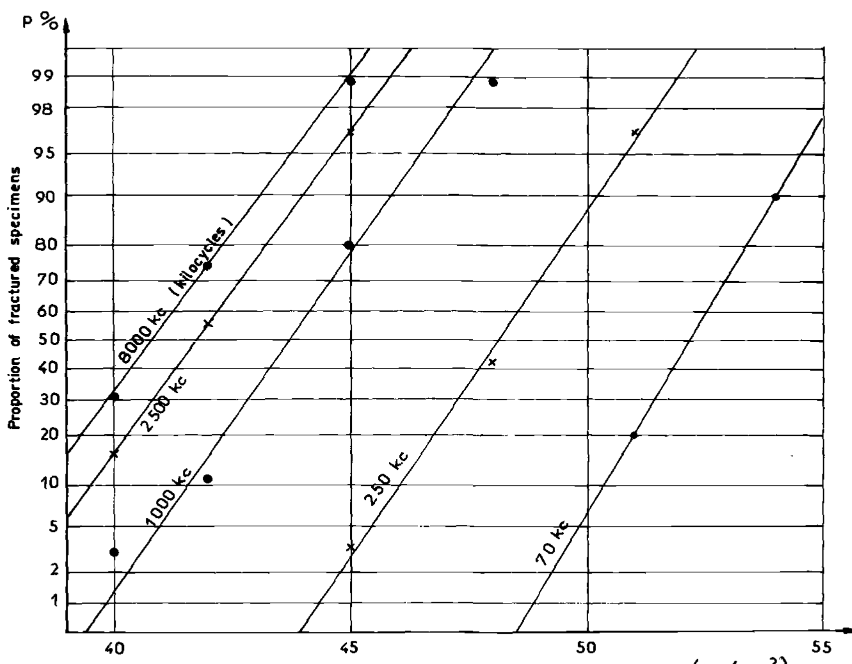

FIG. 4–*Stress-response curves for 35 CD 4 (80 kgf/mm²) steel. (Normal probability scale for frequencies.)*

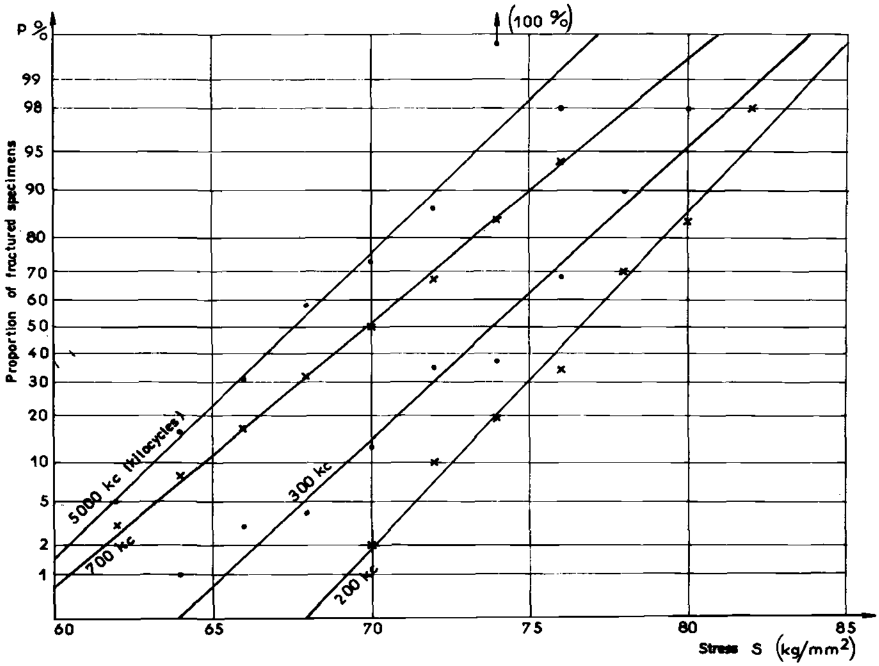

FIG. 5–*Stress-response curves for 35 CD 4 (150 kgf/mm^2) steel. (Normal probability scale for frequencies.)*

have to be normal. One only needs to assume that two parameters—a position parameter μ and a scatter parameter σ—are sufficient to represent these curves which may equally well derive from the normal, logistic, extreme value or some other distribution.

The important point is that, for any given value of N, the probability of fracture can be expressed using the same function of a reduced variate $(S - \mu)/\sigma$. It is obvious that μ and σ depend on N and should really be regarded as two functions $\mu(N)$ and $\sigma(N)$. Denoting the cumulative distribution function of the reduced variate by F, the probability of fracture can be expressed by the following equation

$$P = F\left(\frac{S - \mu(N)}{\sigma(N)}\right) \tag{6}$$

Representation of the Equiprobability Curves Using a Transformed Variate

Equation 6 shows that P = constant if $(S - \mu(N))/\sigma(N)$ is constant. In particular, if $S - \mu(N) = 0$ then $P = F(0)$. The equation of the $F(0)$ equiprobability curve is, therefore,

$$S_{F(0)} = \mu(N) \tag{7}$$

In the preceding section, it has been shown that S_p tends to a limit $E_p \geqslant 0$ when $N \to \infty$. If

$$E = \mu(\infty) \tag{8}$$

and a new function

$$\varphi(N) = \mu(N) - \mu(\infty) \tag{9}$$

is introduced, one can express $\mu(N)$ as

$$\mu(N) = \varphi(N) + E \qquad (\varphi(\infty) = 0) \tag{10}$$

$\varphi(N)$ is a decreasing function of N tending to zero as $N \to \infty$.

Using Eqs 10 and 6,

$$P = F\left(\frac{S - \varphi(N) - E}{\sigma(N)}\right) \tag{11}$$

This equation can be used to account for the main features of the NCF distributions.

To begin with, it is assumed that $\sigma(N)$ does not depend on N. Equation 11 shows that the CDF of the random variate $-\varphi(\text{NCF})$ is the same as the stress-response function. (However, if $\sigma(N)$ does depend on N, its variation is rarely important, and the distributions of $-\varphi(\text{NCF})$ and S are, in practice, similar.)

Using the inverse function φ^{-1}, the distributions of the NCF's can be generated from that of S (in this transformation, $N = \varphi^{-1}$ is infinite for $\varphi = 0$).

Since $\varphi(N)$ decreases with increasing N and tends to zero,

$$\frac{S - \varphi(N) - E}{\sigma(N)} \leqslant \frac{S - E}{\sigma(\infty)} \tag{12}$$

Therefore, in Eq 11, the argument of F can never exceed $(S-E)/\sigma(\infty)$, showing that the proportion of fractured specimens is limited at $F((S-E)/\sigma(\infty))$. This will escape the experimenter's attention if $(S-E)/\sigma(\infty)$ is either very large or very small because in the first case it is almost certain that all the specimens tested will fail, whereas it is the reverse in the second case. Between these two extremes there will be real "runouts."

It is of interest to represent the properties of $\varphi(\text{NCF})$ in a diagram. Replacing the usual S,N system of coordinates by S, φ, the equiprobability curves can be represented in a new diagram.

The equation of the $F(0)$ equiprobability curve is Eq 7. Using Eq 10,

$$S_{F(0)} = \varphi(N) + E \tag{13}$$

is obtained.

This equation shows that by plotting φ instead of N as an abscissa, the $F(0)$ equiprobability curve is represented by a straight line.

More generally, assuming that F is the CDF of a continuous random variate, F is monotonic, and P will be constant in Eq 11 if, and only if, the argument of F is constant, say

$$\frac{S - \varphi(N) - E}{\sigma(N)} = u \tag{14}$$

(u = constant)

This is the general equation of the equiprobability curves which can be written as

$$S_P = \varphi(N) + E + u\sigma(N) \tag{15}$$

Again, if σ does not depend on N, Eq 15 is that of a straight line in the S,φ system of coordinates. This line is parallel to the $F(0)$ equiprobability line represented by Eq 13.

The S,N and S,φ systems of coordinates are superimposed in Fig. 6 to show how they are related.

Putting $N = \infty$ in Eq 15, one finds the ordinate of the asymptote to the S-N curve: $\varphi(\infty) + E + u\sigma(\infty)$ which reduces to $E + u\sigma(\infty)$ since $\varphi(\infty) = 0$. Now, $E + u\sigma(\infty)$ is also the intercept of the S, φ equiprobability curve.

When σ is a constant and the equiprobability curves are straight parallel lines in the S, φ coordinates, it is apparent that the distributions of S and φ are of the same type. This statement still holds approximately if σ is a function of N because one is not concerned in practice with the full range of variation of σ but only with that range between the minimum and maximum values of N in a finite sample of observations.

Figure 6 also shows how the distributions of S and φ do differ. For any given value of N, there is no practical limit to the stress amplitude which can be applied to specimens and the stress-response curve can be explored up to stresses at which the probability of fracture is nearly unity. In contrast with this, an increase in the number of cycles for a given stress value produces a decrease in $\varphi(N)$ which is bounded at zero and the proportion of failures tends to a limit. This can be expressed in Fig. 6 by the fact that a point representing a test

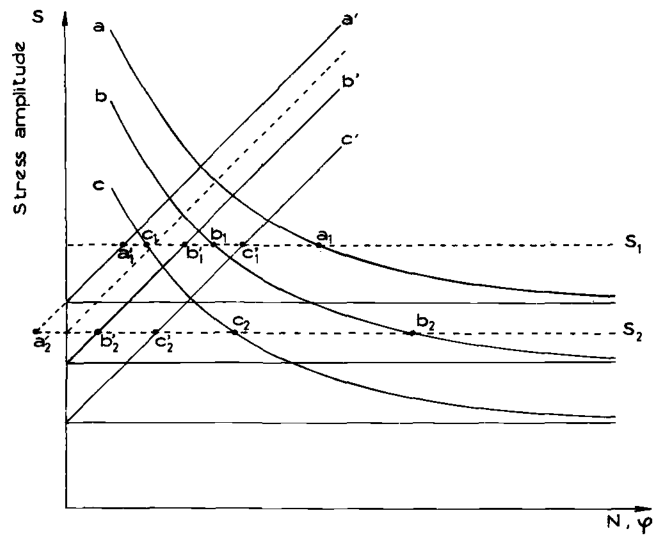

FIG. 6–S, N, *and* S, φ *diagrams.*

duration and moving from right to left parallel to the φ-axis (φ decreases when N increases) will cross a succession of equiprobability lines corresponding to increasing values of P until it reaches the S-axis and thereby the last equiprobability line it can cross whose intercept is obviously equal to the chosen stress value. Figure 6, therefore, illustrates the truncated nature of the distributions of $\varphi(N)$. This figure also shows that the distributions of $\varphi(N)$ at different stress levels differ mainly in location and in the proportion of observations cut off at $\varphi = 0$ but can be expected to be very similar in shape. This is in contrast to the distributions of fatigue lives which (even though plotted on a logarithmic scale) change markedly in shape when the stress changes (Fig. 7 illustrates this fact which has been repeatedly observed–see Refs *1* and *3*). Experience shows that the logarithm of the NCF is distributed normally only at intermediate stress levels. When the stress decreases, the scatter and skewness of these distributions increases to a considerable degree, and the proportion of broken specimens tends to a limit as the number of applied load cycles increases.

Simple Example of the Use of Transformed Fatigue Lives

Using a large variety of fatigue data, it has been shown in Ref *1* that, for large N, $\varphi(N)$ takes the asymptotic form $\varphi(N) = A/N$ where A is a constant.

The range over which this formula is, in practice, applicable depends on the material used and on testing conditions. In some cases, it is a good approximation over quite a large part of the S, N diagram.

Figure 8 is a graph of the NCF reciprocal (multiplied by 10^7 to avoid using very small figures) *versus* stress. The values plotted as ordinates are mean values.

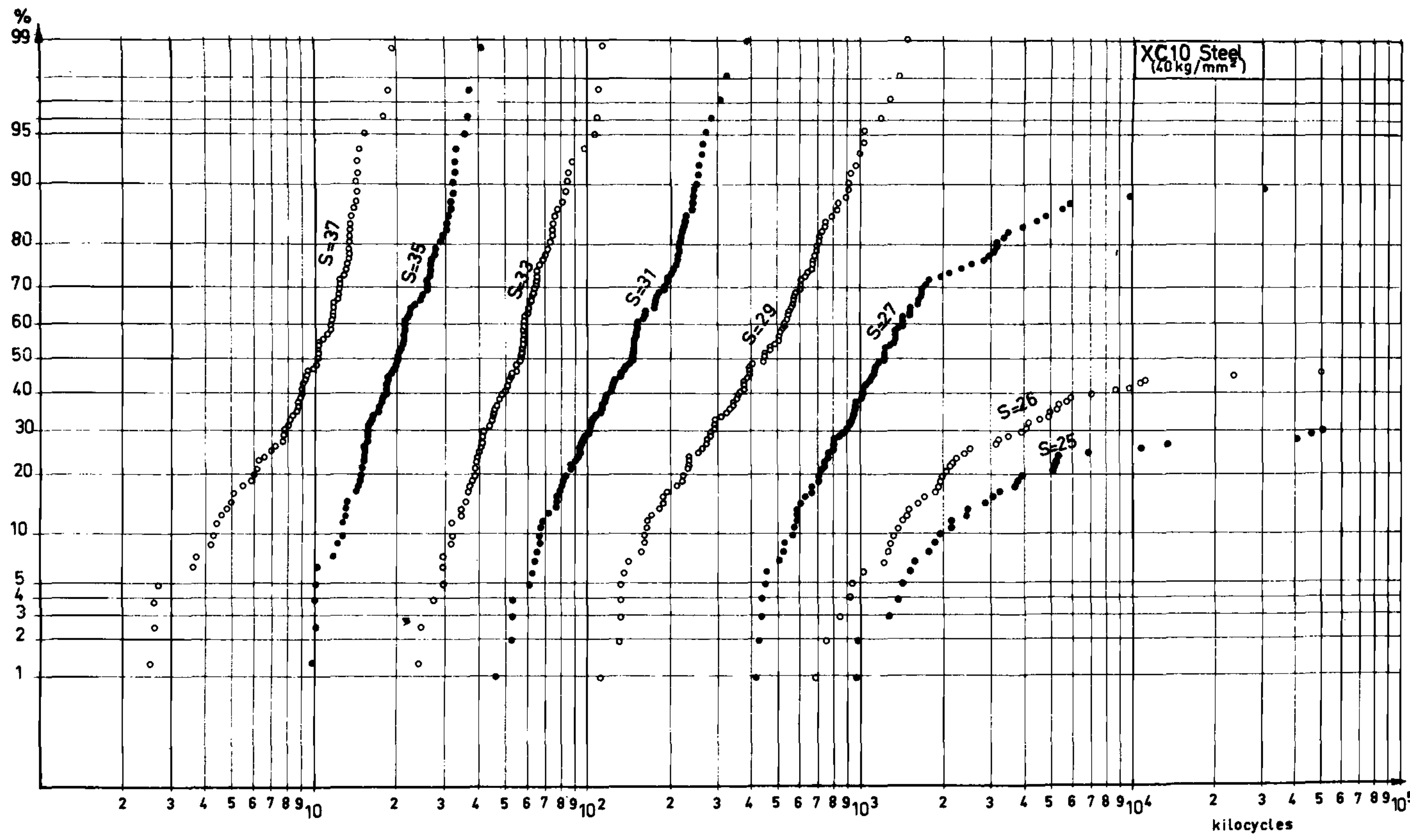

FIG. 7–*Cumulative frequency curves of log* N (*XC 10 steel*). (*Stresses in kg/mm² are indicated on each curve.*)

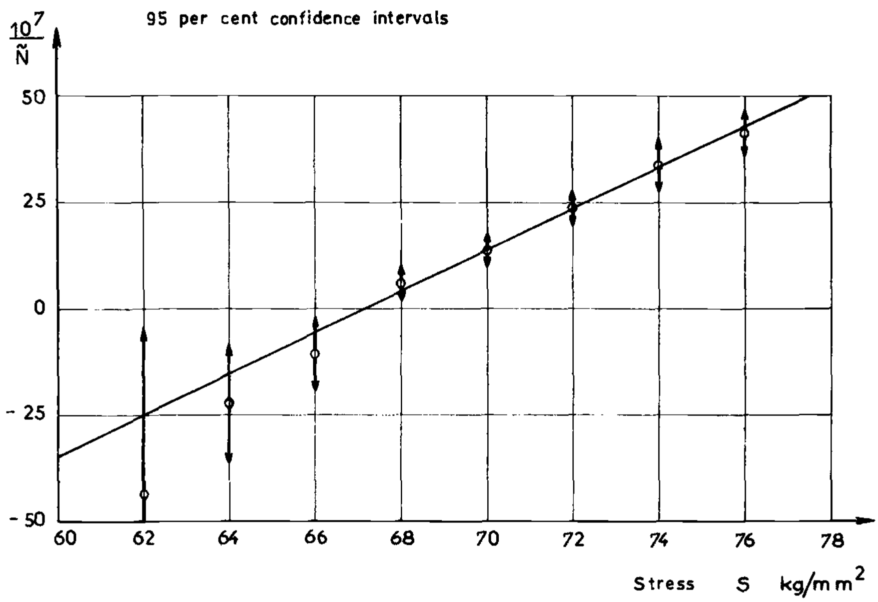

FIG. 8–*Estimated mean of censored distribution of 1/Ñ versus stress (35 CD 4 – 150 kgf/mm²).*

However, it must be noted that, at most test stresses, a number of specimens remained unbroken. In statistical terminology, a sample is said to be *censored* when this occurs. Up to the present paragraph, the term "truncated" has been used which can be understood without further comment. At the time the observations are drawn, however, two possibilities may arise: the statistician may ignore both the values and the number of observations falling outside the limit or he may ignore their values but be informed of their number. In the first case, the sample is really truncated, whereas in the second case it is *censored.* Therefore, it is clear that in fatigue testing one is concerned with censored samples of observations.

The data of Fig. 8 are censored at a number of stress levels. At 62 kgf/mm^2, *95 out of the 100 specimens tested* were *unbroken* at 5 million cycles. At 64 kgf/mm^2, 84 out of 100 specimens were also unbroken. In contrast with this, 87 out of 100 specimens were *broken* at 72 kgf/mm^2 and the proportion rises to 100 percent at the higher levels.

In order to follow the lines of the previous analysis, one must use the means of the *complete* parent distributions out of which the various samples have been drawn if a simple relationship between these means and the stresses is to be found.

It is sufficient to indicate that the mean of a parent distribution can be estimated from a censored sample using a statistical estimation method (for example, Ref *5*). It is intuitive, however, that the precision of the estimate breaks down when the number of observed values (that is, the number of broken specimens) is very small. This explains why the confidence intervals and the deviations of the experimental points from the straight line in Fig. 8 are quite large at 64 and 62 kgf/mm^2. At the upper stress levels, the mean values fall quite nicely on the fitted line.

It is of interest to see the effect of the same transformation on the distributions of fatigue lives. This is shown in Fig. 9, in which only every second cumulative frequency curve of 2×10^6/(NCF), starting from the 62 kgf/mm^2 level, is plotted for better clarity. It can be seen that these distributions are normal, censored at zero. The same transformation applied to the NCF's therefore produces simultaneously two different effects:

1. The transformed NCF's are normal censored (Fig. 9).
2. A straight-line relationship holds between their mean and the applied stress (Fig. 8).

As a final remark in this section, it should be noted that the straight-line relationship in Fig. 8 also holds for negative values of the parent population mean. This may seem strange and needs explanation. Equation 11 shows that the value of φ for which $P = F(0)$ is $\varphi = S - E$. When a value of S less than E is chosen as a test stress, this value is negative though the observed values of φ are all positive. This is so because the central value of a censored distribution can be outside the range of the observed values.

More General Transformation of the Number of Cycles to Fracture

The method in the section on Simple Example of the Use of Transformed Fatigue Lives has been used in a number of instances[*1*], but, unfortunately, $S_{F(0)} = (A/N) + E$ is not always a convenient equation for the median equiprobability curve. This is unfortunate, not only because A/N is a simple function, but also because, if A/N is distributed normally, so is $1/N$. Similarly, if a linear relationship holds between A/N and S, it also holds between $1/N$ and S. No prior knowledge of coefficient A is, therefore, necessary to check the validity of this relationship, and A can be estimated later by means of a linear regression method.

It has been shown in Ref *1* for a number of materials and testing conditions, that the median equiprobability curve can be represented by the following equation:

$$N = \frac{A\exp[-c(S-E)]}{(S-E)} \qquad (16)$$

in which A, c, and E are coefficients.

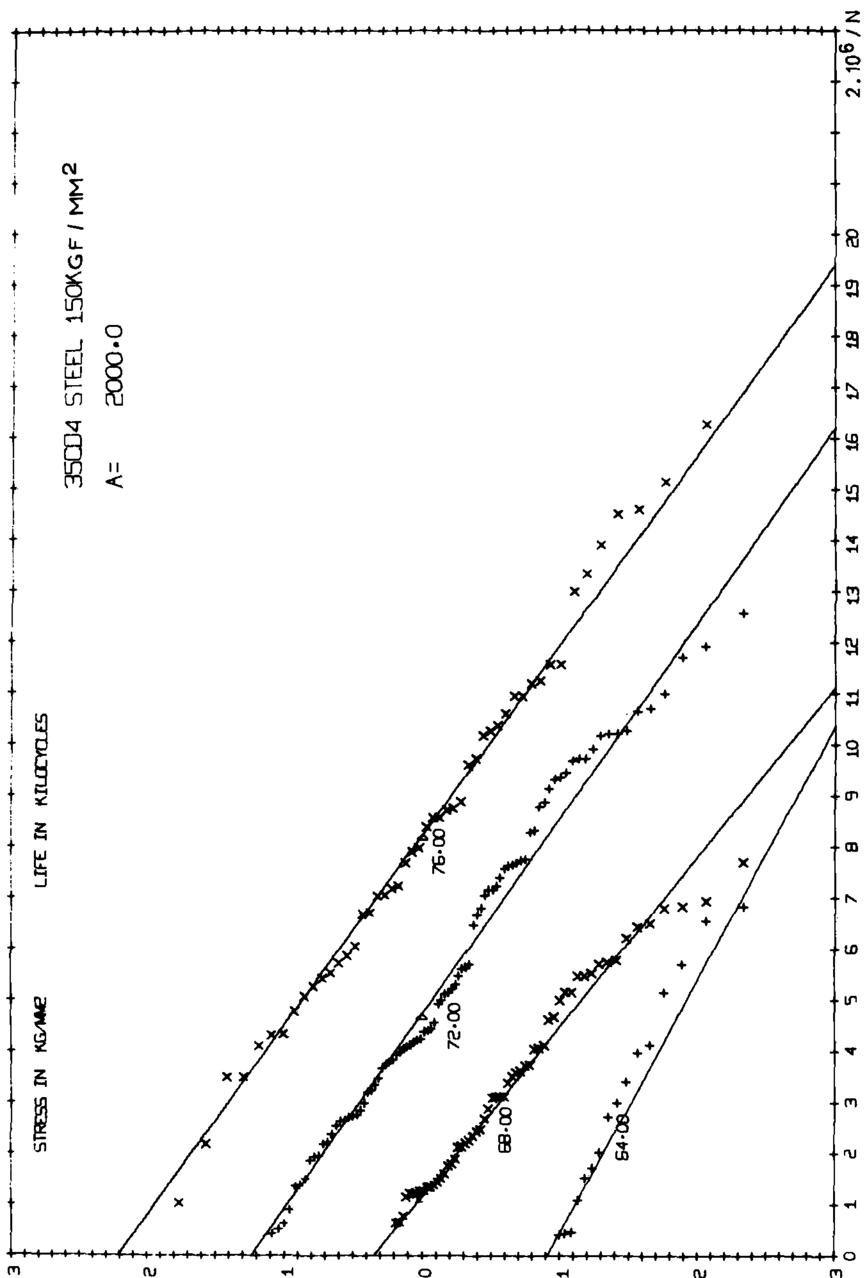

FIG. 9—*Cumulative frequency curves of fatigue-life reciprocal for the 35 CD 4 grade of steel heat treated to 150 kg/mm².*

Making $c = 0$, one gets the equation implicitly used in the previous section ($S = A/N + E$) as a particular case of Eq 16.

A slightly more general formula has been used in Ref *3*:

$$N + B = \frac{A \exp[-c(S - E)]}{(S - E)} \tag{17}$$

where B is an additional coefficient.

The difficulty with Eqs 16 and 17 is that they do not give S explicitly as a function of N, which is needed to express $\varphi(N)$.

If it is assumed that Eq 17 can be used to represent the $F(0)$ equiprobability curve, one may write

$$N + B = \frac{A \exp[-c(S_{F(0)} - E)]}{(S_{F(0)} - E)} \tag{18}$$

The right-hand side of Eq 18 being a monotonically decreasing function of $(S_{F(0)} - E)$, this equation defines a one-to-one correspondence between N and $(S_{F(0)} - E)$. Since $N \rightarrow \infty$ when $S_{F(0)} \rightarrow E$, the converse is also true, and E has the same meaning in Eq 18 as in Eqs 8 to 13. Now, according to Eq 13,

$$\varphi(N) = S_{F(0)} - E \tag{19}$$

Comparing Eqs 18 and 19, $\varphi(N)$ must therefore satisfy the following condition

$$\frac{A \exp[-c\varphi]}{\varphi} = N + B \tag{20}$$

Equation 20 defines $\varphi(N)$ in implicit form for a given set of coefficients A, B, and c.

It is not difficult to solve this equation for φ with an electronic computer. It is, therefore, possible to plot the cumulative frequency curves of φ(NCF) and also the S, φ diagram in much the same way as has been done with A/N in the preceding section, *provided that A, B, and c are known.* The purpose of the next section is to show how these coefficients can be estimated.

Statistical Estimation of the Model Coefficients

It has already been noted in the section on Representation of the Equiprobability Curves Using a Transformed Variate that the distributions of φ(NCF) at the various stress levels are similar, since they are defined by the same cumulative distribution function F. In contrast to this, it has been shown that the distribution of the NCF's changes in shape and is highly skewed at low stress levels. In fact, it has been proved under simple assumptions in an earlier paper [6] that, at any stress level where the proportion of fractured specimens does not tend to unity when the number of applied load cycles increases indefinitely (that is, in the stress range covered by the limit curve in Fig. 1) then, even the lower-order moments of the distribution of the NCF (and among them, the mean and variance) are not defined. (It is shown in Ref 6 that the integrals which define these moments are not convergent.)

Therefore, if the data collected at low stress levels are to be included in a statistical analysis, simple statistics such as the mean and standard deviation of the NCF itself will not be appropriate.

As suggested in the section on Simple Example of the Use of Transformed Fatigue Lives where the NCF reciprocal was used instead of the NCF itself, it will be shown in the next section, using a number of examples, that φ(NCF) is distributed normally or almost normally. The difficulties involved in the use of the NCF when estimating the distribution characteristics will therefore disappear if φ(NCF) is used in place of the NCF.

In order to calculate φ(NCF), however, A, B, and c must be known, as explained at the end of the preceding section. Therefore, one needs to know the coefficients to be estimated!

This situation is not quite as serious as it may seem at first sight. If, to start with, approximate values of A, B, and c are first used to compute transformed values of the NCF's, these will not be distributed exactly as they would, had the true values of A, B, and c been used instead, but it is only necessary that the distributions of φ(NCF) be close enough to normal for the statistical estimation process to work properly with the data.

When this is done, the estimation process will produce new values for A, B, and c which, in turn, will be used to compute a second set of transformed NCF's and so on. This iterative process will be repeated until convergence is obtained.

The method of estimation is a weighted least squares method applied to the estimated means of the φ(NCF) distributions.

At all stress levels where all the NCF's are known, these are the arithmetic means of the φ(NCF)'s. At those levels where some of the specimens are unbroken, the estimated mean is that of the censored distribution of φ(NCF). These estimated means are obviously weighted according to the reciprocals of their respectives variances.

A computer program has been written in FORTRAN language and carries out all computations. The data may enter into four different branches of the program depending on the nature of the function $\varphi(N)$. Experience has shown that Eq 17 may take three degenerate forms:

1. $B = 0; c = 0$

Then Eq 17 can be written

$$1/N = (1/A)(S - E) \tag{21}$$

In this case, there is no necessity to use an iterative process and a linear regression method is applied to $(1/N)$ regarded as the dependent variate and S as the independent variate.

2. $B \neq 0; c = 0$

Equation 17 can be written:

$$(N + B)(S - E) = A$$

This case is dealt with separately because it involves less computational work than cases 3 and 4.

3. $B = 0; c \neq 0$

Equation 17 reduces to Eq 16, and only two parameters have to be estimated.

4. $B \neq 0; c \neq 0$

This is the general form for which three parameters must be estimated.

In all four cases, E and the standard deviation σ of φ(NCF) are also estimated in addition to the above-mentioned parameters.

The standard deviation is estimated separately at each stress level, but these different estimates can be pooled into a single estimate if no significant differences exist.

Application of the Proposed Method to Five Grades of Steel

A large number of test series have already been analysed in Ref *1*. In all, several thousand test results were considered, but, in many instances, the number of test results per stress level was too small to draw valid conclusions regarding the distribution of the NCF or the type of stress-response curve (for example Ravilly's results formerly analyzed by various authors[7]).

Therefore, it was decided at IRSID to carry out an extensive program of fatigue tests aimed at checking the conclusions of Ref *1* with regard to stress-response curves, equiprobability curves, and fatigue-life distributions.

Four grades of steel were used in this investigation, one of them with two different heat treatments (Tables 1 and 2).

All tests were performed under constant moment rotating bending on

TABLE 1–*Chemical composition of the steels used in the investigation.*

AFNOR[a] Steel Designation	Chemical Composition					
	C	Cr	Mo	Si	Mn	Ni
XC 10	0.08			0.14	0.40	
XC 60	0.58			0.37	0.46	
XC 100	1.17	0.17	0.013	0.25	0.39	0.14
35 CD 4	0.34	1.16	0.23	0.32	0.64	0.20

[a] Association Française de Normalisation.

MERL-IRSID[2] type machines at 6000 rpm. For each material, Table 3 indicates the number of specimens tested and the number of load cycles at which the tests were interrupted.

Many tests were carried out below the median endurance limit in order to gather information about fatigue life distributions at low stress levels. At high stresses, testing was limited by specimen heating.

A detailed account of the results of this test program is given in Ref *3*. These data will be used here only to illustrate the described method by examples.

The first step in this method is to put the program into the computer memory either from punched cards or from a magnetic disk. After being punched on cards, the data are fed into the computer and processed according to the program. The data are first printed in order to check the values previously punched on cards. The following results are then printed as the program proceeds:

1. For each stress level, the mean value of φ(NCF) either in the form of the arithmetic mean or in the form of the estimated mean of a censored distribution.

TABLE 2–*Mechanical properties of the steels investigated.*

Steel Grade	Yield Point[a]	Max Tensile Strength[a]	Elongation, %	Yield Point / Max Tensile Strength
XC 10	30.4	40.1	40.6	0.76
XC 60	34.6	68.2	26	0.51
XC 100	86.6	109.2	13.3	0.79
35 CD 4 (80)	58.6	76.7	22.7	0.76
35 CD 4 (150)	143.2	163.6	9.3	0.88

[a] All stress values are given in kilograms per square millimeter, a legally accepted unit of the metric system at the time the investigation began. Use of this unit is maintained throughout to avoid putting more decimals to original figures (1 kg/mm^2 = 1422.3 lb/in^2).

[2] MERL: Mechanical Engineering Research Laboratory, Glasgow, Great Britain. IRSID: Institut de Recherches de la Siderurgie Francaise, Saint-Germain-en-Laye, France.

TABLE 3—*Specimen and load cycle data.*

Steel Grade	Number of Specimens	Fatigue Test Interrupted At
XC 10	740	100 million cycles
XC 60	850	100 million cycles
35 CD 4 (80)	580	8 million cycles
XC 100	940	100 million cycles
35 CD 4 (150)	850	30 million cycles

2. The standard deviation at each stress level.
3. The new estimates of A, B, and c.

This process is resumed until convergence of A, B, and c to limit values is obtained.

The final values of the means and standard deviations of φ(NCF) are then printed together with their confidence intervals.

The schematic diagram of Fig. 6 can now be used to plot real values. This is done in Fig. 10 in which the results for all five materials are plotted together.

The estimated means of φ(NCF) are plotted in abscissas and the stresses in ordinates. The important differences in fatigue strength among the five grades of steel result in widely separated straight lines in the diagram.

The main purpose of this diagram is *not* to plot each *S-N* curve in the form of a straight line: indeed, nearly any relationship can be represented by a straight line using suitable coordinates. This diagram is used here because it suits the purpose of showing the *deviations* of the plotted means from the theoretical line. With this in view it must be noted that, for a given function $\varphi(N)$ (that is, in general, for a given material), any two points having equal abscissas in the *S-N* diagram also have equal abscissas in the $S - \varphi$ diagram while their respective ordinates are unchanged. The vertical deviations of the test points from the straight line in the $S - \varphi$ diagram are, therefore, the same as from a fitted curve represented by Eq 17 in an *S-N* or *S*-log *N* diagram.

As already indicated, the experimental points in Fig. 10 represent estimated mean values. An indication of the scatter which can be expected to arise from sampling fluctuation is given by the 0.95 confidence intervals of these estimates.

Plotting hundreds of individual test results for each material was not feasible on the $S - \varphi$ diagram. A better image of their distributions is given by the cumulative frequency curves shown in Figs. 11-15. These curves have been drawn by a plotter connected to a computer, and, for simplicity of use, the probability scale is graduated in normal deviates rather than proportions. This makes no difference at all for the test points, which fall exactly where they would, had probability paper been used, since the underlying principle of normal probability paper is really to plot the normal deviate for the proportion.

The reader should bear in mind that, in Figs. 11 through 15, $\varphi(N)$ *decreases*

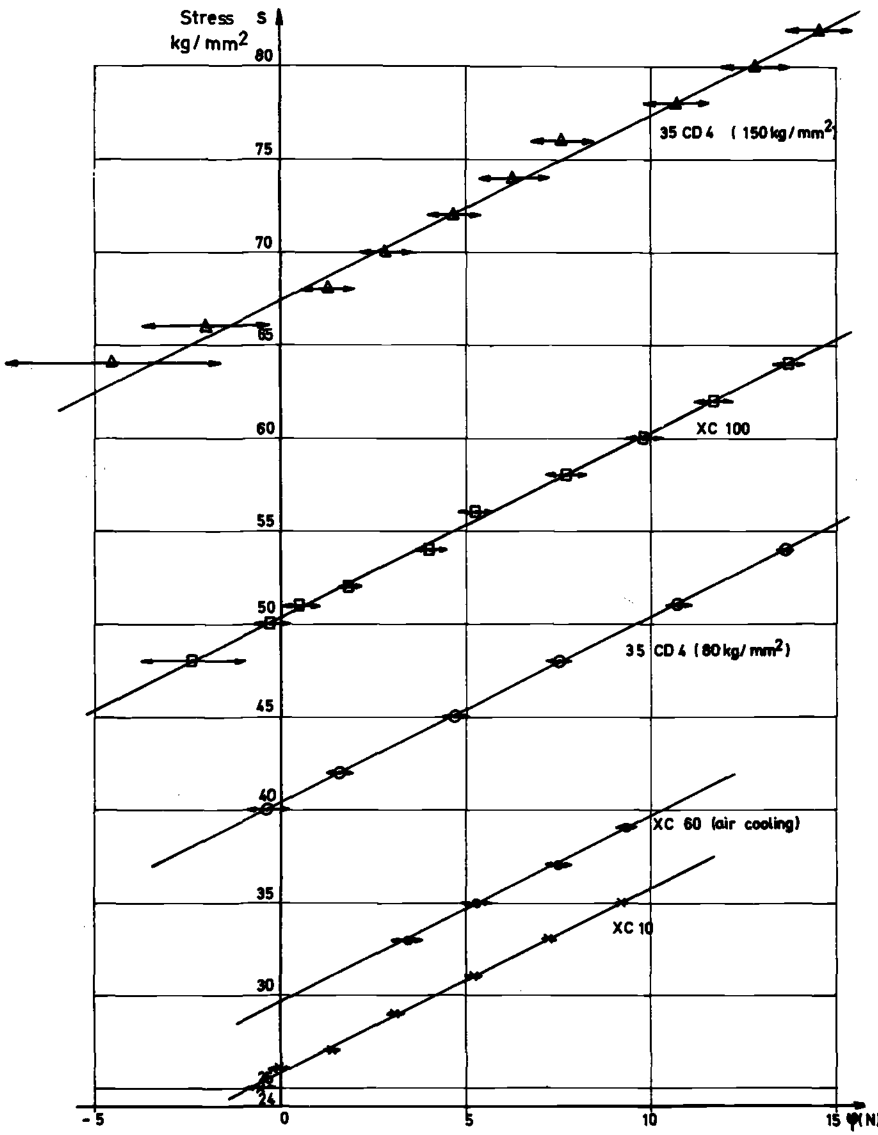

FIG. 10—*Experimental S-φ diagram for the five different grades of steel.*

for increasing N, that is, when the proportion of fractured specimens *increases.* This remark accounts for the negative slope of the cumulative frequency curves since the probability of fracture increases monotonically with the normal deviate. Morever, we know that $\varphi(N) \to 0$ when $N \to \infty$ so that those curves

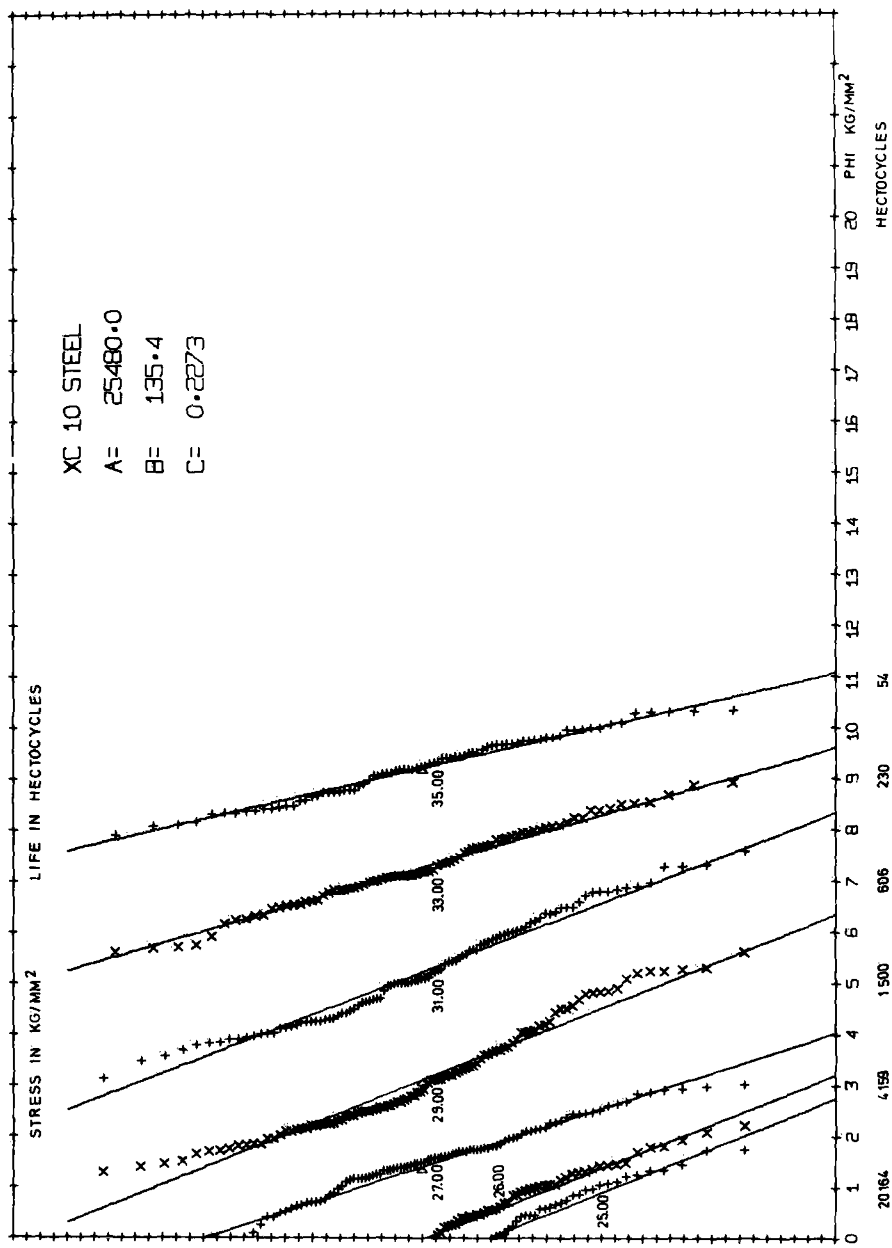

FIG. 11—Cumulative frequency curves of $\varphi(NCF)$ for the XC 10 grade of steel.

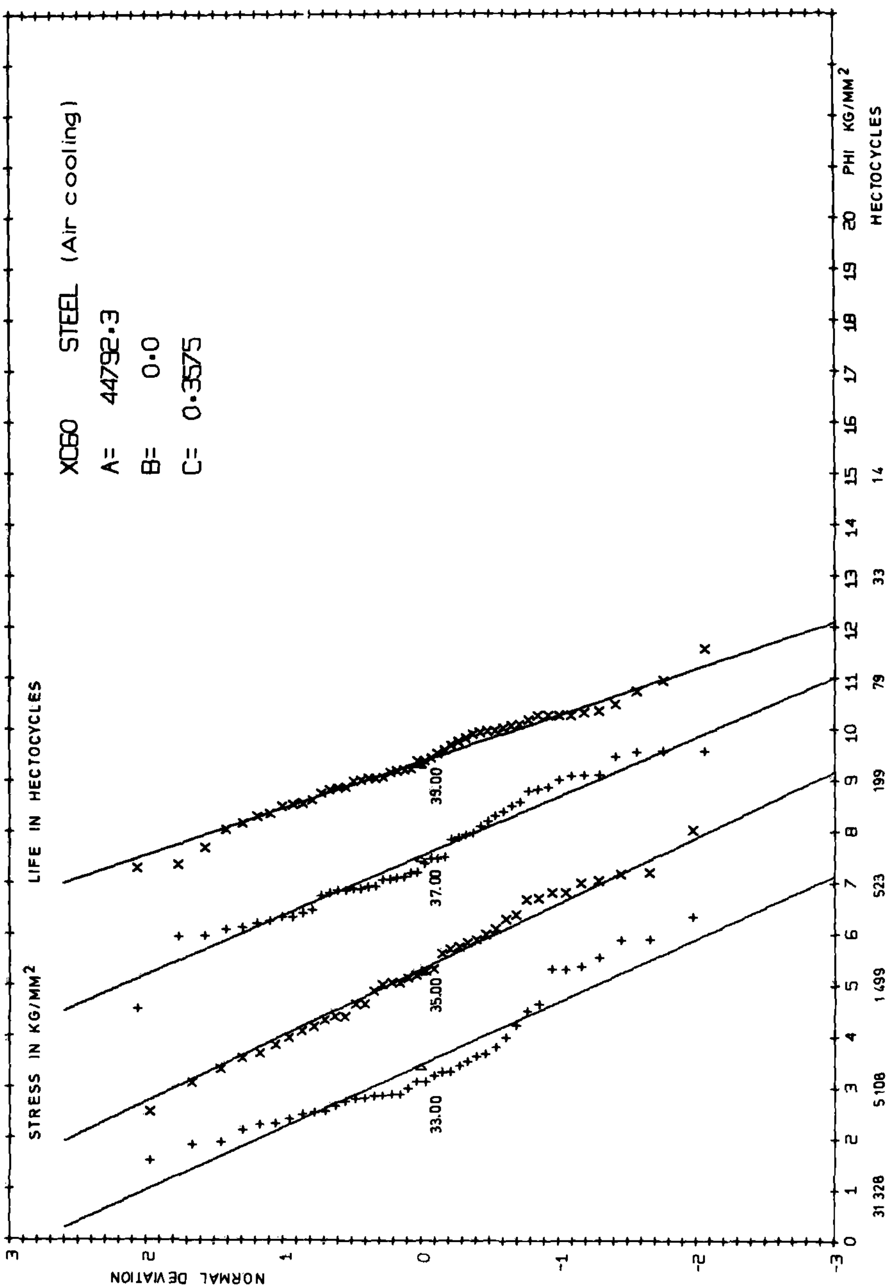

FIG. 12—*Cumulative frequency curves of φ(NCF) for the XC 60 grade of steel.*

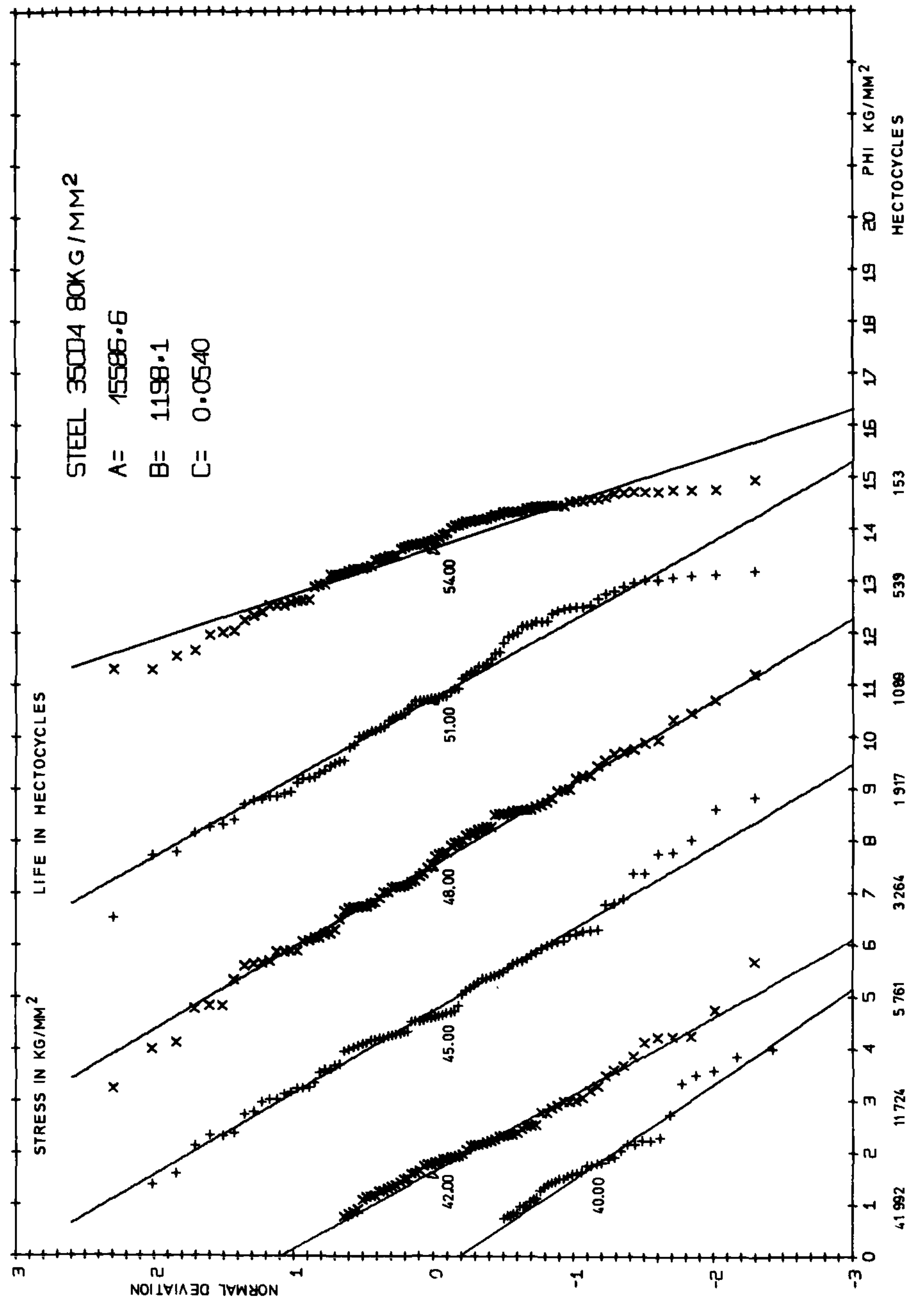

FIG. 13—*Cumulative frequency curves of φ(NCF) for the 35 CD 4 grade of steel heat treated to 80 kg/mm² (maximum tensile strength).*

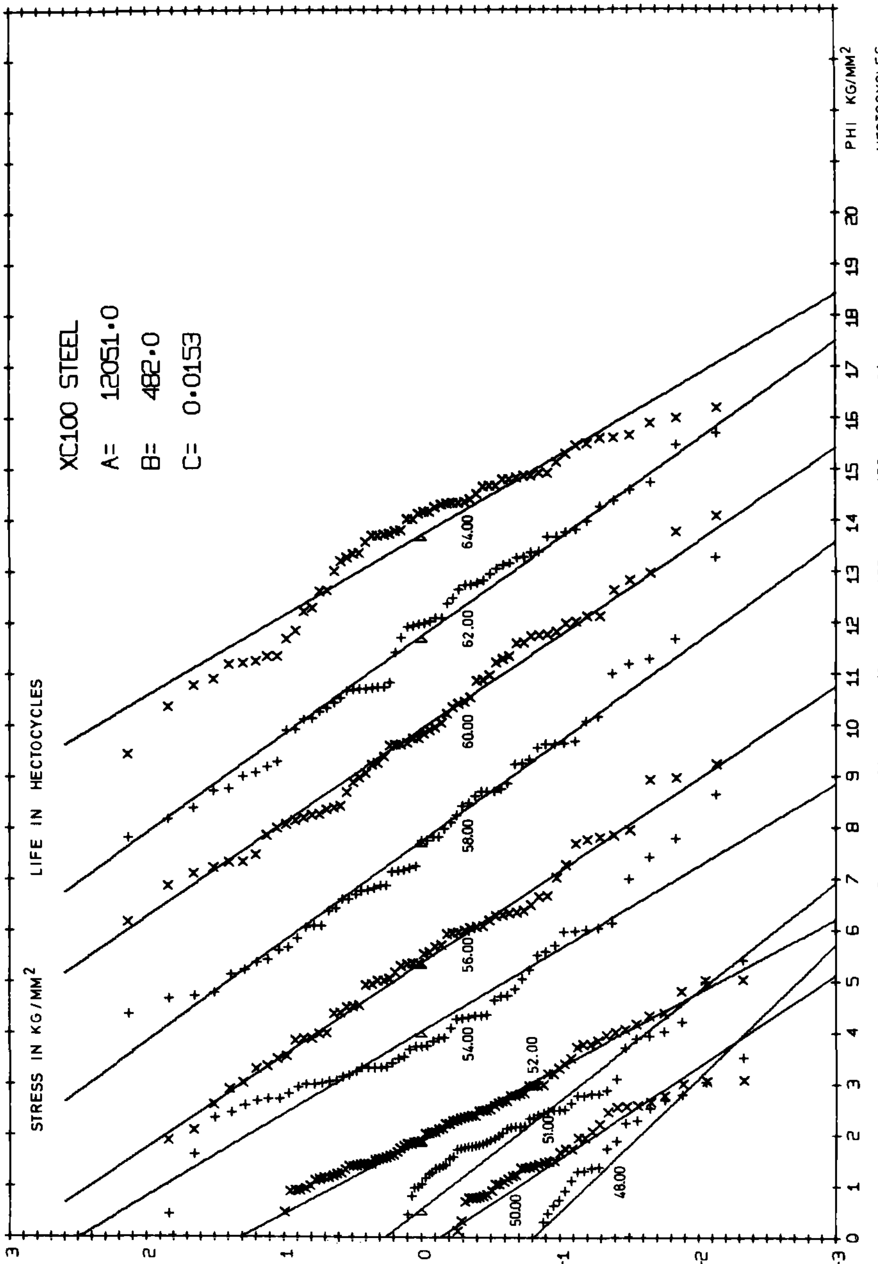

FIG. 14—*Cumulative frequency curves of φ(NCF) for the XC 100 grade of steel.*

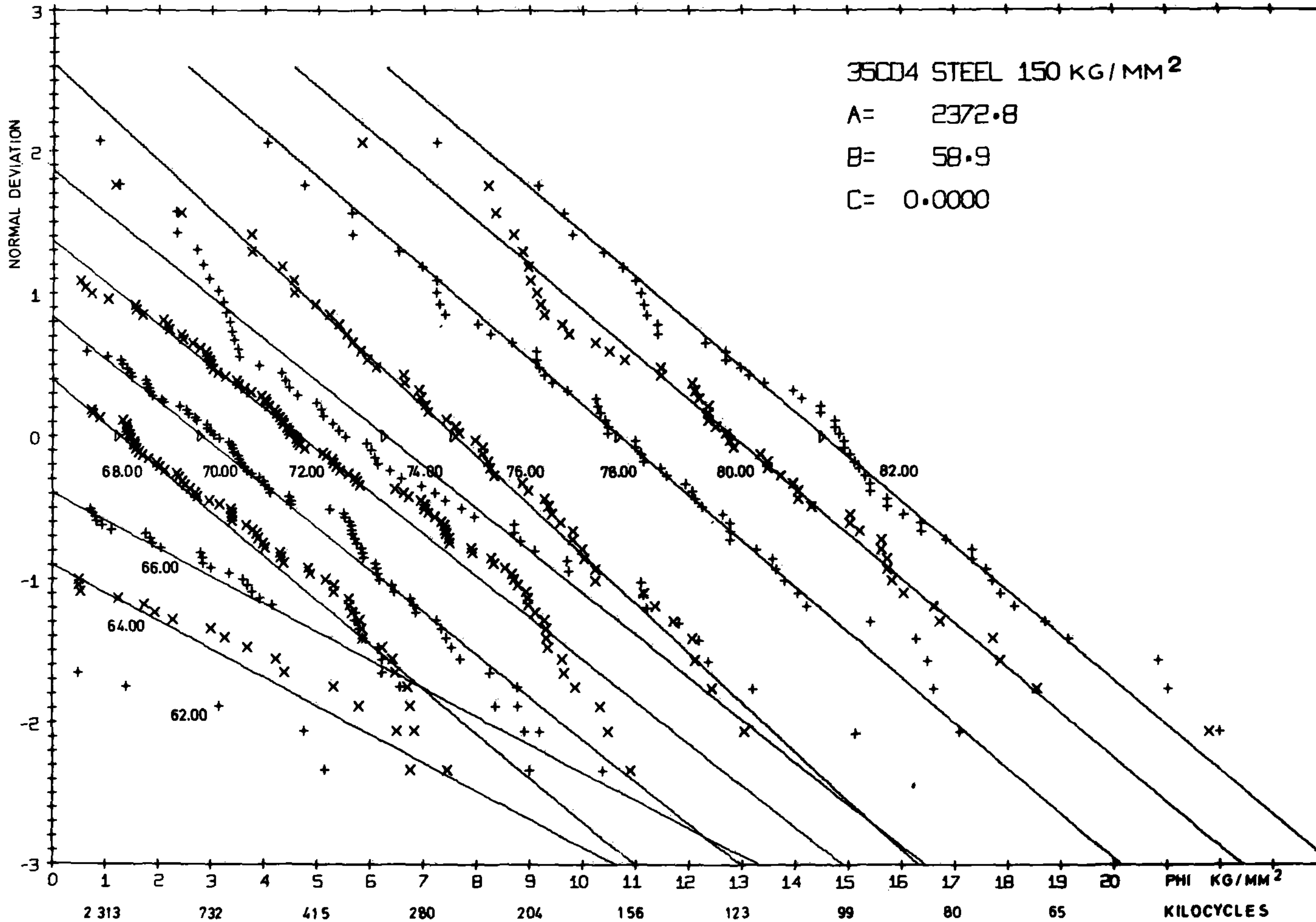

FIG. 15–*Cumulative frequency curves of φ(NCF) for the 35 CD 4 grade of steel heat treated to 150 kg/mm² (maximum tensile strength).*

which end near the vertical axis (Fig. 11) or tend to approach it (Fig. 12) indicate that the proportion of specimens fractured at the corresponding stress level tends to a limit when $N \to \infty$. In other words, the distributions of φ(NCF) are censored at zero (in fact, these distributions are censored at $\varphi(N\,\mathrm{max})$, N max designating the number of cycles where the tests have been interrupted). As expected, this occurs at the lowest stress levels in each test series (stress values in kg/mm^2 are shown at the left of or below the mean point of each curve). The estimates of A, B, and c given by execution of the computer program are given in each figure and a correspondence between φ and the NCF (measured in hecto- or kilocycles) is also given in abscissas.

Discussion

The reader will judge for himself the normality of the cumulative frequency curves (whether the distribution is censored or not) in Figs. 11-15.

In Fig. 14, the distribution of φ(NCF) is definitely skewed at the highest stress level (64 kg/mm^2).

A similar remark applies to Fig. 13 where the next curve (for the 51 kg/mm^2 stress level) is also skewed at its bottom end. These discrepancies from normality should not be attributed to a change in the stress-response curve shape in the corresponding region of the S-N diagram but rather to the inadequacy of Eq 17 in this region. In this respect, the introduction of parameter B in the left-hand side of Eq 17 is not the best step towards improving Eq 16. It can be seen from Eq 20 that there is an upper bound to its root, φ, when $N \to 0$. In fact, since φ increases when N decreases, this upper bound is the solution to

$$\frac{A\exp[-c\varphi_s]}{\varphi_s} = B \tag{23}$$

In these conditions, the largest values of φ are, in some way, "squeezed" against φ_s.

This results in a steep fall at the lower end of the cumulative frequency curve.

At low stress levels, variations in the value of $\sigma(N)$ may also cause departure from normality for the φ(NCF) distributions even if the stress response curves remain sigmoid normal.

In Figs. 14 and 15 there is strong indication that the scatter $\sigma(N)$ increases with N (the slope of the cumulative frequency curves decreases when the stress decreases). Equation 11 then shows that $(S - \varphi(N) - E)/\sigma(N)$ being smaller if $\sigma(N)$ increases with N, the probability of fracture is also smaller than it would be if $\sigma(N)$ was constant. This produces a downward curvature of the cumulative frequency curves.

Conclusions

A relationship is shown to exist between the distributions of the numbers of cycles to fracture and the stress-response function through the *S-N* (stress-number of cycles) relationship. On this basis, a mathematical model of the *P-S-N* (probability-stress-number of cycles) curves is proposed together with a new method of estimation of its coefficients. This method has been programmed in FORTRAN for electronic computers. It has proved successful in the analysis of statistical data obtained in fatigue tests on five grades of steel.

Acknowledgments

I am grateful to my colleague J. G. Stremsdoerfer for his continuous assistance in running and improving the computer program.

References

[*1*] Bastenaire, F. A., "Etude Statistique et Physique de la Dispersion des Résistances et des Endurances à la Fatigue," Ph.D. thesis, Faculty of Sciences, University of Paris, 1960.
[*2*] Freudenthal, A. M. in *Statistical Aspects of Fatigue, ASTM STP 121*, American Society for Testing and Materials, 1952, p. 3.
[*3*] Bastenaire, F. A., Pomey, G., and Rabbe, P., *Mémoires Scientifiques de la Revue de Metallurgie*, MRMTA, Oct. 1971.
[*4*] Bastenaire, F. A., Bastien, M., and Pomey, G., *Acta Technica Academiae Scientarium Hungaricae*, ATSHA, Tomus XXXV-XXXVI.
[*5*] Hald, A., *Skandinavisk Aktuarietidskrift*, SKAKA, Vol. 32, 1949, pp. 119-134.
[*6*] Bastenaire, F. A., *Comptes Rendus des Séances de l'Académie des Sciences*, CRSAA, Vol. 243, 29 Oct. 1956, pp. 1270-1273.
[*7*] Ravilly, E., *Publications Scientifiques et Techniques du Ministère de l'Air*, PSTMA, No. 120, 1938.

R. E. Little [1]

Estimating the Median Fatigue Limit for Very Small Up-and-Down Quantal Response Tests and for *S-N* Data with Runouts

REFERENCE: Little, R. E., "**Estimating the Median Fatigue Limit for Very Small Up-and-Down Quantal Response Tests and for *S-N* Data with Runouts,**" *Probabilistic Aspects of Fatigue, ASTM STP 511,* American Society for Testing and Materials, 1972, pp. 29-42.

ABSTRACT: Much basic fatigue data may be categorized for analytical purposes as small sample quantal response data. For example, both small sample up-and-down test outcomes and most *S-N* data fall into this category. But reliable median fatigue-limit estimates for small samples are not directly available using large sample statistical formulas. Rather, small sample estimates must be examined carefully regarding both their variability under repeated sampling and their "sensitivity" relative to various analytical methods and assumptions. The variability of small sample response estimates has been studied by Dixon and others. This paper considers the sensitivity of these estimates to such key assumption alternatives as, for example, minimum chi square analysis versus maximum likelihood analysis, and an underlying extreme value (smallest) response distribution versus a normal response distribution. Engineering assessment of the "accuracy" of the estimated median fatigue limit requires careful consideration of both its statistical variability and its analytical sensitivity as established herein.

KEY WORDS: fatigue(materials), probability theory, statistical analysis, Weibull density functions, analysis of variance, chi square test, fatigue tests, fatigue limit, *S-N* diagrams, sampling

Nomenclature

- d Uniform spacing of successive stimulus levels
- K Number of stimulus levels used in testing
- L Likelihood
- N_i Number of specimens tested at the ith stimulus level; subscript i is suppressed in Eqs 1 through 4

[1] Professor, University of Michigan, Dearborn, Mich. 48128.

O Specimen did not react (did not fail)
P_i True probability of reacting (failure) at the ith stimulus level
R_i Number of specimens reacting (failed) at the ith stimulus level
S_i Stimulus level, for example, stress or strain amplitudes, or rms values
X Specimen reacted (failed)
Y Linearized response $Y = \alpha + \beta S = F^{-1}(P)$, refer to Table 4
α Intercept of linearized response curve: $\alpha = -\mu/\sigma$
β Slope of the linearized response curve: $\beta = 1/\sigma$
Δ Tabulated factor in the median strength expression $S_{50} = S_0 + \Delta d$
μ Probability density function location parameter
σ Probability density function scale parameter
χ^2 Chi square (statistic)

Subscripts

0 Initial stimulus level used in testing
50 Estimate evaluated at 50 percent probability level

Superscripts

$\wedge$ Estimated value

The up-and-down test method for estimating the true 50 percent response level of quantal data was originally devised to study the impact sensitivity of explosive mixtures [*1*]. In this sensitivity test the common procedure is to drop a weight from various heights on specimens of the same explosive mixture. If the weight is dropped from a very large height, the specimen will explode. On the other hand, if the weight is dropped from only a very small height, the specimen will not explode. For intermediate heights, some specimens explode, whereas others do not. It is supposed in sensitivity testing that each individual specimen has an associated critical height such that the given specimen will explode when the weight is dropped from a greater height, but it will not explode when the weight is dropped from a lesser height. The universe of all explosive specimens of the same mixture is thus characterized by a continuous random variable—the critical height. But this random variable cannot be observed directly. Rather, the test outcomes only establish whether, for each given specimen, the drop height was less than or greater than its critical height. When a number of such response tests are conducted at the same intermediate drop height H_i, the resulting quantal response data take the form: N_i tested at H_i, R_i reacted (and $N_i - R_i$ did not react).

This quantal response situation arises in a number of materials research and development situations, from the testing of armor-piercing projectiles and impact-resistant plastic bottles, to determining the relative resistances of diffusion coatings to corrosion. In quantitative application, quantal response

TABLE 1—*Wöhler's original* S-N *data for wrought Phönix iron.*

Stress centners/zoll^2	Cycles to Failure	Number Tested	Number Failed
320	56 430	1	1
300	99 000	1	1
280	183 140	1	1
260	479 490	1	1
240	909 810	1	1
220	3 632 590	1	1
200	4 917 990	1	1
180	19 186 790	1	1
160	132 250 000 runout	1	0

data may be used to calculate K_{Iscc} based on appropriate stress-corrosion tests on pre-cracked specimens, to calculate the nil ductility transition temperature for keyhole Charpy impact tests[*2*], or of special interest in this paper, to calculate the median fatigue limit based on either *S-N* data or the outcomes of very small up-and-down tests. In over-all perspective, the quantal response situation arises whenever the test performance may be objectively classified into two mutually exclusive categories such as "acceptable" or "not acceptable."

Tables 1 and 2 summarize the fatigue-response data to be analyzed herein. Although the test methods are apparently quite different, the two right-hand columns show clearly the basic similarity of these two methods. Note also that Wöhler's data may be summarized in up-and-down context as XXXXXXXXO.

Theoretical Background (Normal Distribution)

Shortly after World War II Dixon and Mood[*1*] published curves and formulas for a simplified maximum likelihood analysis of normally distributed quantal response data accumulated following the now well-known up-and-down test strategy, Table 2. The effective sample size in their simplified analysis was about one half the actual sample size. Consequently Dixon and Mood cautioned that their asymptotic (large sample) variance expressions "may well be very misleading if the [actual] sample size is less than forty to fifty." In 1953,

TABLE 2—*Typical outcome of a short up-and-down fatigue response test.*[a]

Stress, ksi	1	2	3	4	5	6	Number Tested	Number Failed
65							...	...
60						X	1	1
55			X		O		2	1
50		O		O			2	0
45	O						1	0

[a] X = specimen failed, O = specimen did not fail.

Brownlee et al[3] investigated the small sample behavior of up-and-down tests and concluded that the Dixon-Mood sample-size restriction was unnecessary, namely, they concluded that "the Dixon-Mood formula for the asymptotic variance [of the median normal response estimate] is reasonably reliable even in samples as small as five to ten." Brownlee and his associates also presented a revised expression for the median normal response estimate, which generated a smaller mean square error than the Dixon-Mood estimate when the initial test was conducted at a stimulus level (stress amplitude) some distance from the true median response (refer to Fig. 4, Ref 4). Then, in 1965, Dixon[4] published the results of a digital computer numerical solution to the maximum likelihood equations and presented tabulated quantities which, by easy calculation, provide a median normal response estimate with an even smaller mean square error than the improved estimate suggested in Ref 3. Thus, in certain cases reasonably precise median normal response estimates may now be easily computed for up-and-down tests with sample sizes as small as four or five. These estimates appear in Table 3.

Reliable estimation of the standard deviation σ of the underlying normal response distribution is quite a different matter however. The up-and-down strategy is quite inefficient in this regard. Consequently its σ estimates should be used only in the absence of more reliable prior information.

Dixon[4] took advantage of the lack of precision of the standard deviation

TABLE 3—*Values of Δ for maximum likelihood analyses based on an underlying normal distribution with* $d/\sigma = 1$. S_{50} *equals* $S_0 + \Delta d$, *in which* S_0 *is the stress amplitude used in starting the up-and-down test program.*

Second Part of Series	Δ for Test Series Whose First Part Is			Standard Error of $\hat{S}_{50}$ [4]
	O	OO	OOO	
X	0.50	1.61	2.62	0.88 σ
XO	0.84	1.89	2.89	0.76σ
XX	−0.18	1.00	2.03	
XXO	1.30	2.31	3.32	
XOX	0.50	1.56	2.57	0.67 σ
XXO	0.00	1.12	2.14	
XXX	−0.81	0.45	1.50	
XOOO	1.84	2.85	3.85	
XOOX	1.12	2.14	3.14	
XOXO	0.70	1.74	2.74	
XOXX	0.08	1.17	2.18	0.61 σ
XXOO	0.31	1.37	2.38	
XXOX	−0.31	0.83	1.86	
XXXO	−0.71	0.50	1.54	
XXXX	−1.44	−0.10	0.99	

estimate in up-and-down testing to reduce the maximum likelihood equation to a function of only one variable, the median response S_{50}—by assuming that $d/\sigma = 1$, where d is the uniform spacing between successive stimulus levels (stress amplitudes). This assumption not only circumvents the problem that certain small sample responses are such that the maximum likelihood equations do not yield unique estimates of both σ and S_{50}, it also is consistent with Dixon's major objective of comparing responses of two or more treatments in analysis of variance based on planned experiments. However, when the primary (and perhaps sole) objective is to estimate the median response, then it is clearly necessary to examine carefully the influence of the assumption that $d/\sigma = 1$ on the magnitude of the resulting estimate of S_{50}.

Scope

This paper considers the influence on the magnitude of the resulting median-response estimate of alternative assumptions at three key stages of the analysis: (1) minimum chi square analysis versus maximum likelihood analysis; (2) logistic and extreme value (smallest) response distributions versus the normal response distribution; and (3) stress-amplitude spacing of $d/\sigma = 2/3$ and $d/\sigma = 3/2$ versus $d/\sigma = 1$. These solution alternatives generated $2 \times 3 \times 2 = 12$ different estimates of the median response for each set of possible outcomes listed in Table 3. Then, by examining these twelve sets of estimates it is a fairly simple matter to establish the "sensitivity" of the median-response estimate to each of the three key assumptions enumerated above. Moreover, a study of the dispersion and range of the twelve individual estimates for each data set permits an engineering assessment of both the median response stress amplitude and its "accuracy."

Theory

Whatever the response distribution assumed, it plots as a straight line on the appropriate probability paper. These straight lines are written either as $Y = \alpha + \beta S$ or as $Y = \log \alpha + \beta \log S$, Table 4. But as equal spacing for a logarithmic scale depends on the actual values of S involved, the tabulated values resulting from the following analyses pertain primarily to linear abscissae, that is, these tabulated values may be used for the log-normal, log-logistic, and Weibull distributions only if the independent variable log S is (approximately) equally spaced.[2]

[2] The overwhelming difficulty associated with nonuniform spacing of stress amplitudes lies in trying to find a way to tabulate the desired Δ values. Otherwise, nonuniform spacings present no special estimation problems. Refer to Appendix.

TABLE 4—*Linearizing transformations for straight line* P-S *curves.*

Distribution Function	Expression	Linearizing Transformation[a]	Abscissa Scale[b]
Normal[c]	$P = \frac{1}{\sqrt{2\pi}} \int_{-\infty}^{Y} e^{-\frac{1}{2}u^2} du$	use normal tables, for example	linear
Log-normal[d]		if $P = 0.05$, $Y = -1.645$	logarithmic
Logistic[c]	$P = \frac{1}{1 + e^{-y}}$	$Y = \log_e \left(\frac{P}{1 - P} \right)$	linear
Log-logistic[d]			logarithmic
Extreme value[c] (smallest)	$P = 1 - e^{-e^{Y}}$	$Y = \log_e [-\log_e (1 - P)]$	linear
Weibull[d]			logarithmic

[a] $Y = F^{-1}(P)$, where P is the dependent (observed) variable; Y is plotted linearly along the ordinate of probability paper
[b] S, the independent variable is plotted along the abscissa of probability paper
[c] $Y = \alpha + \beta S$.
[d] $Y = \log \alpha + \beta \log S$.

Maximum Likelihood Analysis

In maximum likelihood estimation the objective is to find those estimates $\hat{\alpha}$ and $\hat{\beta}$ which maximize the likelihood expression

$$L = \prod_{i=1}^{K} \frac{N!}{R!(N-R)!} P^R (1-P)^{N-R} \tag{1}$$

in which the subscript i referring to the K equally spaced stress amplitudes has been suppressed for notational simplicity. In this expression, N_i is the number of specimens tested at stress amplitude S_i, R_i is the number that fail, and P_i is the true probability of failure at S_i. Note that α and β enter Eq 1 through $P_i = F(Y_i)$, Table 4, where $Y_i = \alpha + \beta S_i$.

Likelihood Eq 1 takes on its maximum value when (simultaneously)

$$\frac{\partial [\log L]}{\partial \alpha} = 0 = \sum_{i=1}^{K} \frac{(R-NP)}{P(1-P)} \frac{\partial P}{\partial \alpha} \tag{2a}$$

and

$$\frac{\partial [\log L]}{\partial \beta} = 0 = \sum_{i=1}^{K} \frac{(R-NP)}{P(1-P)} \frac{\partial P}{\partial \beta} \tag{2b}$$

These two nonlinear equations were solved numerically by expanding the right-hand side of the above differential equations in a Taylor's series, and then ignoring higher order terms to compute successive corrections $\delta\alpha$ and $\delta\beta$ in an iterative procedure until the value of the smallest correction term was less than 10^{-8} [5]. Only a few of the small sample responses considered herein yield unique numerical estimates for both α and β. These responses and estimates are given in Table 5, where for the normal distribution, $S_{50} = -\alpha/\beta$ and $\sigma = 1/\beta$. For the remaining responses, a unique numerical solution for $\hat{S}_{50}$ is possible only if σ is specified as some multiple of the spacing d of the stress amplitudes S_i. Table 6 lists Δ values based on maximum likelihood analyses with underlying normal response distributions whose standard deviations are respectively $3/2\ d$ and $2/3\ d$, that is, $d/\sigma = 2/3$ and $d/\sigma = 3/2$. Recall that Table 3 lists Δ values for $d/\sigma = 1$.

Corresponding tables for Δ based on logistic and extreme value (smallest) distributions with identical variances contribute little to this paper and thus have not been presented herein. These tables, however, were used to prepare the over-all summary values of Δ found in Table 7.

TABLE 5 – *Values of Δ (above) and $1/\hat{\sigma}$ (below) for maximum likelihood analyses based on an underlying normal distribution. Only the responses indicated provide unique estimates for both parameter estimates $\hat{S}_{50}$ and $\hat{\sigma}$.*

Second Part of Series	Δ for Test Series Whose First Part Is		
	O	OO	OOO
XXX	. . .	0.33	1.50
	. . .	0.63	0.88
XOOO	3.73	3.86	4.70
	0.29	0.45	0.50
XXXO	−0.81	0.50	1.55
	0.71	0.88	0.99
XXXX	. . .	. . .	0.67
	. . .	. . .	0.31

Minimum Chi Square Analysis

Minimum chi square analysis is well accepted as a reasonable large sample alternative to maximum likelihood analysis. This estimation method also provides estimates which agree closely with the maximum likelihood estimates for small samples, Table 8. These estimates were calculated by finding those values of $\hat{\alpha}$ and $\hat{\beta}$ which minimize the expression

$$\chi^2 = \sum_{i=1}^{K} \frac{(R - NP)^2}{NP(1 - P)} \tag{3}$$

Such values correspond to the situation where (simultaneously)

$$\frac{\partial \chi^2}{\partial \alpha} = 0 = \sum_{i=1}^{K} \frac{(R - NP)}{P(1 - P)} \left\{ \frac{NP - 2PR + R}{NP(1 - P)} \right\} \frac{\partial P}{\partial \alpha} \tag{4a}$$

and

$$\frac{\partial \chi^2}{\partial \beta} = 0 = \sum_{i=1}^{K} \frac{(R - NP)}{P(1 - P)} \left\{ \frac{NP - 2PR + R}{NP(1 - P)} \right\} \frac{\partial P}{\partial \beta} \tag{4b}$$

These equations were also solved numerically such that the maximum error associated with either estimate was less than 10^{-8}. The same small sample

TABLE 6—*Values of* Δ *for maximum likelihood analyses based on underlying normal response distributions whose standard deviations* σ *are respectively equal to 3/2* d *(above) and 2/3* d *(below). In certain cases the magnitude of* Δ *is relatively sensitive to minor changes in* d/σ.

Second Part of Series	Δ for Test Series Whose First Part Is		
	O	OO	OOO
X	0.50 0.50	1.79 1.52	2.86 2.52
XO	1.05 0.70	2.19 1.71	3.23 2.71
XX	−0.37 −0.06	1.00 1.00	2.11 2.00
XOO	1.61 1.11	2.67 2.11	3.69 3.11
XOX	0.50 0.50	1.67 1.51	2.71 2.51
XXO	0.00 0.00	1.24 1.05	2.31 2.05
XXX	−1.10 −0.64	0.35 0.49	1.50 1.50
XOOO	2.20 1.65	3.23 2.65	4.23 3.65
XOOX	1.24 1.05	2.31 2.05	3.33 3.05
XOXO	0.82 0.62	1.93 1.62	2.96 2.62
XOXX	−0.03 0.14	1.17 1.17	2.23 2.17
XXOO	0.42 0.23	1.57 1.25	2.61 2.25
XXOX	−0.42 −0.23	0.83 0.83	1.92 1.83
XXXO	−0.83 −0.62	0.50 0.50	1.62 1.51
XXXX	−1.78 −1.25	−0.26 −0.03	0.93 1.00

responses which yield unique estimates of α and β (S_{50} and σ) for maximum likelihood estimation also yield unique estimates for minimum chi square estimation. The remaining small sample responses, as for maximum likelihood estimation, yield unique estimates of S_{50} only if σ is given in terms of the stress-amplitude spacing. The resulting Δ values for the normal distribution whose standard deviation is such that $d/\sigma = 1$ are given in Table 8 adjacent to the corresponding maximum likelihood values for ease in comparison.

TABLE 7–*Smallest and largest of the twelve Δ values generated by the twelve alternative analyses enumerated in the Scope paragraph. In many practical situations these values may differ negligibly relative to the accuracy actually required in analysis and evaluation.*

Second Part of Series	Δ for Test Series Whose First Part Is		
	O	OO	OOO
X	0.35 0.50	1.46 1.79	2.47 2.86
XO	0.60 1.05	1.61 2.19	2.61 3.23
XX	−0.37 −0.01	0.93 1.03	2.00 2.11
XOO	1.04 1.61	2.04 2.67	3.04 3.69
XOX	0.35 0.50	1.45 1.67	2.45 2.71
XXO	−0.07 +0.03	1.02 1.24	2.02 2.31
XXX	−1.10 −0.35	0.35 0.70	1.50 1.71
XOOO	1.63 2.37	2.63 3.42	3.63 4.43
XOOX	1.02 1.24	2.02 2.31	3.02 3.33
XOXO	0.53 0.82	1.54 1.93	2.54 2.96
XOXX	−0.05 0.21	1.08 1.23	2.13 2.26
XXOO	0.22 0.43	1.23 1.57	2.23 2.61
XXOX	−0.43 −0.20	0.73 0.84	1.77 1.92
XXXO	−0.83 −0.35	0.50 0.71	1.50 1.71
XXXX	−1.89 −0.58	−0.27 0.48	0.93 1.48

Tabulations of minimum chi square Δ values for the normal distribution with $d/\sigma = 2/3$ and $d/\sigma = 3/2$ are omitted herein. These tables, as well as the corresponding Δ tables for the logistic and extreme value (smallest) distributions with identical variances were considered in preparing the summary of results which follows.

TABLE 8–*Values of Δ for maximum likelihood analyses (above) and minimum chi square analyses (below) based on an underlying normal distribution with* $d/\sigma = 1$. *For most responses considered herein these two estimates differ negligibly.*

Second Part of Series	Δ for Test Series Whose First Part Is		
	O	OO	OOO
X	0.50 0.50	1.61 1.56	2.62 2.57
XO	0.84 0.73	1.89 1.76	2.89 2.76
XX	−0.18 −0.11	1.00 1.00	2.03 2.02
XOO	1.30 1.19	2.31 2.20	3.32 3.20
XOX	0.50 0.50	1.56 1.53	2.57 2.53
XXO	0.00 0.00	1.12 1.08	2.14 2.09
XXX	−0.81 −0.73	0.45 0.48	1.50 1.50
XOOO	1.84 1.74	2.85 2.74	3.85 3.74
XOOX	1.12 1.08	2.14 2.09	3.14 3.09
XOXO	0.70 0.63	1.74 1.65	2.74 2.66
XOXX	0.08 0.18	1.17 1.22	2.18 2.23
XXOO	0.31 0.33	1.37 1.37	2.38 2.37
XXOX	−0.31 −0.33	0.83 0.78	1.86 1.79
XXXO	−0.71 −0.71	0.50 0.50	1.54 1.52
XXXX	−1.44 −1.21	−0.10 −0.16	0.99 1.00

Results

Table 3 lists the results of maximum likelihood analysis based on the normal distribution with $d/\sigma = 1$. The right-hand column of this table also lists Dixon's value for the standard error of the estimate $\hat{S}_{50}$ (which is the square root of the error mean square given in Ref *4*). Thus, assuming that $2/3d < \sigma < 3/2d$, Table 3 suffices not only to estimate S_{50}, but, in addition, to compute a crude interval which is likely to trap this true median fatigue strength. However, without additional information regarding the magnitude of σ, this estimation process may not be adequate for the given research and development.

One way to introduce additional information regarding the location of S_{50} is to consider the influence of alternative assumptions on the magnitude of the resulting $\hat{S}_{50}$. If the effect of various alternatives is to change $\hat{S}_{50}$ negligibly relative to the accuracy required in its practical application, then there is no special estimation problem. If, on the other hand, the effect of various assumptions on $\hat{S}_{50}$ is to cause large changes in its value, then this "sensitivity" must be considered carefully in establishing the engineering estimate of the true median response. Table 7 lists the smallest and the largest of the twelve Δ values generated by the twelve alternative solutions enumerated above (see section on Scope). The range established by these two values provides a simple straightforward index to the sensitivity of the median response estimate to the assumptions underlying its computation. It appears that in certain applications the two values given will be identical for practical purposes, in which case either the average of the two entries in Tables 7 or 8 may be used to estimate S_{50}, or the normal maximum likelihood estimate for $d/\sigma = 1$ in Table 3 may be used. On the other hand, if the values listed in Table 7 differ markedly relative to the accuracy required for the given application, then a reliable estimate of the median response has not yet been obtained, and this problem should be duly noted in the appropriate report.

The formats of Tables 3, 6, 7, and 8 may easily be extended to cover test series whose first parts are either OOOO, OOOOO, OOOOOO, etc., or XXXX, XXXXX, XXXXXX, etc. In each case the entry given in the right-hand column is merely increased to account for the increased number of leading O's or X's. For example, if the entry for a test series whose first part is OOO equals 2.62, then the correct Δ value for a test series whose first part is OOOO equals 3.62. Moreover, OOOOO$\Rightarrow$ 4.62, OOOOOO$\Rightarrow$ 5.62, OOOOOOO$\Rightarrow$ 6.62, OOOOOOOO$\Rightarrow$ 7.62, etc.

For test series that start with X's, the corresponding Δ values are obtained from the given tables by (*a*) interchanging the X's and O's before entering the appropriate table, and then (*b*) setting the sign of Δ to minus its tabulated value.

Example

Estimate the fatigue limit for Wöhler's *S-N* data. Solution: from Table 3, interchanging X's and O's and changing the sign of Δ as tabulated, $\Delta = -7.62$ for Wöhler's response of XXXXXXXXO. Thus, $\hat{S}_F = 320 - 7.62 \times 20 = 167.6$ centners/zoll^2. Or, from Table 7, $\Delta_{max} = -7.47$ and $\Delta_{min} = -7.86$. Thus, $\hat{S}_{F,\,max} = 170.6$ and $S_{F,\,min} = 162.8$ centners/zoll^2.[3]

[3] On the basis of published large sample response data it appears that σ for Wöhler's tests is between 0.5 and 2.0 centners/zoll^2. Hence, Wöhler's d/σ is probably somewhere in the

Conclusions

The following conclusions may be drawn from the above analyses of small sample fatigue-limit response data: $\hat{S}_{50}$ values are not markedly influenced by the method of analysis, that is, by maximum likelihood analyses versus minimum chi square analyses. $\hat{S}_{50}$ values based on the symmetric normal and logistic response distributions differ negligibly for both maximum likelihood and minimum chi square analyses. However, the corresponding $\hat{S}_{50}$ values based on the skewed extreme value (smallest) response distribution may differ somewhat from the values pertaining to the symmetric normal and logistic response distributions. $\hat{S}_{50}$ values for all distribution functions and both methods of analysis may differ somewhat as d/σ changes from 2/3 to 3/2. These differences in magnitude are on the same order as those mentioned above. No distribution function, method of analysis, or d/σ ratio consistently yields either the largest or the smallest estimate of $\hat{S}_{50}$ for the small sample responses considered herein.

APPENDIX

Nonuniform Spacing

Tables 6 through 8 pertain only to uniform spacing of stimulus levels. For nonuniform spacing, iterative solutions must be used for all maximum likelihood analyses, as well as for the minimum chi square analyses pertaining to the normal and extreme value distributions. Only the minimum chi square analysis for the logistic function provides an explicit estimate of S_{50}, namely,

$$\hat{S}_{50} = -\frac{\sqrt{3}\hat{\sigma}}{2\pi}\log_e \left\{ \frac{\Sigma N_i p_i^2 \exp -\frac{\pi S_i}{\sqrt{3}\hat{\sigma}}}{\Sigma N_i q_i^2 \exp \frac{\pi S_i}{\sqrt{3}\hat{\sigma}}} \right\}$$

in which

$$p_i = \text{observed proportion failed at } S_i = R_i/N_i$$

and

$$q_i = 1 - p_i$$

Evaluating this expression for $\hat{\sigma}_{min} = S_{ult}/100$ and for $\hat{\sigma}_{max} = S_{ult}/30$ should suffice for steels to provide a reasonable range for the estimate $\hat{S}_{50}$.

range of 10 to 40. As plots of Δ versus d/σ are approximately horizontal for $d/\sigma > 3/2$, more accurate estimates of Δ_{max} and Δ_{min} could be taken as respectively -7.47 (maximum likelihood, extreme value, $d/\sigma = 3/2$) and -7.52 (maximum likelihood, normal, and maximum likelihood, logistic, each with $d/\sigma = 3/2$). However, d/σ in this example is so large that it is clear that all relevant solutions approach the limiting estimate $\Delta_{max} = \Delta_{min} = -7.50$. Hence, $\hat{S}_F$ for Wöhler's S-N data should be estimated as 170 centners/zoll^2.

References

[1] Dixon, W. J. and Mood, A. M., *Journal of the American Statistical Association*, JSTNA, Vol. 43, 1948, pp. 109-126.
[2] Vanderbeck, R. W., Wilde, H. D., Lindsay, R. W., and Daniel, C., *Welding Journal Research Supplement*, WLRVA, American Welding Society, Vol. 32, 1953, pp. 325s-332s.
[3] Brownlee, K. A., Hodges, J. L., Jr., and Rosenblatt, M., *Journal of the American Statistical Association*, JSTNA, Vol. 48, 1953, pp. 262-277.
[4] Dixon, W. J., *Journal of the American Statistical Association*, JSTNA, Vol. 60, 1965, pp. 967-978.
[5] Little, R. E., *Biometrika*, BIOKA, Vol. 55, 1968, pp. 578-579.

B. Mukherjee[1] *and D. J. Burns*[1]

Regression Models for the Effect of Stress Ratio on Fatigue Crack Growth Rate

REFERENCE: Mukherjee, B. and Burns, D. J., "Regression Models for the Effect of Stress Ratio on Fatigue Crack Growth Rate," *Probabilistic Aspects of Fatigue, ASTM STP 511*, American Society for Testing and Materials, 1972, pp. 43–60.

ABSTRACT: Regression models, based on linear elastic fracture mechanics, are used to interpret the effect of stress ratio on fatigue crack growth rate in 7075-T6 aluminum alloy. It is shown that fatigue crack growth rate can be related to range and maximum values of stress-intensity factor. Statistical techniques are used to examine the error which may accumulate when regression equations are used to predict crack growth versus cycles curves.

KEY WORDS: fatigue(materials), crack propagation, probability theory, regression analysis, stresses, stress analysis, statistical analysis, analysis of variance, tension tests, fracture(materials), stress concentration

Nomenclature

a	Half crack length
A, q	Coefficients of the Paris equation
b	Constant
B, j	Coefficients of Forman equation
C	Threshold stress intensity
ΔK	Range of stress intensity factor
K_{max}	Maximum stress intensity factor
K_{mean}	Mean stress intensity factor
K_C	Fracture toughness
m	Correction factor
n	Number of combinations of (da/dN, ΔK, K_{max})
N	Number of cycles
p	Number of coefficients in regression equation
r	Multiple correlation coefficient

[1] Postdoctoral fellow and professor of mechanical engineering, University of Waterloo, Ont., Canada.

R	$\sigma_{min}/\sigma_{max}$ or K_{min}/K_{max}
s	Standard error
SSR	Residual sum of squares
SSW	Residual sum of squares under a given hypothesis
V	Variable
W	Specimen width
σ_{max}	Maximum gross stress
σ_{mean}	Mean gross stress
$\phi_0, \phi_1, \phi_2, \phi_3$	Coefficients of regression equations

There have been numerous publications supporting the argument of Paris and Erdogan [*1*] that fatigue crack growth rate in an elastic structure is primarily a function of the range of the crack-tip stress intensity factor, ΔK. The Paris equation

$$\frac{da}{dN} = A(\Delta K)^q \tag{1}$$

and linear elastic stress analysis provide a straightforward procedure for estimating the influence of crack geometry and stress amplitude on crack growth rate.

It has been argued that Eq 1 is incomplete in that it does not allow for the effect of load ratio, R, and the instability which occurs when the maximum stress intensity factor, K_{max}, approaches the fracture toughness, K_C, of the material. To allow for these effects Forman et al [*2*] modified the Paris equation to

$$\frac{da}{dN} = \frac{B(\Delta K)^j}{(1 - R)K_C - \Delta K} \tag{2}$$

and reported excellent correlation with growth rate data for 7075-T6 and 2024 aluminum alloys. Hudson and Scardina [*3*] also found good correlation between Eq 2 and their very comprehensive growth rate data for 7075-T6 alloy.

However, neither of the aforementioned papers examined the error which may accumulate when Eq 2 is used to predict the crack growth versus cycles curve for a particular specimen. To obtain a measure of this error for Eq 2, it was necessary to reanalyze Hudson and Scardina's data. A set of experiments, chosen with a table of random numbers, is excluded from the regression analysis used to find the coefficients B and j. This set of experiments is then used to test the accuracy of Eq 2 as a predictor. A similar approach is used to assess other equations proposed for predicting the effects of stress ratio on fatigue crack growth.

Fatigue Crack Growth Data

Hudson and Scardina's specimens, 35 in. long by 12 in. wide, were cut from sheet with a nominal thickness of 0.09 in. Tension-compression loading was applied normal to a central, through-thickness notch, initially 0.1 in. long by 0.01 in. wide. The specimens were clamped between lubricated guides to prevent buckling and out-of-plane vibration. Crack growth was measured with a microscope and grids, photographically printed on the specimen.

Tests were conducted at 13 load (stress) ratios, ranging from -1.0 to 0.8. Several stress levels were investigated for each stress ratio. The mean and alternating loads (gross stress) were kept constant throughout each test. Each test was duplicated and an average crack growth curve derived. All of the data analyzed in this paper were obtained from these average curves.

To avoid any ambiguity arising from measurements taken in the early stages of crack propagation, this paper only considers crack growth measurements taken after the crack had grown to a 0.2-in. length. The slope of the straight line, connecting two consecutive points on the crack length versus cycles curve, was taken as the average crack growth rate at the middle point. The range (ΔK), mean (K_{mean}), and maximum (K_{max}) values of stress intensity factor quoted herein correspond to this middle point.

There was a transition from normal to shear mode cracking within the range of crack growth rate, da/dN, of 8.8×10^{-6} and 2.9×10^{-5} in./cycle. Of 290 combinations of ($\Delta K, K_{max}, R, da/dN$) used in this analysis, 30 have da/dN values within or below this transition range. This has been ignored since there was no discontinuity in the slopes of the log (da/dN) versus log (ΔK) curves at the fracture mode transition. Similar observations on fracture mode transition have been reported by Schijve [4] and Hertzberg [5].

Table 1 lists the 46 combinations of mean and semirange of gross stress investigated by Hudson and Scardina. Combinations 21 and 26 have not been considered because of the paucity of crack growth data and the high maximum stress relative to yield stress. Nine other combinations (see Table 1) were chosen using a table of random numbers. The data from these combinations were excluded from the regression analyses so that they could be used to test the regression equations.

Regression Equations for Fatigue Crack Growth Rate

When Hudson and Scardina used the method of least squares to fit Eq 2 to their data they assumed that "the compression portion of a loading cycle did not significantly affect fatigue crack growth." If the same approach is used to analyze only 35 of their 46 sets of data, Eq 2 can be written as

$$\frac{da}{dN} = \frac{10^{-14.36} (\Delta K)^{3.53}}{(1-R)K_C - \Delta K} \tag{3}$$

TABLE 1—*Summary of test program and life calculations.*

Specimen Number	Mean Stress[a]	Semirange of Stress	R	Cycles to Final Crack Length	Predicted Cycles to Final Crack Length Based on 95% Probability Limit	Actual Predicted
1	0	30	−1.0	900	300	3
2	0	25	−1.0	2 140	800	2.7
3	0	20	−1.0	5 430	1 600	3.4
4[b]	0	15	−1.0	15 300	5 500	2.8
5	0	10	−1.0	56 000	26 000	2.1
6	0	5	−1.0	646 000	380 000	1.7
7	2.5	20	−0.8	2 940	1 200	2.5
8	2.5	17.5	−0.8	6 720	2 000	3.3
9[b]	5	25	−0.7	1 285	500	2.6
10	2.5	15	−0.7	8 460	3 400	2.5
11	2.5	12.5	−0.7	16 300	7 000	2.3
12	5	20	−0.6	2 630	1 000	2.6
13	2.5	10	−0.6	27 000	15 000	1.8
14[b]	5	15	−0.5	6 900	2 600	2.7
15	10	20	−0.33	1 083	600	1.8
16	5	10	−0.33	17 900	8 500	2.1
17	2.5	5	−0.33	136 000	135 000	1.0
18	20	30	−0.2	98	80	1.2
19[b]	10	15	−0.2	3 280	1 800	1.8
20	15	20	−0.14	630	380	1.7
21[c]	25	25	0.0			
22	20	20	0.0	410	250	1.6
23	15	15	0.0	1 380	850	1.6
24[b]	10	10	0.0	7 100	5 000	1.4
25	5	5	0.0	62 000	68 000	0.9
26[c]	30	20	0.2			
27[b]	25	16.7	0.2	420	300	1.4
28	20	13.3	0.2	1 440	800	1.8
29	15	10	0.2	4 620	3 000	1.5
30	30	15	0.33	360	260	1.4
31	25	12.5	0.33	1 180	700	1.7
32[b]	20	10	0.33	2 900	1 800	1.6
33	15	7.5	0.33	5 450	3 700	1.5
34	10	5	0.33	28 400	27 000	1.1
35	30	10	0.5	1 760	900	2.0
36	25	8.3	0.5	3 400	1 900	1.8
37	20	6.7	0.5	5 900	3 600	1.6
38[b]	15	5	0.5	24 000	15 000	1.6
39	10	3	0.5	112 500	72 000	1.5
40	30	5	0.7	8 700	4 000	2.2
41	25	4.4	0.7	16 700	8 000	2.1
42	20	3	0.7	75 000	26 000	2.9
43	15	3	0.7	80 000	44 000	1.8
44	10	1.7	0.7	1155 000	300 000	3.9
45	30	3	0.8	42 500	11 000	3.9
46[b]	25	2.8	0.8	55 000	17 000	3.9

[a] All stresses in ksi.
[b] Tests excluded from regression analysis.
[c] Test not included in analysis.

where:

da/dN = in./cycle,
$K = \sigma\sqrt{\pi a}(W/\pi a \tan \pi a/W)^{1/2}$ psi $\sqrt{\text{in.}}$, and
$K_C = 40{,}000\sqrt{\pi}$ psi $\sqrt{\text{in.}}$

It should be noted that Hudson and Scardina defined K as $\sigma\sqrt{a}(W/\pi a \tan \pi a/W)^{1/2}$ so the coefficients in their equation differ from those in Eq 3. The ratio of da/dN predicted by Eq 3 to that predicted by Hudson and Scardina lies within the range 1.01 to 0.89 for ΔK, $(\sigma\sqrt{\pi a})$, between 2000 and 40,000 psi $\sqrt{\text{in.}}$

However, an examination of the raw experimental data casts doubt on the assumption that the compression portion of a loading cycle can be ignored. For example, Fig. 1 shows four of the average crack growth curves. The maximum stress in each case was 30 ksi. There is a systematic increase in the number of cycles required to propagate a crack to a given length, as the minimum load increases from −30 ksi to zero. In view of this, the 35 sets of data were

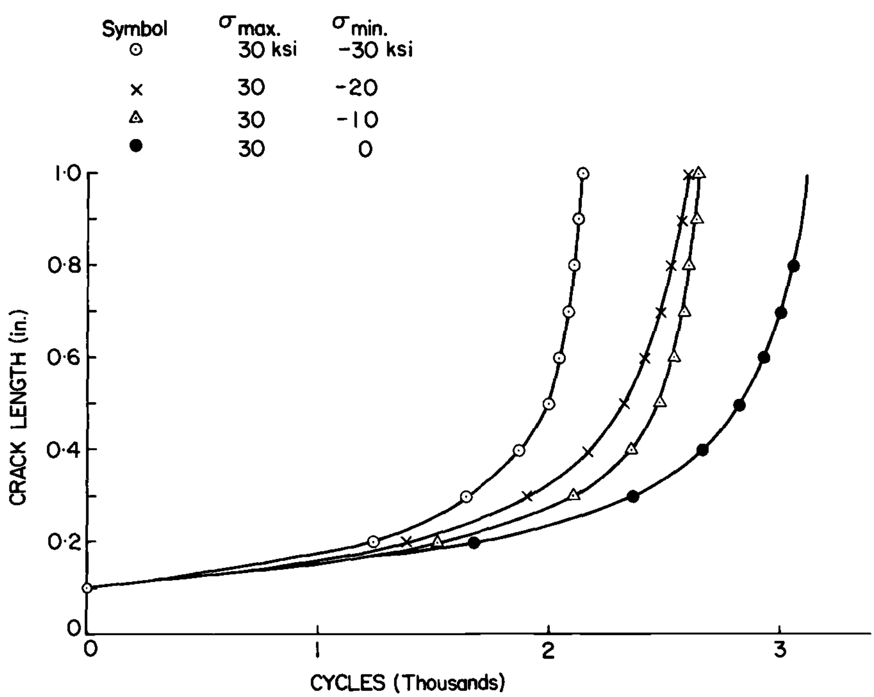

FIG. 1—*Effect of compression loading on crack growth.*

reanalyzed considering tension and compression loads. In this case Eq 2 becomes

$$\frac{da}{dN} = \frac{10^{-11.6}\,(\Delta K)^{2.79}}{(1 - R)K_C - \Delta K} \tag{4}$$

A more general form of Eq 2 is

$$\frac{da}{dN} = \theta_0(\Delta K)^{\theta_1}(V)^{\theta_2} \tag{5}$$

where

$$V = (1 - R)K_C - \Delta K \tag{6}$$

Regression analysis considering tension and compression loads and Eqs 5 and 6 then gives

$$\frac{da}{dN} = \frac{10^{-10.83}\,(\Delta K)^{2.98}}{[(1 - R)K_C - \Delta K]^{1.35}} \tag{7}$$

Table 2 lists the total, regression, and residual sums of squares for Eqs 3, 4, and 7. These and the degrees of freedom (df) have been used to calculate r^2, the square of the multiple correlation coefficient, and s, the standard error. Although Table 2 shows that Eqs 3, 4, and 7 are good fits to the experimental data it does not guarantee that a suitable model equation has been found [6]. Also there is no evidence that it is essential to include K_C directly in the crack growth equations. Forman included K_C in his equation to allow for the instability that occurs when K_{max} approaches K_C. An alternative approach is to put an "external" limit on K_{max}. An advantage of this approach is that it does not require a very accurate value of K_C. It is usually obvious from the shape of the crack length versus cycles curve that instability is very near.

TABLE 2—*Analysis of variance table.*

Equation Number	Total Sum of Squares (corrected)	df	Regression Sum of Squares	df	Residual Sum of Squares	df, ν	Proportion of Variation Explained by Regression Equation, r^2	Standard Error, s
3	238.92	289	220.41	1	18.51	288	0.9220	0.2535
4	238.92	289	223.97	1	14.95	288	0.9360	0.2278
7	238.92	289	228.65	2	10.27	287	0.9570	0.1891
8	238.92	289	226.23	2	12.69	287	0.9469	0.2103
10	238.92	289	226.27	3	12.65	286	0.9470	0.2103

Since ΔK and K_{mean} or ΔK and K_{max} fully define the loading state and crack geometry, it is logical to ask whether K_{mean} or K_{max} can be used instead of $[(1-R)K_C - \Delta K]$ in Eq 5.

If $V = K_{mean}$, data for $K_{mean} \leqslant 0$ cannot be considered. This is a serious limitation, so only $V = K_{max}$ [7,8] will be considered in this paper. Regression analysis then gives

$$\frac{da}{dN} = 10^{-21.07}(\Delta K)^{1.61}(K_{max})^{2.29} \tag{8}$$

Table 2 shows that Eq 8 gives as good a fit to the data as Forman's equation.

To use any of these regression equations as a predictor it is necessary to make certain assumptions about the residuals. In particular, the residuals are independent, follow a normal distribution, have zero mean, and a constant variance [6]. If the regression equation/model is reasonable, the residuals should exhibit tendencies that confirm these assumptions.

Figure 2 shows residual log da/dN plotted against observed log (da/dN) for Eq 8. The residuals are distributed randomly around zero over the full range of log da/dN. Figure 2*a* shows the residuals plotted as a histogram; they follow a normal distribution with zero mean. Therefore, Eq 8 will be used to estimate theoretical crack growth curves and associated probability limits for the nine sets of experimental data not included in the aforementioned regression analyses.

If $(da/dN)_i$ is fatigue crack growth rate calculated using Eq 8 and particular values $(\Delta K_i, K_{max_i})$ then $(1-\alpha)$ percent probability limits on $(da/dN)_i$ are

$$\left(\frac{da}{dN}\right)_i \pm t(\nu, 1 - \tfrac{1}{2}\alpha)\ [s^2 + m]^{1/2}$$

where $t(\nu, 1 - \tfrac{1}{2}\alpha)$ is obtained from a t distribution table for ν degrees of freedom on the residual sum of square (see Table 2); s is the standard error and m is the variance of $(da/dN)_i$.

To calculate a crack length versus cycles curve, it is assumed that $(da/dN)_i$ applies for a small increment of cycles ΔN. This gives a new value for crack length $2(a + \Delta a)$ and new values for ΔK and K_{max}. This iteration is repeated until the required life has been exceeded or an unstable crack length has been reached. The values of ΔN used were related to the frequency of experimental measurements in each test. It can be shown that small changes in ΔN do not significantly influence the predicted curves discussed below.

Figures 3 through 11 show, for Eq 8, predicted mean crack growth curves and curves based on 75, 85, and 95 percent probability limits on log da/dN. All nine experimental curves lie within these predicted limits. If the 95 percent limit had been used as the design limit for these nine specimens, the ratio of actual to

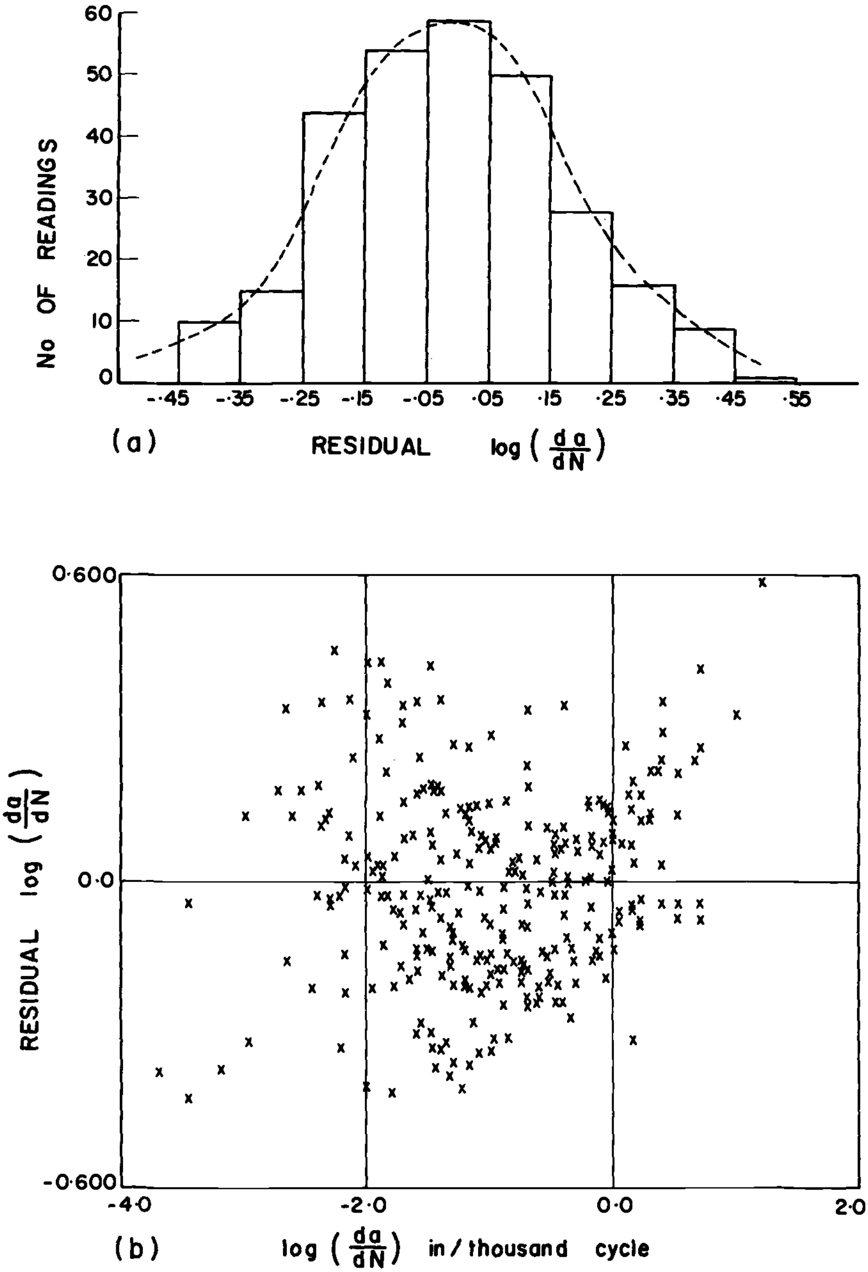

FIG. 2–*Distribution of residual log* da/dN *for Eq 8.*

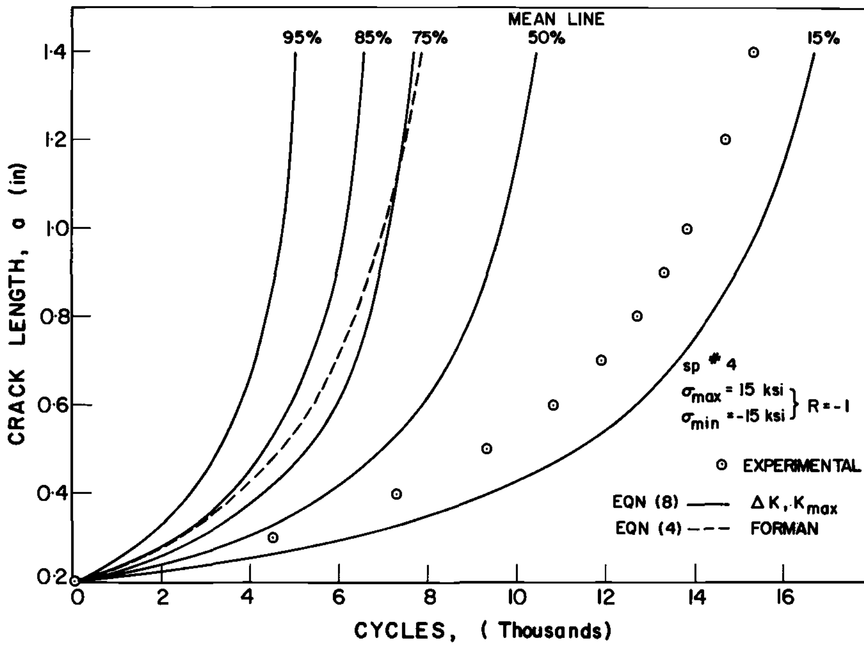

FIG. 3–*Experimental and predicted crack growth curves.*

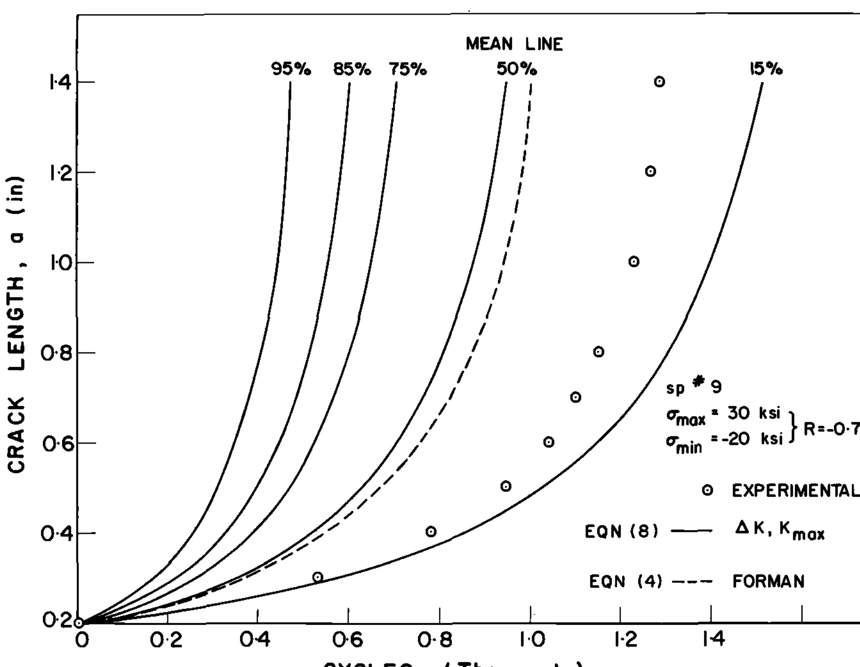

FIG. 4–*Experimental and predicted crack growth curves.*

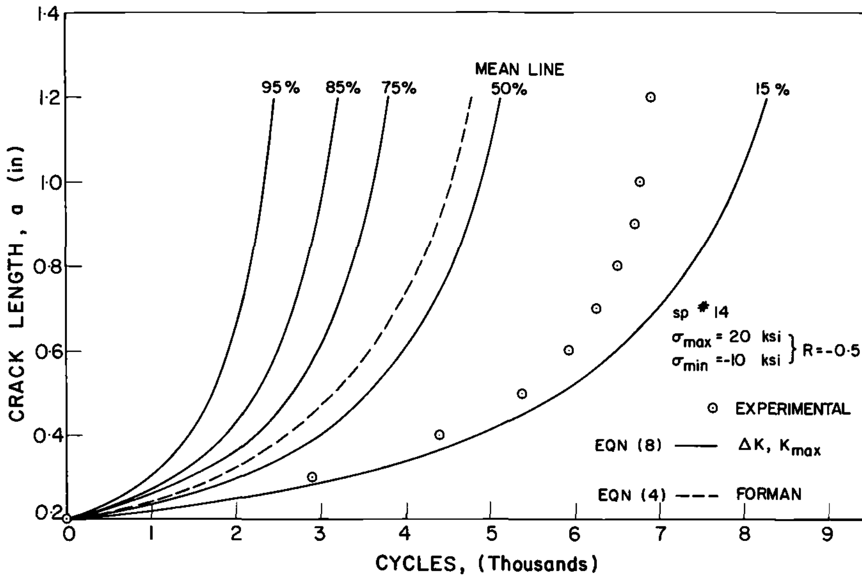

FIG. 5–*Experimental and predicted crack growth curves.*

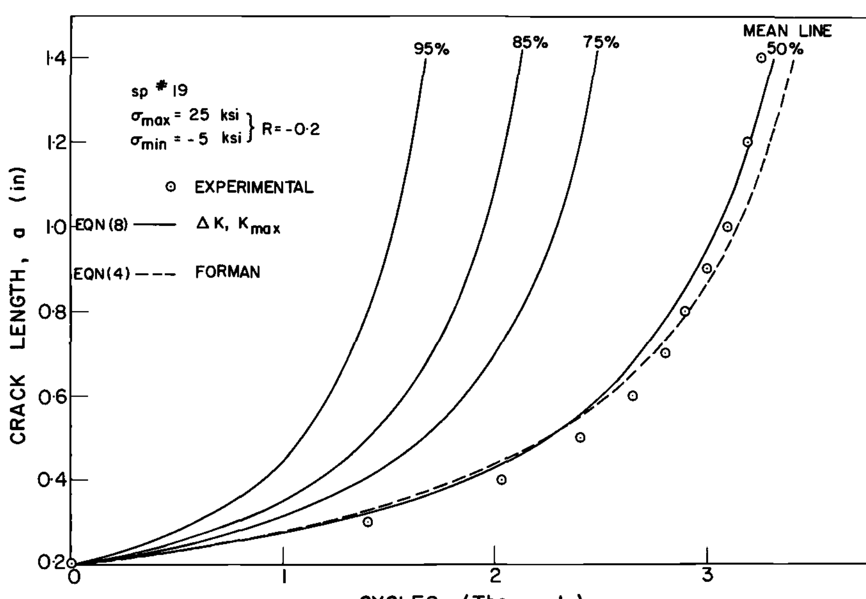

FIG. 6–*Experimental and predicted crack growth curves.*

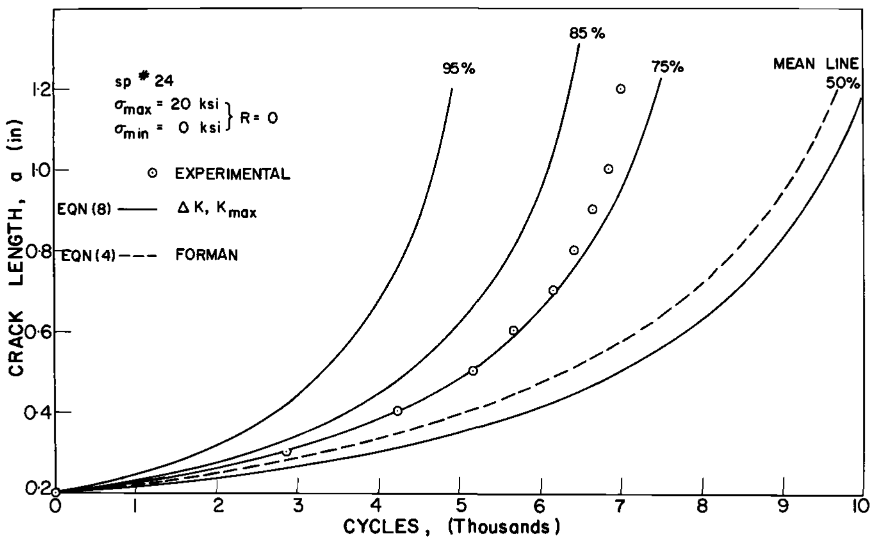

FIG. 7–*Experimental and predicted crack growth curves.*

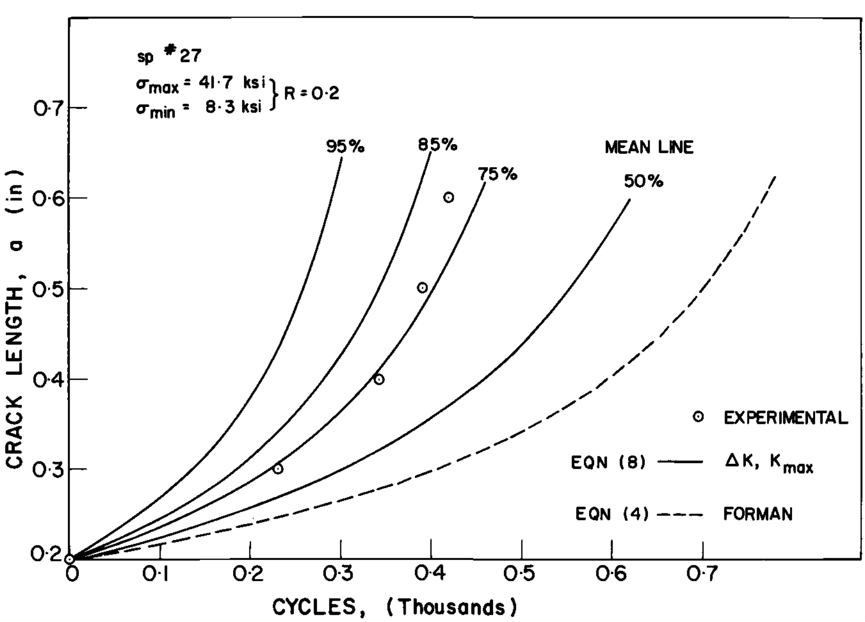

FIG. 8–*Experimental and predicted crack growth curves.*

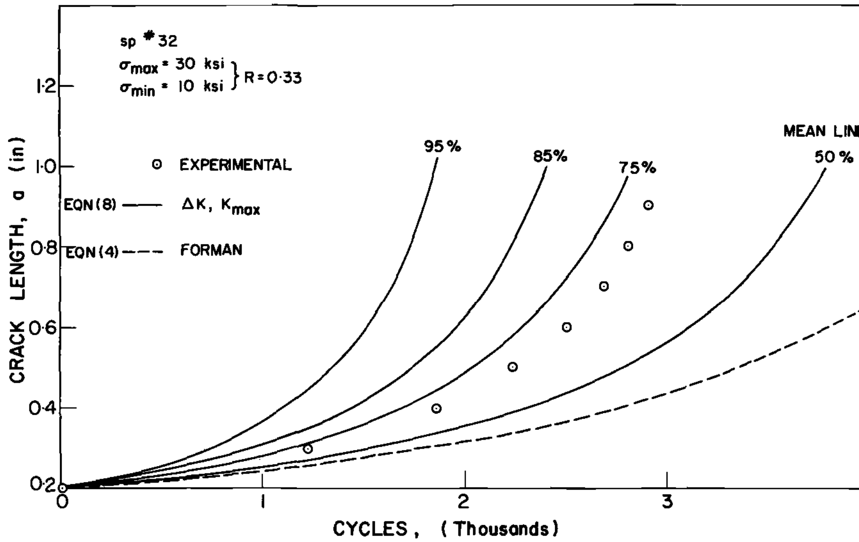

FIG. 9–*Experimental and predicted crack growth curves.*

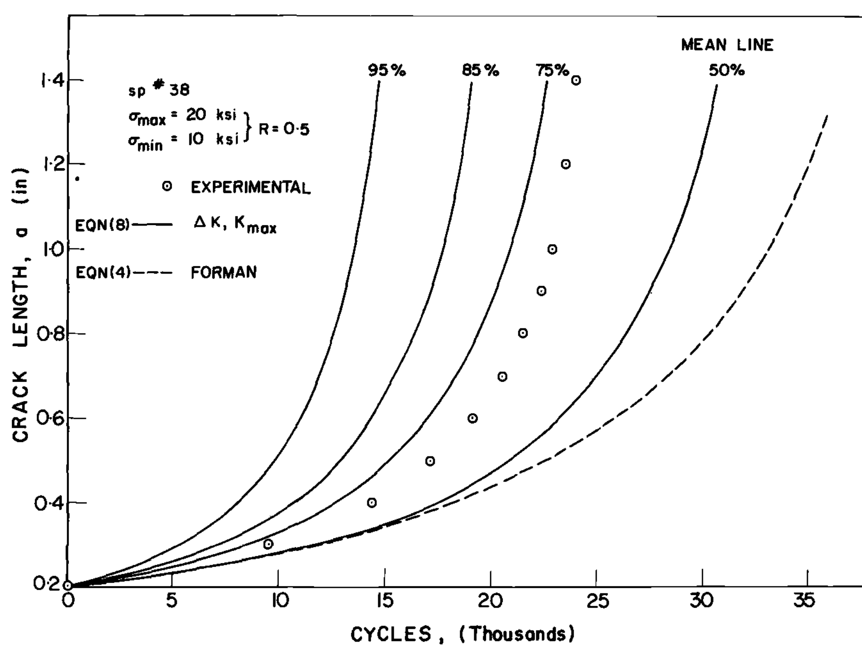

FIG. 10–*Experimental and predicted crack growth curves.*

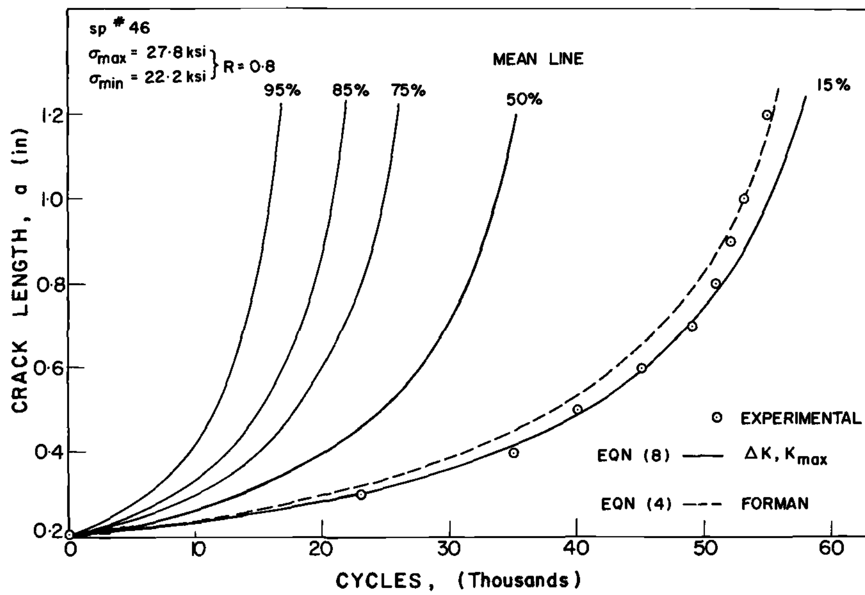

FIG. 11—*Experimental and predicted crack growth curves.*

predicted life would have varied between 1.4 and 3.9. If the mean line had been used as the design limit, the ratio of actual to predicted life would have varied between 0.7 and 1.5.

If the 95 percent probability limit and Eq 8 are used to predict the lives of the 35 specimens used in the derivation of Eq 8, the ratio of actual to predicted life varies between 0.9 and 3.9 (see Table 1). In only one test would this ratio have been less than 1.0.

Since the variance was uniform (see Fig. 2), these ratios of actual to predicted life show that it would have been necessary to design with lines at least two standard deviations below the mean log da/dN versus log ΔK lines. This of course is a well-known design procedure [*9*]. However, the inability of this equation to account for interaction effects, which are known to affect life significantly during variable-amplitude loading [*4*], leaves one in some doubt as to what factor of safety to use in the more general situation.

It can be shown that the residual log da/dN for Eq 4 are also distributed randomly around zero and follow a normal distribution with zero mean. Figures 3 through 11 also show the predicted mean crack growth curves for Eq 4; for convenience of illustration, probability limits are not shown for Eq 4. Since the standard error is of the same magnitude for Eqs 4 and 8 (see Table 2), Figs. 3 through 11 suggest that Eq 4 has little or no advantage over Eq 8 as a predictor. To generalize this conclusion it will, of course, be necessary to examine other materials and geometries.

In view of the large differences between experimental and predicted mean crack growth curves on the figures, it is instructive to examine the lack of fit between experimental and mean log *da/dN* predicted using Eqs 4 and 8. Figure 12 makes this comparison for a sample of the nine specimens excluded from the regression analyses. Figure 12 shows that the agreement between experiment and predicted mean log *da/dN* is reasonably good. A comparison of Figs. 12 and 3 through 11 emphasizes that large cumulative errors can occur when Eqs 4 and 8 are used in iterative calculations, which transform from logarithm to linear scale.

Both Eqs 4 and 8 predict that *da/dN* is zero when K_{max} is zero. It can be argued that *da/dN* may tend to zero when K_{max} is greater than zero. This concept of a "threshold" stress intensity, which must be exceeded for fatigue crack growth, can be examined by letting $V = K_{max} - C$ in Eq 5. Regression analyses were made for values of C, ranging from −60 to 4 ksi $\sqrt{\text{in.}}$ and the

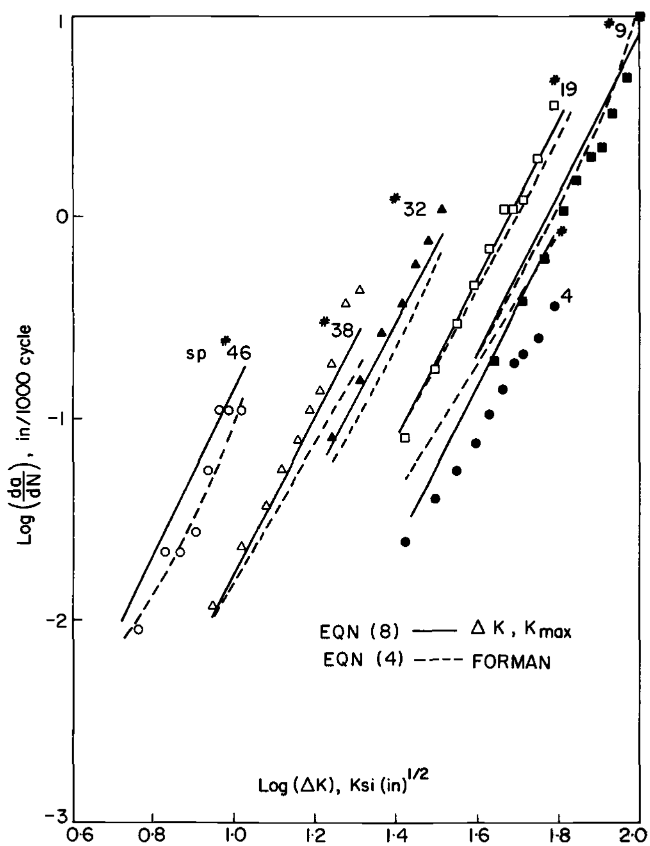

FIG. 12—*Experimental and predicted mean crack growth rate curves.*

residual sum of squares plotted against C, Fig. 13. Although the best fit is obtained when C is -30, any value of C between about -40 and -10 is acceptable. It must be emphasized that C is a mathematical parameter and that the physical "threshold" stress intensity can only be found by experiment. If this physical "threshold" stress intensity is known it can be used as an "external" limit on Eq 5, where $V = K_{max} - C$.

A somewhat different approach to the analysis of these fatigue data is to consider $(\Delta\sigma, \sigma_{max}, a)$ or $(\Delta\sigma, \sigma_{mean}, a)$ as the principal variables, that is, assume

$$\frac{da}{dN} = \phi_0 (\Delta\sigma)^{\phi_1} (\sigma_{max})^{\phi_2} a^{\phi_3} \tag{9}$$

Regression analysis then gives

$$\frac{da}{dN} = 10^{-19.97} (\Delta\sigma)^{1.60} (\sigma_{max})^{2.27} (a)^{2.04} \tag{10}$$

It can be shown that the residual log (da/dN)'s for this equation are distributed randomly about zero, have a constant variance, and follow a normal distribution with zero mean.

In deriving Eq 10 no reference has been made to linear elastic fracture

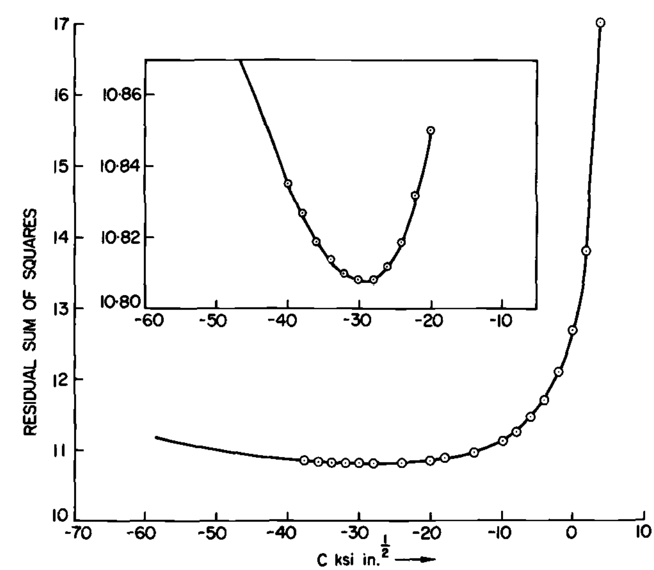

FIG. 13—*Estimation of "apparent" threshold stress-intensity factor.*

mechanics. If a linear elastic fracture mechanics approach is valid, there should be a linear relationship between the coefficients in Eq 10, namely

$$\phi_3 = \frac{\phi_1 + \phi_2}{2} \tag{11}$$

It can be shown (Table 2), for basic data, that the hypothesis $\phi_1 = \phi_2 = \phi_3 = 0$ is rejected [6]. Therefore, hypothesis testing [6] can be used to assess whether the relationship of Eq 11 holds for Eq 10. There are four coefficients (p), that is, ϕ_0, ϕ_1, ϕ_2, and ϕ_3, 290 (n) combinations of $[da/dN, \Delta\sigma, \sigma_{max}, a]$, and the residual sum of squares (SSR) is 12.6457. This sum of squares has $(n - p)$, that is, 286, degrees of freedom.

The hypothesis to be tested is

$$\phi_3 = \frac{\phi_1 + \phi_2}{b} \tag{12}$$

This provides one independent equation relating the coefficients if b is a known number. Substituting Eq 12 into Eq 9 gives

$$\frac{da}{dN} = \phi_0 [\ \Delta\sigma a^{1/b}]^{\phi_1} [\sigma_{max} a^{1/b}]^{\phi_2} \tag{13}$$

Regression analyses can be made for various values of b, each value of b giving a set of values for ϕ_0, ϕ_1, and ϕ_2. The residual sum of squares for these regressions (SSW) has $(n - p + 1)$ degrees of freedom. Since the errors are normally distributed and independent, the differences (SSW – SSR) are the sum of squares due to hypothesis, Eq 12, and have 287–286 degrees of freedom. To test the hypothesis, the ratio

$$F = \left(\frac{\text{SSW} - \text{SSR}}{287 - 286}\right) \bigg/ \frac{\text{SSR}}{(n - p)} \tag{14}$$

is compared with a value taken from a table of the F distribution. For a 95 percent level of significance, the F value with one degree of freedom for the numerator, and 286 degrees of freedom for the denominator is $F_{1,286;0.95} = 3.84$. When $b = 2$, SSW = 12.8099, and $F = 3.73$. Since $F < F_{1,286;0.95}$ the hypothesis $\phi_3 = (\phi_1 + \phi_2)/2$ is not rejected and, this analysis gives

$$\frac{da}{dN} = 10^{-20.08} (\Delta\sigma\sqrt{a})^{1.61} (\sigma_{max}\sqrt{a})^{2.28} (m)^{(1.61 + 2.28)} \tag{15}$$

where $m = 1$.

It can be shown that hypothesis (Eq 12) is not rejected for values of b between 1.8 and 2.0. When b = 1.8, the regression analysis gives

$$\frac{da}{dN} = 10^{-19.83}\left(\Delta\sigma\sqrt{a}(a)^{0.055}\right)^{1.59}\left(\sigma_{max}\sqrt{a}(a)^{0.055}\right)^{2.25}$$

This equation can be rewritten as

$$\frac{da}{dN} = 10^{-19.83}(\Delta\sigma\sqrt{a})^{1.59}(\sigma_{max}\sqrt{a})^{2.25}(m)^{(1.59+2.25)} \qquad (16)$$

where $m = a^{0.055}$.

The terms m = 1 and $m = a^{0.055}$ in Eqs 15 and 16 are analogous to the finite width correction factor $(W/\pi a \tan \pi a/W)^{1/2}$ used previously when examining Eqs 2-8. Figure 14 shows these quantities plotted against crack length, a. Since the finite width correction factor lies close to the envelope defined by m = 1 and $m = a^{0.055}$ it seems reasonable to conclude that Eqs 8 and 10 are related by Eq 11 and the finite width correction factor. If this were not the case, it would be difficult to justify using Eq 8 in preference to Eq 10 without a much more detailed comparison of their value as predictors.

Conclusions

The regression equation $da/dN = \theta_0(\Delta K)^{\theta_1}(K_{max})^{\theta_2}$ can be used to interpret fatigue crack growth data for 7075-T6 aluminum alloy sheet. The

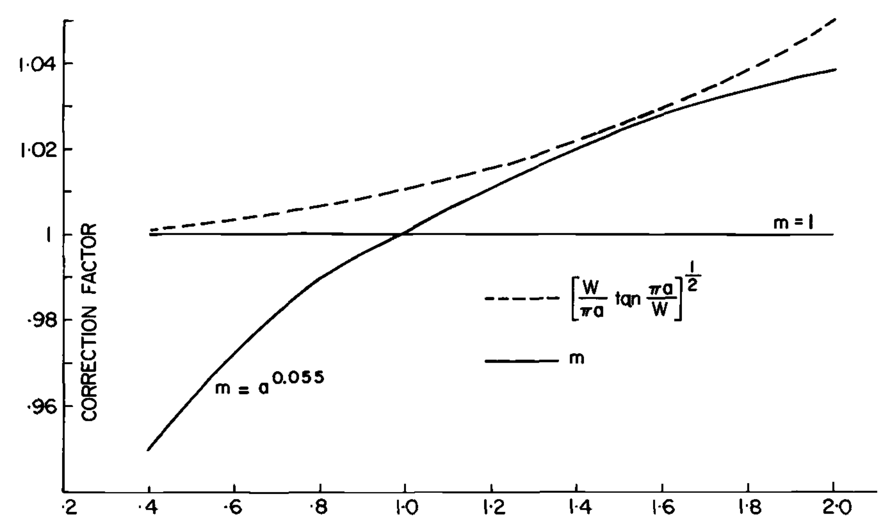

FIG. 14—*Comparison of least squares and finite width correction factors.*

predictions of this equation compare favorably with that of the equation proposed by Forman et al, that is, $da/dN = [B(\Delta K)^{j}] / [(1 - R)K_C - \Delta K]$. Since the first equation does not require a very precise knowledge of fracture toughness, K_C, it may be more useful to the designer.

Large cumulative errors can occur when these or other regression equations are used to predict crack growth versus cycles curves, that is, transformation from logarithm to linear scale and integration. If the residuals do not violate certain assumptions, these cumulative errors can be allowed for by using upper probability limits on fatigue crack growth rate.

Acknowledgments

This research was supported by a grant from the National Research Council of Canada. The analysis is based on experimental data obtained by C. M. Hudson and J. T. Scardina of NASA Langley Research Center. The advice of J. Mukherjee is gratefully acknowledged.

References

[1] Paris, P. and Erdogan, F., *Journal of Basic Engineering,* American Society of Mechanical Engineers, JBAEA, No. 4, Dec. 1963, pp. 528-534.
[2] Forman, R. G., Kearney, V. E., and Engle, R. M., *Journal of Basic Engineering,* American Society of Mechanical Engineers, JBAEA, Vol. 89, No. 3, Sept. 1967, pp. 459-464.
[3] Hudson, C. M. and Scardina, J. T., *Engineering Fracture Mechanics,* EFMEA, Vol. 1, No. 3, 1969, pp. 429-446.
[4] Schijve, J. in *Fatigue Crack Propagation, ASTM STP 415,* American Society for Testing and Materials, 1967, p. 415.
[5] Hertzberg, R. W., "Application of Electron Fractography and Fracture Mechanics to Fatigue Crack Propagation in High Strength Aluminum Alloys," Ph.D. thesis, Lehigh University, May 1965.
[6] Draper, N. R. and Smith, H., *Applied Regression Analysis,* Wiley, New York.
[7] Erdogan, F., *Crack Propagation Theories,* NASA CR, 901, National Aeronautics and Space Administration, 1967.
[8] Walker, K. in *Effect of Environment and Complex Load History on Fatigue Life, ASTM STP 462,* American Society for Testing and Materials, 1970.
[9] Raithby, K. D., *Journal of the Royal Aeronautical Society,* AENJA, Vol. 65, 1961, pp. 729-738.

G. H. Jacoby[1] *and H. Nowack*[2]

Comparison of Scatter Under Program and Random Loading and Influencing Factors

REFERENCE: Jacoby, G. H. and Nowack, H., "**Comparison of Scatter Under Program and Random Loading and Influencing Factors,**" *Probabilistic Aspects of Fatigue, ASTM STP 511,* American Society for Testing and Materials, 1972, pp. 61–74.

ABSTRACT: The paper deals with the scatter under program and random loading. For the explanation of the results, constant amplitude tests and tests with biharmonic loading are also included in the study. The basis of the comparison of the data is the logarithmic normal distribution and its parameters. It was found that scatter under program, random, and biharmonic loading is identical and is similar to the scatter derived in constant amplitude tests in the life range of about 10^5 load cycles. This is true for life as well as for crack propagation. Miner's rule overestimates the scatter, which occurs in tests simulating irregularly varying service loads. An important influence on scatter is due to the testing machine.

KEY WORDS: fatigue(materials), probability theory, probability distribution functions, crack propagation, crack initiation, reliability, loading, scattering, fatigue life, constant life fatigue diagrams, statistical analysis, fatigue tests, loads(forces)

A cumulative damage analysis is the foremost problem in estimating the fatigue life of structures, which encounter irregularly varying service loads. Such an analysis may include the following possible damage parameters: life, crack initiation time, crack propagation rate, residual strength, and failure location in complicated structures with several degrees of freedom for fracture. All these data are of a statistical nature, and their scatter must be included in fatigue life or reliability analysis.

An essential question is whether a distribution function such as a logarithmic normal or a Weibull distribution can be related to fatigue data. If a known

[1] Carl Schenck, GmbH, Darmstadt, Germany.

[2] Deutsche Forschungs- und Versuchsanstalt fuer Luft- und Raumfahrt e.V. (DFVLR), Institut fuer Werkstoff-Forschung, Porz-Wahn, Germany

distribution function applies to the data, the statistical treatment is very appropriate. This is, however, not just a question of curve fitting and extrapolation; a specific model of failure may belong to a certain distribution function. Such a model can be based, to a certain extent, on the behavior of real materials and may be described by the growth of a crack or the multiplication of the number of cracks by advancing slip lines, increasing weakness of grain boundaries, etc. So far, distribution functions and their validity describing fatigue behavior were checked mainly for constant amplitude loading. It is known, however, from cumulative damage studies, that many materials show pronounced interaction effects, with respect to the load sequence. For this reason, load sequence has to be included in a discussion concerning scatter of fatigue data.

In the present paper scatter under conventional 8-step program loading and digital random loading is dealt with. This treatment is based on a study of scatter and several influencing factors under constant amplitude loading for several damage parameters.

As an intermediate step between program loading and random loading on one side and constant amplitude loading on the other, biharmonic loading is also included. Biharmonic loading offers the possibility of studying cumulative damage effects in a clear and systematic manner.

Distribution Functions

There are several distribution functions that have been applied to fatigue data. However, the logarithmic normal and the Weibull distributions have been used most frequently. Both were found to be applicable to a wide range of materials and testing conditions. Moreover, within certain limits, there is no real difference between these distribution functions although they are based on different failure models[*1,2*]. Both models seem to be reasonable from a physical point of view for describing the fatigue process as it is known today. The Weibull distribution is more adjustable, because it has three free parameters, which are N_0, the minimum life parameter, N_a, the characteristic life parameter (up to N_a 63.2 percent of the population have failed) and b, the Weibull shape parameter. Runouts, which may occur near the fatigue limit, can also be included. The Weibull distribution is often preferred, because it leads to a realistic reliability analysis[*3*]. The logarithmic normal distribution is described fully by two parameters, which are very distinctive and enable an easy comparison of data from different test series. Besides that, a minimum life, $\bar{N}_0$, can also be incorporated into the logarithmic normal distribution. In this case the log $(N_i - N_0)$ values are normally distributed. Figure 1*a* and 1*b* show data from two groups of 77 constant amplitude fatigue tests, each fitted by a logarithmic normal and by a Weibull distribution. From the figure it can be concluded, that there is no reason to favor one of the distribution functions for

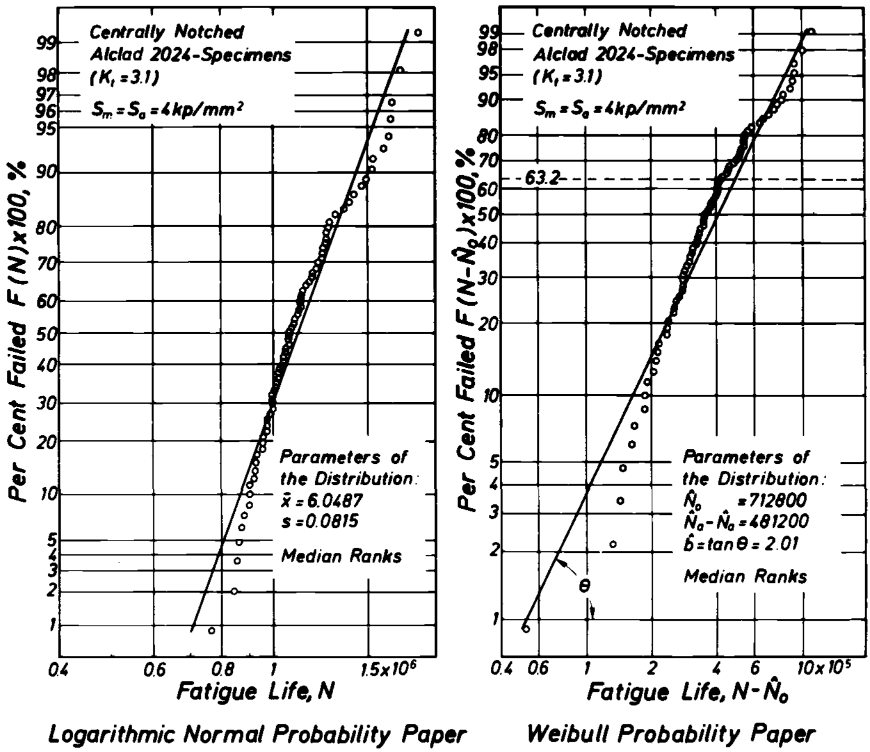

FIG. 1*a*–*Fatigue life data from constant amplitude tests with specimens taken from sheets in rolling direction.*

the representation of the data. Hence, because of the mentioned simplicity, the logarithmic normal distribution is used throughout this paper, to represent fatigue data. The fatigue behavior will be described by the sample arithmetic mean of the log-transformed life data

$$\bar{x} = \frac{1}{n} \sum_{i=1}^{n} \log N_i$$

and the sample standard deviation of the log-transformed life data

$$S = \sqrt{\frac{1}{n-1} \sum_{i=1}^{n} (\log N_i - \bar{x})^2}$$

which are sample estimates for the respective data of the population.

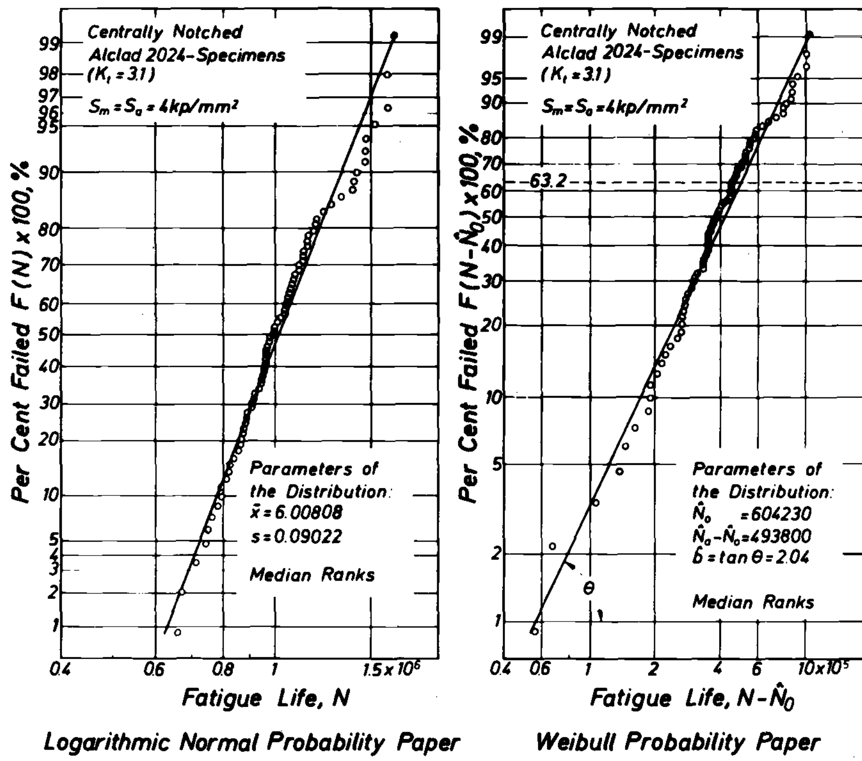

FIG. 1*b*–*Fatigue life data from constant amplitude tests with specimens taken from sheets transverse the rolling direction.*

Factors Influencing Scatter

As can be seen from many studies, the scatter under constant amplitude loading is influenced by many factors. These are: type of material and its condition; type of loading; size and shape of a specimen or structure; and the environment. The damage parameter considered probably influences the resulting scatter also. It should be noted, that the scatter is also a function of mean stress and amplitude (see for instance Ref *4*). Figure 2 shows *S-N* curves and the respective scatterband for a certain life range. This life range has been chosen because a correlation may exist between the scatter from constant amplitude and program loading [*4-6*].

Figure 2 shows that the scatter below about 10^5 load cycles to failure is nearly constant and independent of stress. Therefore, it can be concluded that the life is the dominant factor on scatter and not stress, although both are correlated. The data, shown in Fig. 2, were also evaluated for crack propagation. Considered were the numbers of load cycles N_f required to grow a crack from a

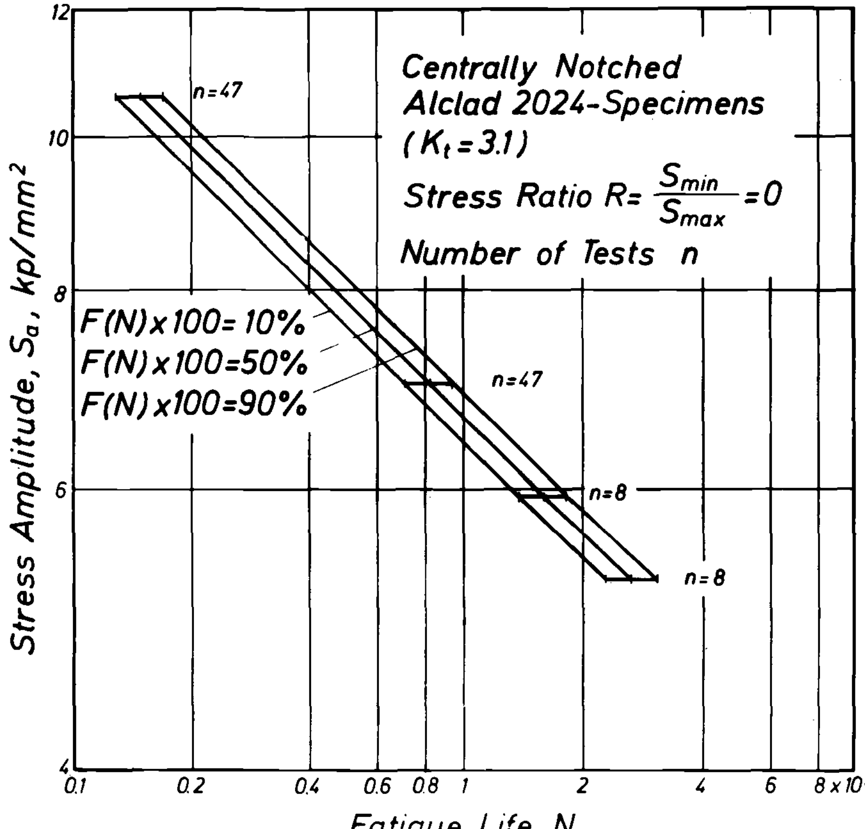

FIG. 2–S-N *curves for a stress ratio* R = 0, S_{max} = *constant and different probabilities of failure.*

length of $l = 0.5$ mm to the critical crack length l_f at final failure. N_f may be defined as the macrocrack propagation stage of the whole fatigue process. The scatter data for the crack propagation stage are compiled in Table 1. Also shown are the scatter values for the total fatigue life as derived from Fig. 2 and other constant amplitude tests. A comparison leads to the conclusion that scatter in both cases is very similar for fatigue lives $\leqslant 10^5$ load cycles. It has to be considered, however, that the confidence in crack propagation stage data is somewhat limited because of some experimental difficulties involved in measuring the $N_{l\,=\,0.5\text{ mm}}$ values. The similarity between the scatter of life and crack propagation data is documented in the literature also [7-9]. There an increasing scatter was often found with decreasing stress. In the present study the scatter for the crack propagation stage was found to be independent of stress, because it is formed by the scatter for life until a crack length of

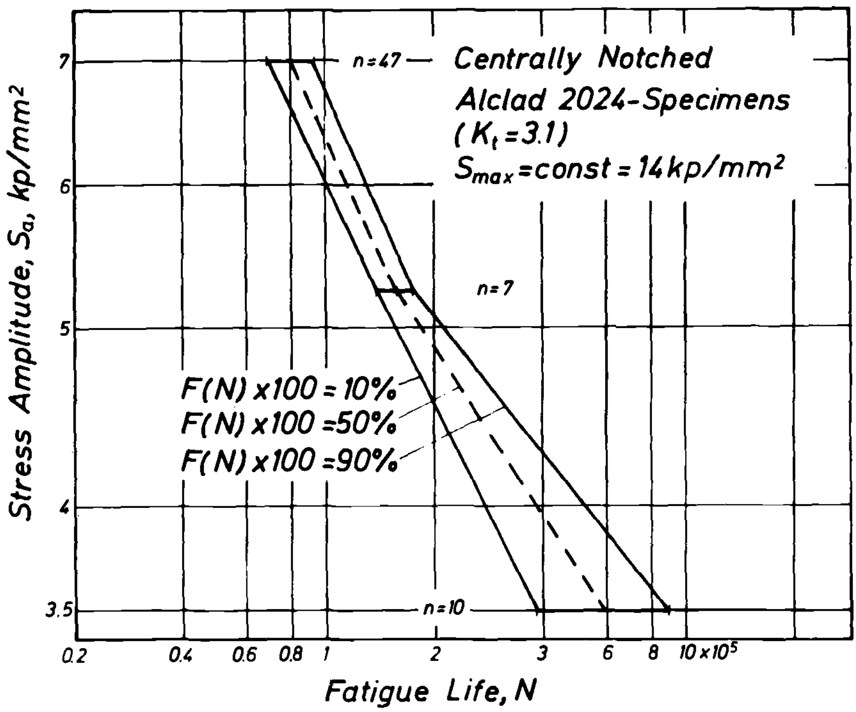

FIG. 2—*Continued.*

TABLE 1—*Parameters of the distributions of total fatigue life and crack propagation stage as derived from Fig. 2 and other constant amplitude tests (centrally notched Alclad 2024-specimens,* K_t = *3.1).*

Stress Amplitude, S_a kp/mm²	Stress Ratio $R = \frac{S_{min}}{S_{max}}$	Range of Total Fatigue Life [F(N) x 100 = 50%]	Parameters of the Distributions of Total Fatigue Life		Parameters of the Distributions of N_f (Crack-Propagation Stage)	
			$\bar{x}$	s	$\bar{x}$	s
14.0	-1	$N < 10^5$	4.229	0.043	—	—
14.8	-1	$N < 10^5$	—	—	3.837	0.046
4.13	0	$N > 10^5$	5.945	0.090	4.681	0.041
7	0	$N < 10^5$	4.905	0.0497	—	—
8.25	0	$N < 10^5$	4.623	0.0485	3.426	0.059
10.6	0	$N < 10^5$	4.171	0.0473	—	—
5.25	0.25	N near 10^5	5.193	0.042	—	—
6.2	0.25	N near 10^5	—	—	3.663	0.043
3.5	0.5	$N > 10^5$	5.769	0.137	—	—
4.13	0.5	$N > 10^5$	—	—	4.112	0.040

$l = 0.5$ mm is reached. If these data change in the same manner, the crack propagation stage must not be influenced. The physical explanation for this effect may be that the behavior of a crack of $l = 0.5$-mm length is already governed by stress and strain considerations on a macroscopic scale. The stress-strain field around the crack tip is responsible for crack propagation as well as for the residual strength and is relatively independent of the microstructural details in a material. The crack initiation stage, which here is arbitrarily defined by the number of load cycles till a crack of $l = 1\ \mu$ has formed, would probably show a much higher scatter. This statement, however, has not been proved up to now because of experimental difficulties.

Biharmonic Loading

A biharmonic load-time function is generated by the superposition of two sine waves with different frequencies, phase angles, and amplitudes. For studying fatigue damage accumulation, biharmonic load-time functions with frequency ratios of the two sine waves of 2:1 and phase angles of $-\pi/4$ or $+\pi/4$ are very appropriate. They enable the explicit study of the influence of sequence effects as caused by two consecutive load cycles with different amplitudes and mean stresses. A biharmonic load generation system and the definitions for biharmonic load traces are described elsewhere [*10,11*].

As can be seen, the scatter occurring in biharmonic tests does not differ much from the scatter in constant amplitude tests with the same load range $|S_{max} - S_{min}|$[3] and the same mean load. At first glance this is astonishing, since the scatter in constant amplitude tests with the amplitude and mean load of the smaller load cycles within the biharmonic load cycles is higher (see Fig. 2 and Table 1).

The described results of tests with biharmonic loading lead in a straightforward manner to the conclusion that the scatter in fatigue tests with varying amplitudes is determined mainly by the highest load range and mean load within the load-time function. An explanation for this fact may proceed from the idea that, to a certain extent, high loads eliminate differences in local stress concentrations. The given explanation could be verified in low cycle fatigue tests, where the stress-strain behavior was measured with a special pick-up at the notch root. Figure 3 shows typical examples of hysteresis loops as derived from a biharmonic and a constant amplitude test. It is seen that there is no difference in the overall appearance, which means that the plastic deformation behavior must be identical.

In Table 2 data are listed for the scatter within the crack propagation stage as already defined. The scatter seems to be somewhat higher than for the total life data, but this may be due to the already mentioned uncertainties in measuring $N_{l\,=\,0.5\ mm}$.

[3] See Table 2.

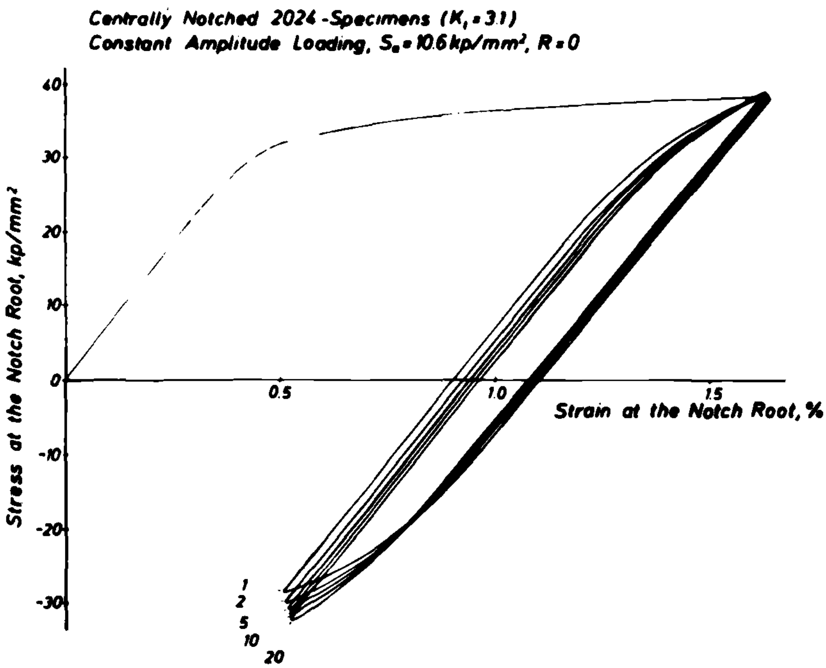

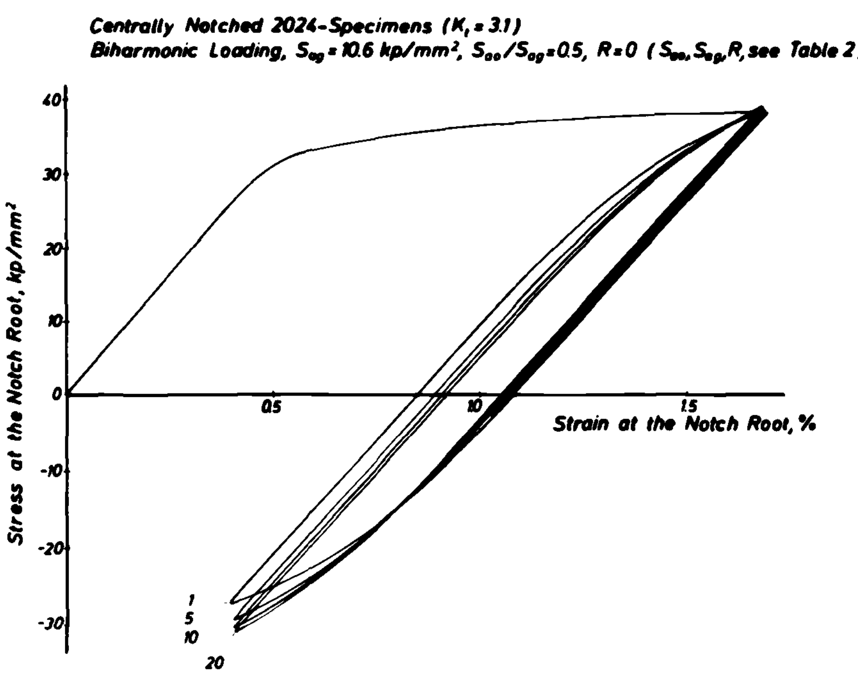

FIG. 3–*Hysteresis loops as derived from tests with constant amplitude loading and biharmonic loading.*

TABLE 2–*Parameters of the distributions of total fatigue life and crack propagation stage as derived from tests with biharmonic loading (centrally notched Alclad 2024-specimens,* $K_t = 3.1$*).*

Biharmonic Loading, Definitions	Stress Ratio	Amplitude Ratio	Parameters of the Distributions of the Total Fatigue Life $S_{max} = 14$ kp/mm² $\bar{x}$	s	Parameters of the Distributions of N_f (Crack Propagation Stage) $S_{max} = 16.5$ kp/mm² $\bar{x}$	s
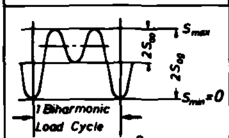 Amplitude Ratio: $\frac{S_{ao}}{S_{ag}}$ Stress Ratio: $\frac{S_{min}}{S_{max}}$	0	$\frac{S_{ao}}{S_{ag}} = 0.25$	4.832	0.043	3.382	0.058
	0	$\frac{S_{ao}}{S_{ag}} = 0.5$	4.756	0.048	3.296	0.049
	0	$\frac{S_{ao}}{S_{ag}} = 0.75$	4.608	0.047	3.125	0.061
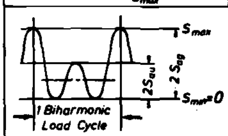 Amplitude Ratio: $\frac{S_{au}}{S_{ag}}$ Stress Ratio: $\frac{S_{min}}{S_{max}}$	0	$\frac{S_{au}}{S_{ag}} = 0.25$	4.909	0.045	3.408	0.060
	0	$\frac{S_{au}}{S_{ag}} = 0.5$	4.878	0.031	3.397	0.057
	0	$\frac{S_{au}}{S_{ag}} = 0.75$	4.802	0.042	3366	0.046
	0	$\frac{S_{ao}}{S_{ag}} = \frac{S_{au}}{S_{ag}} = 0$	4.905	0.0497	3.426	0.059
	0	$\frac{S_{ao}}{S_{ag}} = \frac{S_{au}}{S_{ag}} = 1$	4.611	0.046	2.891	0.052

Cumulative Damage Hypotheses

An essential question in estimating cumulative damage effects, and particularly fatigue life, is the applicability of a cumulative damage hypothesis. Most studies dealing with this problem included scatter by summing up the damage ratios derived for a constant probability of survival. This method, however, leads to an overestimation of scatter, because the latter, as already described, is determined by the highest load amplitudes. An example to support this statement is shown in Fig. 4. The lives from biharmonic tests with an amplitude ratio of $S_{ao}/S_{ag} = 0.5$ and a calculated life distribution for the same loading condition using the Palmgren-Miner hypothesis are plotted. The higher scatter of the calculated distribution is due to the high scatter of the fatigue life data in constant amplitude tests with the same load range and mean load as the smaller load cycle within the biharmonic load cycle (see Fig. 2 and Table 1).

Scatter Under Program and Random Loading

Cumulative damage fatigue life analysis (or the analysis of any other damage parameter) is often performed in program tests or by the application of a cumulative damage hypothesis. As a more recent method random testing, which simulates real service conditions more closely, has to be considered also. There

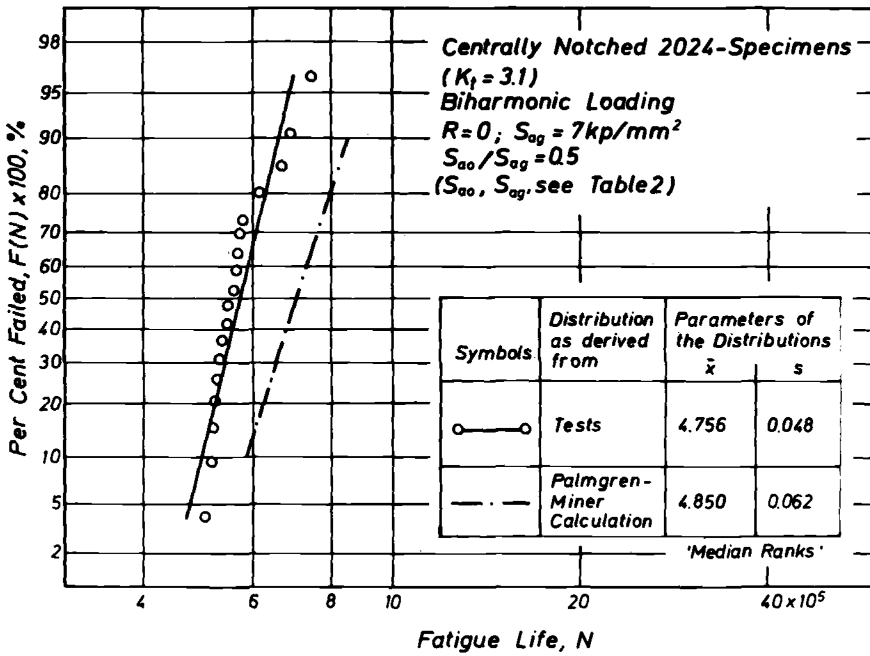

FIG. 4–*Fatigue-life distributions as derived from tests with biharmonic loading and as calculated by the Palmgren-Miner hypothesis.*

are, however, still several reasons which favor the application of program tests or of a cumulative damage hypothesis [*12*]. Because of these reasons, several studies were performed to check the accuracy of the different methods and to compare the results. There are many influencing factors, which can lead to different cumulative damage analyses [*12-14*]. The main factor, however, seems to be the type of load spectrum. So far, nearly all studies performed dealt with fatigue life and crack propagation, and the sample means were compared. But nearly nothing is known about the scatter under program and random loading or by using a cumulative damage hypothesis, respectively.

In Figure 5 the results of program and random tests are shown. The data stem from tests with digital random and conventional 8-step program loading. The basis for these tests is described elsewhere [*12-15*]. Figure 5 shows that though there is a pronounced difference in life, which can be attributed to interaction effects, there is nearly no difference in scatter. This fact supports the statement already made, that scatter depends mainly on the highest load range occurring in a load-time function. In the present study the influence of the stress level on scatter under program or random loading was not considered. According to several other studies, however, the scatter under program loading is nearly constant for a large range of stress levels and lives. This is in contrast to the

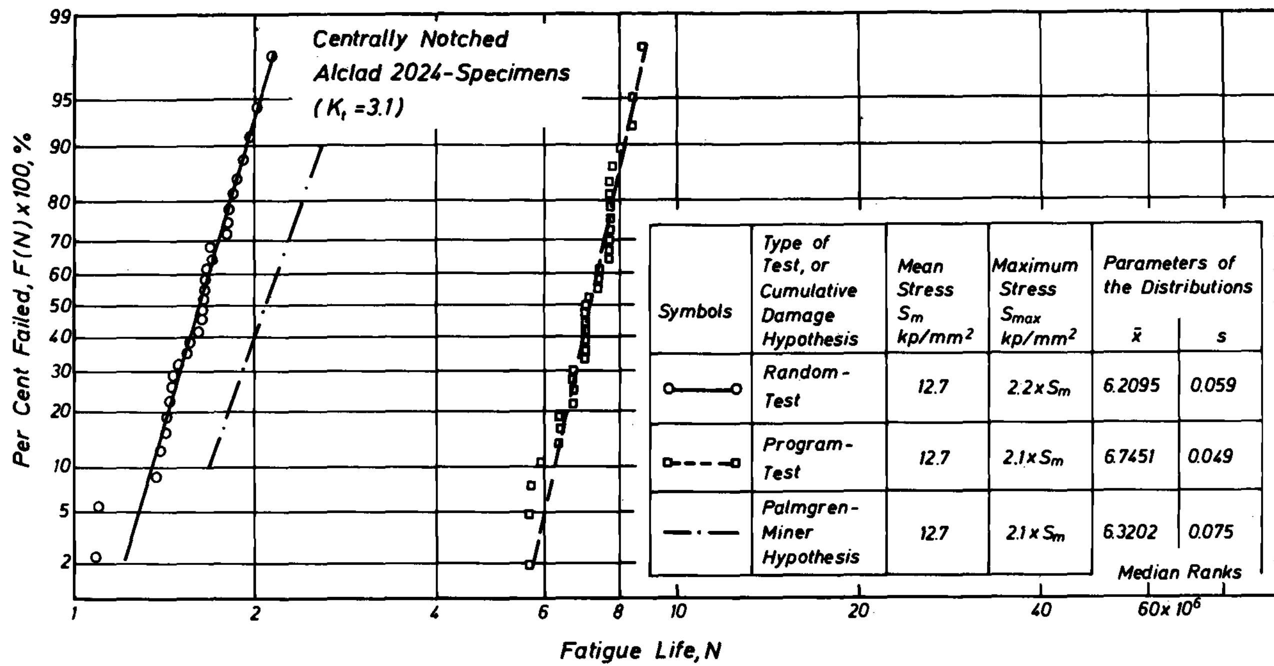

Symbols	Type of Test, or Cumulative Damage Hypothesis	Mean Stress S_m kp/mm²	Maximum Stress S_{max} kp/mm²	Parameters of the Distributions $\bar{x}$	s
o———o	Random-Test	12.7	$2.2 \times S_m$	6.2095	0.059
□- - - -□	Program-Test	12.7	$2.1 \times S_m$	6.7451	0.049
—·—	Palmgren-Miner Hypothesis	12.7	$2.1 \times S_m$	6.3202	0.075

FIG. 5—*Fatigue-life distributions as derived from random tests and program tests and as calculated by the Palmgren-Miner hypothesis.*

behavior of scatter along an *S-N* curve for constant amplitude loading and higher fatigue lives (above 10^5 load cycles). The present study also confirms many results mentioned in the literature that scatter under constant amplitude loading in a life range below about 10^5 load cycles is about the same as the scatter under program or random loading (see for instance [*4-6*]). The life distribution as calculated by the Palmgren-Miner hypothesis is also shown in Fig. 5. The scatter of this distribution is higher than the scatter as derived from program or random tests. This is again a result of the increasing scatter along an *S-N* curve. A similar result was also mentioned in Ref *16*.

Influence of Testing Machine

In all the considerations so far the scatter caused by the testing machine or installation has been neglected. This, however, may be an important influence [*17-19*]. The scatter caused by the testing machine can be attributed to many factors, for instance to misalignment of specimens due to careless clamping, to errors in the load-measuring system, to deviations in the control circuit, to faulty cycle counters, or simply to the various skills of different persons handling a machine. In Fig. 6 data are shown from program tests with a servohydraulic testing machine. For the tests an 8-step program has been used, which exhibits a variation in load amplitudes of 1:10 (see for instance Ref *12* and a frequency range of 1:50 Hz. In one case the data exhibit a high scatter, in the other the scatter is much less. In the case with the higher scatter, the

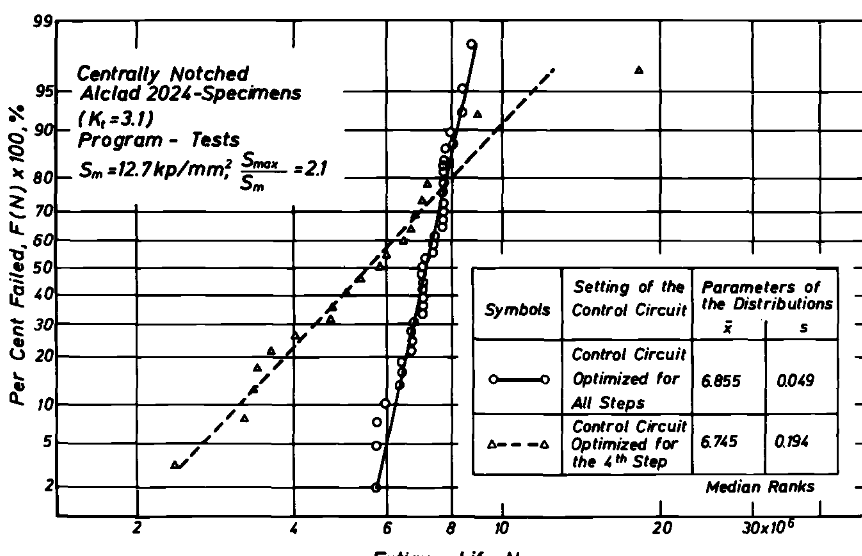

Symbols	Setting of the Control Circuit	Parameters of the Distributions $\bar{x}$	s
o——o	Control Circuit Optimized for All Steps	6.855	0.049
Δ- - -Δ	Control Circuit Optimized for the 4th Step	6.745	0.194

FIG. 6–*Scatter in program tests as influenced by the setting of the control circuit of a closed loop servohydraulic testing machine.*

machine-control circuit has always been optimized in step 4 of the 8-step program. For this step the combined error (control and measuring) was less than 1 percent. In all other steps the error could be higher. This method of optimization is often used in program testing.

In the second series of program tests, which show a much lower scatter, the machine was optimized carefully for all steps during the tests. This led to an error of less than 1 percent in all steps. This optimization may be performed by means of a computer in a more effective manner.

Conclusions

For a comparison of fatigue data derived under different testing conditions, it is convenient to apply the logarithmic normal distribution with its main parameters: arithmetic mean and standard deviation of the log-transformed cycle lives. This is valid for a finite life range only.

The scatter is influenced by many factors such as material, material processing, geometric shape, type of loading, environment, and the damage parameter under consideration. Especially important are mean stress and amplitude and the life range.

For constant amplitude tests the scatter in life and crack propagation rate is similar. This holds also for biharmonic loading.

Biharmonic loading is an appropriate method for studying the accumulation of damage under consecutive load cycles with varying amplitudes and mean stresses. The scatter under biharmonic loading is nearly identical with the scatter in constant amplitude tests, if the constant amplitude tests are run with the same total load range as the total load range of the biharmonic loading. That means that the scatter under variable amplitude loading is determined mainly by the highest load level.

The scatter under program and random loading was found to be nearly identical with the scatter in constant amplitude tests in the life range of about 10^5 load cycles.

The results mentioned in the preceding two paragraphs lead to the conclusion, that the scatter in variable load tests of any kind is determined by the highest loads.

The application of the Palmgren-Miner hypothesis overestimates scatter.

In all studies on scatter, the influence of the testing installation has to be considered.

For the performance of a reliability analysis for structures subjected to irregularly varying service loads, the standard deviation of the log-transformed cycle lives of the population should be known. Instead, an estimated standard deviation has to be used, which can be derived from program or random tests [*7,20*]. From the present test results it is seen that an estimate for the standard deviation can be derived from program as well as from random tests.

References

[1] Gertsbakh, I. B. and Kordonskij, Kh. B. in *Engineering Science Library*, Springer-Verlag, Berlin, 1969.
[2] Freudenthal, A. M. and Gumbel, E. J., *Advances in Applied Mechanics*, AAMCA, Vol. 4, 1956, pp. 117-158.
[3] Freudenthal, A. M. and Shinozuka, M., "Structural Safety Under Conditions of Ultimate Load Failure and Fatigue," Wadd Technical Report 61-177, Aeronautical Systems Division, Oct. 1961.
[4] Schijve, J. in *Full-Scale Fatigue Testing of Aircraft Structures*, F. J. Plantema and J. Schijve, Eds., Pergamon Press, London, 1961, pp. 41-59.
[5] Schijve, J. and Jacobs, F. A., "Program-Fatigue Tests on Notched Light Alloy Specimens of 2024 and 7075 Material," NLL-Report M 2070, National Lucht- en Ruimtevaartlaboratorium, Amsterdam, 1960.
[6] Gassner, E. and Schütz, W. in *Full-Scale Fatigue Testing of Aircraft Structures*, F. J. Plantema and J. Schijve, Eds., Pergamon Press, London, 1961, pp. 14-40.
[7] Schijve, J. and Jacobs, F. A., "Fatigue Crack Propagation in Unnotched and Notched Aluminum Alloy Specimens," NLR-TR M. 2128, National Lucht- en Ruimtevaart-laboratorium, Amsterdam, 1964.
[8] Gassner, E. and Jacoby, G., *Luftfahrttechnik-Raumfahrttechnik*, LTRTA, Vol. 10, 1964, pp. 6-20.
[9] Barrois, W. G., "Manual on Fatigue of Structures," AGARD-MAN 8-70, NATO Advisory Group for Aerospace Research and Development, 1970.
[10] Nowack, H., *Fortschritt-Berichte VDI-Z*, FBVBA, Reihe 5, No. 7, 1969, pp. 91-114.
[11] Nowack, H., "Ein Beitrag zur Untersuchung der Schadensakkumulation auf der Grundlage biharmonischer Belastungsabläufe," DLR Forschungsbericht 71-23, Abteilung Wissenchaftliches Berichtswesen der Deutschen Forschungs- und Versuchsanstalt für Luft- und Raumfahrt E. V., Ed., Porz-Wahn, 1971.
[12] Jacoby, G. in *Proceedings*, Third Conference on Dimensioning and Strength Calculations, Hungarian Academy of Sciences, 1968, pp. 81-95.
[13] Jacoby, G. in *Effect of Environment and Complex Load History on Fatigue Life, ASTM STP 462*, American Society for Testing and Materials, 1970, pp. 184-202.
[14] Jacoby, G., *Fortschritt-Berichte VDI-Z*, FBVBA, Reihe 5, No. 7, 1969, pp. 63-90.
[15] Jacoby, G., *Zeitschrift für Flugwissenschaften*, ZEFLA, Vol. 18, 1970, pp. 235-258.
[16] Gassner, E., Griese, F. W. and Haibach, E., *Archiv für das Eisenhüttenwesen*, AREIA, Vol. 35, 1964, pp. 255-267.
[17] Weibull, W., *Fatigue Testing and Analysis of Results*, Pergamon Press, London, 1961.
[18] Heywood, R. B., *Design against Fatigue*, Chapman and Hall Ltd., London, 1962.
[19] Jacoby, G., "Prüfmaschinen für metallische Werkstoffe," *International RILEM-Symposium*, Stuttgart, Germany, 1968, DVL-Bericht Nr. 865.
[20] Haibach, E., *Luftfahrttechnik-Raumfahrttechnik*, LTRTA, Vol. 13, 1967, pp. 188-193.

Sigge Eggwertz [1]

Investigation of Fatigue Life and Residual Strength of Wing Panel for Reliability Purposes

REFERENCE: Eggwertz, Sigge, "Investigation of Fatigue Life and Residual Strength of Wing Panel for Reliability Purposes," *Probabilistic Aspects of Fatigue, ASTM STP 511,* American Society for Testing and Materials, 1972, pp. 75-105.

ABSTRACT: In the reliability analysis for a fail-safe structure, statistical information regarding service time until fatigue crack initiation as well as subsequent reduction in residual strength is indispensable. Safety during the service life requires that critical cracks be detected at inspections before the probability of the damaged structure meeting a load exceeding its residual strength has reached an unacceptable level. About 20 sheet panels of 2024-T3 aluminum have been fatigue tested until cracks of various lengths appeared, using a flight-by-flight load program. The fatigue panels had four rows, with four small strips of the same sheet material in each row. The strips were attached to the sheet by two rivets, forming 32 stress concentrations in each panel. After fatigue cycling, the strips were replaced by continuous stringers and the residual tensile strength of the panels was determined. The mean of the logarithm of the number of flights to crack initiation amounted to 4.43, that is, 27,000 flights, while the standard deviation was 0.17. The relationship between the residual strength of the stiffened panel and the critical crack length shows rather little stochastic variation. When the residual strength is plotted versus the crack propagation time, however, the scatter does not seem to be negligible.

KEY WORDS: fatigue(materials), reliability, probability theory, statistical analysis, distribution theory, Weibull density function, crack propagation, crack initiation, stress analysis, fatigue limit, tensile properties, fatigue tests

Nomenclature

f	Frequency in cycles per second
$G(t)$	Probability of failure of structure containing a crack, during time t after crack initiation

[1] Structures Department, The Aeronautical Research Institute of Sweden, Stockholm, Sweden.

H	Expected number of times per hour a load amplitude s_a is exceeded
H_0	Load spectrum parameter, $H_0 = 0.2$ used in numerical example
h	Load spectrum parameter, $h = 20$ used in numerical example
l	Crack length, l_c is length of critical crack in static test
M	Order number of fatigue life of test specimen
m	Number of equally fatigue-sensitive elements in a test panel
N	Total number of test specimens
n	Number of inspection intervals during service life
P, P_ν	Probability of complete failure during service life, during interval ν
P_c, P_{c1}	Probability of crack initiation, first crack initiation
P_u	Probability of ultimate static failure of undamaged structure
p_c	Frequency function of crack initiation
R	Parameter of residual static margin function, $R = 10{,}000$ used in numerical example
S	Stress or load
S_a	Load or stress amplitude
S_m	Mean load or stress
S_o	Original static margin
S_c	Ultimate residual strength of panel containing crack
S_u	Ultimate static strength of undamaged structure
s_a	Normalized load amplitude, $s_a = S_a/S_o$
s_t	Normalized static margin at time t after crack initiation, $s_t = S_t/S_o$
T	Service time in hours, or number of flights
T_{ci}	Service time until crack initiation, index $i = 1, 2, \ldots$ indicating crack No. $1, 2, \ldots$
T_L	Limit service life
T_o	Parameter of Weibull distribution
T_u	Parameter of Weibull distribution, indicating lower limit of service time until crack initiation
T_ν	Service time until end of interval No. ν
t	Service time from crack initiation
t_i	Length of inspection interval
α	Parameter of Weibull distribution
μ_c	Mean value of logarithm of time to crack initiation
ν	Order number of inspection and inspection interval
σ_c	Standard deviation for logarithm of time to crack initiation

Fatigue has been a problem for a very long time in the design of certain structures, especially in mechanical engineering with moving parts such as wheel axles, propeller shafts, turbine blades, and so forth. In the aeronautical field it was commonly agreed around 1950 that fatigue was to be a serious problem in the primary structure of an aircraft, also. The building industry seems to have only recently become aware of the problems that fatigue cracks may cause in modern structures. It is true that railway bridges and high towers have been built with regard to fatigue for several decades. In the near future, however, it will be necessary to take fatigue into account in a large percentage of main structures in buildings and bridges, at least where steel and other metals are involved. Wherever complicated built-up structures of high strength materials will be utilized, technicians in all specialities are likely to meet with the fatigue problem.

Fatigue damage is revealed in a structural component by the initiation of a visible crack which propagates until it has reached such a length that complete failure occurs due to a peak load. Several stochastic variables are involved: time to crack initiation, crack propagation rate, and residual strength corresponding to a certain crack length in the component. The magnitudes of the load amplitude may in many cases also be considered to vary randomly, although official regulations and human behavior will often influence this variation. It has not proved feasible to cover the safety problem concerning fatigue in general by applying a limited number of safety factors on the load or the life time. A statistical treatment is the only way of obtaining an adequate safety level. In a specific case, safety factors may be used when the basic reliability analysis has first been carried out.

The original attitude towards fatigue, as expressed in the "safe-life" philosophy [*1,2*], was that cracks should not be allowed to occur during the service life of a structure. This is a natural policy concerning a vital, simple structural part with no static redundancy. In a complicated structural system built up from a large number of members, it may be extremely difficult to realize even a comparatively short crack-free life.

The aircraft manufacturers, in this predicament, invented the "fail-safe" principle and the "damage-tolerant" structure. The idea is that the component will still be able to carry a considerable load for a long time after crack initiation. The crack will be easy to discover at inspections which are performed at regular, predetermined intervals, when other necessary repairs are also made. It may be argued that inspection of fatigue-sensitive structures has been performed for a long time, not only in the aeronautical field, but also, for example, on railway bridges [*3*]. But a regular reliability approach based on controlled crack propagation and inspections has, so far, to the knowledge of the author, only been applied for aircraft [*4,5*]. It seems likely that it will be utilized in the near future in many other fields.

Several theoretical studies of the reliability of fail-safe structures have been presented [*6-10*]. Experimental results are available only to a limited extent [*10-12*], which is quite natural since it is extremely expensive to build and test a large number of full-scale structural components. It is necessary, however, to obtain a better knowledge of the scatter in the various phases of a fatigue failure and to understand the causes of this scatter.

The present investigation involves the fatigue testing of approximately 20 identical panels which are rather simple and cheap to manufacture but are thought to be fairly representative of the tension skin of a riveted box-beam wing aluminum-alloy structure. After fatigue cycling until various crack lengths were obtained, the residual strength of panels with longitudinal stiffeners has been determined.

In some of the panels the test was continued until two or more cracks were detected at the 32 rivet holes which constituted the stress concentrations. From the results of the first crack initiation, the parent distribution of crack initiation in one single stress concentration has been evaluated and estimates made of the service time until second crack initiation.

Reliability Analysis for Fail-Safe Structure

The reliability of a fail-safe airframe component such as a wing panel has been studied, mainly theoretically, at the Aeronautical Research Institute of Sweden (FFA) with the intention of determining the length of inspection intervals so that a reasonably low risk of fatigue failure is not exceeded during the service life of the aircraft [*10,13,14*]. Since the present investigation is meant to provide experimental data to be included in the calculations and also to form a basis for judging the validity of the assumptions and approximations introduced, a brief description of the procedure developed at FFA is included.

The risk of complete fatigue failure during an interval between two inspections is obtained by combining the probability of crack initiation and the probability that the structure is subjected to a load which is heavy enough to cause total failure in the fatigue-damaged structure. The probability, P_c, of crack initiation during a given flight time, T, is a function increasing with T. In the analysis, a log-normal distribution with a standard deviation $\sigma_c = 0.2$ has been assumed. A logarithmic mean life of 50,000 h has usually been chosen for the numerical calculations.

The frequency of high loads on a component depends very much on which part of the aircraft is considered and also on the operational use of the aircraft. In the general study which has been performed, it was considered satisfactory to adopt a simple exponential distribution function. The expected number of times H per hour that a load amplitude, s_a, will be exceeded has thus been expressed as

$$H = H_0 e^{-h s_a} \tag{1}$$

where the two parameters H_0 and h have been given values which apply to a wing of a civil transport aircraft operating on medium ranges.

The moment when the crack is normally detected is called the crack initiation. It has been assumed that the residual strength of the structure decreases linearly with the service time from the crack initiation until the static margin, that is, the difference between the ultimate strength and the mean load, is zero, which will happen after a constant time, R. Usually the value $R = 10{,}000$ h has been employed in the calculations. No stochastic variation of the residual strength function has been taken into account. The normalized static margin, s_t, t hours after crack initiation is written as

$$s_t = 1 - t/R \tag{2}$$

Complete fatigue failure occurs when the load amplitude exceeds the static margin

$$s_a \geqslant s_t \tag{3}$$

Combining the load-distribution function, Eq 1, and the strength-reduction formula, Eq 2, gives the following expected number of times the residual strength is exceeded in a cracked structure

$$H_t = H_0 e^{-h(1 - t/R)} \tag{4}$$

The probability of failure during a time increment, Δt, may be written as

$$G(\Delta t) = [1 - G(t)]H_t \Delta t \tag{5}$$

Dividing by Δt and taking the limit as $\Delta t \to 0$

$$\frac{dG(t)}{dt} + H_t G(t) = H_t \tag{6}$$

The general solution of this differential equation is

$$G(t) = 1 - e^{[F(0) - F(t)]} \tag{7}$$

where

$$F(t) = \int H_t dt \tag{8}$$

Introducing Eq 4 into Eq 8 and integrating gives, after entering into Eq 7,

$$G(t) = 1 - \exp\left[\frac{RH_0}{h} 1\left(- \exp\frac{ht}{R}\right)\exp(- h)\right] \tag{9}$$

The function $G(t)$ is presented in Fig. 1 for a structure already having a crack at the beginning of the service life, $T = 0$. The residual strength parameter has been given the value R = 10,000 h, while the load parameters are $H_0 = 0.2$ and $h = 20$. The latter two values are applicable to a civil transport aircraft on ranges of medium length, assuming an ultimate design load factor of 3.75 [*10*]. In an undamaged structure the probability of ultimate failure may be determined as

$$P_u(t) = 1 - e^{-H_u t} \tag{10}$$

where H_u is obtained from Eq 1, entering $s_a = 1$. Since $H_u t << 1$, Eq 10 is approximated by

$$P_u(t) = H_u t = H_0 t e^{-h} \tag{11}$$

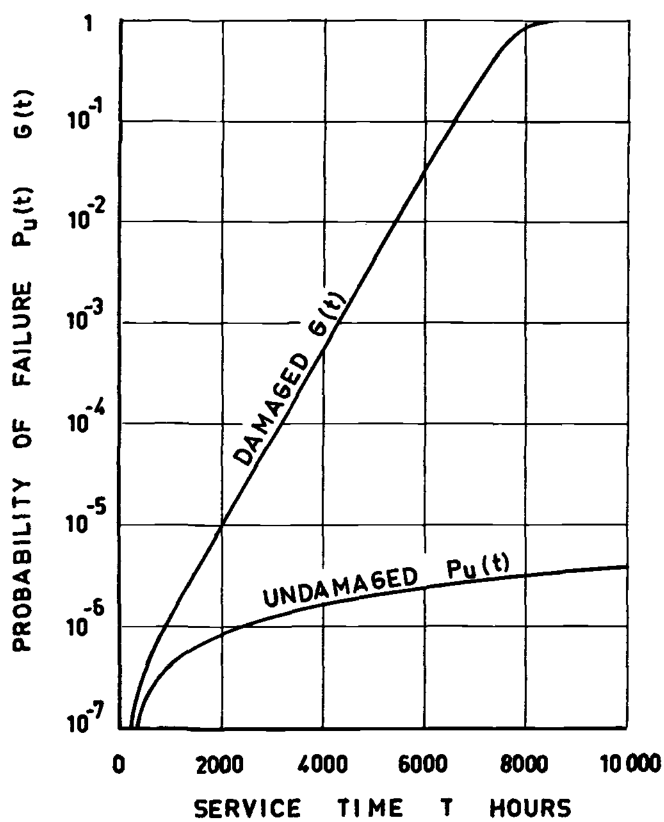

FIG. 1—*Probability of failure due to a gust load in damaged and undamaged structure during service life,* T.

This function has also been included in Fig. 1. It grows linearly with time. In the damaged structure the increase is much more rapid. After 2000 h, the ratio between the two functions has exceeded the value of 10.

A time schedule is shown in Fig. 2 for the inspections of a structural component from the delivery of the aircraft until retirement from service. The total number of inspection intervals is n, and a given interval number ν is considered, beginning at the time $T = T_{\nu-1}$ and ending at $T = T_\nu$. The probability P_ν of complete failure during the interval ν is determined as the time integral of the product of the function $G(t)$ for the cracked structure with decreasing residual strength and the probability of crack initiation $p_c \Delta T$ during a time increment ΔT.

$$P_\nu = \int_{T_{\nu-1}}^{T_\nu} G_t(T_\nu - T) p_c(T) dT \tag{12}$$

Numerical calculations have been carried out for a large number of ages, $T_{\nu-1}$, at the beginning of the interval, and also a large number of lengths of inspections intervals, $t_{i\nu} = T_\nu - T_{\nu-1}$. In Fig. 3 is plotted the computed probability of failure versus the inspection interval with the age $T_{\nu-1}$ as a parameter. This diagram covers inspection intervals up to 10,000 h, while Fig. 4 gives the failure risks for longer intervals up to 20,000 h.

It is obvious that the diagrams of Figs. 3 and 4 can be used for determining the probabilities of failure for all inspection intervals during the service life, one after the other. As long as the probabilities are small, which should be the case, the probability of failure during the whole life is obtained as the sum of the probabilities for the intervals.

$$P = \sum_{\nu=1}^{n} P_\nu \tag{13}$$

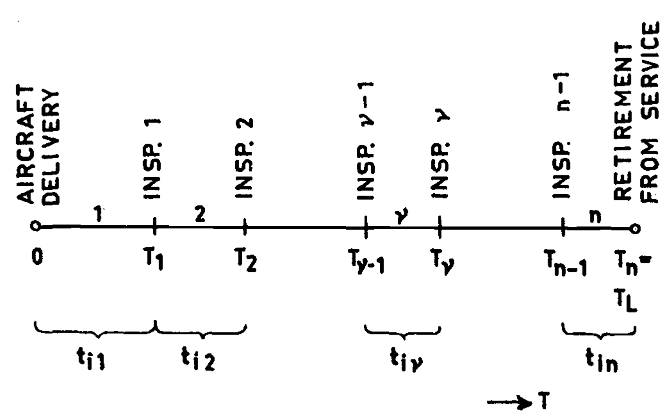

FIG. 2—*Time schedule for inspections of component of major aircraft structure.*

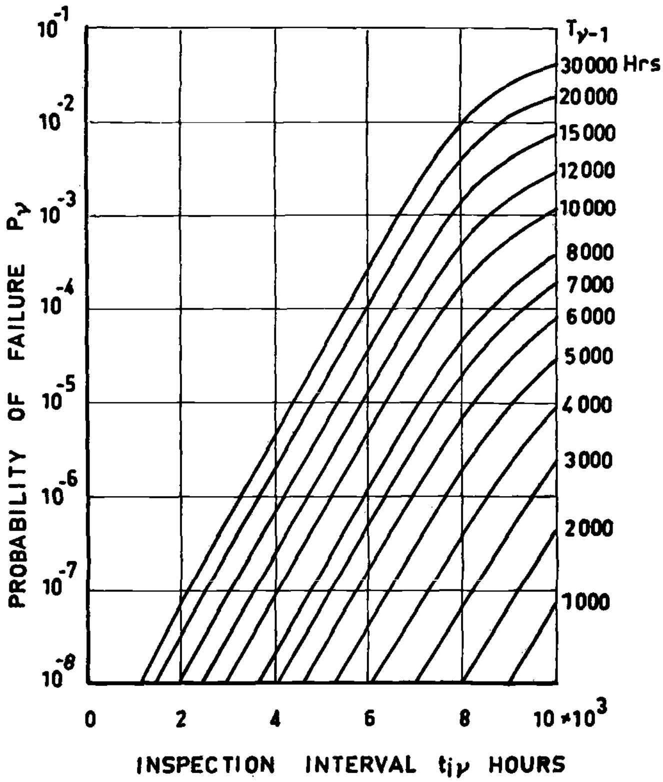

FIG. 3–*Probability of fatigue failure during an inspection interval,* $t_{i\nu}$, *for different ages of aircraft,* $T_{\nu-1}$, *at the beginning of the interval, Part 1.*

The simplest case is periodic inspection, which means that all inspection intervals are equally long. Figure 5 gives the probability of failure during a service life which is divided into a number of intervals of constant length from 1000 to 10,000 h. The risk of failure has also been computed for $n = 1$, that is, no intermediate inspections. Furthermore, the probability P_c of crack initiation has been included for comparison. If the risk of failure is limited to $P = 10^{-5}$ during a service life of 30,000 h, the diagram suggests an inspection interval $t_i \leqslant 4000$ h, implying eight inspection intervals during the life time. A closer study of Figs. 3 and 4 indicates that the total number of inspections would be reduced, particularly if the first interval is made much longer than the following ones. It must be pointed out that this conclusion is valid only under the assumption that the fatigue quality of the structure is known in advance, before the inspection intervals are planned. During the initial period of the service life, unexpected cracks may occur, which make it necessary to apply rather short intervals between the inspections.

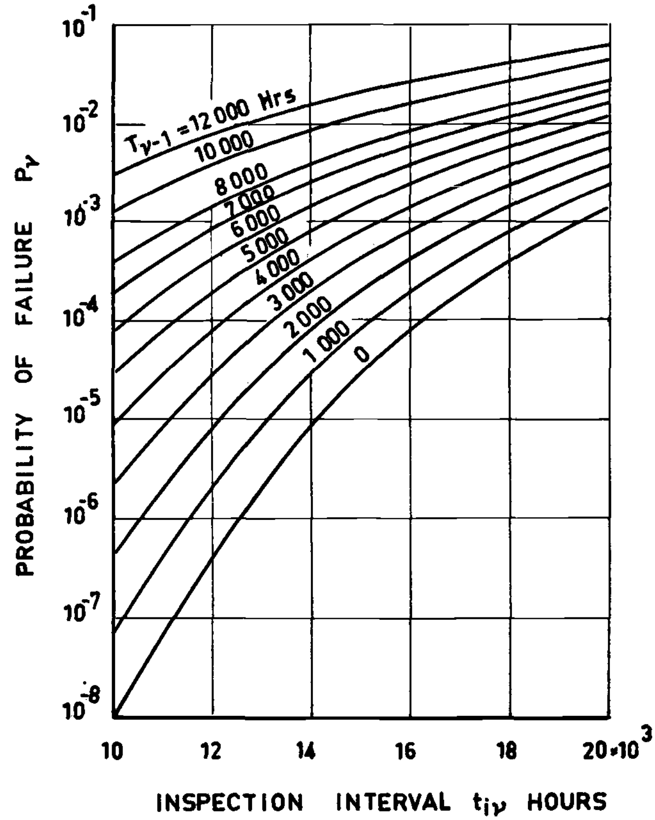

FIG. 4–*Probability of fatigue failure during an inspection interval,* $t_{i\nu}$, *for different ages of the aircraft,* $T_{\nu-1}$, *at the beginning of the interval, Part 2.*

Test Specimens

Many fatigue tests on wing panels have included a riveted joint [*15-20*]. This is natural since on many aircraft in service the wing-skin joints are among the most fatigue-critical points in the airframe. The following reasons were stated, however, for not including a joint in the present investigation:

(1) Various types of skin joints occur in aircraft wings with quite different fatigue qualities depending on the detail design of the joint. Any selection of a special type of joint would make the investigation specialized, whereas the aim has been to produce test results with an applicability as general as possible.

(2) At the present state of knowledge it is possible to attain for a joint the fatigue life required by a rather moderate sacrifice of weight. By locally increasing the skin thickness the stress may be reduced to a level which is acceptable with regard to the stress concentration of the joint. This implies that

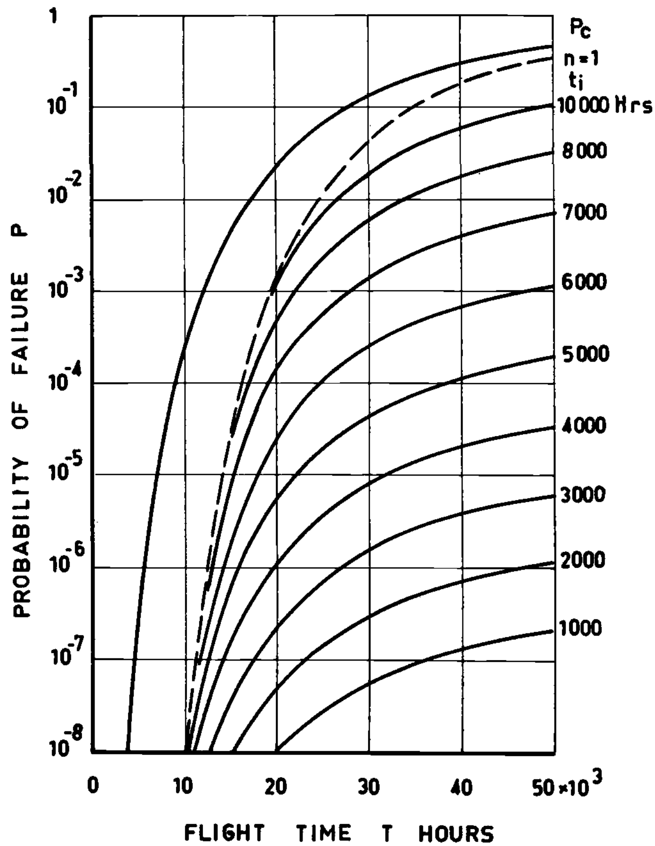

FIG. 5—*Probability of fatigue failure during service life,* T, *assuming periodic inspection with interval,* t_i. *Curve denoted* n = *1 gives risk of failure when no inspection is carried out, and* P_c *indicates risk of crack initiation.*

joints will probably not be the most critical details in a new airframe design, and also that the stress level in joints will vary considerably from one structure to another.

(3) The stress in the base structure can be affected only at the expense of large weight increase. The base panel sets an upper limit for the fatigue quality that can be attained with a given sheet material and a given type of connection (riveted, bolted, or glued joint) between sheet and stringer. Results from tests on base panels may yield information concerning fatigue life, which is generally valid for a commonly used material and method of connection.

In an actual wing panel a certain load transfer takes place between sheet and stringer which is of importance from the point of view of fatigue [*15*]. This is not the case if the panel is subjected to pure axial load. A load transfer can be achieved, however, by cutting the stringers between every second rivet. Since the stringer is not normally fatigue critical, it may be replaced by a sheet strip of rectangualar cross section. The load transfer can be adapted to a suitable magnitude by varying the dimensions of the sheet strip. By experiments on small sheet specimens with a cross section of 120 × 2.5 mm, it was found that a strip with a width of 20 mm and a thickness of 2.5 mm fixed by two rivets, ϕ 5 mm, center to center 20 mm, would be adequate for the purpose. The load transfer to the strip was determined by the aid of two strain gages on the edges of the strip. After fatigue testing of the small specimens, the rivets were removed and the relation between strain-gage reading and loading on the rivet holes was determined in a special calibration jig. The load transfer, which varied considerably during the fatigue cycling, amounted to around 3 percent of the total tensile load on the sheet specimen, a magnitude considered realistic for a normal wing panel.

The large sheet panel for fatigue testing was manufactured according to Fig. 6. Within the test length it consists of a 2.5-mm sheet of 2024-T3 aluminum, clad and anodized (SAAB specification 3526-68), with a width of 480 mm. The sheet was provided with four parallel rows of small strips of the same material, four in each row. Each strip, 38 by 20 by 2.5 mm, was fastened to the panel by two 5-mm rivets of 2024 material, hand-driven and countersunk on the free side of the sheet. In all, the panel has 2 × 4 × 4 = 32 rivet holes. In order to minimize bending, the two outer rows of strips were attached to one side and the inner rows to the other side of the panel. The design of the test panels meets the very important requirement that the manufacturing cost per specimen should be low in order to allow 22 panels to be produced at a reasonable total cost. The panels were cut from four 3600 by 1000-mm sheets of the same delivery.

After fatigue testing, the damaged panels, and some panels without cracks, were loaded statically in tension to determine their residual strength. Since the intention was to obtain experimental information for a realistic stringer-stiffened wing panel, the strips were removed from the sheets before this test and replaced by stringers, continuous along the whole length of the panel, as shown in Fig. 6. The stringers were made of channel-section bars, 41 by 36 by 2.7 mm, of extruded 2024-T4 aluminum (SAAB specification 3526-4). The total stringer area, 4 × 300 = 1200 mm^2, is equal to the cross-sectional area of the main sheet.

Fatigue Tests

The investigation was divided into two parts. Twelve panels were tested in the first part and ten panels in the second. One of the panels was intended for a static test only.

The fatigue cycling was carried out in a servo-hydraulically controlled testing

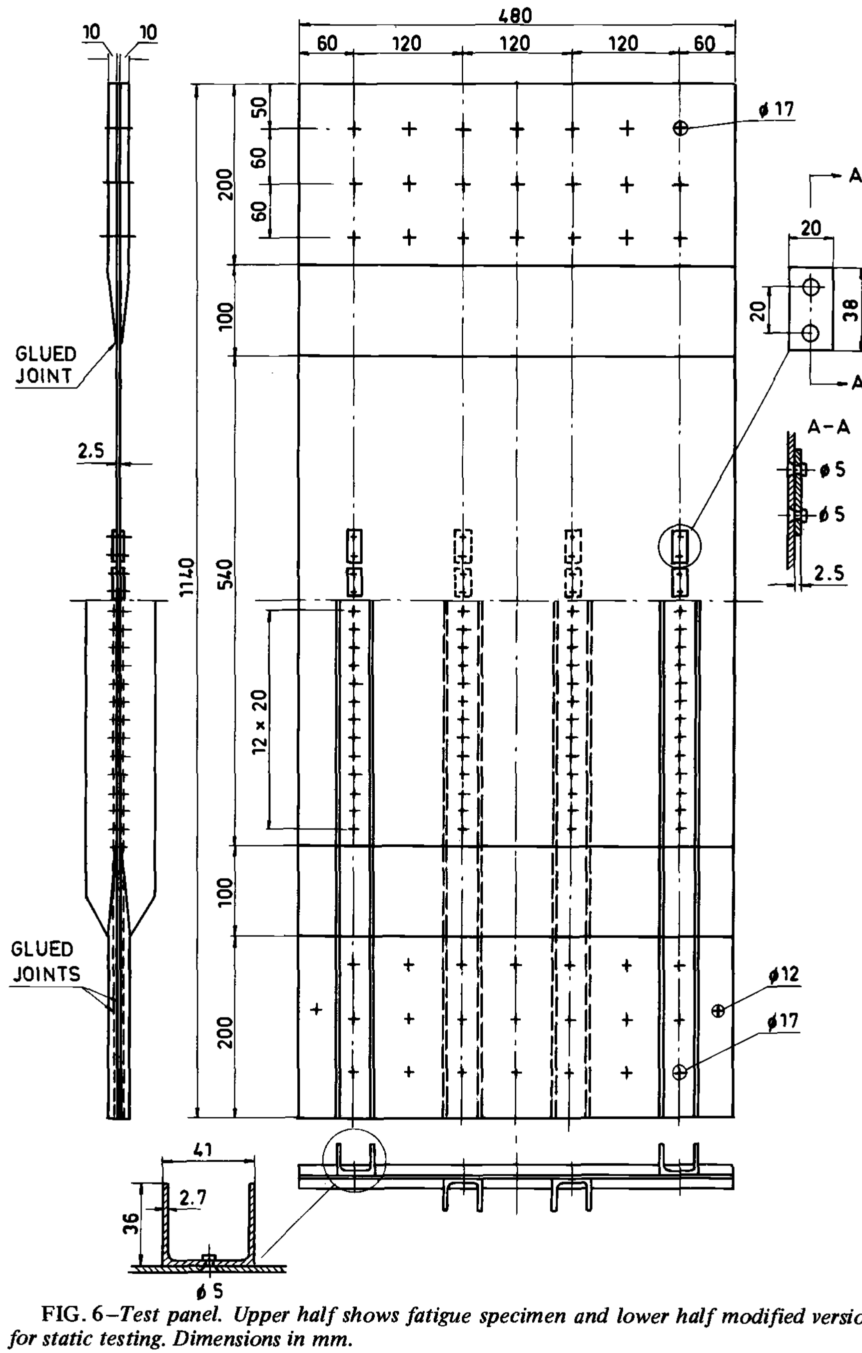

FIG. 6—*Test panel. Upper half shows fatigue specimen and lower half modified version for static testing. Dimensions in mm.*

machine with a maximum loading capacity of ±0.20 MN. In the first part the original controlling and programming units of the machine were utilized, which automatically provided a repeated load program including eight different steps. Since these units did not work well in the long run without much supervision and maintenance, they were replaced in the second part by a punched-tape-operated program and a home-built control unit. The only nominal difference in the loading was that the latter system had to be run at a lower speed, approximatively 70 percent of the speed of the original system.

Published results from program or random-loading fatigue tests have revealed that the ground-air-ground cycle and its position in the load sequence has a pronounced influence on the fatigue life [*16,21,22*]. A realistic fatigue test should thus be run "flight by flight." Each program block, corresponding to one flight, should preferably include a large number of different load amplitudes in a randomized sequence but with an amplitude distribution according to measured applicable load spectra.

The programming unit of the fatigue machine could only provide a very limited number of different loads, and all cycles of the same magnitude had to be run consecutively. On the basis of experimental experience, it was judged that such a simplified flight-simulation loading would yield results of practical significance. Probably the most serious objection is that the program does not include higher loads than those normally occurring in every flight. Loads occurring seldomly could not be achieved automatically, since all flights had to be identical, and it would have been too time-consuming to introduce them manually. It is known that, occasional very high loads usually have a beneficial effect on fatigue life and should, therefore, be omitted. It has not yet been established where the truncation of the load spectrum should be made, but it is likely that the minimum fatigue life would be obtained at a slightly higher limit than was used in the present investigation [*23,24*].

The simplified flight-simulation program is shown in Fig. 7. It has been obtained from a normal load spectrum for a jet transport, assuming a flight duration of 1 h. This spectrum is not strictly exponential, while the reliability analysis, Eq 1 assumes an exponential distribution function for the high loads. This involves no contradiction, however, since the common loads occurring in every flight, which produce the dominant part of the fatigue damage, must not necessarily have the same distribution as the heavy loads causing ultimate failure.

The load program starts with a ground condition with compression stress, $S_{\min} = -25$ MN/m^2, all taxiing loads being omitted. The mean stress is then changed to tensile stress corresponding to flight condition, $S_m = 88$ MN/m^2, and seven steps with amplitudes varying from 10.3 to 30 MN/m^2 are cycled around this mean stress. The program includes 89 load cycles and was completed in 4.35 s in the first part of the investigation. The tape-operated flight in the second part took 6.0 s. Each test was completed in 40 to 50 h running time in

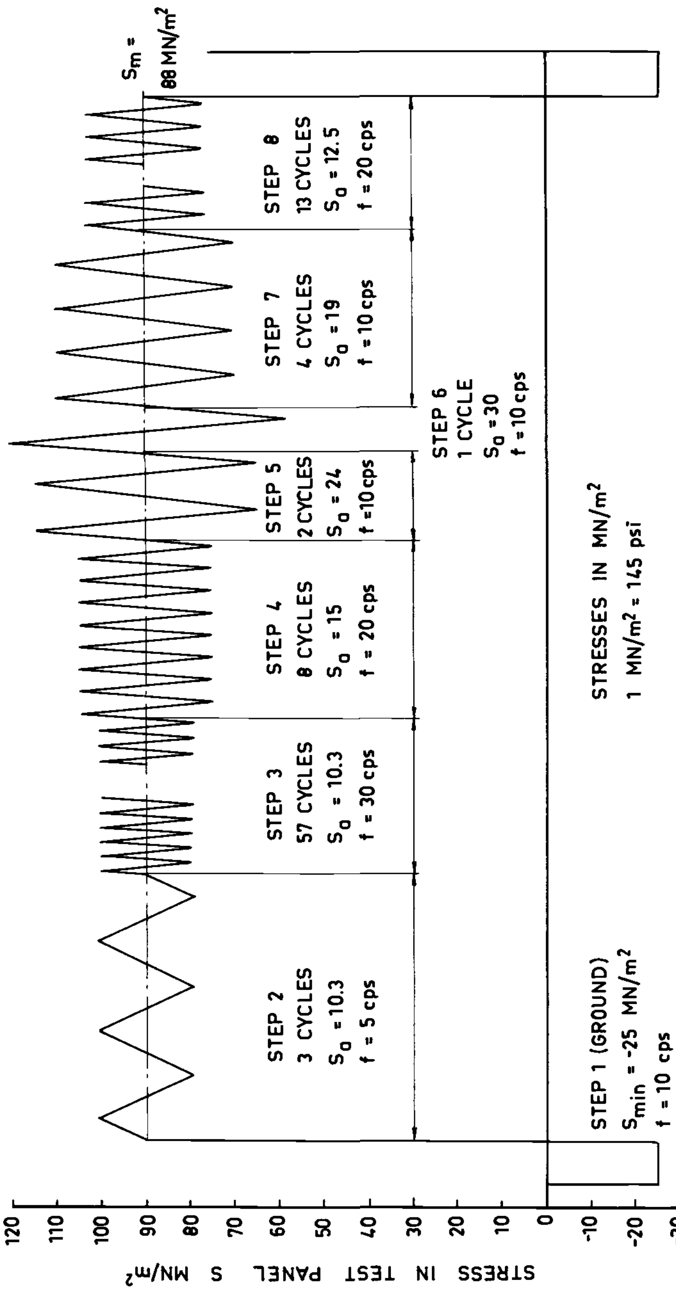

FIG. 7—*Program for simulation of 1-h flight in fatigue test.*

the machine. The stress levels quoted have been used in all fatigue tests but one, where both mean stress and stress amplitudes were lowered by 14 percent after the first 20,000 flights. This was done by mistake, but the results have been included to show the effect of a stress reduction.

The steel clamping jaws and the device used to prevent buckling caused by compression loads, are shown in Fig. 8. The stiffeners were provided with a teflon nose to reduce friction. The stress distribution over the width of the panel was checked by a number of strain gages. The longitudinal strain in the small sheet strips was also measured on two panels.

The cracks were detected with the aid of a crack wire, which was glued in a loop around the rivet holes, on the free side of the sheet. When the wire was

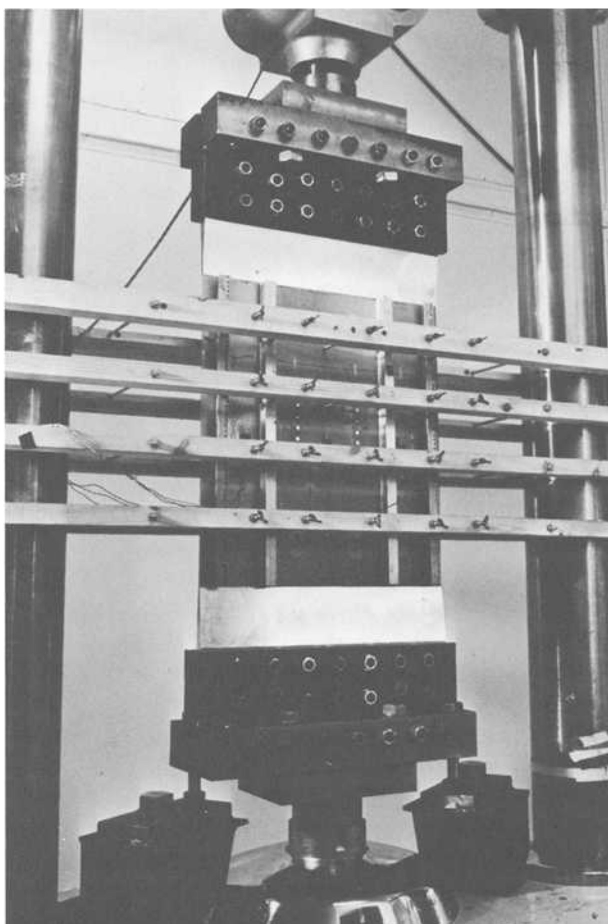

FIG. 8—*Clamping and stiffening of fatigue panel to prevent buckling.*

broken the testing machine stopped automatically. The crack detection occurred at varying crack lengths. Usually the crack, located on one side or both sides of the hole, had a length of about 10 mm measured from the center of the rivet hole. This means that the crack had propagated some 5 mm from the edge of the countersunk rivet head.

In panel 1, fatigue testing was continued until complete failure. The first crack was arrested, after it had propagated during some 3000 flights, by pressing a steel ball against the sheet surface just in front of the crack tip. This crack did not grow afterwards, but crack 3 developed into failure of the whole sheet. Panel 18 was also cycled to failure, since the crack wire did not function when the crack occurred during a night. Unfortunately, only the total number of flights could thus be recorded for this specimen. Panel 3 buckled when a high compressive load was induced accidentally by the servo control unit. Panel 4 was subjected to 47,000 simulated flights without any visible crack. Since the gluing between the sheet and the stiffening plates at the ends had started to yield, the fatigue test was discontinued at this stage. The other 17 fatigue panels were cycled until they developed cracks of lengths varying between 10 and 91 mm. The propagation of the crack was followed with a magnifier and recorded at short intervals.

Ultimate Static Tests

After the fatigue panels had been modified as described above, the clamping jaws which had been used in the fatigue machine were installed in a 5.0-MN uniaxial testing machine. In this machine, 18 panels fatigue tested without complete failure and one panel which had not been fatigue cycled were subjected to increasing tension until ultimate failure.

The stress distribution was carefully studied during the whole test on two panels with the aid of ten strain gages on the sheet and twelve on the stringers. On the other panels the stress distribution was only checked with three pairs of gages. When the critical crack started to propagate, its length was recorded by an automatic camera at a rate of about one picture per second. The critical crack was always the longest crack, which turned out to develop into total failure.

Test Results

The results of the fatigue tests and the static tests have been compiled in Table 1. Specimen 3 has been omitted for reasons stated above.

The second column gives the number of flights, T_{c1}, until detection of the first crack. It varies from 13,000 to 55,000 for the panels with the ordinary stress level, whereas it was increased to 74,000 when the stress was decreased by 14 percent after 20,000 flights. The next columns refer to the second and subsequent cracks. It should be noted that after the fatigue tests had been completed, a closer study revealed further small cracks in several panels which have not been included in the table. Many fatigue-crack nuclei could be detected in the fracture surface at the rivet holes, especially after the static failure. The first crack started from one of the inner rivet rows in 13 panels, while the origin was the outer rows in the 6 other panels where cracks occurred.

The distribution curve for log T_{c1} has been plotted on Gaussian probability paper in Fig. 9, using the 17 test results which were available at the same stress level. A straight line has been drawn through the computed logarithmic mean value $\mu_{c1} = (\overline{\log T_{c1}}) = 4.432$ with a slope corresponding to the computed standard deviation of log T_{c1}, $\sigma_{c1} = 0.172$. The logarithmic mean thus corresponds to 27,000 flights.

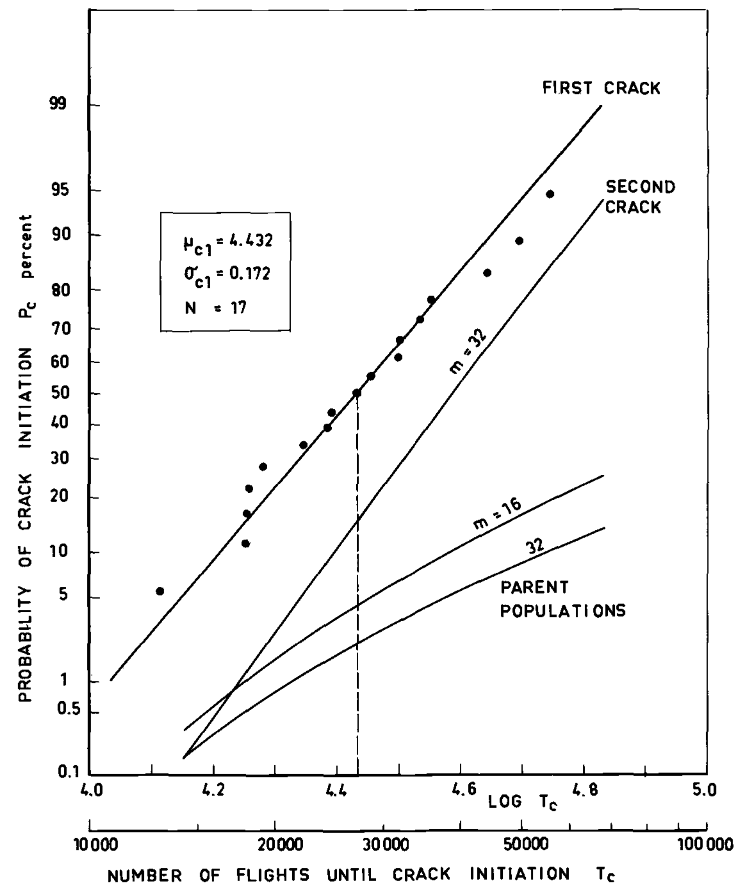

FIG. 9–*Distribution curve on Gaussian probability paper for number of flights to initiation of first crack, obtained from 17 panel fatigue tests. Distribution curves for "parent" populations, assuming number of identical members* m = *16 and 32. Distribution of second crack initiation with* m = *32.*

Columns 8 and 9 of Table 1 present the total number of flights, T_L, when the fatigue tests were stopped, and the number of flights that the critical crack had endured from detection, $T_L - T_c$. The next column gives the length of the longest crack, which was always critical in the ultimate static test. The first crack was critical in all panels but 1 and 10. In panel 8 the fatigue cycling was discontinued immediately after the crack wire had been broken. The one-sided crack then had a length of 8 mm from the center of the rivet hole. The table gives the value as $l_c = 8 + 2.5 = 10.5$, that is, the crack is measured from the other edge of the hole. The critical cracks of all other panels have branches in two directions, the length being measured between the crack tips. The crack in panel 21 did not pass through a rivet hole. It was situated about one hole diameter from the edge of the nearest hole.

The detection of the critical cracks was made at crack lengths varying from 7.5 to 23 mm, measured from the center of the rivet hole, or from the other crack tip. The collection of all crack-propagation curves in Fig. 10, where the abscissa represents the number of flights since the crack was detected, reveals a large scatter. This is not unexpected, since a longer crack usually grows faster than a shorter one, and the cracks have been discovered at various lengths. The one-sided cracks have been given in the diagram as measured from the opposite edge of the rivet hole. The connection between the last point where only one branch of a crack had been found and the first observation point for the double-sided crack has been drawn as a dotted line.

In Fig. 11 it has been assumed that all cracks were detected at a length of 15 mm, from tip to tip. Those cracks which were found at later stages have been extrapolated backwards using a mean-propagation curve from the test results available. They have thus been moved to the right in the diagram, which should give a more adequate picture of the scatter in crack propagation.

The ultimate residual strengths, S_c, of all panels which did not fail during the fatigue testing have been compiled in the next to the last column of Table 1. The variation of residual strength with the length of the critical fatigue crack is shown in Fig. 12. The residual strength has been normalized with respect to the ultimate strength of an undamaged panel, $S_u = 0.92$ MN. The eight test points show surprisingly little scatter around a fitted curve, considering that the errors in the measured values of S_c are of 1 to 2 percent magnitude. Test results from panels with the critical crack in an inner row have been represented by triangles, while those corresponding to the more scarce outer-row cracks are denoted by circles. The latter type of crack seems to result in a slightly lower residual strength. The only triangle that deviates perceptibly from the curve belongs to panel 13, which was fatigue tested at a lower stress level than the other specimens.

During the ultimate static tests the load was raised in steps as long as the length of the crack was stable. When the crack started to grow at constant load,

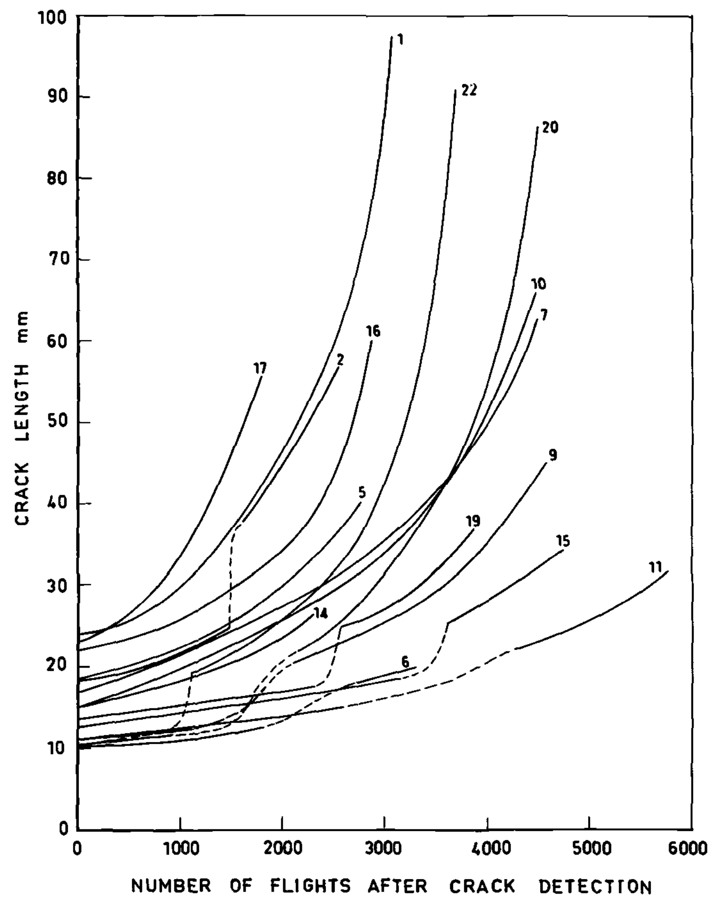

FIG. 10—*Crack propagation curves for 15 fatigue panels.*

or when plastic deformation occurred, the loading was increased continuously and the crack was photographed at short intervals. The exposures were marked automatically on the load-time recorder. The crack propagation could thus be followed all the time until rapid failure, which occurred at a certain combination of crack length and load.

For small critical fatigue cracks the slow crack-propagation period was very short. In panel 8 the maximum load was attained almost at the same moment as the crack started to grow, and the ultimate failure came a few seconds later. One of the most successful recordings of slow crack propagation was obtained for panel 10, as shown in Fig. 13. The length of the initial fatigue crack was 66 mm. The crack started to grow at a load of 0.56 MN. At 0.69 MN, with a crack length of 90 mm, the continuous load increase was started (time zero).

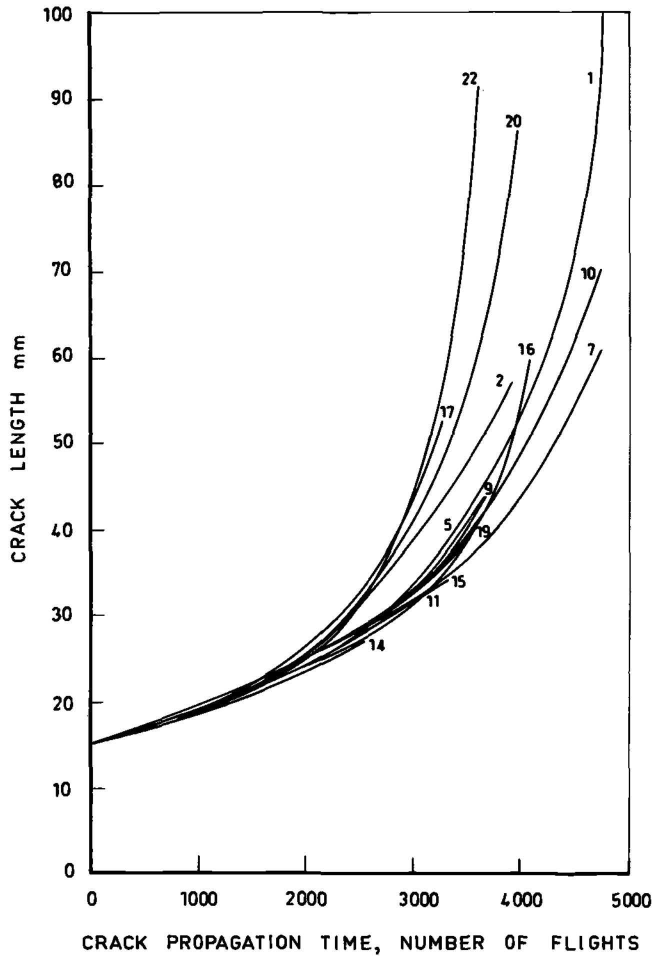

FIG. 11–*Crack propagation curves brought to coincide at a total crack length of 15 mm.*

Discussion

In statistical evaluations of data from fatigue tests it has often been assumed that the number of cycles, or simulated flights, until crack initiation has a log-normal distribution. The main reasons seem to be that this distribution is convenient to handle and that comparisons have shown that other distributions do not generally give better agreement with test results[25,26]. The present investigation contains too few test specimens to allow any significant statement regarding the probability distributions of wing panels. The aim has been, in the first place, to obtain information on the magnitude of the scatter. Since each

TABLE 1—*Results of fatigue tests and ultimate static tests.*

Panel Number	Number of Flights to Crack 1 T_{c1}	2 T_{c2}	3 T_{c3}	$\log T_{c1}$	Order Number, M	Probability, $P_{c1} = \frac{M}{N+1}$	Total Number of Flights, T_L	Crack Propagation, $T_L - T_c$	Critical Crack Length, mm l_c	Residual Strength, MN S_c	Remarks
1	24 320	28 700	30 530[a]	4.386	7	0.389	33 850	3 320	~180	. . .	fatigue tested to failure
2	43 920	. . .	. . .	4.643	15	0.833	46 360	2 440	57	0.73	
4	. . .	. . .	. . .	. . .	. . .	. . .	47 740	. . .	. . .	0.90	no crack
5	35 470	. . .	. . .	4.550	14	0.778	38 230	2 760	40	0.76	
6	49 350	. . .	. . .	4.693	16	0.889	52 640	3 290	20	0.83	
7	24 590	28 950	. . .	4.391	8	0.444	29 070	4 480	63	0.73	
8	28 450	. . .	. . .	4.454	10	0.556	28 450	0	10.5	0.85	
9	19 130	. . .	. . .	4.282	5	0.278	23 690	4 560	45	0.75	
10	17 960	19 940	. . .	4.254	3	0.167	24 420	4 480	66	0.72	
11	55 270	. . .	. . .	4.742	17	0.944	61 120	5 850	32	0.77	
12	. . .	. . .	. . .	. . .	. . .	. . .	. . .	. . .	. . .	0.92	not fatigue tested
13	74 120	. . .	. . .	. . .	. . .	. . .	88 210	14 090	75	0.73	0.86 of normal stress
14	27 060	. . .	. . .	4.432	9	0.500	29 340	2 280	27	0.81	
15	34 270	34 270	34 270	4.535	13	0.722	39 000	4 730	35	0.77	
16	22 200	. . .	. . .	4.346	6	0.333	25 230	3 030	61	0.73	
17	31 670	31 670	. . .	4.501	12	0.667	33 390	1 720	55	0.71	
18	. . .	. . .	. . .	. . .	. . .	. . .	22 220	. . .	~200	. . .	fatigue tested to failure
19	17 890	17 890	. . .	4.253	2	0.111	21 750	3 860	37	0.74	
20	18 160	. . .	. . .	4.259	4	0.222	22 660	4 500	86	0.69	
21	31 590	. . .	. . .	4.500	11	0.611	32 650	1 060	16	0.83	crack outside hole
22	13 020	. . .	. . .	4.115	1	0.056	16 730	3 710	91	0.69	

[a] Cracks 3, 4, and 5.

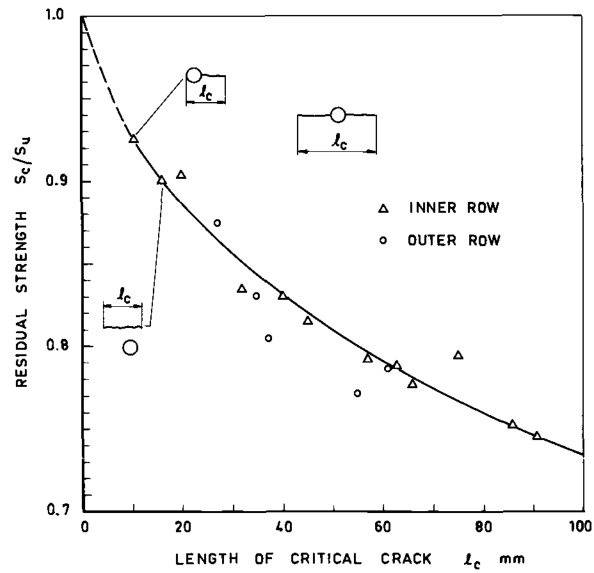

FIG. 12—*Residual strength of damaged panel plotted versus crack length.*

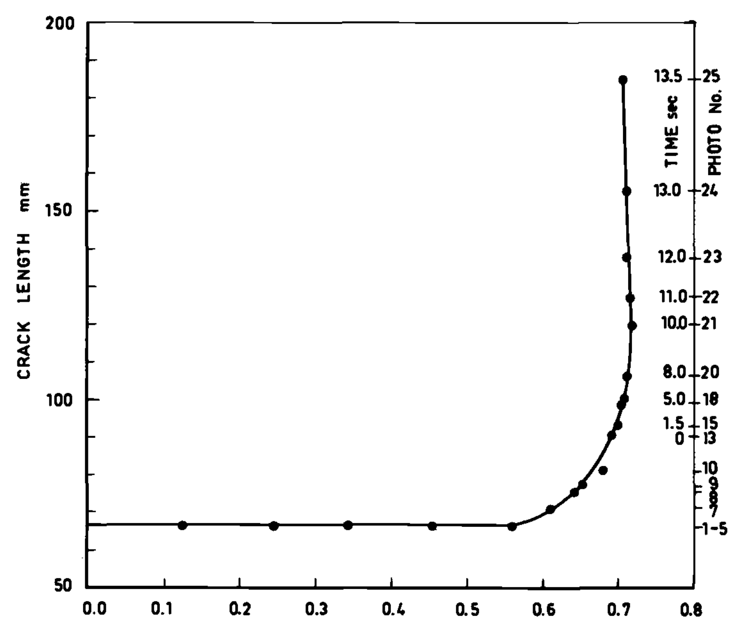

FIG. 13—*Crack propagation versus tensile load in ultimate static test on panel 10.*

tested panel includes 32 similar stress concentrations where fatigue cracks may be expected, the total number of fatigue-sensitive spots involved in the investigation is considerable. By regarding the test results as service times until first failure, and by studying also the following crack initiations, where these were discovered, it may be possible to obtain more basic information, as advocated by Freudenthal [*27*].

The straight line drawn on Gaussian probability paper in Fig. 9 corresponds to the computed parameters, the mean value, and the standard deviation, $\mu_{c1} = 4.432$ and $\sigma_{c1} = 0.172$. This line does not seem to be very well adapted to the test points in the outer parts. It would be possible to get a slightly better fit by decreasing the slope. The discrepancy has to do with the method of computing the mean plotting position for the test results

$$P_{c1} = M/(N+1) \tag{14}$$

where M is the order number of the test point and N is the total number of results. The latter number is obviously too small to justify the use of the simple Eq 14. A chi-square test with six classes gave $\chi^2 = 1.91$, to be compared to $\chi^2{}_{0.90} = 9.24$. The test results thus do not deviate from the log-normal distribution on a 90 percent significance level.

If P_c is the probability of crack initiation in a single rivet hole, called the "parent" distribution, the probability P_{c1} of the first crack among m identical holes is obtained using the Bernoulli theorem [*27,28*].

$$P_{c1} = 1 - (1 - P_c)^m \tag{15}$$

The total number of rivet holes in a test panel is 32. There is a variation in tensile stress over the panel width, implying higher stress for the inner rows of rivet holes. On the other hand, the bending stresses in the panel seem to be somewhat higher in the outer rows. The first crack has occurred more often in the inner rows. It is interesting, therefore, to derive the parent distribution for both $m = 32$ and $m = 16$. Such distributions have been drawn in Fig. 9, using Eq 15 with P_{c1}-values determined in the tests. They are slightly curved, implying that they are not log-normal, and have less slope than the experimentally determined curve for the first crack. It may be concluded that test results for single rivet holes would show a median value of around 150,000 flights, and a standard deviation of about 0.4.

The probability of the second crack initiation may also be simply expressed in terms of the probability of the parent population [*28*].

$$P_{c2} = 1 - (1 - P_c)^m - mP_c(1 - P_c)^{m-1} \tag{16}$$

The distribution function of the second crack has been computed from the parent distributions. It is almost a straight line, as shown in Fig. 9 for $m = 32$. The distribution corresponding to $m = 16$ is very close to the curve presented, as might be anticipated. The median value of the second crack initiation is about 39,000 flights, implying an expected number of 12,000 flights between the first and the second cracks. A second crack has only been observed in six panels (Table 1); in three of these, the second cracks were observed at the same time the first cracks were detected, and in the other three, the interval between the first and the second cracks varied from 2000 to 4400 flights. No panel with the normal stress level was fatigue cycled more than 5850 flights after the detection of the first crack. It is not possible, therefore, to compare the test results with the computed distribution curve. It should be noted that the theoretical curve presupposes that the 32 fatigue-sensitive spots are identical and independent, which is probably not an acceptable approximation when the first crack has reached a considerable length.

It has been stated that the log-normal distribution does not fit the physical model regarding fatigue crack initiation [29]. From this point of view the extreme value distribution has definite advantages. The test results from initiation of the first fatigue crack have also been plotted in Fig. 14 on an extreme value probability paper, where the probability is expressed as

$$P_{c1} = 1 - e^{-(T_{c1}/T_o)^{\alpha}} \tag{17}$$

A straight line has been fitted by eye, in the first place to the central test points, with the following values of the two parameters

$$T_o = 31{,}900 \text{ flights}, \alpha = 2.60$$

The value of α indicates that the log-normal distribution cannot be considered a good approximation for the extreme value distribution, but that the two functions have a similar course [28,30]. The deviation from the test points at the lower end of the straight line seems to suggest that the introduction of a lower limit, as a third parameter of the distribution function, Eq 17, would result in a better agreement [31].

The Weibull distribution

$$P_{c1} = 1 - \exp\left[-\left(\frac{T_{c1} - T_u}{T_o}\right)^{\alpha}\right] \tag{18}$$

with its three parameters, T_u, T_o, and α, is usually more adaptable to a given set of test results than the two-parameter functions used above. On the other hand,

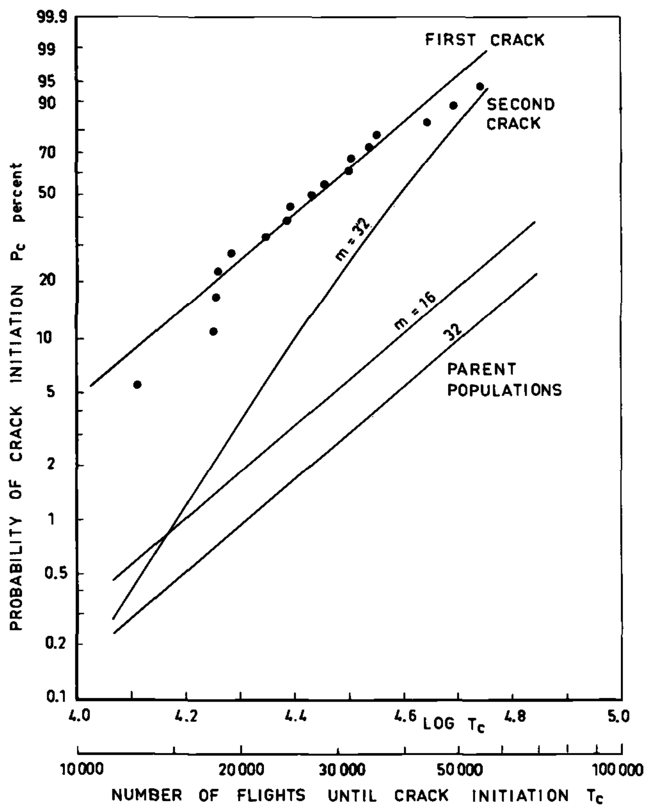

FIG. 14–*Distribution curve for number of flights to initiation of first crack, obtained by plotting test results on extreme value probability paper. Distribution curves for parent populations, assuming* m =*16 and 32, and distribution of second crack initiation with* m = *32.*

the proper assessment of the parameters is no longer a simple transaction. A method of statistical moments given by Weibull[32] has been employed, together with a number of other procedures. It was found, however, that in this case a simple method of least squares, carried out by searching the minimum on an electronic computer, gave the most satisfactory result.

$$T_u = 11{,}100 \text{ flights}, T_o = 20{,}400 \text{ flights}, \alpha = 1.52$$

The logarithm of the difference $(T_{c1} - T_u)$ has been plotted in Fig. 15 *versus* the same double-logarithmic extreme value ordinate as used in Fig. 14. The straight line corresponding to the computed parameters fits the test results rather well, the lowest values excepted. A chi-square test with ten classes gives

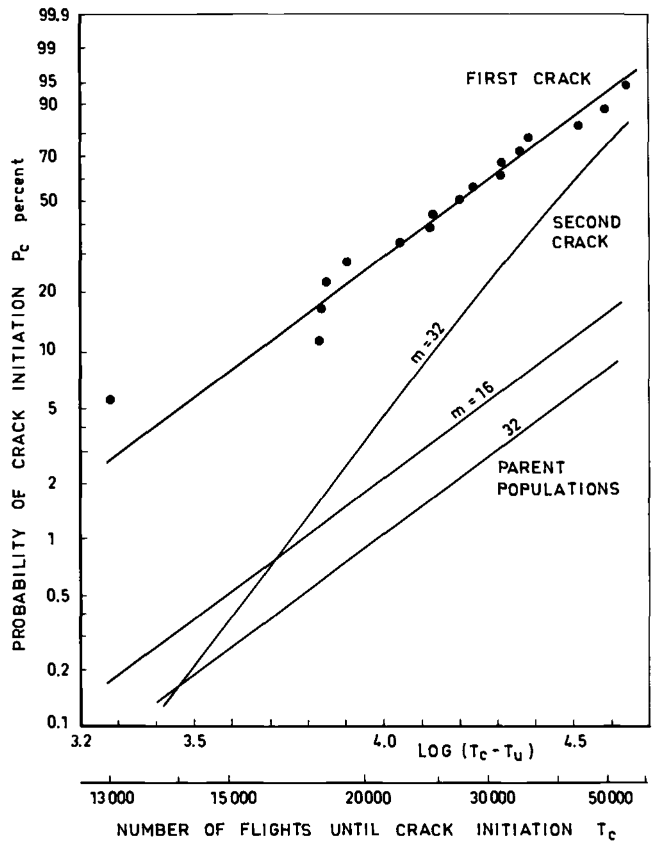

FIG. 15–*Weibull distribution for number of flights to initiation of first crack, obtained by plotting test results on extreme value probability paper. Distribution curves for parent populations assuming* m = *16 and 32, and distribution of second crack initiation with* m = *32.*

χ^2 = 7.41, implying no significant deviation of the test results on a 90 percent level.

One main advantage with the extreme value distributions is that the parent distributions will also be represented in the diagram of Figs. 14 and 15 as straight lines, parallel with the distribution of the first crack initiation. A comparison with the parent curves obtained in Fig. 9 indicates that somewhat shorter fatigue lives, about 100,000 flights, corresponding to P_c = 50 percent, will be predicted for the single stress concentration, using the extreme value distributions, compared to 150,000 flights when the log-normal distribution was adopted. The expected number of flights between the first and the second cracks on the 50 percent level is rather similar in all three diagrams. While the second crack distribution is almost parallel to the log-normal first crack distribution in

Fig. 9, the lower parts become much steeper using the extremal first-crack distributions in Figs. 14 and 15.

The scatter of the residual strength for a panel with a fatigue crack of a given length is quite small, as shown in Fig. 12. The length of a crack at a given number of flights after detection is subjected to large stochastic variations, as clearly illustrated by Fig. 10. In panel 17 a crack length of 30 mm was reached in less than 1000 flights, while in the nominally identical panel 11 it took about 5500 flights to obtain the same crack length. The crack-propagation diagram in Fig. 11 which was derived by letting all cracks start at a length of 15 mm, indicates that the main part of the scatter is to be attributed to crack detection. In the panel tests, crack detection was dependent on the crack wire. It is possible that continuous surveying by an experienced fatigue-test staff might have given earlier crack detection in some cases. The situation for an aircraft on a service inspection is probably not more favorable than in the present investigation.

In Fig. 16 the residual strength is plotted versus the number of cycles to which the panels had been subjected after crack detection. The point within parentheses represents panel 1, which was fatigue cycled until complete failure. The residual strength of the 2.5-mm sheet is thus known as the maximum load of the flight-simulation program, which must have caused the failure. To this

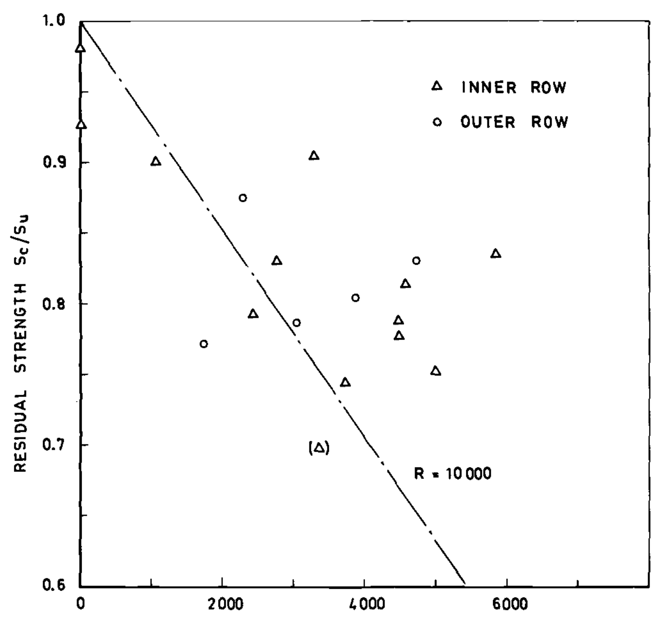

FIG. 16—*Residual strength of panel in static test plotted versus number of flights after detection of critical fatigue crack.*

strength has been added the computed ultimate load taken by the stringers. The straight line, with $R = 10{,}000$ flights or hours, which has been used in the reliability calculations, is also shown in the diagram. The line seems to represent a rather conservative approximation.

An alternative presentation of the residual strength versus crack propagation time has been tried in Fig. 17. The total number of flights, T_L, to which the panel was subjected, has been normalized with respect to the number of flights, T_{c1}, until crack detection. The scatter is somewhat less than in Fig. 16, which seems to indicate a relationship between slow crack propagation and long time to crack initiation. The point-dotted curve which has been obtained by assuming $R = 10{,}000$ flights and $T_{c1} = 10^{\mu_{c1}} = 27{,}000$ flights, seems to form a rather good approximation of the test results for short cracks in the upper part. Longer cracks give a higher residual strength than indicated by the curve, except the very long crack in panel 1 that caused ultimate failure in the fatigue test. It must be remembered, however, that the residual panel strength has been computed in this case, and that the panel further contained two long cracks.

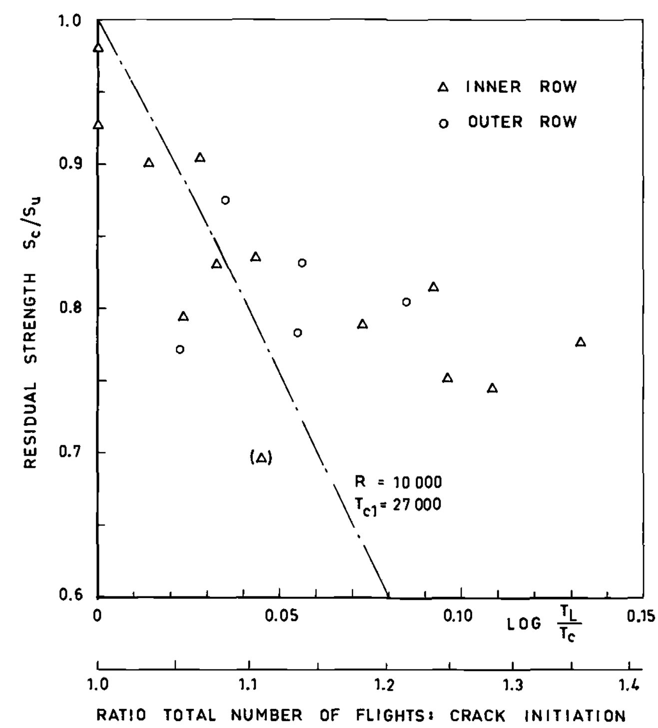

FIG. 17–*Residual strength of damaged panel plotted versus ratio between total number of flights and number of flights to crack detection.*

It seems rather obvious from Fig. 16 that the assumption made in the reliability analysis presented above—namely, that the relationship between the residual strength and the number of flights after crack initiation is a unique function—is not in good agreement with the real conditions. At least the scatter in length of cracks at detection must be included.

Conclusions

The logarithmic mean of the number of flights, or hours of flight, to first crack initiation in a basic wing panel with 32 rivet holes was determined from 17 fatigue tests at a normal stress level to be about 30,000, with a log standard deviation of 0.17. Using log-normal and extreme value distributions, the crack initiation time for a single rivet hole was computed to be 100,000-150,000 flights at 50 percent probability. The median time between the first and the second cracks was estimated at slightly over 10,000 flights, which is probably an exaggerated value.

The relationship between the residual strength of a damaged panel and the crack length was obtained from 19 static tests without much scatter. When the residual strength was plotted as a function of the number of flights after crack initiation, it was not possible to establish a unique relationship, which was due less to the scatter in crack propagation than to the large variation of the length of the cracks at detection. It was concluded, therefore, that this scatter in detectable length must be considered in a reliability analysis of a fail-safe structure.

Acknowledgments

The investigation was supported by the Swedish Board for Technical Development, Stockholm. I also thank Dr. L. E. Jarfall, FFA, for suggesting the design of the test specimens.

References

[*1*] Walker, P. B., *Journal of the Royal Aeronautical Society*, AENJA, Vol. 57, No. 505, Jan. 1953, pp. 12-18.
[*2*] Tye, W., "Philosophy of Airworthiness," AGARD Report 58, Advisory Group for Aeronautical Research and Development, North Atlantic Treaty Organization, Aug. 1956.
[*3*] Fountain, R. S., Munse, W. H., and Sunbury, R. D., *Journal of the Structural Division*, American Society of Civil Engineers, JSDEA, Vol. 94, No. ST12, Dec. 1968, pp. 2751-2767.
[*4*] Asvitt, C. A., Heap, H. F., and Storey, H. L., "Aircraft Structure Sampling Inspection Programs," FAA Maintenance Symposium, *Continued Reliability of Transport-Type Aircraft Structure*, Washington, D.C., Nov. 1966.
[*5*] Rich, M. J. and Linzell, L. E., "Damaged Static and Fatigue Stress Analysis of VTOL Structures," AIAA Paper 69-214, AIAA/AHS VTOL Research, Design and Operations Meeting, Georgia Institute of Technology, Atlanta, Feb. 1969.
[*6*] Ferrari, R. M., Milligan, I. S., Rice, M. R., and Weston, M. R. in *Proceedings*, ICAF-AGARD Symposium on Full Scale Fatigue Testing of Aircraft Structures, Amsterdam, June 1959, Pergamon Press, London, 1961, pp. 413-426.

[7] Heller, A. S., Heller, R. A., and Freudenthal, A. M. in *Fatigue–An Interdisciplinary Approach,* Syracuse University Press, New York, 1964; also, U.S. Air Force Technical Report ML-TDR-64-160, June 1964.
[8] Lardner, R. W., *Journal of the Mechanics and Physics of Solids,* JMPSA, Vol. 14, 1966, pp,141-150.
[9] Yoshimura, T. and Yokobori, T., *Report of the Research Institute on Strength and Fracture of Materials,* Tohoku University, Vol. 3, No. 2, 1967, pp. 95-102.
[10] Lundberg, B. K. O. and Eggwertz, S., "A Statistical Method for Fail-Safe Design with Respect to Aircraft Fatigue," FFA Report 99, Aeronautical Research Institute of Sweden, Stockholm, 1964.
[11] Freudenthal, A. M. and Payne, A. O., "The Structural Reliability of Airframes," AFML-TR-64-401, Air Force Materials Laboratory, Air Force Systems Command, Dayton, Ohio, Dec. 1964.
[12] Stagg, A. M., "An Investigation of the Scatter in Constant Amplitude Fatigue Test Results of Aluminum Alloys 2024 and 7075," ARC CP 1093, Aeronautical Research Council, London, 1970.
[13] Eggwertz, S. and Lindsjö, G., "Analysis of the Probability of Collapse of a Fail-Safe Aircraft Structure Consisting of Parallel Elements," FFA Report 102, Aeronautical Research Institute of Sweden, Stockholm, 1965; also, U.S. Air Force Technical Documentary Report RTD-TDR-63-4210, Feb. 1964.
[14] Eggwertz, S. and Lindsjö, G., "Study of Inspection Intervals for Fail-Safe Structures," FFA Report 120, Aeronautical Research Institute of Sweden, Stockholm, 1970.
[15] Jarfall, L. E., "Optimum Design of Joints: The Stress Severity Factor Concept," *Proceedings of the 5th ICAF Symposium on Aircraft Fatigue–Design, Operational and Economic Aspects,* Melbourne, May 1967.
[16] Schijve, J., Broek, D., de Rijk, P., Nederveen, A., and Sevenhuysen, P. J., "Fatigue Tests with and Without Ground-to-Air Cycles. A Comparative Study on Full-Scale Wing Center Sections," NLR-TR S. 613, National Aerospace Laboratory, Amsterdam, 1965.
[17] Spaulding, E. H. in *Metal Fatigue,* G. Sines and J. L. Waisman, Eds., McGraw-Hill, New York, 1959.
[18] Stone, M. in *Proceedings of the 4th ICAF Symposium on Fatigue Design Procedures,* E. Gassner and W. Schütz, Eds., Pergamon Press, Oxford, 1969.
[19] Stone, M. in *Proceedings of the 6th ICAF Symposium on Advanced Approaches to Fatigue Evaluation,* Miami Beach, May 1971.
[20] Doty, R. J. in *Proceedings of the 6th ICAF Symposium on Advanced Approaches to Fatigue Evaluation,* Miami Beach, May 1971.
[21] Gassner, E. and Jacoby, G., *Luftfahrttechnik-Raumfahrttechnik,* LTRTA, Vol. 11, No. 6, June 1965, pp. 138-148.
[22] Naumann, E. C., "Evaluation of the Influence of Load Randomization and of Ground-Air-Ground Cycles on Fatigue Life," NASA TN D-1584, National Aeronautics and Space Administration, Washington, D.C., 1964.
[23] Schijve, J., Jacobs, F. A., and Tromp, P. J., "Crack Propagation in Aluminum Alloy Sheet Materials under Flight Simulation Loading," NLR-TR 68117, National Aerospace Laboratory, Amsterdam, 1968.
[24] Schijve, J., *Journal of the Royal Aeronautical Society,* AENJA, Vol. 74, No. 714, June 1970, pp. 517-532.
[25] Kaechele, L., "Probability and Scatter in Cumulative Fatigue Damage," Memorandum RM-3688-PR, Rand Corp., Santa Monica, Dec. 1963.
[26] Stagg, A. M., "Scatter in Fatigue: Elements and Sections from Aircraft Structures," Technical Report 69155, Royal Aircraft Establishment, Farnborough, 1969.
[27] Freudenthal, A. M. in *Proceedings of the 5th ICAF Symposium on Aircraft Fatigue–Design, Operational and Economic Aspects,* Melbourne, May 1967.
[28] Heller, R. A. and Heller, A. S., *Annals of Reliability and Maintainability,* ANRMA, Vol. 5, 1966, pp. 722-728, Fifth Annual Conference, ASME/AIAA/SAE/ASTME/ASTM/AIChE/EIA; also, U.S. Air Force Report AFML-TR-66-168, June 1966.

[29] Gumbel, E. J., *Journal of the Engineering Mechanics Division,* American Society of Civil Engineers, JMCEA, Vol. 89, No. EM5, Oct. 1963, pp. 45-63.
[30] Choi, S. C. and Enochson, L. D., "Random Fatigue Test Sampling Requirements," AFFDL-TR-65-95, Air Force Flight Dynamics Laboratory, Research and Technology Division, Air Force Systems Command, Wright-Patterson AFB, Ohio, 1965.
[31] Weibull, W., "Scatter of Fatigue Life and Fatigue Strength in Aircraft Structural Materials and Parts," FFA Report 73, Aeronautical Research Institute of Sweden, Stockholm, 1957.
[32] Weibull, W., "New Methods for Computing Parameters of Complete or Truncated Distributions," FFA Report 58, Aeronautical Research Institute of Sweden, Stockholm, 1955.

A. O. Payne[1]

A Reliability Approach to the Fatigue of Structures

REFERENCE: Payne, A. O., "A Reliability Approach to the Fatigue of Structures," *Probabilistic Aspects of Fatigue, ASTM STP 511*, American Society for Testing and Materials, 1972, pp. 106–155.

ABSTRACT: In recent years, due to the progressive development of higher performance aircraft, the fatigue strength of aircraft structures has become an increasingly important problem.

In the present paper, a method of assessing structural safety in fatigue is proposed in which a statistical model for the fatigue process is used to carry out a reliability analysis, enabling the probability of failure to be estimated at any stage of the life. The statistical variability in crack-propagation rate and residual strength of the cracked structure is included together with the effect of any prescribed inspection procedure.

The method is applied to a structure of high strength steel typifying a "safe-life" structure and to a redundant aluminum alloy structure representative of the "fail-safe" construction.

It is concluded that the reliability analysis can be applied to both fail-safe and safe-life structures and provides a quantitative basis for ensuring their safe operation, including the planning of an inspection procedure if feasible. In this regard the method represents an advance on the existing procedures but inherent in the quantitative approach it employs is the adoption of an acceptable safety level. The most appropriate way of defining safety level is discussed and a suitable measure is proposed. An extensive amount of data is required in applying the procedure but it is suggested that in the case of aircraft structures this difficulty can be overcome by using results from the comprehensive structural testing program normally carried out, together with relevant data from similar structures.

KEY WORDS: fatigue(materials), reliability, statistical analysis, probability theory, distribution theory, failure, quality control, design criteria, structures, structural design

Nomenclature

a Crack length

a_F Crack length for complete collapse under the mean load

[1] Principal Research Scientist, Aeronautical Research Laboratories, Department of Supply, Melbourne, Australia.

$F = \dfrac{P(N)}{V \cdot N}$	Average probability of failure per mile travelled in life N
$F_t(t_1)$†	Probability of a variate t exceeding some particular value t_1
l	Relative crack length $\dfrac{a}{a_F}$
l_D	The minimum crack length detectable by inspection
$\widetilde{l}_N, \widetilde{l}_n$	Median values of the distributions of l at life N and relative life n
$L(n)$	Probability of survival to the life n (also called the Survivorship Function)
$L_F(n), L_S(n), L_I(n), L_I{}^*(n), L_{FT}(n), L_{SL}(n)$	Survivorship Functions at relative life n, corresponding to the risk functions, $r_F(n), r_S(n), r_I(n), r_I{}^*(n), r_{FT}(n), r_{SL}(n)$
N	Life of a structure expressed as a number of load applications
N_i	Life to first formation of a fatigue crack (also called life to initial failure)
$\widetilde{N}_i$	Median of the distribution of N_i
n	Relative life $\dfrac{N}{\widetilde{N}_i}$
n_l	Relative life to crack length l for any structure
$n_{l,Z}$	Life of a structure which has a life Z times the median life at the same crack length l
n_F	Relative life to complete collapse of a structure under the mean load
n_D	Relative life to produce a crack of length l_D
$\widetilde{n}_l, \widetilde{n}_F, \widetilde{n}_D$	Medians of the distributions of n_l, n_F, and n_D
n_S	Relative life corresponding to a particular service life N_S
n_{SL}	Relative safe life calculated by the conventional safe-life philosophy
$n_{I(1)}, n_{I(2)}, n_{I(m)}$	Relative lives to first, second, and m^{th} inspections carried out to detect fatigue cracks
$p_R(R{:}\mu_R)$	Probability-density function of residual strength R with a mean value μ_R
$p_X(X_1)$†	Probability-density function of a variate X at a particular value X_1

† Where no confusion can arise, the subscript for the variate may be omitted.

$P_X(X_1)$†	Probability distribution of a variate X at a particular value $X_1 \cdot P_X(X_1) = Pr\{X \leqslant X_1\}$
$P(N)$	Probability of failure up to the life N
$R(l)$	Strength of a structure containing a fatigue crack of relative length l
$r(N)$	Probability of failure in the remaining fleet at the N^{th} load application, or the risk of failure at life N
$r(n)$	Risk of failure at the relative life n
$r_S(n)$	Risk of static fracture due to fatigue at life n—defined as failure at life n at a fatigue crack in a structure which is still able to sustain an applied service load exceeding the mean load
$r_F(n)$	Risk of fatigue fracture at life n—defined as failure at life n due to a fatigue crack reaching such an extent that the structure is unable to sustain the mean load
$r_{FT}(n)$	The total risk of fatigue failure at the life n $(r_S(n) + r_F(n))$
$r_{SL}(n)$	Risk of failure at the life n as calculated by the conventional "safe-life" procedure
$r_I(n; l_D, n_I)$	Risk of fatigue failure at life n in a population of structures which have all been previously inspected at the life n_I, with an inspection procedure which detects crack lengths greater than l_D
$r_I{}^*(n; l_D, n_I)$	Risk of fatigue failure at life n when cracks of greater length than l_D are detected by inspection at n_I and are then repaired and the structures returned to service
$r_I(n; l_D, n)$	Risk of fatigue failure at the life n when all structures are continuously inspected to detect crack lengths greater than l_D
$r_I(n; l_D, r_{max})$	Risk of fatigue failure at life n with an inspection procedure detecting crack lengths greater than l_D at inspection intervals designed to limit the risk below some specified value r_{max}
$r_D{}^*(n_{I(m)}; l_D, n_{I(m-1)})$	Probability of detecting cracks by inspection at life $n_{I(m)}$ in structures previously inspected at $n_{I(m-1)}$ according to a procedure by which cracks of length greater than l_D are detected and are then repaired and the structures returned to service

$\bar{r}(N)$	The average failure rate up to life N, $\bar{r}(N) = \dfrac{\int_0^N r(n)\cdot dn}{N}$
R_o	Ultimate strength of an uncracked structure
S	An applied service load
S_{ult}	Ultimate design load
S_m	Mean load on the structure
U	Gust velocity
V	Aircraft ground speed
W	Aircraft all-up weight
Y	Relative service load $\dfrac{S}{S_{\text{ult}}}$
μ, σ^2 †	General symbols for mean and variance of a population used with a suffix to denote the variate
μ_0	Mean strength (failing load) of uncracked structures
$\mu_R(l)$	Mean strength of structures containing cracks of length l
$\tilde{l}_n = g(\tilde{n}_l)$	Median crack-propagation curve for the population of structures
$\dfrac{\mu_R(l)}{\mu_0} = \phi(l)$	Mean residual strength expressed nondimensionally as a function of crack length l
$X(l) = \dfrac{R(l)}{\mu_R(l)}$	Relative strength of any structure containing a crack length l
$Z = \dfrac{N_{l,Z}}{\tilde{N}_l}\ \dfrac{n_{l,Z}}{\tilde{n}_l}$	Comparative life, or life factor of a structure with a life to crack length l of Z times the median life to the same crack length

Fatigue has been a major cause of failure in structures and structural components since the early days of fatigue failures in railway rolling stock and wrought iron bridges. However, in recent years, fatigue of airframes has become progressively more important with the continuing trend towards high performance aircraft. This paper is concerned primarily with the fatigue of aircraft structures, but the procedure developed here can be readily applied to structures in general.

In the early days of the aircraft fatigue problem the fatigue life of the structure was estimated and then divided by a scatter factor to give a safe operating life. The scatter factor was used primarily to make allowance for the variability in fatigue life of the fleet and to ensure that the probability of failure was acceptably low.

The disadvantage of this procedure was that a very large percentage of the population (all but the very few structures weak in fatigue) were retired from service long before their useful fatigue life had been reached. This led to the development of the fail-safe philosophy which essentially relied on leaving structures in service until fatigue cracks were detected by a planned inspection procedure before they reached a dangerous extent.

Problems arise with this method, however, in that the structure should have sufficient residual strength to provide safety until cracks are detected and furthermore an inspection procedure is needed to minimize the comprehensive and costly inspections that are carried out. The current airworthiness requirements for operation on the fail-safe principle specify a minimum residual strength for the structure with a detectable crack present. This is a practicable requirement but it takes no account of the progressively increasing risk of static failure due to a growing fatigue crack.

Various efforts have been made to establish the risk of failure as a function of life, but this is a very complex problem requiring extensive data on the static and fatigue strength characteristics of the structure.

One of the early papers on this subject was written by Shaw in 1954[*1*]. An expression for the risk of failure in an inspection interval is derived based on the probability of a structure developing a detectable crack combined with the probability of occurrence of a service load exceeding the corresponding residual strength. The variability in fatigue life and applied service loads are therefore taken into account, but there is no consideration of residual strength or crack-propagation characteristics.

In 1959 Ferrari et al[*2*] developed a procedure for estimating the risk of failure and showed that the current airworthiness requirement of a limit-load residual strength for civil aircraft may be inadequate. Their approach considers the variability in fatigue life to initial cracking and assumes a linear reduction in static strength throughout the succeeding life. The probability of failure under an exponential gust-load spectrum is then derived. This was an advance over Shaw's method, in that a progressive reduction in static strength is postulated but no account is taken of variability in crack-propagation rate or residual strength. A similar approach was developed by Eggwertz[*3*] and was applied to investigate the effect of inspection at constant intervals.

These methods provide a quantitative approach, but they all involve major simplifying assumptions despite the considerable amount of basic data required.

In 1963 Eggwertz and Lindsjö proposed a method in which the structure is replaced by several simple parallel elements[*4*]. As parallel elements fail by fatigue, the load is assumed to be redistributed over the remainder in accordance with the conditions of static equilibrium. From experimental results for a single element, the influence of the load level on time to crack initiation and on the consequent decrease of static strength can be determined. The probability of failure for a gust-load spectrum has been calculated on this basis, assuming a linear decrease in static strength of an element with time but ignoring the statistical variability in the static strength property.

This approach was considerably extended by Heller and Heller[5]. They assume uniform load distribution among all of the parallel members and as members fail, the load on the remainder is increased proportionately. The fatigue life to failure in the various elements is predicted from basic data on a single element, using a reliability analysis which includes the variability in static strength of the elements.

The idealization of the structure as a system of simple parallel elements enables the static and fatigue-strength characteristics to be synthesized from the extensive data that can be readily obtained from tests on a number of single elements. However, the representation of a complex structure by such a system is open to some question.

The failure of a highly redundant aircraft structure under either ultimate load or fatigue-loading conditions usually follows a well defined sequence of events involving a complex load and stress redistribution throughout the structure as failure proceeds.

In the present paper a fully probabilistic approach to the problem is presented which calculates the risk of failure under any prescribed load spectrum, taking account of the variability in static and fatigue strength and the variability in crack-propagation rate. A model of the fatigue process is developed to derive the crack-propagation and residual strength characteristics of the structure from the results of a full-scale fatigue test in conjunction with other representative data.

The Fatigue Process in a Complex Structure

Considering a structure in service subjected to repeatedly applied loads from the service-load spectrum, there will be a period during which the fatigue process leads to the formation of a macroscopic crack. This is called the life to initial failure. The fatigue crack then extends progressively as the life continues with a progressive reduction in the residual strength of the structure as shown in Fig. 1.

During this period there is an increasing probability, at each successive application of a service load, that the structure will fail statically. Failure of a structure in this way is termed here "static fracture by fatigue." However, if the structure continues to survive this risk, the crack will eventually reach some length a_F, at which failure will occur under the steady mean load. (In practice, the crack-propagation curve becomes so steep that it is almost vertical, at which stage the residual strength falls to the mean load and failure occurs.) This is termed "fatigue fracture" to distinguish it from "static fracture by fatigue" which is dependent on the chance occurrence of a service load exceeding the static strength.

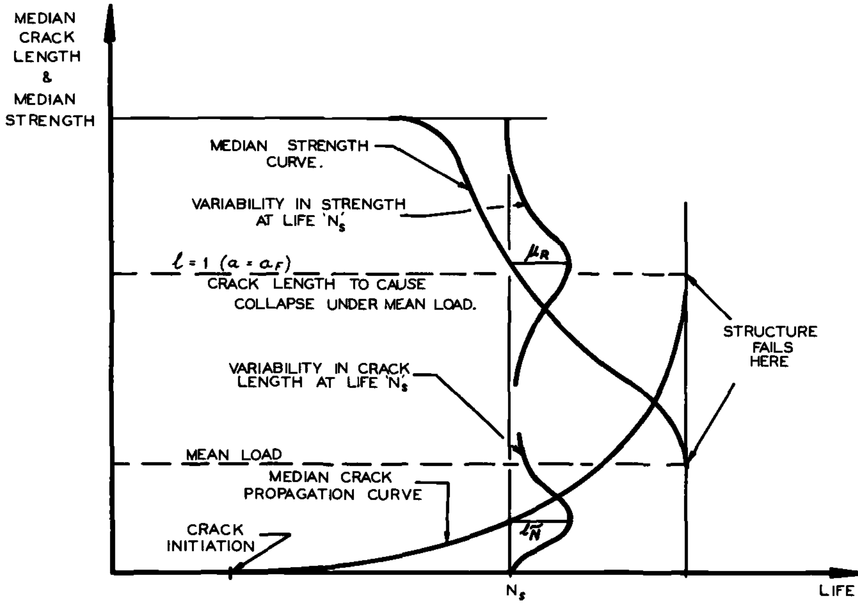

FIG. 1—*The risk of structural failure by fatigue.*

Although fatigue fracture could also be regarded as static failure of the structure under the mean load, it is essentially a failure due to the fatigue process itself. It is instructive to identify these two risks and consider them separately since they give some physical insight into the problem especially as regards the significance of the fail-safe and safe-life philosophies and the influence of an inspection procedure.

Consider a structure cracked to some crack length a which may be expressed nondimensionally as a relative crack length $l = a/a_F$. If the residual strength of the structure is $R(l)$ the probability of static fracture by fatigue under a load from the service-load spectrum $F_S(S)$ is given by $F_S\left\{R(l)\right\}$, where $F_S(S)$ is the probability of exceeding a service load S.

If we now look at all members of the population at any particular service life N_S, we will find a variation in their residual strength due to the following causes: (1) variability in fatigue performance resulting in structures being cracked to a varying extent and; (2) variability in the static strength of structures all cracked to the same extent.

The evaluation of the risk of static failure by fatigue must therefore take into account the variability in the residual strength of a structure due to these two causes. As discussed in the Appendix these two sources of variation may be assumed to be statistically independent.

Variability in Fatigue Performance

Considering the complete population of structures, there is a complete series of crack propagation curves as shown in Fig. 2 ranging from structures very weak in fatigue to those very strong in fatigue. At any particular service life there is therefore a probability distribution of crack length or, correspondingly, at a given crack length there is a probability distribution of fatigue life.

As discussed in the Appendix a survey of data on fatigue crack propagation supports the assumption of a log-normal distribution of fatigue life N_l at a constant crack length l, having a characteristic variance which is independent of the crack length. That is,

$$\log N_l \sim N(\log \widetilde{N}_l, \sigma_{\log N}{}^2) \tag{1}$$

where $\widetilde{N}_l$ is the median fatigue life to a crack length of l and $\sigma_{\log N}{}^2$ is the variance of $\log N$ and is the same for all values of l.

It is also shown in the Appendix that it follows from the above assumption that the fatigue life $N_{l,\,Z}$ of any particular structure in the population bears a constant ratio to the median fatigue life $\widetilde{N}_l$ at the same crack length as illustrated in Fig. 2.

That is to say, if we consider the median crack-propagation curve $l = g\left(\dfrac{\widetilde{N}_l}{\widetilde{N}_i}\right)$

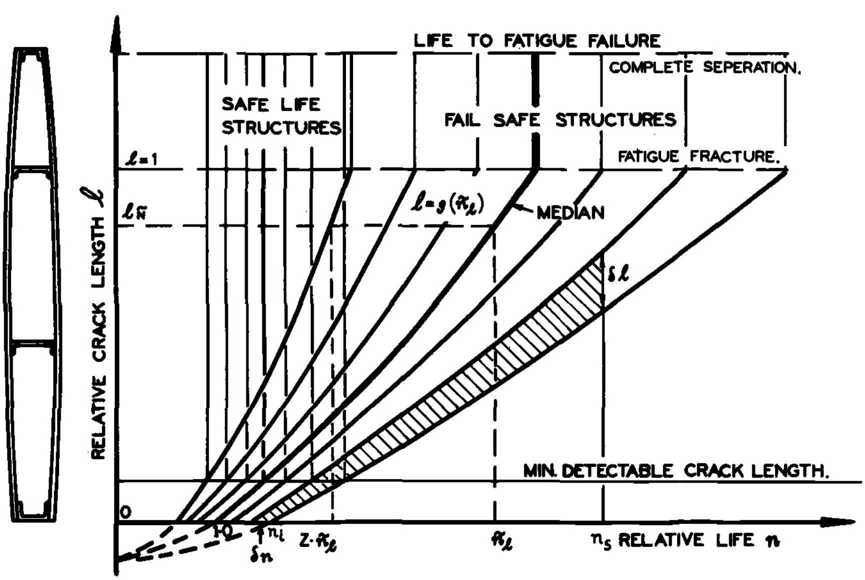

FIG. 2—*Model of the fatigue process.*

relating the crack length l to the median life $\widetilde{N}_l$, then the life of any particular structure in the population will bear a constant ratio to the median life, $\widetilde{N}_l$, at the same crack length for all points on the crack-propagation curve.

This ratio is called here the life factor Z and if the life of the structure is denoted by $N_{l,\ Z}$ it follows that for all values of l,

$$N_{l,\ Z} = Z \cdot \widetilde{N}_l \tag{2}$$

As stated in the Appendix, this model of the crack propagation behavior is supported by test data on both steel and aluminum alloy specimens.

Variability in the Static Strength Property

The mean of the residual strength $\mu_R(l)$ is a decreasing function of the crack length and it is assumed in this analysis that at any crack length l the residual strength $R(l)$ has a characteristic distribution about the mean value $\mu_R(l)$. In other words, it is assumed that the relative residual strength $X = \dfrac{R(l)}{\mu_R(l)}$ has the same distribution function at all values of crack length l. This infers that the variability in residual strength is mainly due to the variability in material properties and the variations in manufacture. There is experimental evidence to show that this is a realistic assumption as discussed in the Appendix.

Application to Reliability Analysis

With the model of the fatigue process developed above, it is possible to derive the risk of static fracture by fatigue and the risk of fatigue fracture, together with the corresponding survivorship functions. This is done by a reliability analysis in the following section.

Derivation of the Risk and Survivorship Functions

The model of the fatigue process developed above is assumed to apply, together with the assumptions discussed in the Appendix.

Static Fracture due to Fatigue

To derive the risk of static fracture due to fatigue, at any life N consider first those members of the population which are all cracked to some specific crack length l. The residual strength $R(l)$ of these structures will have a probability distribution with a mean value $\mu_R(l)$ and the probability of failure at the N^{th} load from a load spectrum $F_S(S)$ may be derived using the classical reliability approach.

Pr $\{$ Failure at the N load in structures with mean strength $\mu_R(l)$ $\}$
$= Pr$ $\{$ $R \leqslant S$ in all structures with crack length l at life N $\}$

$$= r(N/\mu_R(l)) = \int_0^\infty p_R(R\colon \mu_R)\cdot F_S(R)\cdot dR \tag{3}$$

where $r(N/\mu_R(l))$ is the risk of failure at life N in those structures which have a mean residual strength $\mu_R(l)$ and $p_R(R\colon\mu_R)$ is the probability-density function of residual strength R with a mean value μ_R.

It is now convenient to express quantities nondimensionally; R is transformed to the dimensionless variate $X = R/\mu_R$ which is the relative residual strength and is assumed here to have the same probability-density function at all crack lengths; the service life or number of service-load applications N is expressed in terms of the median life to initial failure $\tilde{N}_i$ to give the relative life $n = N/\tilde{N}_i$; the crack length, a, has already been expressed as the relative crack length $l = a/a_F$ where a_F is the crack length at which the structure will collapse under the mean load.

With this nomenclature and taking $p(R)\cdot dR = p(X)\cdot dX$, we can rewrite Eq 3 for the risk of failure of structures with crack length l at a particular service life n_S, as

$$r\left\{n_S/\mu_R(l)\right\} = \int_0^\infty p_X(X)\cdot F_S(X\cdot\mu_R)\cdot dX \tag{4}$$

It is assumed that $p_X(X)$ applies for all values of l (see Appendix), but the mean residual strength $\mu_R(l)$ must be a known function of the relative crack length l.

$$\mu_R(l) = \mu_0\cdot\phi(l) \tag{5}$$

where μ_0 is the mean strength in the uncracked condition of all structures in the population.

Substituting in Eq 4 gives -

$$r\left\{n_S/\mu_R(l)\right\} = \int_0^\infty p_X(X)\cdot F_S\left[X\mu_0\cdot\phi(l)\right]dX$$

To derive the total risk of failure at n_S, it is necessary to integrate over all relative crack lengths between 0 and 1.

Then

$$r\left\{n_S\right\} = \int_0^1\int_0^\infty p_X(X)\cdot F_S\left[X\cdot\mu_0\cdot\phi(l)\right]\cdot p(l)\cdot dl\cdot dX \tag{6}$$

We now transpose the variate of crack length l to one of fatigue life for which the probability density function is known. By reference to Fig. 2 it can be seen by considering the shaded element representing crack lengths between l and $(l + dl)$ that the structures which have crack lengths between l and $(l + dl)$ at life n_S are those which have fatigue life to initial failure between n_i and $(n_i + dn_i)$ (neglecting any effect on the probability density function of n_i due to the very few structures that have failed between their initial life and the life n_S). That is,

$$p(l)\cdot dl = -p(n_i)\cdot dn_i = -p\left(\frac{N_i}{\tilde{N}_i}\right)\cdot d\left(\frac{N_i}{\tilde{N}_i}\right)^{\dagger\dagger}$$

$$= -p(Z)\cdot dZ$$

Hence, instead of the crack length l at life n_S we consider the corresponding life to initial failure, taking

$$n_i = \frac{n_S}{\tilde{n}_F} \text{ at } l = \frac{a_F}{a_F} = 1 \text{ for the lower limit of integration}^{\dagger\dagger}$$

and

$$n_i = n_S \text{ at } l = \frac{0}{a_F} = 0 \text{ for the upper limit of integration.}^{\dagger\dagger}$$

Now using the equation for the median crack-propagation curve

$$l = g(\tilde{n}_l) = g\left(\frac{n_l}{Z}\right) \tag{7}$$

we can transform the variate from l to n_i in Eq 6.

$$r_S(n_S) = \int_{\frac{n_S}{\tilde{n}_F}}^{n_S} \int_0^{\infty} p_X(X)\cdot F_S\left\{X\cdot\mu_0\cdot\phi\left[g\left(\frac{n_S}{Z}\right)\right]\right\} p_Z(Z)\cdot dX\cdot dZ \tag{8}$$

where r_S is used with the subscript S to denote the risk of static fracture due to fatigue.

The corresponding probability of survival for static fracture due to fatigue can then be calculated from the basic relationship [6].

$$L(n_S) = e^{-\int_0^{n_S} r(n)\cdot dn}$$

†† A change of sign is introduced because increasing values of l correspond to structures with decreasing values of life to initial failure, n_i.

Hence

$$L_S(n_S) = \exp\left[-\int_{n=0}^{n=n_S} \int_{z=\frac{n}{\tilde{n}_f}}^{z=n} \int_{x=0}^{x=\infty} F_S\left\{X\mu_0\phi\left[g\left(\frac{n}{Z}\right)\right]\right\} p(X)\cdot p(Z)\cdot dX\cdot dZ\cdot dn\right] \tag{9}$$

Fatigue Fracture

Reference to Fig. 3 shows that at the service life n_S those structures with lives to initial failure n_i less than $n_S/\tilde{n}_F$ would have cracked to the extent of $l = 1$ corresponding to failure under the mean load. Therefore, if we again neglect the effect on the probability density function of n_i of structures that fail by static fracture due to fatigue, the probability of survival for fatigue fracture at n_S is given by

$$L_F(n_S) = 1 - \int_0^{n_S/\tilde{n}_F} p(n_i)\cdot dn_i$$

$$= 1 - \int_0^{n_S/\tilde{n}_F} p(Z)\cdot dZ$$

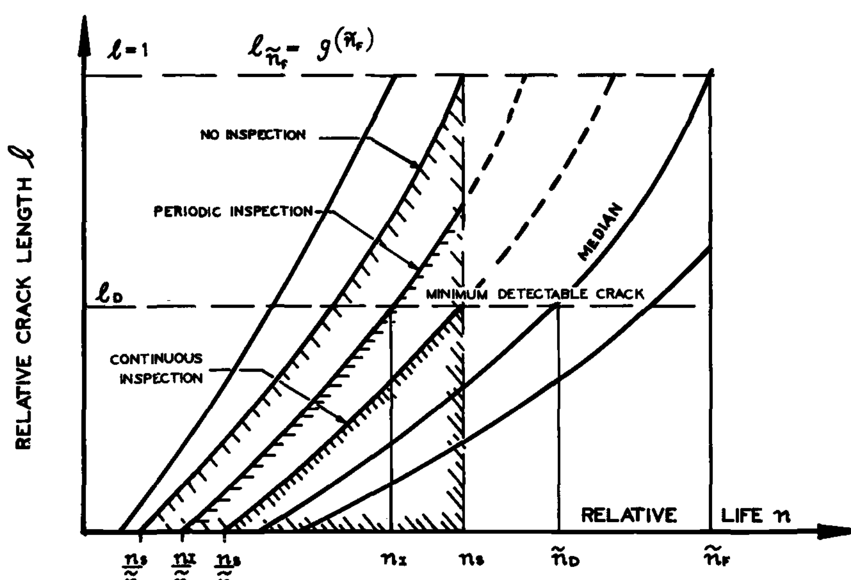

FIG. 3 –*Integration of risk function for various inspection procedures.*

since $Z = N_i/\widetilde{N}_i = n_i$ or

$$L_F(n_S) = \int_{n_S/\tilde{n}_F}^{\infty} p(Z)\cdot dZ \tag{10}$$

and the risk of fatigue fracture,

$$r_F(n_S) = \frac{p_Z\left(\frac{n_S}{\tilde{n}_F}\right)}{\int_{n_S/\tilde{n}_F}^{\infty} p_Z(Z)\cdot dZ} \tag{11}$$

Total Risk of Fatigue Failure

In the model proposed here a structure can fail either by static fracture due to fatigue or, if it survives this risk, it will fail by fatigue fracture. Static fracture due to fatigue and fatigue fracture are therefore regarded as two separate events and the total risk of fatigue failure is given by the sum of the two separate risks.

$$r_{FT}(n_S) = r_S(n_S) + r_F(n_S) \tag{12}$$

The corresponding probability of survival can be similarly calculated.

$$L_{FT}(n_S) = L_S(n_S)\cdot L_F(n_S) \tag{13}$$

The Effect of Inspection

The effect on the risk of failure of various inspection procedures in service can be investigated by using the expressions for the risks derived above.

Continuous Inspection

Consider the case where every structure is continuously inspected by an inspection technique which detects cracks exceeding a certain detectable length l_D corresponding to a life $\tilde{n}_D$ on the median crack-propagation curve.

As soon as cracks reach the detectable length l_D the structure is taken out of service and therefore fatigue fracture is prevented so the risk of fatigue fracture is zero.

The only risk of fatigue failure is therefore the risk of static fracture due to fatigue at crack lengths between 0 and l_D (Fig. 3). In practice, when cracks are detected they are usually repaired and the structures are restored to service. In this event there is no depletion of the fleet by the inspection process and the risk of static fracture by fatigue can be obtained directly from Eq 6 by integrating between limits $l = 0$ to $l = l_D$. By reference to Fig. 3 it can be seen that this corresponds to integrating from $Z = n_S/\tilde{n}_D$ to $Z = n_S$ in Eq 8 and hence

$$r_I^*(n_S; l_D, n_S) = \int_{n_S/\tilde{n}_D}^{n_S} \int_0^{\infty} F_S\left\{ X \cdot \mu_0 \cdot \phi \left[g\left(\frac{n_S}{Z}\right)\right]\right\} p(X)p(Z)dX \cdot dZ \qquad (14)$$

where $r_I^*(n_S; l_D, n_S)$ denotes the risk of failure, with repair, of detectable cracks. (In this nomenclature $r_I(n_S; l_D, n_I)$ is the risk of failure at n_S, following an inspection to detect cracks of length l_D at the life n_I.) The probability of detecting cracks at the life n_S is given by

$$r_D^*(n_S; l_D, n_S) = p_Z\left(\frac{n_S}{\tilde{n}_D}\right) \qquad (15)$$

Where cracked structures are not repaired but are retired from service the probability distribution of fatigue life to initial failure suffers a significant truncation at $n_S/\tilde{n}_D$ as can be seen by reference to Fig. 3.

Since the risk of failure at n_S is the probability of failure in the population remaining at n_S it can be obtained for this case from Eq 14 by dividing by the normalizing factor

$$\int_{\frac{n_S}{\tilde{n}_D}}^{\infty} p(Z) \cdot dZ$$

to allow for the truncation of the distribution.

$$r_I(n_S; l_D, n_S) = \frac{r_I^*(n_S; l_D, n_S)}{\int_{\frac{n_S}{\tilde{n}_D}}^{\infty} p(Z) \cdot dZ}$$

$$= \frac{\int_{\frac{n_S}{\tilde{n}_D}}^{n_S} \int_0^{\infty} F_S\left\{X\mu_0\phi\left[g\left(\frac{n_S}{Z}\right)\right]\right\} p(X)p(Z)dXdZ}{\int_{\frac{n_S}{\tilde{n}_D}}^{\infty} p(Z) \cdot dZ} \qquad (16)$$

The probability of detecting cracks at the life n_S is now given by

$$r_D(n_S; l_D, n_S) = \frac{p_Z\left(\frac{n_S}{\tilde{n}_D}\right)}{\int_{\frac{n_S}{\tilde{n}_D}}^{\infty} p(Z)\cdot dZ} \tag{17}$$

Periodic Inspection

In practice it is usually not feasible to inspect structures continually but inspections are carried out at a series of lives $n_{I(1)}$, $n_{I(2)}$. . . . Until the first inspection at $n_{I(1)}$, the conditions in the fleet are the same as for no inspection. Cracks initiate and grow undetected and the risks of static fracture by fatigue, and fatigue fracture, are given by Eqs 8 and 11, respectively.

When an inspection is made at $n_{I(1)}$, however, all structures with cracks exceeding a length of l_D are eliminated and at this stage the conditions in the population are the same as for continuous inspection.

Therefore, taking the practical case where structures are repaired and returned to service, the risk of static fracture by fatigue at the time of the first inspection at $n_{I(1)}$ is obtained from Eq 14.

$$r_I^*(n_{I(1)}; l_D, n_{I(0)}) = \int_{\frac{n_{I(1)}}{\tilde{n}_D}}^{n_{I(1)}} \int_0^{\infty} F_S\left\{X\cdot\mu_0\cdot\phi\left[g\left(\frac{n_{I(1)}}{Z}\right)\right]\right\} p(X)p(Z)dXdZ \tag{18}$$

However, as the service life proceeds beyond $n_{I(1)}$, cracks grow unchecked and at some later life n_S as shown in Fig. 3 the risk of static fracture is obtained by integrating over the cracked structures which have lives to initial failure ranging from $n_{I(1)}/\tilde{n}_D$ to n_S.

Hence

$$r_I^*(n_S; l_D, n_{I(1)}) = \int_{\frac{n_{I(1)}}{\tilde{n}_D}}^{n_S} \int_0^{\infty} F_S\left\{X\cdot\mu_0\cdot\phi\left[g\left(\frac{n_S}{Z}\right)\right]\right\} p(X)\cdot p(Z)\cdot dXdZ \tag{19}$$

However, it will be seen by reference to Fig. 3 that if the service life n_S continues to $(n_{I(1)}/\tilde{n}_D)\cdot n_F$, the structures with life to initial failure of $n_{I(1)}/\tilde{n}_D$ have developed cracks to the full length $l = 1$. At this stage the risks of failure in the fleet have become the same as if no inspections had been made.

Therefore, with periodic inspections the risk of static fracture by fatigue $r_S(n)$ and the risk of fatigue fracture $r_F(n)$ increase as for no inspection until the first inspection is made at $n_{I(1)}$. The risk of static fracture by fatigue is reduced at the first inspection to the same value as for continuous inspection. As the life continues beyond this, however, cracks will extend past the detectable length l_D and the risk of static fracture will rise again and if another inspection is not carried out it will become equal to the value of the risk for no inspection at a life $(n_{I(1)}/\tilde{n}_D)\cdot\tilde{n}_F$.

The risk of fatigue fracture remains zero after the first inspection until the life $(n_{I(1)}/\tilde{n}_D)\cdot\tilde{n}_F$ is reached when it rises to the value corresponding to the no inspection case. This behavior is illustrated in Fig. 3.

It can be seen therefore that although the probability of survival is improved by periodic inspection, the risk of failure can fluctuate between the risk for continuous inspection and the risk for no inspection. In general it is necessary to limit the risk of failure since exposure to a high risk even for a short time is to be avoided.

The maximum inspection interval that will ensure some reduction in risk at all times is that corresponding to the situation where cracks with length just short of l_D at the first inspection at $n_{I(1)}$ have just reached the full length $l = 1$ at the next inspection at $n_{I(2)}$.

It follows from the above that

$$n_{I(2)} = n_{I(1)}\cdot\frac{\tilde{n}_F}{\tilde{n}_D} \tag{20}$$

Therefore for this condition the inspection times form a geometric progression with progression ratio $\tilde{n}_F/\tilde{n}_D$.

Inspection for Limited Risk

For safety reasons it may be necessary to maintain the risk or failure rate below a certain acceptable value at all times. This provides a basis for planning the inspection intervals which must now be chosen so that the risk of failure fluctuates between the risk for continual inspection and a specified maximum value. Provided the specified value of risk exceeds the risk under continuous inspection, the procedure is always possible, although it may require frequent inspections. (An example will be discussed in the section on Application to Fail-Safe and Safe-Life Structures and is shown there in Fig. 13.)

Probability of Structures Being Eliminated by Periodic Inspection

It is of interest to consider the probability of cracks being detected at each inspection since this gives the fraction of the fleet that can be expected to require repair and modification before continuing in service.

Reference to Fig. 3 shows that at the first inspection all structures with crack lengths between $l = l_D$ and $l = 1$ are eliminated by the inspection. This corresponds to structures being eliminated with initial lives between $n_{I(1)}/\tilde{n}_D$ and $n_{I(1)}/\tilde{n}_F$.

Hence the fraction of the population in which cracks are detected at the first inspection is given by

$$r_D{}^*(n_{I(1)}; l_D, n_{I(0)}) = \int_{\frac{n_{I(1)}}{\tilde{n}_D}}^{\frac{n_{I(1)}}{\tilde{n}_F}} p(Z) \cdot dZ \tag{21}$$

Similarly for the m^{th} inspection, provided that the inspection intervals are short enough to limit at all times the risk of failure below the risk of failure for no inspection, the probability of elmination of structures is given by

$$r_D{}^*(n_{I(m)}; l_D, n_{I(m-1)}) = \int_{\frac{n_{I(m-1)}}{\tilde{n}_D}}^{\frac{n_{I(m)}}{\tilde{n}_D}} p(Z) \cdot dZ \tag{22}$$

Calculation of the Probability of Survival

With the data and assumptions referred to above, the risks of static fracture due to fatigue and fatigue fracture can be evaluated as functions of life from Eqs 8 and 11. The total risk of fatigue failure and the corresponding probability of survival are then evaluated according to Eqs 12 and 13.

If an inspection procedure is applied, the risk of failure is given by the risk of static fracture. For continuous inspection the risk of failure is given by Eq 14 or Eq 16 according to whether or not there is repair and replacement of structures in which cracks are detected. With periodic inspection at specified times $n_{I(m)}$, the risk of failure is given by $r_I{}^*(n_S; l_D, n_{I(m)})$ in the case of replacement (by substituting $n_{I(m)}$ for $n_{I(1)}$ in Eq 19).

The corresponding probabilities of survival can be calculated as before from the appropriate risk function.

$$L(n_S) = e^{-\int_0^{n_S} r(n) \cdot dn}$$

The probability of cracks being detected at the m^{th} inspection at life $n_{I(m)}$ follows from Eq 22 and is given by

$$r_D{}^*(n_{I(m)}; l_D, n_{I(m-1)}) = \int_{\frac{n_{I(m-1)}}{\tilde{n}_D}}^{\frac{n_{I(m)}}{\tilde{n}_D}} p(Z) \cdot dZ$$

assuming that the number of structures that fail is small compared to the number in which cracks are safely detected.

The main difficulties in evaluating the risk functions are to obtain the basic data required and to evaluate the difficult integrals involved. With the modern digital computer the second difficulty can be largely overcome and a procedure has been developed which enables these double integrals to be evaluated quite efficiently [7].

The data required for a complex structure are usually difficult to obtain and the method proposed here is to use representative data from other structures in conjunction with test data obtained on the actual structure in the course of the initial design proving tests.

Input Data

The following input data are required in evaluating the risk and survivorship functions.

(1) The load spectrum $F_S(S)$ defining the probability of exceeding the service load, S.

(2) The average ultimate strength, μ_0.

(3) The average residual strength, $\mu_R(l)$.

(4) The probability distribution $P_X(X)$ of the relative strength $X = R/\mu_R$ which is assumed to apply at any crack length.

(5) The median crack-propagation curve for the population of structures $l_n = g(\widetilde{n}_l)$.

(6) The probability distribution $P_Z(Z)$ of the comparative life or life factor $Z = n_{l,\ Z}/\widetilde{n}_l$, which is assumed to apply at any crack length l.

(7) The limits of integration for the risk function. These are determined by the end points of the crack-propagation curve and by the inspection procedure applied.

Calculation for Typical Aircraft Structures

Because of the requirement for minimum weight and the extensive prototype testing now undertaken in the design of aircraft, it offers considerable scope for the application of reliability analysis. The foregoing procedure will now be applied to the estimation of safe operating conditions for typical cases in the aeronautical field.

Two different types of aircraft structures are considered—a high tensile steel monolithic structure typical of a safe-life design on the one hand and a redundant aluminum alloy structure typical of the fail-safe construction on the other. For each type of structure two quite different service conditions are considered, ranging from the military fighter aircraft role to civil air carrier operation.

Typical Structures—Details of the two types of structure considered are as follows:

Structure A is a high-strength steel, nonredundant structure with an average

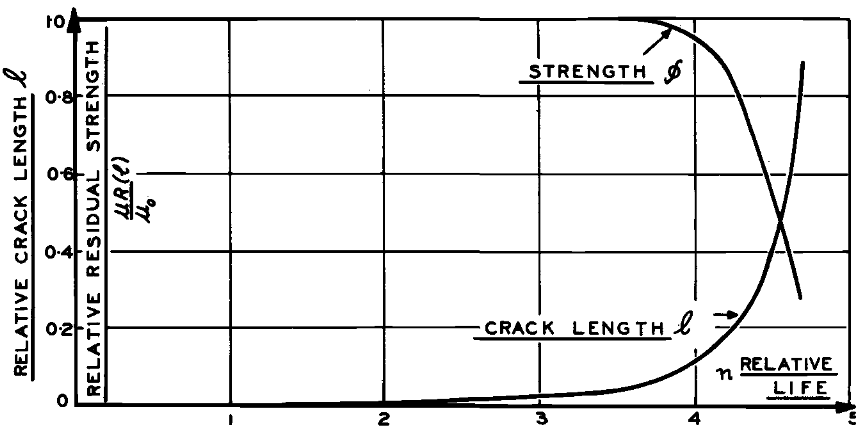

FIG. 4—*Fatigue characteristics of high strength steel structure (type A).*

critical crack length, a_F, to failure under the mean load of approximately 1g. A typical crack-propagation curve obtained from a full-scale fatigue test on such a structure is shown in Fig. 4 and this has been used to obtain the residual strength curve shown, using the relationship

$$l = \frac{a}{a_F} = \frac{A}{\left(\frac{\mu_R}{\mu_0}\right)^2}$$

based on fracture-mechanics theory. A is a constant dependent on the fracture toughness of the material, and can be estimated from the failing load of the structure tested to destruction in the fatigue test. Data on the variability in residual strength were obtained from a large sample of results from ultimate tensile strength tests on a high strength structural steel [*8*].

These data expressed in terms of the dimensionless variate R/μ_R have been fitted by the three parameter Weibull distribution:

$$P_X(X) = 1 - \exp - \left\{\frac{X - 0.824}{1.017 - 0.824}\right\}^{2.55}$$

The distribution of fatigue life to final failure is assumed to be logarithmic normal with a variance of $\sigma_{\log}{}^2{}_N = 0.02$ and in accordance with the model of the fatigue process proposed above it is assumed to apply at any given crack length l.

The residual strength relationship

$$\frac{\mu_R}{\mu_0} = \phi[g(\widetilde{n}_l)] = \phi\left[g\left(\frac{n_l}{Z}\right)\right]$$

was obtained directly from Fig. 4 and put into the digital computer as a set of ordered pairs $\left(\frac{\mu_R}{\mu_0}, \widetilde{n}_l\right)$. If the structure were operated on the safe-life principle, inspection would not be relied on; but to enable the reliability analysis to be carried out including an investigation of the effect of inspection, a detectable crack length of $l_D = 0.40$ was adopted. This corresponds to the critical crack length for limit load on the structure and gives a crack length of 0.40 in. and a crack depth of 0.20 in. for a semicircular crack. These crack dimensions would be near the lower limit of positive detection by normal in-service inspections using current techniques.

Structure B is a redundant aluminum alloy structure typical of the fail-safe construction, for which representative data have been taken from extensive fatigue investigations on aluminum alloy wings conducted at the Aeronautical Research Laboratories (ARL)[9]. A functional relationship was derived for the crack-propagation curve as shown in Fig. 5. The ARL results were pooled with

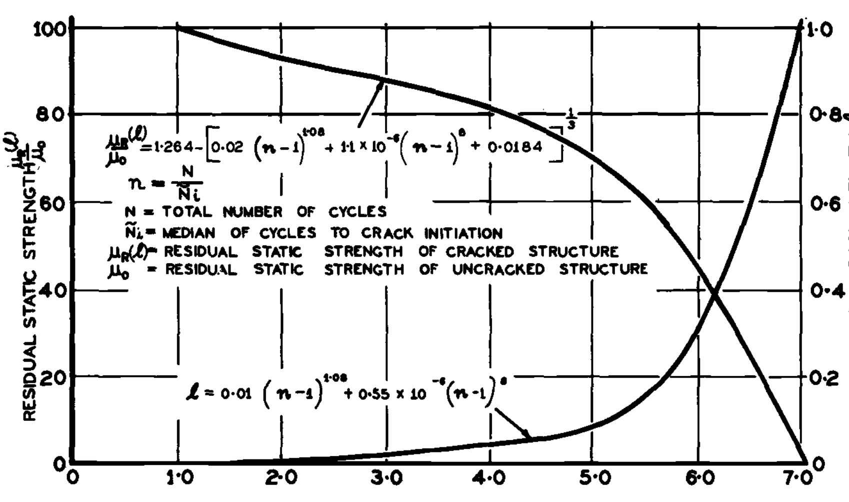

FIG. 5–*Fatigue characteristics of aluminum alloy structure (type B).*

residual strength data from similar structures to obtain a characteristic relationship for residual strength in terms of crack length.

$$\frac{\mu_R(l)}{\mu_0} = \phi\left(\frac{l}{l_0}\right)$$

A normal distribution has been assumed for the residual strength expressed as $R(l)/\mu_R(l) = X$, with a standard deviation $\sigma_X = 0.04$, by reference to the results of an analysis of representative data in Ref *10*. A log-normal distribution of fatigue life has been assumed with a standard deviation $\sigma_{\log N} = 0.20$ and as before this is assumed to apply to the fatigue life for any given crack length l. In this case the mathematical expressions for crack length $l = g(\widetilde{n}_l)$ and average residual strength $\mu_R/\mu_0 = \phi(l)$ are incorporated in the computer program for the evaluation of the risk function.

A detectable crack length of $l_D = 0.021$ has been adopted corresponding to a crack 3 in. long in a wing structure having a 12-ft effective chord.

Typical Loading Conditions—Details of the two service-load spectra are as follows:

Spectrum I is derived from load-frequency data on American jet fighter operations presented by Mayer and Hamer[*11*] in the form of a relative frequency distribution of $\Delta n/\Delta n_L$, where Δn is the incremental acceleration due to a service load S, and Δn_L is the incremental acceleration for limit load.

These data have been expressed in terms of a relative service load $Y = S/S_{\text{ult}}$.

The applied service load $S = (1 + \Delta n)W$, where W is the all-up weight.

The ultimate design load $S_{\text{ult}} = 1.5(1 + \Delta n_L)W$, where 1.5 is the ultimate design load factor.

Hence

$$Y = \frac{1 + \Delta n}{(1 + \Delta n_L)1.5}$$

and the corresponding service load spectrum is shown in Fig. 6 as a relative frequency distribution of Y.

Mayer and Hamer[*11*] also give typical values of load counts per hour for various aircraft types from which an average figure of ten positive load peaks per hour has been taken.

Since the nondimensional life $n = N/\widetilde{N}_i$ is used in this analysis,[2] the number of load counts in the median life to initial failure $\widetilde{N}_i$ is required when using the load spectrum in Fig. 5 since this gives the relative frequency of occurrence of

[2] The various risk functions have been expressed in terms of the dimensionless variate Z but they are compared on a common basis in the figures using the relative life $n = N/\widetilde{N}_i$.

each load. A life of 2000 h is assumed typical of this type of aircraft, giving a total of 20,000 load counts in the median life to initial failure.

Spectrum II has been based on results from the National Advisory Committee for Aeronautics investigations on gust frequencies in thunderstorms [*12*] where the probability of exceeding a given gust velocity U is expressed by

$$F_U(U) = e^{-0.197U}$$

Adopting the normally specified 99 fps gust as the ultimate design-load condition, it follows that

$$\frac{U}{99} = \frac{S - S_m}{S_{\text{ult}} - S_m}$$

where S_m is the mean load, S_{ult} the ultimate design load for the structure, and S is the service load corresponding to an up-gust U.

Assuming that a mean load of 20 percent of the ultimate is representative of a civil transport,

$$U = 124\left(\frac{S}{S_{\text{ult}}} - 0.2\right)$$

$$= 124\,(Y - 0.2)$$

transposing to the relative service load $Y = S/S_{\text{ult}}$. This leads to $F_Y(Y) = e^{-24.4(Y-0.2)}$ as shown in Fig. 6.

Tolefson [*12*] lists the total frequency of occurrence of gusts for the thunderstorm gust spectrum as a function of altitude. From these data an average frequency of two thunderstorm gusts (including both up-gusts and down-gusts) per hour has been taken, corresponding to operation at an altitude between 20,000 and 40,000 ft at 400 to 500 mph. Since upward loads are those causing static fracture by fatigue, this corresponds to one load per hour. Assuming $\tilde{N}_i = 20{,}000$ h as a realistic figure for this type of aircraft operation, there would be a total of 20,000 loads in the median life to initial failure.

Calculation of Risk and Survivorship Functions

The computer program developed by Mallinson [7] enables the risk functions to be evaluated for static fracture due to fatigue and for fatigue fracture as given in Eqs 8 and 11, respectively. This has been done for each type of structure (A and B) and each type of load spectrum (I and II), giving four cases, A-I, A-II, B-I, B-II, and the results are shown in Figs. 7 to 10. The corresponding probabilities of survival are compared in Fig. 11.

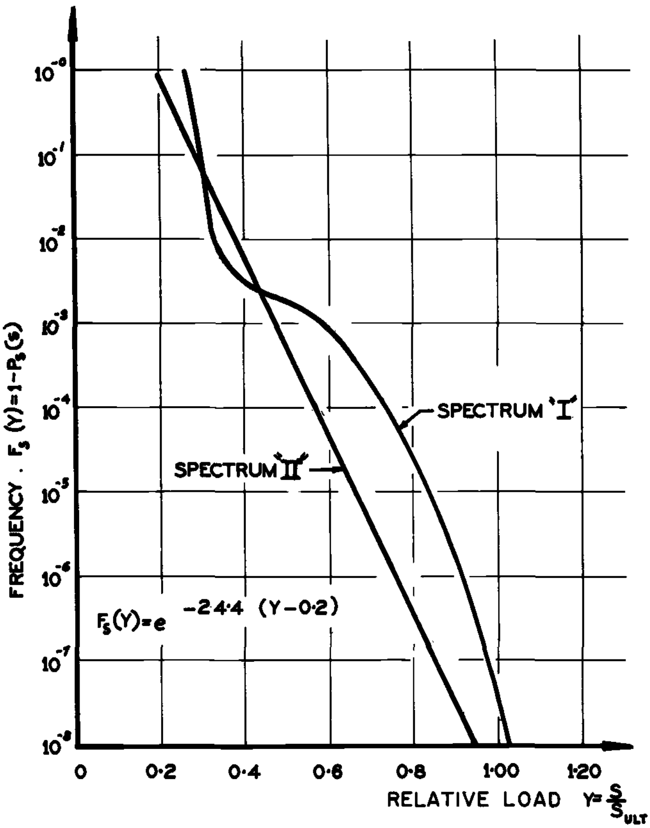

FIG. 6—*Load spectra.*

These four cases have been selected to test various aspects of the method. A wide range of service load spectra and crack propagation characteristics is represented and the range of life considered is, for the no-inspection condition, well beyond the limits that would apply, for the safety levels acceptable in service.

The risk function r_I for the optimum condition of continuous inspection has been evaluated in each case together with the probability of crack detection r_D and these results are also plotted for comparison with the risk functions for no inspection. It can be seen from these comparisons that the increase in safety level achieved by inspection is much greater for the highly redundant type B structure than for the type A structure. The effect of inspection for this case is studied further in Figs. 12 and 13. In Fig. 12 the effect on the risk function of inspection with repair and replacement is shown for case B-I by plotting r_I*

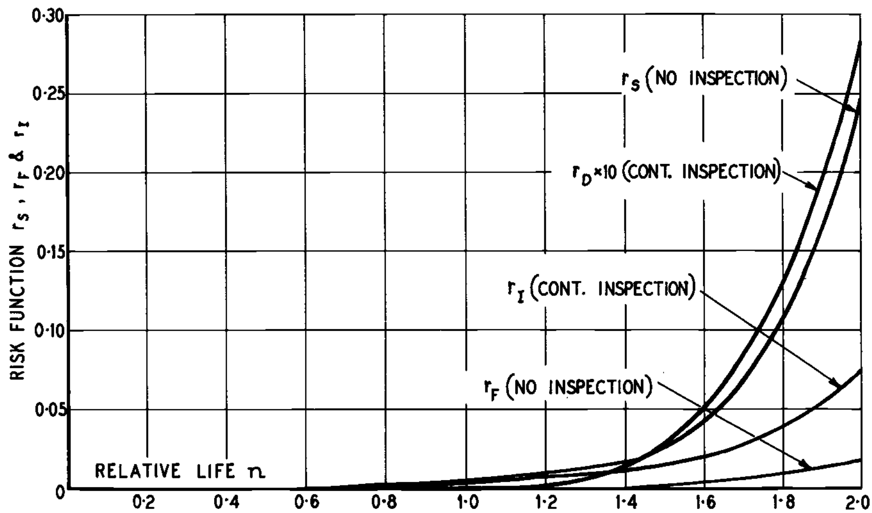

FIG. 7—*Risk function, case A-I.*

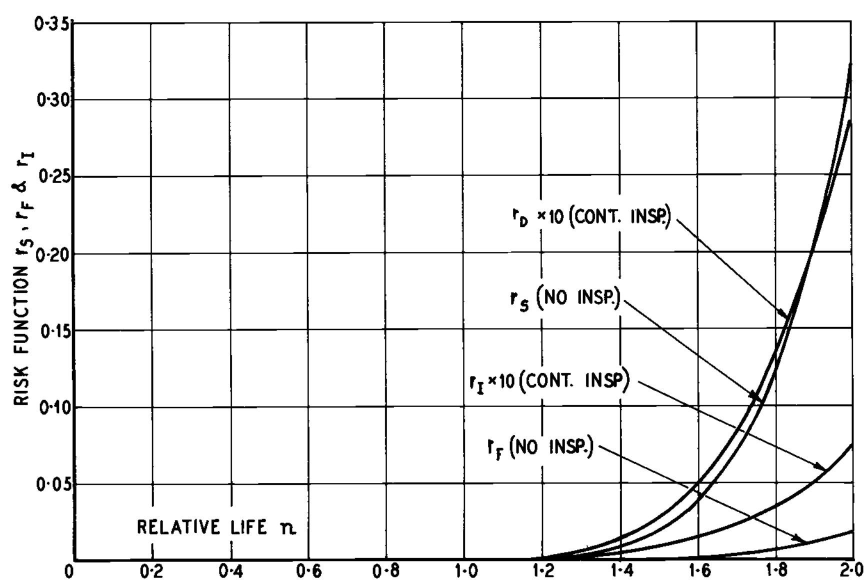

FIG. 8—*Risk function, case A-II.*

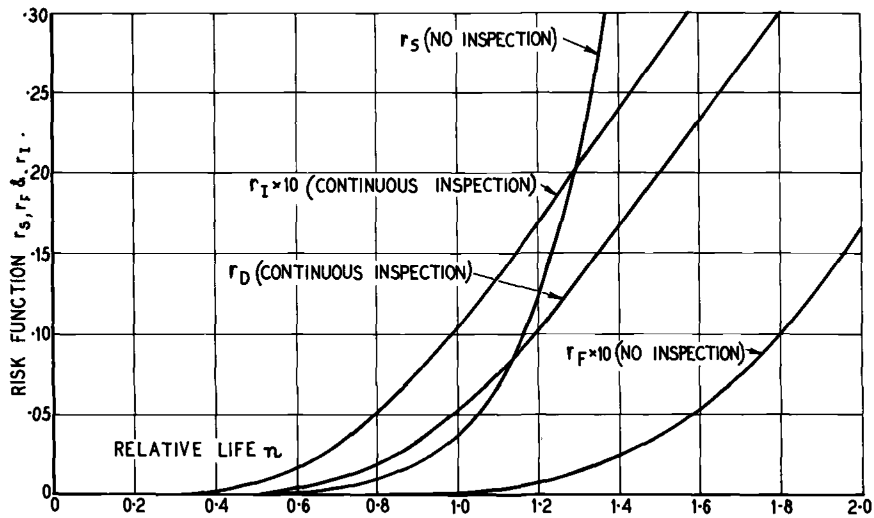

FIG. 9—*Risk function, case B-I.*

calculated from Eq 14. The comparison of r_I and r_I* shows that there is little effect on the risk functions from the reduction of the population due to the elimination of cracked structures by inspection over the range of service life which is of practical interest.

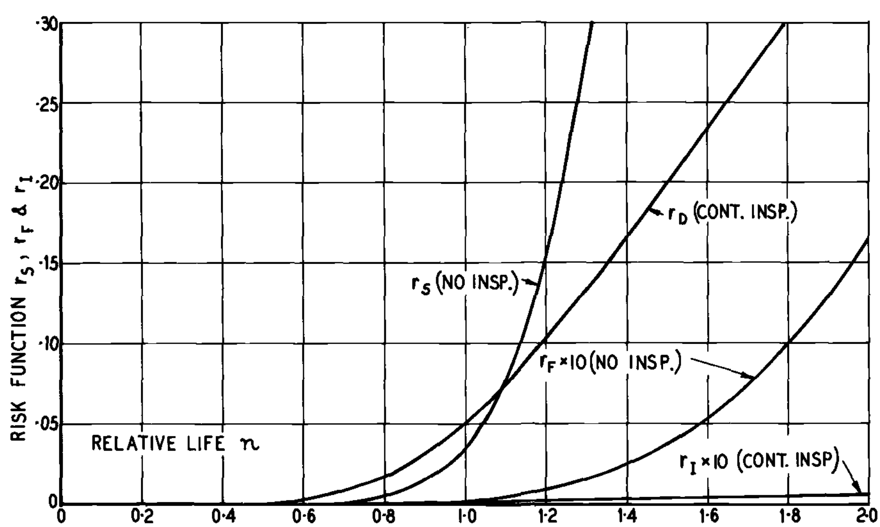

FIG. 10—*Risk function, case B-II.*

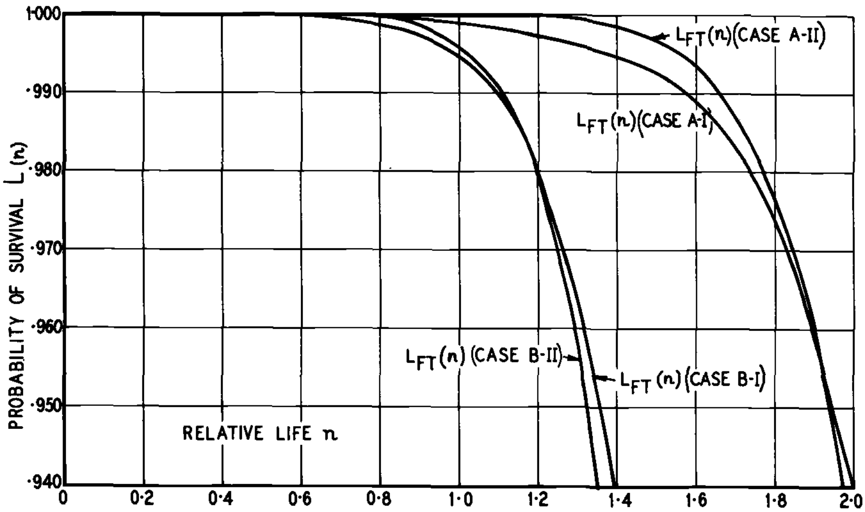

FIG. 11—*Survivorship functions, no inspection.*

The usual application of in-service inspection procedures to redundant structures of civil aircraft is represented by case B-II. For this case the risk and survivorship functions for limited risk have been calculated. Inspections were performed at relative lives $n_{I(r)}$ of 0.68, 1.23, 1.67, and 1.97 to limit the risk of failure below a specified value (0.001 in this case). This is a particular case of

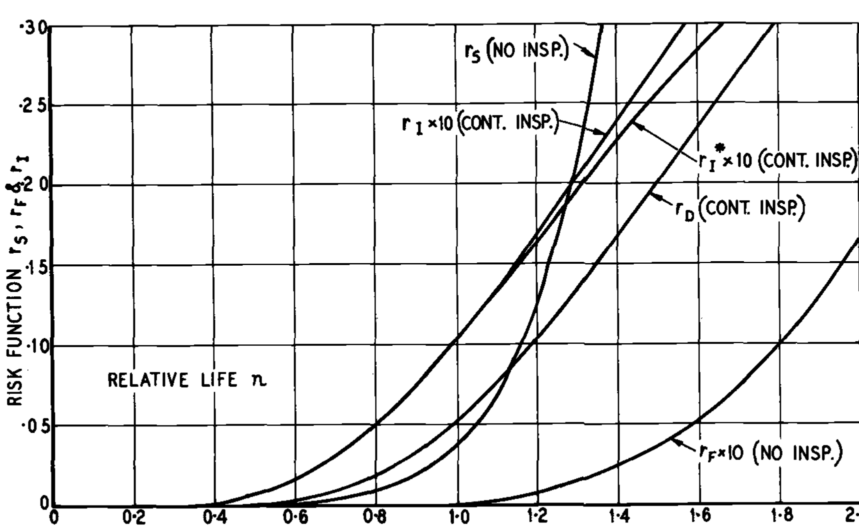

FIG. 12—*Effect of inspection on risk function, case B-I.*

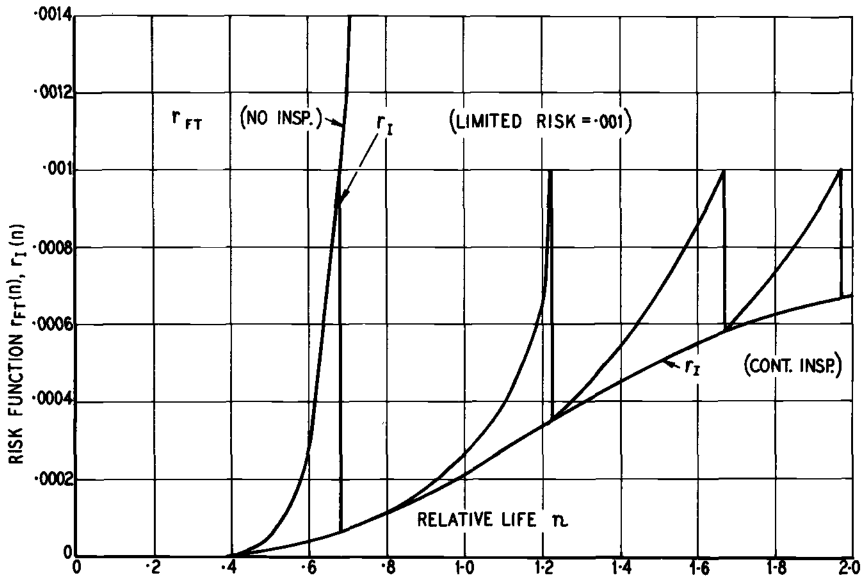

FIG. 13—*Risk of fatigue failure, case B-II. Various inspection procedures.*

periodic inspection in which inspections are carried out on the whole fleet at a series of prescribed intervals. The risk and survivorship functions for no inspection, continuous inspection, and inspection for limited risk are compared for case B-II in Figs. 13 and 14.

It will be seen by reference to Fig. 13 that the risk function for periodic inspection returns to the continuous inspection curve at each inspection and subsequently rises until it is checked by the next inspection. The continuous inspection curve therefore has a basic significance since it indicates the maximum extent to which the risk of failure can be controlled by inspection. It has therefore been investigated here, although it is a procedure which is not normally used.

Results have been presented only up to values of n for which the losses in the population due to fatigue failures are relatively small. In practice, service lives are adopted which give a probability of failure of approximately 0.001 [*15*] and a value as high as 0.01 would be quite unacceptable. At higher values of n the increasing proportion of structural failures may produce a significant distortion of the probability distributions of fatigue strength and static strength. This question is discussed further under "Basic Data and Assumptions."

Application to Fail-Safe and Safe-Life Structures

There are two procedures currently used for assessing the safety in fatigue of aircraft structures. These are the safe-life and fail-safe philosophies referred to

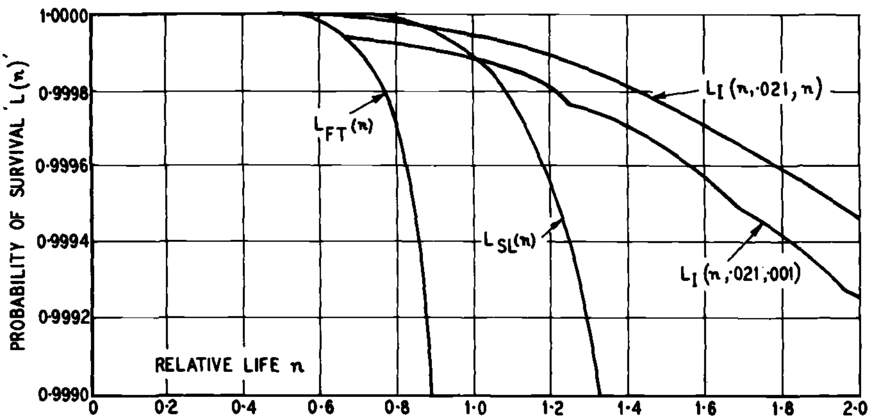

FIG. 14–*Probability of survival, case B-II. Various inspection procedures. Legend for survivorship functions:*

L_{SL}–safe life
L_{FT}–total risk, no inspection
$L_I(n,$ 0.021 in., 0.001)–limited risk = 0.001
$L_I(n,$ 0.021 in., n)–continuous inspection with L_D = 0.021 in.

earlier and their performance will now be investigated using the foregoing method of reliability analysis.

Safe-Life Philosophy

For a nonredundant structure in which the crack propagation time to failure is short, the safe-life approach estimates a mean life to failure from a fatigue-test result on the actual structure or from other representative data. To allow for scatter, this mean life is then divided by a factor (scatter factor) to give a safe operating life. The risk of static fracture by fatigue is neglected and the risk of failure is assumed to be the risk of fatigue fracture. This is based on the assumption that the crack propagation time is negligible and the life to produce a detectable crack is virtually the same as the life to fatigue fracture. In practice there is usually a significant crack-propagation time and the "safe life" will therefore vary according to the crack length (or failing load) at which the failure is defined.

This is illustrated by the risk functions in Figs. 7 to 10 which show that even for a type A structure which is typical of safe-life structures, the risk of static failure due to the growing fatigue crack (that is, the risk of "static fracture due to fatigue") is by no means negligible.

A direct comparison has been made between the probability of survival calculated by the reliability analysis and the probability of survival predicted by the safe-life approach for the four cases, A-I, A-II, B-I, and B-II. To apply the safe-life approach, a mean life has been taken for each of the four cases corresponding to failure at limit load in a fatigue test on the structure. Based on this criterion of failure, a safe life has been calculated to give a probability of survival of 0.999 assuming a log-normal distribution of life with appropriate variance as given for Structures A and B above. These safe lives designated n_{SL} are tabulated for the four cases in Table 1.

Reference to Table 1 indicates that the probability of survival as calculated by the reliability analysis procedure is substantially lower than that derived by the safe-life method which does not take full account of the effect of static fracture due to fatigue.

This difference is more marked for Structure B but it is quite significant for Structure A which is nonredundant and typical of the safe-life construction.

It is concluded that in practice there is always some departure from the idealized safe-life structure, in that there is a significant period of crack propagation with reducing static strength—the risk of failure of a structure during this period of its life being the risk of "static fracture due to fatigue" as defined earlier. This risk is not taken into full account in the current safe-life approach, which adopts a mean life corresponding to failure at a particular crack length, as determined in a fatigue test relating to the structure.

As a result, the estimate of safe life based on this mean may be in error and, depending on the conditions, this error can be in the nonconservative direction.

TABLE 1—*Safety achieved by safe-life and fail-safe procedures as calculated by reliability analysis.*

	Safe-Life Criterion			Fail-Safe Criterion		
(1)	(2)		(3)	(4)	(5)	
	Safe-Life Estimate				Life at which *Pr* Survival $L_T(n)$ = 0.999	
Type of Aircraft	Relative Life, n_{SL}	Life, h, N_{SL}	*Pr* of Survival at Safe Life $L_{FT(N_{SL})}$	Life at which Residual Strength = Limit Load	Relative Life	Life, h
A-I	1.625	3 250	0.987	4.4	0.98	1 960
A-II	1.625	3 250	0.993	4.4	1.36	2 720
B-I	1.31	26 200	0.962	5.2	0.77	15 400
B-II	1.31	26 200	0.953	5.2	0.87	17 400

Col. (1)—I = fighter-load spectrum; II = gust-load spectrum; A = safe-life structure; B = fail-safe structure

Col. (2)—n_{SL}, N_{SL} = safe life for $P_r\{\text{survival}\}$ = 0.999; estimated by safe life procedure using average life to failure under limit load

Col. (3)—$L_{FT(n_{SL})}$ = Probability of survival at n_{SL} calculated by the reliability analysis

Col. (4)—Life at which fail-safe criterion applies: median residual strength = limit load

Col. (5)—Life at which $Pr\{\text{survival}\}$ = 0.999 as calculated by the reliability analysis

Fail-Safe Philosophy

In highly redundant structures there is usually an extensive period of crack propagation during a large part of which there is no very marked loss in strength due to a detectable crack. Such structures may be operated on the fail-safe philosophy: a life is calculated in the same way as in the safe-life procedure, except that the mean life may be based on the life to some observed crack length in the fatigue test, and instead of retiring the structure from service when the calculated safe life has been reached, an inspection is carried out.

A risk is incurred that structures containing undetected cracks may fail under an applied service load and this is the risk of static fracture due to fatigue as defined in this paper. To meet this situation, the current civil airworthiness requirements for fail-safe structures specify a minimum strength to be demonstrated for the structure with clearly detectable failures present.[3]

The reliability analysis developed in this paper provides a more quantitative approach by calculating the risk of static fracture due to fatigue. This is shown by Figs. 7 to 10 where the risk of static fracture due to fatigue for the four cases taken are presented as functions of life. It is clear that the risk of static fracture due to fatigue is quite significant in all cases and depends on the type of structure and the loading spectrum.

To investigate the suitability of the airworthiness requirement the life at which the mean strength of cracked structures has fallen to limit load is shown for the four cases in Table 1 and it can be seen by reference to the survivorship functions in Fig. 11 that operation up to this stage in service would lead to an unacceptably high probability of failure in all four cases. A similar finding is reported by Ferrari et al [*2*].

This indicates that the present airworthiness requirement for fail-safe structures is not entirely adequate. It is suggested that successful operation of the fail-safe philosophy has largely depended on early detection of cracks in those aircraft of the fleet which are first to show fatigue cracking. This is then followed by modifications to aircraft in the rest of the fleet to eliminate the fatigue weaknesses before extensive cracks develop.

In those cases where each aircraft in the fleet has been operated until fatigue cracks have been detected before undertaking modifications, it is most likely that the residual strength with detectable cracks present is considerably higher than limit load.

A more reliable method of maintaining safety is proposed in which an inspection procedure based on reliability analysis is carried out to limit the probability of failure to a specified value.

[3] The Air Registration Board (United Kingdom) specifies $66^2/_3$ percent of the ultimate load. The Federal Aviation Agency (United States) requirements correspond to 55 percent of ultimate load with a factor of 1.15 to be applied unless the test load is maintained on the structure while the members are being cut.

Safety by Planned Inspection

As stated earlier, continuous inspection gives the maximum improvement in the probability of survival and although it is not normally a very practicable procedure, it provides a measure of the potential value of inspection in any particular case.

In Figs. 7 to 10 the risk function for continuous inspection is compared with the risk for no inspection. It is apparent from these results that the advantages of inspection are greater in the case of the redundant type B structure than for the type A structure because of the much shorter relative crack length that is detectable. Inspection is also more effective under the gust-load spectrum than under the maneuver load spectrum because with the latter there is a much greater probability of occurrence of high loads that will cause failure of structures containing the small cracks that can escape detection. This indicates that the operation of redundant structures on the fail-safe principle offers a considerable advantage in civil aircraft operation.

With continuous inspection the risk of fatigue fracture $r_F(n)$ is zero since no cracks are allowed to grow beyond the detectable length l_D and there is, instead, the probability of elimination by inspection $r_D(n)$ given by Eq 15 or Eq 17. In Figs. 7 to 10, $r_D(n)$ is plotted for each of the four cases and it will be seen that it is much greater than the risk of static fracture by fatigue $r_S(n)$ which is now very much reduced due to the elimination of cracked structures by the inspection process.

Since the risk of fatigue fracture is zero, the risk of static fracture by fatigue becomes the risk of fatigue failure and as stated earlier there are two cases to be considered.

If structures in which cracks are detected are retired from service, the risk of fatigue failure with inspection $r_I(n)$ is given by Eq 16, while if the cracked structures are repaired and replaced in service the risk of fatigue failure with inspection and replacement is $r_I{}^*(n)$ presented in Eq 14.

These two risks are compared for Case B-I in Fig. 12 and it will be seen that the difference between them is small for values of service life considered here. However, since repair and replacement of structures in service is the usual procedure, $r_I{}^*(n)$ has been used in the following consideration of inspection procedures.

In practice, some form of periodic inspection is required and an inspection procedure which limits the maximum value of the risk is proposed here. An example of this is shown in Fig. 13 for Case B-II where the computer program has been arranged to apply the inspection condition automatically when the risk reaches a predetermined value of 0.001. The risk functions for no inspection and continuous inspection with replacement are plotted for comparison and the corresponding survivorship functions are shown in Fig. 14.

Also shown is the survivorship function for a safe-life structure with a median life to failure of 5.2 $\tilde{N}_i$, corresponding to failure of the structure at limit load, and with a log-normal distribution of fatigue life having variance $\sigma^2 = 0.04$ as used in the reliability analysis.

Reference to Fig. 13 shows that the inspection procedure for a risk limit of 0.001 involves four inspections at 0.68 $\tilde{N}_i$, 1.22 $\tilde{N}_i$, 1.67 $\tilde{N}_i$, and 1.97 $\tilde{N}_i$. This situation corresponds, for the conditions of B-II, to a risk limit of 5×10^{-8} failures per hour with four inspections at 13,600, 24,400, 33,400, and 39,400 h.

By reference to Fig. 14 it can be seen that for a probability of survival of 0.999, the limited-risk procedure provides an operating life of 2.3 $\tilde{N}_i$ (46,000 h) as compared to 0.9 $\tilde{N}_i$ (18,000 h) for no inspection and 2.6 $\tilde{N}_i$ (52,000 h) for continuous inspection.

This procedure can be compared with the conventional fail-safe approach. Reference to the survivorship function $L_{SL}(n)$ in Fig. 14 shows that planning inspection periods by the fail-safe philosophy would be quite unsatisfactory if the criterion for inspection were taken as a probability of 0.001 of cracks being present that will cause failure under limit load. This would indicate that the first inspection should be carried out at a life of 1.32 $\tilde{N}_i$, but at this stage the probability of failure in the fleet would be unacceptably high.

A more satisfactory criterion is to inspect when there is a probability of 0.001 that detectable cracks are present. In the present case the detectable crack length is given as $l_D = 0.021$ corresponding to a life of 3.0 $\tilde{N}_i$. With a standard deviation of $\sigma = 0.2$ and a mean life of 3.0 $\tilde{N}_i$ a probability of 0.001 corresponds to a life of 0.72 $\tilde{N}_i$.

This gives a probability of 0.001 that there are detectable cracks present and it compares reasonably well with the life of 0.68 $\tilde{N}_i$ for first inspection calculated by the reliability analysis. However, the method does not provide an estimate of the number and frequency of subsequent inspections based on an acceptable safety level.

Discussion

The application of the foregoing procedure to structural safety in fatigue will now be considered. While the method has the advantage that it provides a quantitative estimate of the risk of failure as a function of the life, it involves a number of assumptions and requires a considerable body of basic data.

Basic Data and Assumptions

The method relies largely on using representative data in conjunction with a number of important physical assumptions as discussed below.

Basic Assumptions—(1) The service load S is assumed to be independent of the structural resistance R. The assumption infers that any increase in flexibility of the structure as a fatigue crack extends does not affect its response to the applied loads. This is a quite valid assumption for structures in which there is a relatively short crack length to failure, as in the type A structure used in the foregoing examples. For highly redundant structures there will be a local increase in flexibility, which could increase the elastic response, but it is considered that in such an event it would be very likely that the effect on the trim of the aircraft would result in detection of the failure (see Appendix).

(2) It is assumed that there is no correlation between the residual strength of a cracked structure and its fatigue strength. The evidence in support of this assumption is presented in the Appendix.

(3) The relative residual strength $X = R(l)/\mu_R(l)$ of structures cracked to some crack length l has a characteristic probability distribution which applies for any value of l. There is experimental evidence to support this assumption as discussed in the Appendix.

(4) At all points on the crack-propagation curve of any structure the fatigue life $N_{l,\,Z}$ bears a constant ratio to the median life $\tilde{N}_l$ at the same crack length $N_{l,\,Z}/\tilde{N}_l = Z$.

Since $N_{l,\,Z}$ is distributed about the median value $\tilde{N}_l$ it follows from this assumption that Z has a median value of 1 and has the same distribution for all crack lengths.

The experimental evidence to support this assumption is discussed in the Appendix.

(5) As the life increases and structures fail and are thus eliminated from the population, it is assumed that there is no change in shape of the probability distributions of static and fatigue strength. In general some distortion of the probability distributions of fatigue life and residual static strength will arise since the weaker than average structures will tend to fail first. In practice, however, this effect should not be very significant since, over the operating range of service life, the proportion of failures in the population is necessarily very small.

Basic Data—(1) The service-load spectrum $F_S(S)$ must be known. This can be estimated from representative data initially and then subsequently obtained from actual service records. However, for the high loads of rare occurrence some extrapolation of the data may be necessary.

(2) The mean value of the ultimate failing load μ_0 of the structure is required. This is used to express the mean residual strength $\mu_R(l)$ nondimensionally as $\mu_R(l)/\mu_0 = \phi(l)$.

(3) The probability distribution of the relative strength $X = R(l)/\mu_R(l)$ is required. As stated in the Assumptions the same distribution is taken to apply at all values of crack length l.

(4) The median crack-propagation curve for the structure must be known. It is proposed to rely on the crack-propagation curve obtained in fatigue testing a prototype specimen of the structure in the design stage. However, the shape of the curve may be indicated by basic considerations such as by the application of fracture mechanics theory in the case of the monolithic type A structure in the foregoing examples.

(5) The mean residual strength $\mu_R(l)$ must be known as a function of crack length and expressed nondimensionally as $\mu_R(l)/\mu_0 = \phi(l)$. This function may be estimated by calculation or from representative data, in conjunction with the results from static failure of the structure tested to destruction in a fatigue test.

(6) The distribution of the fatigue life $N_{l,Z}$ to a given crack length is required. As stated in the Assumptions, the comparative life $N_{l,Z}/N_l = Z$ is taken to have a characteristic distribution which is the same at all crack lengths.

Applications to Airworthiness

The procedure developed here considers two separate risks of fatigue failure: (1) fatigue fracture defined as failure following growth of the fatigue crack to the stage where collapse occurs under the steady mean load, and (2) static fracture by fatigue defined as failure of the structure under a service load during the crack propagation stage.

By separating these two risks it is possible to make a quantitative estimate of the total risk of failure due to fatigue, taking account of the variability in structural resistance and crack propagation rate together with the probability distribution of service loads. This is not done in the safe-life and fail-safe procedures, neither of which takes full account of the risk of static failure in the structure, progressively weakened by the growing fatigue crack. The present airworthiness philosophies are at a notable disadvantage in this regard and as shown by the foregoing examples they can be significantly in error in the unconservative direction.

Reliability in Fatigue—It is therefore suggested that the safety of both types of construction should be established by a probabilistic procedure such as the one presented in this paper. The approach considers reliability in fatigue and embraces both the safe-life and fail-safe philosophies. In many safe-life structures the life to failure includes a considerable crack-propagation period and there is no essential difference from the fail-safe structures—both have similar characteristics only in varying degree. In safe-life structures in which crack propagation is very rapid, the risk of failure during the growth of the fatigue crack is negligible and the risk of failure is then the same as the risk of fatigue fracture.

In both cases the risk of fatigue failure for the safe-life structure is given by the reliability analysis which includes both the risk of fatigue fracture and the risk of static fracture by fatigue.

As illustrated by the above examples, the reliability analysis provides a rational assessment of fatigue performance, including the calculation of inspection intervals, and it also enables the effect of structural parameters to be investigated. Its application in the four cases discussed has shown that inspection has a great potential advantage and in view of the increasing size, complexity, and cost of modern aircraft there is likely to be an increasing trend to rely on safe detection of cracks in service. A probabilistic approach to planned inspection procedures in conjunction with modern nondestructive inspection techniques could make an important contribution in this regard.

Specification of the Safety Level—Specification of a required probability of survival is essential to the reliability approach. For all engineering structures some risk of failure exists, however remote, and there is a general trend to more efficient and rational design procedures based on a probabilistic approach[*13,14*]. It is therefore suggested that the airworthiness authorities should consider specifying a required safety level. A required probability of survival is already contained indirectly in some airworthiness requirements[*15*] which specify safe lives at three standard deviations below the mean life.

The required safety level may be specified in a number of ways the most important of which are:

(1) The probability P of any aircraft suffering a fatigue failure within its operating life N. This definition is very useful when considering a fleet of aircraft, since P then defines the fraction of the total that would be expected to suffer fatigue failure. However, it has the disadvantage that it takes no account of the operating life and hence of the time of exposure to risk. Various authorities[*15,16*] quote safe lives, three standard deviations below the mean in relation to a normal distribution of log life, corresponding to $P = 0.0013$. Experience has indicated[*17*] that for civil aircraft an approximate value of $P = 0.001$ is achieved.

(2) The risk of failure $r(N)$, in the fleet at any life N, or the failure rate per hour.

$$r = \frac{\dfrac{dP}{dN}}{1 - P(N)}.$$

This is the risk function derived in the reliability analysis. It gives the probability of a failure in the fleet at any stage of the life N, but it gives no average of performance throughout the life.

(3) The average failure rate $\bar{r}(N)$ in the fleet for life N.

$$\bar{r}(N) = \frac{\int_0^N r(n) \cdot dn}{N}$$

$$r(n) = \frac{\dfrac{dP}{dn}}{1 - P(n)} \approx \frac{dP}{dn}$$

Since $P(n)$ is necessarily small in the operational life N.

Therefore, we may take:

$$\bar{r}(N) = \frac{P(N)}{N}$$

This gives the average failure rate over the life for the fleet, or for a number of (similar) fleets, and is therefore a useful measure of safety for Civil Airworthiness Authorities. Assuming an average operating life N of 20,000 h, the value of $r(N)$ corresponding to P = 0.001 in (1) is:

$$r(N) = \frac{0.001}{20{,}000} = 5 \times 10^{-8}$$

In a survey of accident statistics for United Kingdom and United States civil aircraft, Freudenthal and Payne[*10*] found an average structural failure rate of 3×10^{-7} for ultimate load failure and 2×10^{-7} for fatigue failure.

Pugsley[*18*] reports a structural accident rate of 10^{-7} per hour in the United Kingdom for military aircraft in the 1930's. Black[*19*] states that in the 1970's the target level of reliability should be 10^7 h, including fatal accidents for all systems failures, with any individual cases not exceeding 1 to 10 percent of the total. This indicates an accident rate for structural failure of about 10^{-8} per hour. Lundberg[*20*] also suggests 10^{-8} per hour as an average failure rate for structural fatigue with 10^{-9} as a target in view of the rapid expansion taking place in civil air transport.

(4) The average probability of failure per mile, $F = P/V{\cdot}N$ where V is the average ground speed. This definition enables a comparison of the safety of different modes of travel from place "A" to place "B" but it rather favors air travel because of its high speed.

From a consideration of the above it is suggested that the most suitable measure of safety is the average failure rate per hour $[\bar{r}(N)]$. This is readily compared with operational statistics and it represents an average risk throughout the life.

In addition it is proposed that a maximum permissible figure should be specified for the instantaneous failure rate or risk $r(N)$. This is suggested because if an inspection procedure is adopted to limit the total probability of failure, the risk of failure may rise to quite a high value for a short period before each inspection.

The proposed safety condition for reliability in fatigue is therefore: $r_{FT}(N) \leqslant 10^{-7}$/h and $\bar{r}_{FT}(N) \leqslant 10^{-8}$/h.

General Conclusions

The reliability analysis of the risk of structural fatigue failure which has been developed here takes into account the crack-propagation and residual strength characteristics in estimating the probability of failure of the structure under the service load spectrum.

From a comparison of this method with the fail-safe and safe-life procedures for four typical cases that have been taken on aircraft structures it is concluded that the current methods can be unconservative in certain instances.

This arises because both the fail-safe and safe-life procedures are affected by, but only partly take account of, the probability of failure of the structure during the period in which it is being progressively weakened by the growing fatigue crack.

The procedure proposed here for reliability in fatigue is applicable to both fail-safe and safe-life structures and for a prescribed safety level it will show whether inspection is feasible and, if not, it will evaluate the life to replacement. From investigation of the four cases considered, it is apparent that the potential advantage of inspection may prove to be very considerable. The analysis then enables an efficient inspection procedure to be planned using the crack-propagation and residual strength characteristics of the structure determined in a fatigue test, and information on the crack-detection capability of the inspection technique.

However, as stated above, the procedure involves a number of assumptions and a considerable body of data, and for structures in general the method should be regarded at the present stage as a means of comparing the effect of various design parameters on the fatigue performance in order to obtain an efficient design.

In the aeronautical field on the other hand, it is suggested that the structural design and development practice and the relevant background data are comprehensive enough to warrant development of the method to provide safety against fatigue failure. The procedure is based on the characteristics of the structure determined from structural tests and design analysis in conjunction with pooling of other representative data. This is an extension of the policy already adopted with the current philosophies for aircraft structures.

Acknowledgments

I wish to acknowledge the efforts of my colleagues in the Structures Division of the Aeronautical Research Laboratories who have assisted with the preparation of material for this paper. Special recognition is due to G. Mallinson, assisted by Patricia Diamond, for developing the numerical techniques and carrying out the computations.

APPENDIX

Discussion of Assumptions

In the main body of this paper a statistical model for structural fatigue failure has been proposed which involves the following important assumptions regarding the static and fatigue strength of the population of structures:

(1) Static strength and fatigue strength are independent.

(2) Service load S is independent of static strength R.

(3) For all points on the crack-propagation curve of any structure, the fatigue life bears a constant ratio to the median life at the same crack length.

(4) The fatigue life to any given crack length has a log-normal distribution with constant variance independent of the crack length.

(5) For structures all cracked to the same crack length l, the relative residual strength $R(l)/\mu_R(l)$ has a characteristic distribution which is the same for all crack lengths.

These assumptions are discussed below and supporting evidence is presented.

Independence of Static and Fatigue Strength

As far as the basic material properties of static and fatigue strength are concerned, experimental evidence indicates that no definite correlation exists[*21-23*]. For fabricated structures there is further indirect evidence, in that static ultimate load failure usually occurs in a different area, and by a different mechanism, to fatigue failure. This has been found in static and fatigue tests conducted on aluminum alloy structures[*24,25*] and similar results have been reported for welded steel components[*26*]. It can therefore be inferred that static failure through a cracked section will not be directly related to the factors that govern fatigue cracking.

Independence of Service Load and Static Strength

There is the possibility that a fatigue crack may increase the flexibility of the structure to the stage where the elastic response to gusts is markedly affected. However, experimental evidence suggests that this would require a very extensive crack, mainly because the crack causes only a local increase in flexibility of the structure. In fatigue testing aircraft wings at the Aeronautical Research Laboratories by the resonant vibration method it was found[*24,27*] that the primary modes of vibration were very little affected even by substantial cracks. It is therefore suggested that the extensive cracking required to cause an appreciable effect on structural response would be detected, either by visual inspection or by a marked change in trim of the aircraft.

Constant Life Factor for Any Member of the Population

Crack-propagation data such as that given in Refs *28* and *29* for test replications on a number of nominally identical specimens indicates that there is a constant factor Z relating the life to a crack length l of any particular specimen to the median life $\widetilde{N}_l$ at the same crack length. That is,

$$N_{l,\,Z} = Z \cdot \widetilde{N}_l \tag{23}$$

for all values of crack length l.

This condition is in fact a corollary to the assumption in (4) of a log-normal distribution of life $N_{l,\ Z}$ with constant variance σ^2 for all values of l. This follows, since if $\log N_l \sim N(\log \widetilde{N}_l, \sigma^2)$ then

$$\log N_l - \log \widetilde{N}_l = \log \frac{N_l}{\widetilde{N}_l} \sim N(0, \sigma^2) \tag{24}$$

and this applies for all values of l since the log-normal distribution is assumed to apply for all values of l with the same variance σ^2.

Therefore, for any particular specimen, there corresponds a constant α such that $\log N_l/\widetilde{N}_l = \alpha \cdot \sigma$. Therefore, $N_l/\widetilde{N}_l = e^{\alpha \cdot \sigma}$ = constant Z, since α and σ are constant for all values of l.

Log-Normal Distribution of Fatigue Life at Constant Crack Length

This is a major assumption which is essential to the model of the fatigue process proposed in the paper and it has been examined in some detail. Three separate investigations, each based on an extensive body of experimental data, provide evidence in support of the assumption as follows:

(1) Comprehensive surveys of fatigue-test data on various aluminum alloy structures[*30,31*] have shown that the fatigue life to complete failure of fabricated structures has a probability distribution which is approximately logarithmic normal with a constant variance. Ford et al[*31*] propose a characteristic value of 0.20 for the standard deviation of the logarithm of fatigue life for aluminum alloy structures. This result indicates that at least at the terminal point of the crack propagation curve a logarithmic normal distribution of fatigue life applies.

(2) Ford and Payne[*32*] have analyzed data from Mustang wings tested under constant amplitude loading. Groups of structures were tested at each of a number of load ranges and the maximum load of the loading cycle for each group varied from 16 to 80 percent of the ultimate failing load.

Failure in each group of structures of course occurred at a crack length corresponding to the maximum load of the fatigue cycle and the data therefore comprise results for fatigue failure at a series of quite different crack lengths.

Ford and Payne[*32*] have pooled the data from these groups by taking the median $\widetilde{N}_k$ and the standard deviation S_k for any group k and for each test result N_k in the group the standardized variate $(\log N_k - \log \widetilde{N}_k)/S_k$ has been calculated.

The test results from all of the groups have been pooled in this way to give a total of 84 data points. It has been found that these pooled data form a large homogeneous sample which shows reasonable agreement with a logarithmic normal distribution. This provides evidence in support of a logarithmic normal distribution of fatigue life at any crack length.

(3) A comprehensive investigation on this subject has been undertaken by Ingham and Grandage[*33*] using fatigue data from Mustang wings[*34*], fatigue data from C46 wings[*35*], and F-29A wings[*36*].

From a study of these data it was found that following crack initiation the crack-propagation curves were practically linear over a considerable part of the life.

That is, for each structure

$$N_l - N_i = \beta \cdot l \tag{25}$$

where N_l is the life of the structure to crack length l, N_i is the life to initial failure, and β is the slope of the crack-propagation curve for the structure.

Similarly for the median

$$\tilde{N}_l - \tilde{N}_i = \tilde{\beta} \cdot l$$

where $\tilde{\beta}$ is the slope of the median crack-propagation curve. Therefore,

$$\frac{N_l - N_i}{\tilde{N}_l - \tilde{N}_i} = \frac{\beta}{\tilde{\beta}} \tag{26}$$

The data again came from groups of structures tested at each of a series of load ranges. The slope β from the crack-growth curve of each structure in a particular group was obtained and divided by the median slope from the group $\tilde{\beta}$ to give a series of values of $\beta/\tilde{\beta}$.

The assumption under test was that the life to any crack length l had a log-normal distribution with constant variance. It has been shown in the section on Constant Life Factor for Any Member of the Population, that under this assumption, for any structure,

$$N_{l,\ Z} = Z \cdot \tilde{N}_l \tag{27}$$

for any crack length l. In particular, $N_{i,\ Z} = Z \cdot \tilde{N}_i$. Hence it would follow that

$$\frac{N_l - N_i}{\tilde{N}_l - \tilde{N}_i} = Z \tag{28}$$

where $\log \underset{\sim}{Z} \sim N(0, \sigma^2_{\log Z})$. It follows from Eqs 26 and 28 that the assumption requires $\beta/\tilde{\beta} = Z$, and therefore

$$\log \left(\frac{\beta}{\tilde{\beta}}\right) \sim N(0, \sigma^2_{\log \beta}) \text{ with } \sigma_{\log \beta} = \sigma_{\log Z}$$

The values of $S^2_{\log \beta}$ for each of the three different types of structures were obtained by pooling the relevant data in each case. For the Mustang wings a value of 0.22 was obtained for $S_{\log \beta}$ which is in good agreement with the value of 0.20 recommended for $S_{\log Z}$ by Ford et al[*31*]. For the C46 and T29A structures, however, $S_{\log \beta}$ was significantly greater than this value in each case. This could be attributed to the much smaller sample size for these data combined with the difficulty in obtaining an accurate record of crack growth throughout the fatigue test.

In testing the experimental data against the log-normal distribution the values of $\log (\beta/\tilde{\beta})$ for each group of tests on a particular type of structure were divided by the value of $S_{\log \beta}$ for the structure to give a standardized variate

$$\nu = \frac{\log \beta - \log \tilde{\beta}}{S_{\log \beta}} \tag{29}$$

All the values were then pooled to give a total of 115 data points and these are shown plotted in Fig. 15 reproduced from Ingham and Grandage[*33*]. It will

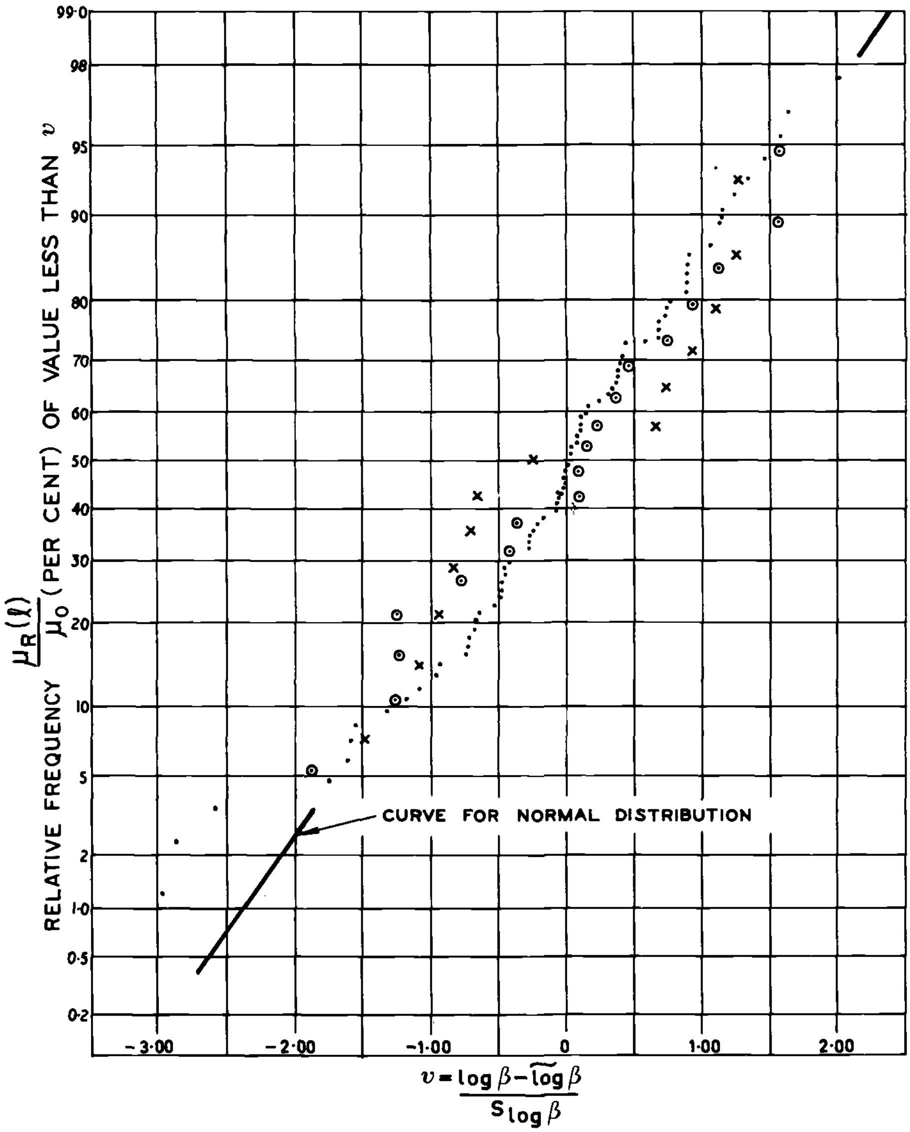

FIG. 15—*Probability distribution of life to given crack length (reproduced from Ref 33).*

$\beta = \frac{Ne - Ni}{l}$ • Mustang P51D wings 84 tests $S_{\log\beta} = 0.22$

X C-46 wings 13 tests $S_{\log\beta} = 0.45$

⊙ T29A wings 18 tests $S_{\log\beta} = 0.35$

be observed that the plotted points show reasonably good agreement with the straight line of the normal distribution.

Since these data represent the initial period of crack growth in the three different types of structures tested under a variety of different types of loading conditions, it is considered that the results provide good justification for the assumption of a log-normal distribution of fatigue life at any stage of the crack propagation.

Characteristic Distribution for Residual Strength for Cracked Structures

It is stated in the main body of the paper that for a structure of monolithic construction of high strength steel the residual strength R_l at any crack length is given by fracture mechanics theory and this assumption is well supported by experimental data.

For a through crack of length l it can then be shown that

$$R_l = K\sqrt{\frac{2}{\pi}} \cdot \frac{1}{\sqrt{l}} \tag{30}$$

where K is the fracture toughness for the material of the particular specimen. In the general case where the crack originates from the surface of the material and the crack front may have a more complex shape, Eq 23 then takes the form

$$R_l = K \cdot \alpha \cdot \frac{1}{\sqrt{l}} \tag{31}$$

where α is a factor determined by the shape of the crack front.

Similarly for the median values

$$\mu_R(l) = \tilde{K} \cdot \alpha \cdot \frac{1}{\sqrt{l}}$$

where $\tilde{K}$ is the median value of fracture toughness.

Hence the relative residual strength

$$X(l) = \frac{R(l)}{\mu_R(l)} = \frac{K}{\tilde{K}}$$

is independent of the crack length l.

This shows that for the monolithic structure the probability distribution of residual strength $X(l)$ is the same for all crack lengths, and is in fact equivalent to the probability distribution of fracture toughness for the material.

There is also evidence to show that the assumption of a characteristic distribution of relative residual strength applies to fabricated structures. The variability in ultimate strength of uncracked aircraft structures of aluminum alloy has been investigated by Freudenthal and Payne[*10*] using multiple test data from eleven different types of structure and nine types of mainplane panels. The panels were all loaded to failure in compression but the different types of structure were tested to destruction under differing loading cases and tension, compression and shear failures were represented in these results. For each type of structure the dimensionless variate R_0/μ_0 was taken for each structure and thus all results were transformed to have a mean value of 1.0 and were then pooled to give a total of 170 data points from the 19 different types represented.

It was found that these data formed a homogeneous sample with a pooled standard deviation of 0.043, and the normal distribution gave a good fit over a considerable range of the variate R_0/μ_0. This suggests that a single distribution of the ultimate failing load about the mean value can be obtained irrespective of the type of structure considered or its mode of failure. Furthermore it infers that the variability in residual strength of cracked structures is unlikely to be influenced by factors affecting the local load distribution in the structure such as the length of a crack, but is mainly dependent on the variability in material properties and variations in manufacture. This is supported by the results of residual strength tests on Vampire wings[*37*]. These specimens had all been fatigue tested to the stage where the main spar boom was cracked through resulting in a loss of approximately 20 percent of the total tension area. All specimens therefore contained the same failure of well defined extent and were loaded statically to destruction. The coefficient of variation of the failing load (or the standard deviation of relative residual strength $R(l)/\mu_R(l)$) was 0.042. This is in good agreement with the value of 0.043 for the standard deviation in relative strength of uncracked structures, found by Freudenthal and Payne[*10*], referred to above, and indicates that the variability in relative strength is little affected by even substantial cracking.

References

[*1*] Shaw, R. R., *Journal of the Royal Aeronautical Society,* AENJA, Vol. 58, No. 526, Oct. 1954, pp. 720-723.

[*2*] Ferrari, R. M., Milligan, I. S., Rice, M. R., and Weston, M. R. in *Proceedings of the Symposium on Full Scale Fatigue Testing of Aircraft Structures,* Amsterdam, 1959, F. J. Plantema and J. Schijve, Eds., Pergamon Press, Oxford, 1963, pp. 413-426.

[*3*] Eggwertz, Sigge in *Proceedings of the Symposium on Fatigue of Aircraft Structures,* Paris, 1961, W. Barrois and E. L. Ripley, Eds., MacMillan Co., New York, 1963, pp. 345-362.

[*4*] Eggwertz, Sigge and Lindsjö, G., "Analysis of the Probability of Collapse of a Fail-Safe Aircraft Structure Consisting of Parallel Elements," FFA Report HU-961, The Royal Aeronautical Research Institute of Sweden, Stockholm, 1963.

[*5*] Heller, R. A. and Heller, A. S., "A Probabilistic Approach to Cumulative Fatigue Damage in Redundant Structures," Fatigue Institute Report 17, Contract NONR 266-91, Columbia University, New York, 1965.

[*6*] Freudenthal, A. M. and Shinozuka, M., "Structural Safety under Conditions of Ultimate Load Failure and Fatigue," WADD Technical Report 61-177, Aeronautical Systems Div., USAF, Wright-Patterson AFB, Ohio, 1961.

[*7*] Mallinson, G. D., "Note on the Numerical Evaluation of the Risk Function," Structures Internal Report, Aeronautical Research Laboratories, Melbourne, 1970.

[*8*] *Metals Handbook,* 8th ed., Vol. 1, Chapman and Hall Ltd., London, 1961, pp. 87-94.

[*9*] Payne, A. O. in *Proceedings of the Symposium on Full Scale Fatigue Testing of Aircraft Structures,* Amsterdam, 1959, F. J. Plantema and J. Schijve, Eds., Pergamon Press, Oxford, 1963, pp. 76-132.

[*10*] Freudenthal, A. M. and Payne, A. O., "The Structural Reliability of Airframes," AFML-TR-64-401, Air Force Materials Laboratory, Dayton, Ohio, 1964.

[*11*] Mayer, J. F. and Hamer, H. A., "Applications of Power Spectral Analysis Methods to Manoeuvre Loads Obtained on Jet Fighter Airplanes During Service Operations," TN D-902, National Aeronautics and Space Administration, Langley Research Center, 1961.

[*12*] Tolefson, H. B., "Summary of Derived Gust Velocities Obtained from Measurements

within Thunderstorms," NACA Report 1285, National Advisory Committee for Aeronautics, Langley Research Center, 1956.

[13] *The Structural Engineer,* May 1955, Committee of the Institution of Structural Engineers, pp. 141-149.

[14] Julian, O. G. in *Proceedings of the American Society of Civil Engineers,* PACEA, Vol. 83, July 1957, pp. 1-22.

[15] "Design Requirements for Aircraft for the Royal Navy," Ministry of Aviation Publication, AVP 970, Vol. 1, Part 2, leaflet 200/7, para. 8.1.

[16] Raithby, K. D., *Journal of the Royal Aeronautical Society,* AENJA, Vol. 65, Nov. 1961, pp 729-738.

[17] Russell, A. E. in *Proceedings of the 6th Anglo-American Aeronautical Conference,* Royal Aeronautical Society, Folkestone, 1957.

[18] Pugsley, A., *The Safety of Structures,* Edward Arnold Ltd., London, 1966.

[19] Black, H. C. in *Proceedings of the International Conference on Structural Safety and Reliability,* Smithsonian Institute, Washington, D.C., April 1969.

[20] Lundberg, B., *Journal of the Aeronautical Sciences,* JASSA, Vol. 22, No. 6, 1955, pp. 349-413.

[21] Mann, J. Y. and Vann, A. W. N., "Variation in Fatigue Properties between Batches of DTD 363A Aluminum Alloy," ARL SM Note 331, Aeronautical Research Laboratories, Melbourne, 1967.

[22] Mann, J. Y., "A Note on the Fatigue Properties of Welded Low Alloy Structural Steels," ARL SM Technical Memo 87, Aeronautical Research Laboratories, Melbourne, 1960.

[23] Stallmeyer, J. E. and Munse, W. K., *British Welding Journal,* MCBWA, Vol. 7, No. 4, April 1960, pp. 281-287.

[24] Johnstone, W. W., Patching, C. A., and Payne, A. O., "An Experimental Determination of the Fatigue Strength of CA-12 Boomerang Wings," ARL SM Report 160, Aeronautical Research Laboratories, Melbourne, 1950.

[25] Kepert, J. L., Patching, C. A., Rice, M. R., and Robertson, J. G., "Fatigue Characteristics of a Riveted 24S-T Aluminum Alloy Wing, Part III: Test Results," ARL SM Report 248, Aeronautical Research Laboratories, Melbourne, 1956.

[26] Munse, W. K. and Stallmeyer, J. E., *British Welding Journal,* MCBWA, Vol. 7, No. 3, March 1960, pp. 188-200.

[27] Kepert, J. L., Patching, C. A., and Robertson, J. G., "Fatigue Characteristics of a Riveted 24S-T Aluminum Alloy Wing, Part I: Testing Techniques," ARL SM Report 246, Aeronautical Research Laboratories, Melbourne, 1956.

[28] Christensen, R. F. in *Proceedings of Crack Propagation Symposium,* Aeronautical Research Council, Cranfield, Sept. 1961, pp. 326-374.

[29] Schijve, J., Jacobs, F. A., and Tromp, P. J., "Crack Propagation in 2024 T-3 Alclad under Flight-Simulation Loading. Effect of Truncating High Gust Loads," NLR TR 69050U, National Aerospace Laboratory, The Netherlands, June 1969.

[30] Impellizeri, L. F. in *Structural Fatigue in Aircraft, ASTM STP 404,* American Society for Testing and Materials, Nov. 1966, pp. 136-156.

[31] Ford, D. G., Graff, D. G., and Payne, A. O. in *Proceedings of the Symposium on Fatigue of Aircraft Structures,* Paris, 1961, W. Barrois and E. L. Ripley, Eds., MacMillan Co., New York, 1963, pp. 179-208.

[32] Ford, D. G. and Payne, A. O., "Fatigue Characteristics of a Riveted 24S-T Aluminum Alloy Wing, Part IV: Analysis of Results," ARL SM Report 263, Aeronautical Research Laboratories, Melbourne, 1958.

[33] Ingham, Jennifer and Grandage, J. M., "Investigation into the Probability Distribution of the Crack Propagation Rate in Fabricated Structures," ARL Structures Div. Internal Report, Aeronautical Research Laboratories, Melbourne, Feb. 1967.

[34] Parry-Jones, G. in *Proceedings of the Third Congress of the International Council of Aeronautical Sciences,* Stockholm, 1962, T. Von Karman and T. Roy, Eds., Spartan Books, Washington, 1964, pp. 801-813.

[35] Whaley, R. E., McGuigan, M. J., and Bryan, D. L., "Fatigue-Crack Propagation and Residual-Static-Strength Results on Full Scale Transport Airplane Wings," NACA Report NT 3847, National Advisory Committee for Aeronautics, Langley Research Center, 1956.
[36] Castle, C. B. and Ward, J. L., "Fatigue Investigation of Full Scale Wing Panels of 7075 Aluminum Alloy," NASA Report TN D-635, National Aeronautics and Space Administration, Langley Research Center, 1961.
[37] Bruton, R. A. and Patching, C. A., "Fatigue Investigation of Vampire Wings," ARL SM Report, Aeronautical Research Laboratories, Melbourne, in process for publication.

DISCUSSION

F. H. Hooke[1] (*written discussion*)—The "risk function," "hazard rate," "force of mortality," or "instantaneous failure rate"[2,3] is, by definition, the rate of failure at time t or n of survivors of the population at time t or n. It is usually denoted $r(n)$ and is related to the reliability or probability of survival $L(n)$ by the basic equation quoted by Dr. Payne.

$$L(n) = e^{-\int_0^n r(n)dn}$$

and $r(n)dn$, putting $dn = 1$, gives the probability of failure at the next load cycle of a member of the population which has survived to the nth load cycle. If, in the bivariate population of Dr. Payne's example, which is distributed in the variates l and R, we choose an element $dldR$, the probability of failure at the next cycle of a member which has survived to n is:

$$r(n)_{\text{element}} = r(n \mid l, R) = F_S(R)$$

as is implied in Eq 3 where $F_S(R)$ is the probability of the service load $F_S(S)$ exceeding the element's strength R. The reliability or probability of survival of the element is shown to be[4]

$$L(n)_{\text{element}} = L(n \mid l, R) = e^{-\int_0^n F_S(R)dn}$$

and the contribution of this element to the reliability of the singly distributed element in which l is constant is:

$$dL(n \mid l) = e^{-\int_0^n F_S(R)dn} p(R)dR$$

[1] Senior principal research scientist, Structures Division, Aeronautical Research Laboratories, Department of Supply, Melbourne, Australia.

[2] Myers, R. H., Wong, K. L., and Gordy, H. M., *Reliability Engineering in Electronic Systems*, John Wiley & Sons, New York, 1964.

[3] Bazivski, I., *Reliability Theory and Practice*, Prentice Hall, 1962.

[4] Hooke, F. H., "Analysis of Safe Fatigue Life and Safe Inspection Intervals by Reliability and Conventional Theory," ARL Report SM 335, 1971.

The conditional reliability of this population element dl in which l is constant while R is distributed about the mean value $\mu_R(R)$ with density $p_{R,\ \mu_R}(R)$ is:

$$L(n|l) = \int_{R=0}^{R=\infty} e^{-\int_0^n F_S(R)dn} p_{R,\ \mu_R}(R)dR.$$

The risk function for this element dR is

$$r(n|l) = \frac{-\dfrac{d}{dn}\left[\displaystyle\int_{R=0}^{R=\infty} e^{-\int_0^n F_S(R)dn} p_{R,\ \mu_R}(R)dR.\right]}{\displaystyle\int_{R=0}^{R=\infty} e^{-\int_0^n F_S(R)dn} p_{R,\ \mu_R}(R)dR}$$

to which Dr. Payne's Eq 3 is an approximation.

By a simple extension, the reliability for the whole bivariate population in l and X is:

$$L(n) = \int_{X=0}^{X=\infty} \int_{l=0}^{l=1} \left\{e^{-\int_0^n F_S(X\mu_0\phi[l])dn}\right\} p(l)p_X(X)dldX$$

so that

$$r(n) = \frac{-\dfrac{d}{dn}\left[\displaystyle\int_{X=0}^{X=\infty} \int_{l=0}^{l=1} \left\{e^{-\int_0^n F_S(X\mu_0\phi[l])dn}\right\} p(l)p_X(X)dldX\right]}{\displaystyle\int_{X=0}^{X=\infty} \int_{l=0}^{l=1} \left\{e^{-\int_0^n F_S(X\mu_0\phi[l])dn}\right\} p(l)p_X(X)dldX}$$

to which Dr. Payne's Eq 6 is an approximation, which amounts to averaging the probability of failure over all members of the population at a given time n. The approximation is, of course, exact where the risk is the same for all elements of the population, and is good where the probability of failure of an element is small.

Equation 8 is Eq 6 with a change of variable; however, to proceed to Eq 9 from Eq 8 by way of the basic relationship $L(n_S) = e^{-\int_0^{n_S} r(n)dn}$ would appear to lead to the result:

$$L_S(n_S) = \exp\left[\int_{n=0}^{n=n_S} \int_{\substack{n_S \\ Z=\overline{n}_F}}^{Z=n_S} \int_{X=0}^{X=\infty} p(X)F_S\left(X\mu_0\phi\left[g\left(\frac{n_S}{Z}\right)\right]\right) p_Z(Z)dXdZdn\right]$$

which has the same proviso as before, namely that it is approximate.

In the example studied by Dr. Payne, there are several regimes in the lifetime of each member of the population, and in his Example A-I the regimes are as follows:

(i) The uncracked period, from $n = 0$ to $n = N_i$, during which $F_S(R)$ is the probability of a service load exceeding the virgin strength.

(ii) The undetectably cracked and unweakened period, from $n = N_i$ to $n = 3.6N_i$, during which $F_S(R)$ is, again, the probability of a service load exceeding the virgin strength.

(iii) The undetectably cracked but weakened period, from $n = 3.6N_i$ to $N = 3.8N_i$ during which the probability of failure is increasing above its initial value.

(iv) The period of detectable cracking and weakening, until the mean strength reaches limit load: this period is from $n = 3.8N_i$ to $4.4N_i$.

(v) The instant at which the mean strength reaches limit load, or two thirds of the virgin strength, at $n = 4.4N_i$.

(vi) The period during which the structure has less than limit load strength, that is, for $n > 4.4N_i$.

(vii) The instant when R becomes equal to the mean load, and $F_S(R) = 1$.

The reliability may be partitioned into its components by attention to the limits of integration of $F_S(X\mu_0\phi[l])$ thus:

$$L(n) = \int_{X=0}^{X=1} \int_{l=0}^{l=\infty} \left\{ e^{-\int_0^{N_i} \cdots dn} \times e^{-\int_{N_i}^{3.6N_i} \cdots dn} \times e^{-\int_{3.6N_i}^{3.8N_i} \cdots dn} \right\} dXdl$$

It may perhaps be overlooked at the first reading that Dr. Payne's analysis suppresses failures in regime (i), defines as "static failures due to fatigue" regimes (ii) to (vi) and separately calculates those of regime (vii) as "fatigue failures." At short lives, that is, in regions where the probability of failure is small, the contributions from regimes (i) and (ii) are a major part. Rigorous calculation of the risk of failure from loads exceeding the virgin strength is easy. Some philosophical questions arise when one is considering whether to separate failures of uncracked structures from failures of undetectably cracked and unweakened structures, and also whether to separate failures of weakened structures under loads greater than their current strengths but less than their virgin strengths from failures of the same weakened structures under loads larger than their virgin strengths.

Studies published elsewhere[4] suggest that if one adds to the conventionally calculated probabilities of fatigue failure the probabilities of failure through exceeding the virgin strength, the result will be in close agreement with the probabilities of failure as calculated by reliability theory. In view of the second paragraph of the General Conclusions, this matter requires further investigation.

It is the forte of reliability theory to take into account the risks of failure of structures whose strength has fallen to some value between their virgin strength and the largest load applied in the fatigue test. The latter is often, for military aircraft, limit load, and for civil aircraft often about three quarters of limit load. Dr. Payne's Spectrum I has limit load ($S = 0.67S_{\mathrm{Ult}}$) exceeded with a probability of 3×10^{-4}, which is six times in a life of 20,000 load counts. A load of $0.77S_{\mathrm{Ult}}$ is exceeded with a probability of 5×10^{-5}, that is, once per aircraft lifetime of 20,000 load counts, a load of $0.87S_{\mathrm{Ult}}$ once in the lifetime of ten aircraft, $0.93S_{\mathrm{Ult}}$ once in the lifetime of 100 aircraft, and $0.99S_{\mathrm{Ult}}$ once in the lifetime of 1000 aircraft.

Such "rare events" have an intrinsic variability, similar to the classic observations of von Bortkiewicz on the number of men killed by the kick of a horse in certain corps of the Prussian army (1875-1894).[5] The spectrum is "fuzzy" in this region, being an extrapolation from actual records on a fleet of much more limited size, and this "fuzziness" is communicated to the calculations of risk rate and reliability. It is thought that the acquisition of more data may improve confidence in the estimations: it is not yet clear whether such improved confidence can be predictive or merely retrospective.

A. O. Payne (*author's closure*)—Dr. Hooke has made three interesting comments on the paper: The first comment on the derivation of the risk function as given in Eq 6 of the paper, concerns the assumption which I have discussed under "Basic Assumptions" namely, as structures fail and are thus eliminated from the population, it is assumed that the effect of these losses on the shape of the probability distributions of static and fatigue strength may be neglected.

In the derivation that he has presented, Dr. Hooke allows for the effect of such losses on the probability distribution of crack length l at a given life (which is in effect the probability distribution of fatigue strength). In determining the probability of survival ($L(n)_{\mathrm{element}}$) for structures with residual strength R containing cracks of any given length l, he obtains an exact expression for the probability of survival of such structures at life n.

$$L(n)_{\mathrm{element}} = L(n/l, R) = e^{-\int_0^n F_S(R)\cdot dn}$$
$$= e^{-\int_0^n F_S(X\cdot\mu_0\cdot\phi[l])\cdot dn}$$

However, in proceeding to integrate this probability over all values of R (or X)

[5] von Bortkiewicz, L., "Das Gesetz der kleinen Zahlen," Teubener, Leipsiz, 1898; quoted in *An Introduction to the Theory of Statistics,* G. M. Yule and M. G. Kendall, Griffin and Co., 1945.

to give the probability of survival for all structures with a crack length l, the expression

$$L(n/l) = \int_{R=0}^{R=\infty} e^{-\int_0^n F_S(R)\cdot dn} \cdot p(R)\cdot dR$$

is obtained which ignores the progressive change in shape of the probability distribution of residual strength R (represented in the equation by $p(R)$) due to the fact that at any crack length l, the weaker than average structures will tend to fail first.

This effect will be quite significant as indicated by the service load spectra in Fig. 6 of the paper which show that structures which have a strength 10 percent less than structures of average strength will have a probability of failure ten times greater.

Dr. Hooke's final expression for $r(n)$ is therefore, like the one given in Eq 6 of the paper, an approximation which will involve small errors provided the probability of failure in the population is very small. In view of the small probabilities of failure that will be acceptable in practice, together with the uncertainties in our knowledge of the shape of the original distributions of fatigue life and residual strength, this appears to be a reasonable approximation although it warrants further investigation.

However, Dr. Hooke's final expression giving the risk function as the derivative of a term involving three integrations is open to the objection that additional computational inaccuracies are involved as compared to the simpler expression for the risk function in Eq 6 which involves a double integration. The numerical analysis procedure developed by Mallinson[7] has made possible the application of the reliability procedure in the general case but the inaccuracies involved in even a double integration are by no means negligible and this aspect is still being investigated.

Regarding the second comment, the model of the fatigue process developed in the paper considers only the failure of structures containing a macroscopic fatigue crack—uncracked structures are not included in the calculations for the risk of fatigue failure. Since any structure containing a macroscopic crack is taken to have suffered some reduction in its static strength the regimes (i) and (ii) postulated by Dr. Hooke do not occur in my model of the fatigue process.

His regimes (iii) to (vi) are all concerned with cracked structures that may fail by chance occurrence of a service load in excess of the mean load and are therefore included in what I have termed the risk of static fracture due to fatigue.

Regime (vii) concerns structures cracked to such an extent that failure will occur under the mean load and this is considered in the risk of fatigue fracture.

As stated in the paper, the identification of these two risks gives a physical insight into the problem especially as regards the significance of the fail safe and safe life philosophies and the influence of an inspection procedure.

In an ARL report[4], Dr. Hooke took a different model of the fatigue process in which he postulates that fatigue cracks originate in the whole population of structures at zero life and in this case the various regimes he defined could be identified. He used[4] this model to calculate the probability of survival for some specific cases and he has not included the variability in residual strength of structures cracked to a given crack length which has a very significant effect on the risk of failure. His results are therefore not comparable with the calculations carried out in this paper.

The relevance to the present case, of the good agreement found by von Bortkiewicz between the frequency of deaths by horse kick in the Prussian Army and the Poisson probability distribution for the occurrence of rare events is not altogether clear.

It is true that the service-load spectrum may have to be extrapolated to the high loads approaching the ultimate, by using experimental data for lower loads. However, the lower tails of the distributions of fatigue life and residual strength are more significant in the reliability approach, and are more difficult to obtain, than the distribution of service loads. The uncertainty in the form of the probability distribution of fatigue life presents a similar problem in the application of the currently used safe-life approach.

R. C. Linsley[1] *and B. M. Hillberry*[2]

Random Fatigue of 2024-T3 Aluminum under Two Spectra with Identical Peak-Probability Density Functions

REFERENCE: Linsley, R. C. and Hillberry, B. M., "Random Fatigue of 2024-T3 Aluminum under Two Spectra with Identical Peak-Probability Density Functions," *Probabilistic Aspects of Fatigue, ASTM STP 511,* American Society for Testing and Materials, 1972, pp. 156–167.

ABSTRACT: Broad-band and bimodal spectra random fatigue tests were performed on 2024-T3 aluminum alloy specimens. The specimens were axially loaded through an electrohydraulic closed loop test system. The two spectra were produced by filtering the output of a random noise generator. These filters were adjusted to provide nearly identical ratios of the number of zero crossings with positive slope per second to the number of positive peaks per second for the two signals. There was no significant difference in mean fatigue lives of both spectra at the 0.01 significance level.

KEY WORDS: fatigue(materials), stress analysis, probability theory, density functions, failure(materials), fatigue tests, random processes, loading, aluminum alloys

Nomenclature

B	Material constants used in representing constant amplitude sinusoidal fatigue curve
b	Reciprocal of negative slope of constant amplitude sinusoidal fatigue curve
D	Fatigue damage
$E(x)$	Expected value of argument
M	Number of positive peaks per second
N_0	Number of zero crossings with positive slope per second
N_p	Number of positive peaks to failure
$N, N(\sigma)$	Number of cycles to failure in constant amplitude, sinusoidal fatigue test at stress amplitude

[1] President, Linsley Enterprises, Inc., Lansing, Mich.; formerly graduate research assistant, School of Mechanical Engineering, Purdue University, Lafayette, Ind. 47907.

[2] Associate professor, School of Mechanical Engineering, Purdue University, Lafayette, Ind. 47907.

α	$(N_0/M)^2$
$p(x)$	Peak-probability density function of x, where x is instantaneous value of signal
erf	Error function
n_i	Number of cycles at stress amplitude, σ_i
N_i	Number of cycles to failure at stress amplitude, σ_i
$p(\sigma)$	Probability density function of peak stress
σ	Stress amplitude, ksi, also used for standard deviation

The phenomenon of fatigue of metals has been recognized for over a century. During this time interval investigators of metal fatigue have developed a considerable body of knowledge on the life of metals under constant-amplitude sinusoidal loading conditions. However, by far the majority of load spectra applied to loaded members in machinery and equipment are not comprised of only one load amplitude and frequency, but the applied load produces a randomly varying stress in the member.

Many theories of cumulative damage have been proposed to help the designer predict the life of machine parts subject to loads of varying amplitude based on the presently available constant-amplitude fatigue response of materials. Miner[1] in 1945 proposed a linear cumulative damage rule that predicted failure when the summation of cycle ratios equalled unity. This rule has experienced wide acceptance among designers because no other proposed cumulative damage theory has emerged with significantly greater predictive accuracy.

Other investigators, Shanley[2] and Liu et al[3], have proposed a modification to the exponent on stress to account for sequence or stress interaction effects.

A number of investigators, Corbin and Naumann[4], Naumann[5,6], Leybold and Naumann[7], Marsh and Mackinnon[8], and Heller et al[9] have performed randomized block tests.

Kowalewski[10] tested 2024 aluminum alloy specimens in cantilever bending with filtered random noise as the input to an electromagnetic shaker. Three power spectra were generated providing three $\sqrt{\alpha}$ ratios. A linear cumulative damage rule predicted the 50 percent probability of failure accurately over the life range of 10^4 to 10^6 zero crossings to failure.

Swanson[11] conducted random fatigue tests with two $\sqrt{\alpha}$ ratios. Considerably different fatigue lives were reported for the two spectra except at 9 ksi rms.

Bussa[12] and Clevenson and Steiner[13] investigated different $\sqrt{\alpha}$ ratios with five and six different power spectra, respectively.

Hillberry[14] proposed an equivalent-crack-length theory which predicts failure when the expected crack length reaches a length equal to the critical crack length in an equivalent-constant-amplitude test. The equivalent-constant-amplitude stress level is selected as that stress level with a probability of occurrence of a peak stress equal to or exceeding this magnitude of 0.001 based on the peak-probability density function of the applied spectrum. This theory produced good agreement with experimental results for both broad-band ($\sqrt{\alpha} = 0.79$) and narrow-band ($\sqrt{\alpha} = 1.0$) loading.

Hillberry [*14*] as well as others based their predictions on the distribution of peak stresses occurring in the life history. In this investigation, random fatigue tests were run with two entirely different power spectra, but with nearly identical $\sqrt{\alpha}$ ratios. The peak-stress distributions are the same for identical $\sqrt{\alpha}$ ratios. As shown below, two different spectra with identical peak-stress distributions should produce the same fatigue lives at the same rms stress level.

Peak-Probability Density Function and Cumulative Damage

The peak-probability density function for a continuous random process with Gaussian distributed instantaneous values, x, is given by Broch [*15*]

$$p(x) = \frac{\sqrt{1-\alpha}}{\sigma\sqrt{2\pi}} \exp\left[\frac{-x^2}{2\sigma^2(1-\alpha)}\right] + \frac{x\sqrt{\alpha}}{2\sigma^2}\left[1 + erf\left(\frac{x}{\sigma}\sqrt{\frac{\alpha}{2(1-\alpha)}}\right)\right] \exp\left[\frac{-x^2}{2\sigma^2}\right] \quad (1)$$

where

$$\alpha = \left(\frac{N_0}{M}\right)^2$$

σ = standard deviation of x.

Thus, the shape of the peak-probability density function depends on the parameter α only.

The Palmgren-Miner cumulative damage rule can be represented as

$$\sum_{i=1}^{i} \frac{n_i}{N_i} = 1 \quad (2)$$

where

n_i = number of cycles at stress amplitude, σ_i
N_i = number of cycles to failure at stress amplitude, σ_i

For constant amplitude test results the relationship between stress amplitude and cycles to failure can be represented by an equation of the form

$$N\sigma^b = B \tag{3}$$

The Palmgren-Miner damage theory can be extended to random loading by assuming that the damage produced by each positive peak is the same as the damage produced in a constant-amplitude fatigue test with the same stress amplitude. If N_p is the total number of positive peaks to failure in random loading, the expected number of positive peaks to failure between σ and $\sigma + d\sigma$ is

$$n(\sigma) = N_p p(\sigma) d\sigma \tag{4}$$

The expected damage of all positive peaks in the interval from σ to $\sigma + d\sigma$ is

$$\frac{n(\sigma)}{N(\sigma)} = \frac{N_p p(\sigma) d\sigma}{N(\sigma)} \tag{5}$$

The total expected damage is then

$$E(D) = N_p \int_{-\infty}^{\infty} \frac{p(\sigma)}{N(\sigma)} d\sigma \tag{6}$$

Substituting Eq 3 into Eq 6 gives

$$E(D) = \frac{N_p}{B} \int_{-\infty}^{\infty} \sigma^b p(\sigma) d\sigma \tag{7}$$

Using the normalized peak-probability function, $p(z)$, with the standardized variable z with zero mean and unit variance, Eq 7 becomes

$$E(D) = \frac{N_p}{B} \sigma_{\text{rms}}^{(b+1)} \int_{-\infty}^{\infty} z^b p(z) dz \tag{8}$$

Using the same material with constants b and B identical, the value of the integral will be the same for two spectra, which have the same peak-probability density of stress, $p(z)$. Therefore, if tests of the same material are run at the same rms stress and with identical peak-probability density functions, the number of positive peaks to failure, N_p, will be equal regardless of the value of the exponent b or the constant B. This assumes that the value of the expected damage is identically equal at failure.

Experimental Method and Test Results

Equipment

The fatigue tests for this investigation were performed on an MTS Systems Corporation electrohydraulic closed-loop fatigue machine which consisted of a 20-gpm, 3 000-psig hydraulic power supply, a servo amplifier with an ac input module, two 15-gpm servovalves, a 20-kip load cell, a 5-kip actuator with an 8-in. stroke, and a three-post load frame for the sinusoidal fatigue tests. For the random tests, a 20-kip actuator with a 5-gpm and a 15-gpm servovalve was used. Figures 1 and 2 are schematics of the constant-amplitude and random-loading fatigue-test systems. For the random tests, the output of a Gaussian noise generator was filtered to produce a broad-band and a bimodal spectra. For the sinusoidal tests a sine-wave function generator was used as the command signal.

The frequency response of the test system was flat within ±0.4 db from 0.1 to 65 Hz with sinusoidal input and the output measured on an oscilloscope.

Specimen

The specimens used in this investigation were machined from 2024-T3 aluminum alloy rod, ½ in. in diameter. The dimensions are indicated in Fig. 3. All specimens were hand polished using successively finer grades of emery cloth or silicon paper. First a fine grade emery cloth was used longitudinally to remove the turning marks. Polishing was continued until the machining marks were no longer visible. Then a 600 grit wet or dry silicon carbide paper was used transversely until the previous polish marks were no longer visible. Finally, the

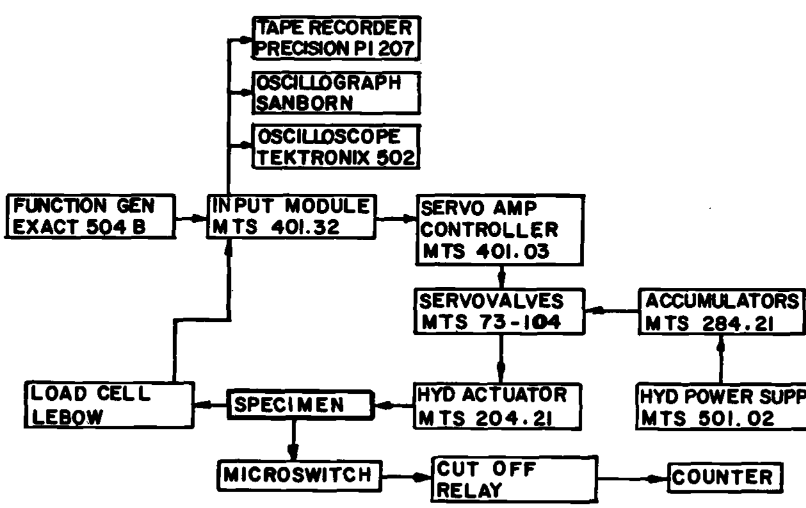

FIG. 1–*Schematic of sinusoidal loading fatigue test system.*

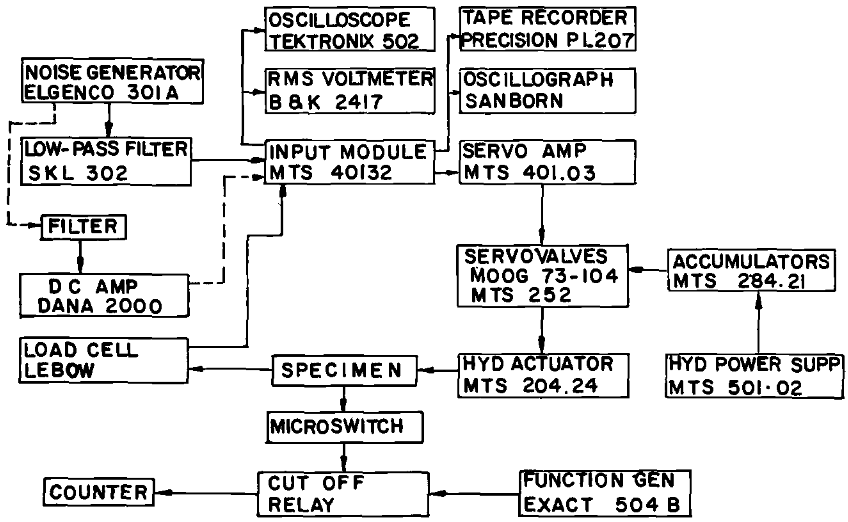

FIG. 2–*Schematic of random loading fatigue test system.*

specimen was polished longitudinally with crocus cloth until the preceding polish marks were not visible. A light lubricating oil film was applied to all specimens to reduce humidity effects.

Specimen Grips

Woods metal (a low-melting-point alloy) grips were designed to minimize bending. The specimen was threaded into the top grip and a disk and lock nut attached to the bottom thread of the specimen. Molten Woods metal was poured into a cylindrical ring in the bottom grip which was threaded into the actuator rod. The actuator rod was moved upward so that the molten Woods metal surrounded the disk. A cap was placed on the top of the ring and after the molten metal solidified, the specimen was loaded.

Results of strain-gage measurements taken on three gaged specimens yielded bending strains no greater than 3.07 percent of the theoretical strain using the applied load and the measured cross sectional area.

Sinusoidal Fatigue Tests

Constant-amplitude fatigue tests were conducted using a sine-wave-function generator as the command signal. Six specimens were tested at each of six stress levels from 26.1 to 49.5 ksi. Most samples were run at a frequency of 40 Hz.

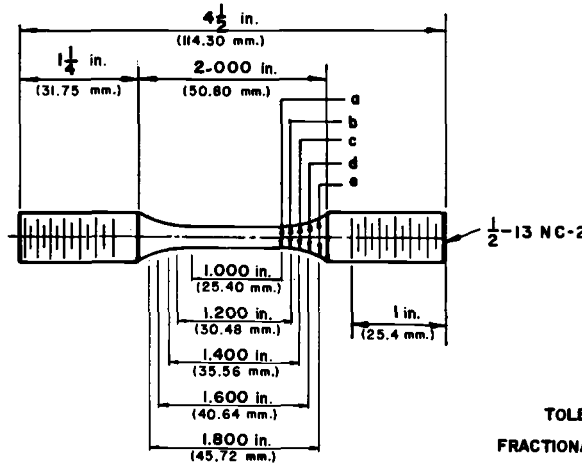

DIA	IN	mm.
a	0.250	6.35
b	0.260	6.60
c	0.270	6.86
d	0.300	7.62
e	0.350	8.89

TOLERANCES

FRACTIONAL $\pm \frac{1}{64}$ ($\pm$0.40 mm.)

DECIMAL $\pm$ 0.001 ($\pm$0.025 mm.)

FIG. 3–*Aluminum specimen.*

Random Fatigue Tests

In order to determine the effect of the peak-probability density on fatigue life, tests were conducted using a low-pass filter and a combination of two narrow-pass filters which produced a bimodal power spectrum with two resonant frequencies. A Gaussian noise generator was used as a signal source for both the broad-band and bimodal spectra. The broad-band tests were run with a N_0/M, or $\sqrt{\alpha}$, ratio of 0.70. For the bimodal spectrum, a filter using "twin-tee" rejection filters in the feedback loops of two operational amplifiers was used. The final stage gains were adjusted until the $\sqrt{\alpha}$ ratio for this spectrum was nominally the same as that of the broad-band spectrum. The measured value was 0.68. The two spectra were measured with a spectrum analyzer and averager with 0.2 Hz bandwidth filter and are presented in Fig. 4. Oscillograph traces of load or stress versus time for both spectra are shown in Fig. 5.

Test Results

The constant-amplitude test results are presented in Fig. 6 and random-fatigue test results are plotted in Fig. 7. The open and solid circles represent the logarithmic mean of cycles to failure or positive peaks to failure and the bars indicate the range. Failure in this paper is defined as rupture or separation of the specimen into two pieces. The test results are listed in Tables 1 and 2.

Statistical Analysis of Data

Two parametric and two nonparametric tests were performed on the random-fatigue results. The two parametric tests were designed to determine

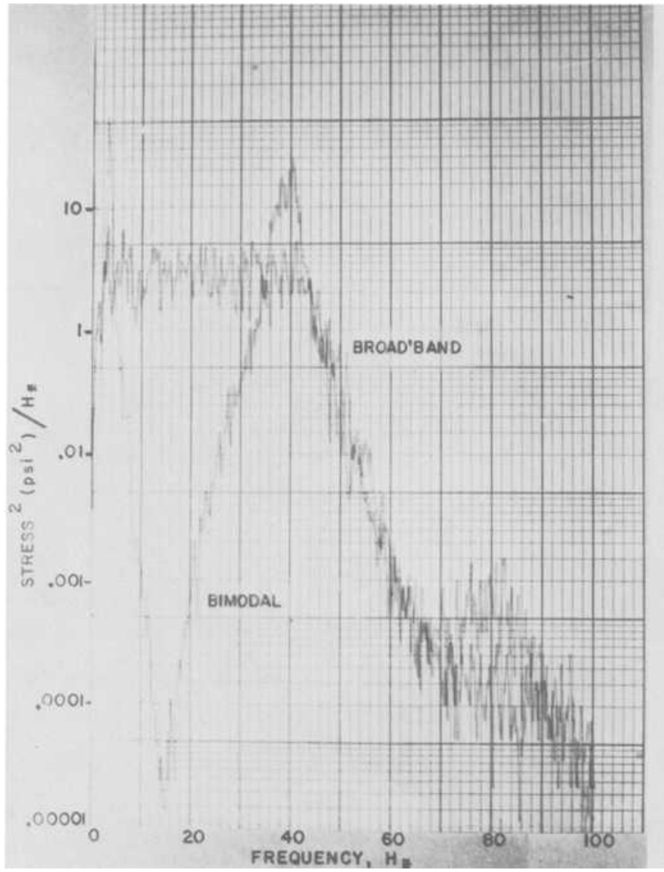

FIG. 4–*Bimodal and broad-band random loading spectra.*

whether the two sample populations represented by the two spectra at identical stress levels were from the same or different underlying populations. A comparison was made of sample means using the Student's t test. This tested the hypothesis that the population mean lives with each spectrum (at one rms stress level) were the same. The Type I error under this hypothesis was set at 0.01. The results of this comparison indicated the hypothesis should be accepted at the 0.01 significance level for all three rms stress levels. Since an assumption of equal variances was assumed in the above comparison of means, the second test (F test) was a two-sided comparison of the sample variances at each of the three stress levels. A Type I error of 0.02 was used. The variance ratios at all three stress levels fell within the acceptance interval and the hypothesis of equal

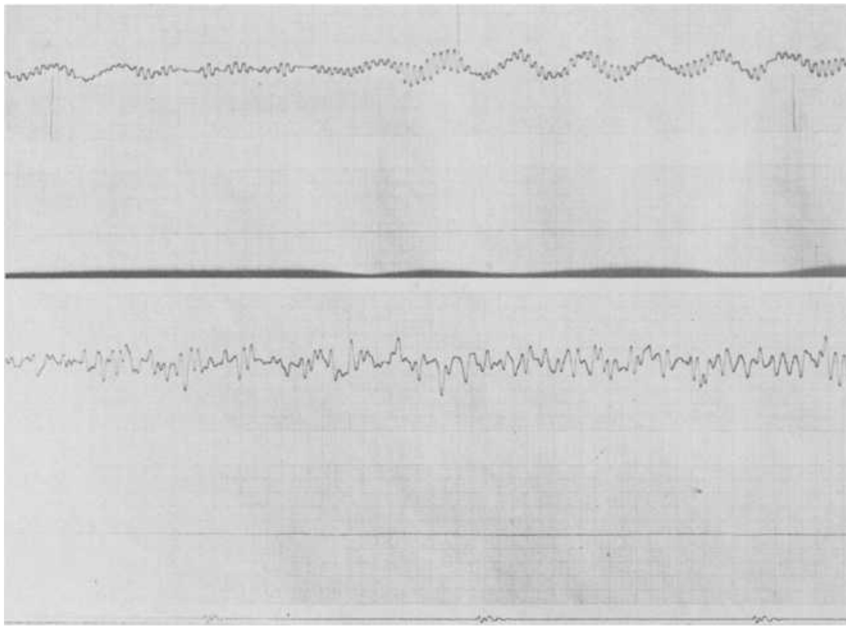

FIG. 5—*Oscillograph traces of broad-band and bimodal random loading response.*

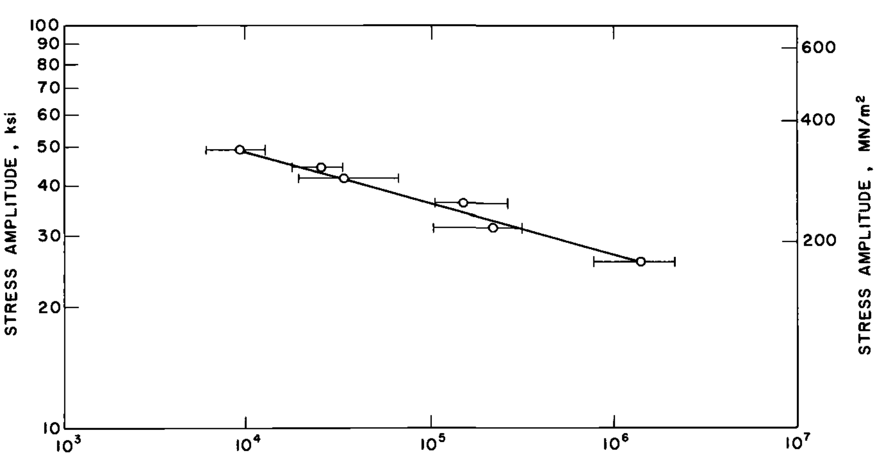

FIG. 6—*Constant amplitude sinusoidal fatigue test results.*

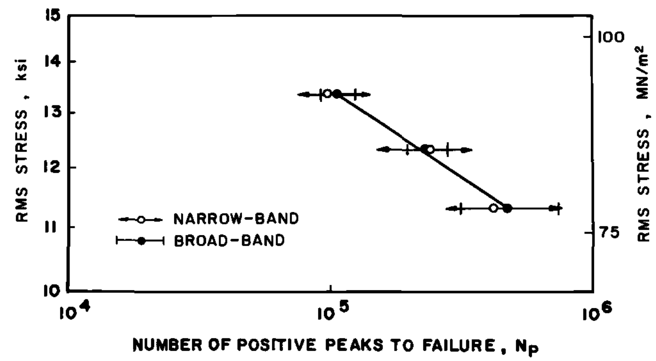

FIG. 7—*Random loading fatigue test results.*

variances was accepted at this significance level. However, at a significance level of 0.10, the hypothesis of equal variances was accepted at two stress levels but was rejected at 12.3-ksi rms stress level.

The two nonparametric statistical tests were also used on these data. Identical populations were again hypothesized for the "sign test" [*16*]. Two minus signs and four minus signs were obtained at the 12.3- and 11.3-ksi rms stress levels, respectively. A test at the higher stress level was not made due to the small number of samples for the broad-band spectrum. Using a binomial distribution, the conditional probability of fewer than three plus signs or fewer than three minus signs from 14 paired observations given that the probability of selecting a plus sign is 0.50 was calculated at 0.013. This defined a Type I error as 0.013. Thus, the result indicated acceptance of the hypothesis of identical populations at the 0.013 significance level. A second nonparametric test, the Wilcoxon-Mann-Whitney test [*16*] was made at all three stress levels to test the identical distribution hypothesis. The results of this test at the 13.3, 12.3, and 11.3-ksi

TABLE 1—*Mean and standard deviation of constant-amplitude fatigue tests.*

Stress Amplitude		Number of			
ksi	MN/m²	Specimens	$\overline{N}^a$	$\overline{X}^b$	S^c
49.5	341	6	9 500	3.9777	0.130
45.0	310	6	25 840	4.4124	0.109
41.7	288	6	34 830	4.5420	0.184
36.0	248	6	159 100	5.2016	0.146
31.5	217	6	225 800	5.3538	0.174
26.1	180	6	1 412 000	6.1497	0.167

[a] $\overline{N}$ = Antilog of average of log N
[b] S = Standard deviation of log N
[c] $\overline{X}$ = Average of log N

TABLE 2–*Mean and standard deviation of random fatigue tests.*

rms Stress						
ksi	MN/m²	Spectrum	Number of Specimens	$\overline{X}^a$	$\overline{N}_p{}^b$	S^c
13.3	91.7	Broad-band	2	5.0302	1.072×10^5	0.097
12.3	84.8	Broad-band	8	5.3645	2.315	0.055
11.3	77.9	Broad-band	7	5.6716	4.694	0.119
13.3	91.7	Bimodal	7	5.0081	1.019	0.119
12.3	84.8	Bimodal	7	5.3990	2.506	0.134
11.3	77.9	Bimodal	7	5.6356	4.321	0.148

^{a} $\overline{X}$ = Average of log Np
^{b} $\overline{N}p$ = Antilog of average of log Np
^{c} S = Standard deviation of log Np

rms stress levels were within the acceptance interval at the 0.044, 0.007, and 0.007 significance levels, respectively.

Conclusions

In this investigation, there was no significant difference at the 0.01 significance level between the fatigue lives using two entirely different power spectra with identical peak-probability density functions at three rms stress levels. This indicates that the distribution of stress peaks is an important parameter in random fatigue.

This investigation implies that the shape of the power spectrum influences the fatigue life under random-loading conditions only through its influence on the peak-probability density function. If this holds true for other $\sqrt{\alpha}$ ratios, then laboratory simulation studies should be performed with the same peak-probability density function of stress, or equivalently the same $\sqrt{\alpha}$ ratio, as the actual field-stress spectrum.

Any $\sqrt{\alpha}$ between 0 and 1.0 could be duplicated by using dual discrete resonances in the power spectrum or by adjusting the slope of the power spectrum with a bandwidth ratio of 100 or greater. Thus, laboratory studies of an ergodic process could produce accelerated test results using a filtered spectrum with higher center frequencies than the field data by maintaining the same $\sqrt{\alpha}$ ratio.

References

[1] Miner, M. A., *Journal of Applied Mechanics,* American Society of Mechanical Engineers, JAMCA, Vol. 12, 1945, pp. 159-164.

[2] Spence, H. R. and Luhrs, H. N., *Journal of the Acoustical Society of America,* JASMA, Vol. 3, No. 3, 1961, pp. A1098-1101.

[3] Marsh, K. J. and Mackinnon, J. A., *Journal of Mechanical Engineering Science,* JMESA, Vol. 10, Feb. 1968, pp. 48-58.

[4] Corbin, P. L. and Naumann, E. C., "Influence of Programming Techniques and of

Varying Limit Load Factors on Maneuver Load Fatigue Test Results," Technical Note D-3149, National Aeronautics and Space Administration, Jan. 1966.

[5] Naumann, E. C., "Evaluation of the Influence of Load Randomization and of Ground-air-ground Cycles on Fatigue Life," Technical Note D-1584, National Aeronautics and Space Administration, Oct. 1964.

[6] Naumann, E. C., "Fatigue Under Random and Programmed Loads," Technical Note D-2629, National Aeronautics and Space Administration, Feb. 1965.

[7] Leybold, H. A. and Naumann, E. C. in *Proceedings*, American Society for Testing and Materials, ATMPB, Vol. 63, 1963, pp. 717-734.

[8] Marsh, K. J. and Mackinnon, J. A., *Journal of Mechanical Engineering Science*, JMESA, Vol. 10, 1968, pp. 48-58.

[9] Heller, R. A., Seki, M., and Freudenthal, A. M. in *Proceedings*, American Society for Testing and Materials, ATMPB, Vol. 64, 1964, pp. 516-535.

[10] Kowalewski, J. in *Full Scale Testing of Aircraft Structures*, F. J. Plantema and J. Schijve, Eds., Pergamon Press, New York, 1961, pp. 60-75.

[11] Swanson, S. R., "An Investigation of the Fatigue of Aluminum Alloy Due to Random Loading," University of Toronto Institute of Aerophysics, Report 84, 1964.

[12] Bussa, S. L., "Fatigue Life of Low Carbon Steel Notch Specimens Under Stochastic Conditions," MTS Systems Corp. Technical Report 900.21-1, 1967.

[13] Clevenson, S. A. and Steiner, R., "Fatigue Life Under Random Loading for Several Power Spectral Shapes," Technical Report R-266, National Aeronautics and Space Administration, 1967.

[14] Hillberry, B. M. in *Effects of Environment and Complex Load History on Fatigue Life, ASTM STP 462*, American Society for Testing and Materials, 1970, pp. 167-183.

[15] Broch, J. T. in *Bruel & Kjaer Technical Review*, No. 3, 1963.

[16] Lingren, B. W. and McElrath, G. W., *Introduction to Probability and Statistics*, 2nd ed, Macmillan Co., New York, 1966, chapters 4 and 9-11.

H. Itagaki[1] *and M. Shinozuka*[1]

Application of the Monte Carlo Technique to Fatigue-Failure Analysis under Random Loading

REFERENCE: Itagaki, H. and Shinozuka, M., "Application of the Monte Carlo Technique to Fatigue-Failure Analysis under Random Loading," *Probabilistic Aspects of Fatigue, ASTM STP 511*, American Society for Testing and Materials, 1972, pp. 168–184.

ABSTRACT: Analyzing the fatigue damage of a notched specimen subjected to a random-stress history of narrow-band characteristics, the crack propagation factor is treated as a homogeneous random process reflecting statistical variations of material property within the specimen. On the basis of the proposed statistical-mechanical model of fatigue failure, into which a crack propagation model and a fracture criterion are incorporated, statistical distribution of fatigue life is predicted with the aid of the Monte Carlo technique by digitally simulating the stress history and the crack propagation factor as random processes. The results indicate that the spacial randomness in material property can, and in fact should be considered in order to account for the larger scatter of fatigue life observed in the experiment performed under the conditions compatible with the assumptions used in the analysis.

KEY WORDS: fatigue(materials), fracture(materials), statistical analysis, random processes, loading, stress analysis, crack propagation, Monte Carlo technique, fatigue tests

As is well known, a majority of important structures such as air and spacecraft, ships, and bridges are subject to loading of a random nature during their operation and the mechanical property of the material of which these structures are made exhibits micro as well as macroscopic spacial statistical variations.

The problem of fatigue failure of structural components or specimens under the conditions of random loading has so far been a subject of study in a large number of papers without, however, considering the spacial variation of material strength parameters. As a first step, therefore, this paper attempts to study the effect of such randomness of material property (of specimen along its fracture

[1] Visiting senior research associate, and professor of civil engineering, respectively, Columbia University, New York, New York 10027.

path x) on the process of crack propagation within a notched specimen under conditions of random loading.

For this purpose, it is assumed as usual that: (1) the stress history, $s(t)$, due to loading is of the form of a narrow-band stochastic process with mean zero (the mean zero assumption is not essential to the following analysis); and (2) the crack-propagation process can be completely described by the sequence of "stress peaks" of the process $s(t)$ (consisting of absolute values of local peak and trough stresses), which can be interpreted as point process[*1*] $s_1, s_2, \ldots, s_n$ with s_i indicating the absolute value of the i^{th} local extreme of the process $s(t)$ (see Fig. 1).

Under further usual assumptions as to the law of (stable) crack propagation, the cumulative fatigue damage, $D(c_n)$ can be written as

$$D(c_n) - D(c_{n-1}) = k_n f(s_n) \tag{1}$$

or

$$D(c_n) - D(c_0) = \sum_{i=1}^{n} k_i f(s_i) \tag{2}$$

where

$D(c_n)$ = fatigue damage; a function of fatigue crack length c_n existing immediately after the application of s_n

$f(s_i)$ = a function of stress peak s_i

$k_i = k(x_i)$, crack propagation factor; a random function of location, x_i, of crack tip along the fracture path immediately before the application of s_i.

In the present study, the process $k(x)$ and the sequence s_i will be digitally simulated with the aid of the methods respectively developed in Refs *2* and *3*.

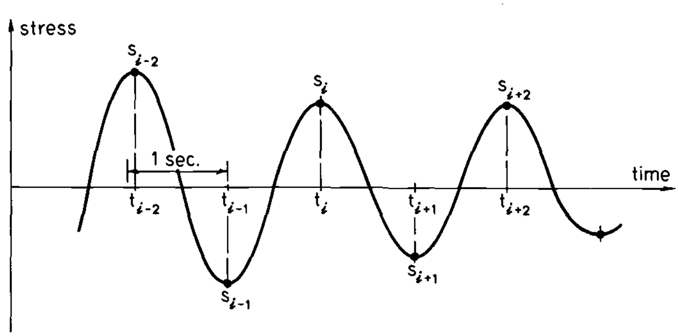

FIG. 1–*Stress history and stress peaks.*

This will make it possible to perform a digital experiment evaluating $D(c_n)$ numerically with the aid of Eq 1. Therefore, repeating the same computation on a sample of nominally identical specimens, each with a set of simulated realizations of $k(x)$ and s_i, one can produce a sample of $D(c_n)$ from which the empirical distribution of $D(c_n)$ can be obtained. At the same time, with an appropriate failure criterion, a sample of fatigue life, N, and therefore its empirical distribution can be simulated.

A similar digital experiment, however, has been performed with a constant crack propagation factor (determined from a fatigue test under various constant-stress amplitudes). The result is plotted on extremal probability paper in Fig. 2 (open circles), together with the experimental result (solid circles) [3]. The numerical simulation indicated in this diagram is performed under the following reasonable assumptions [4]: (1) the initial crack length c_0 is identical for all the specimens (if c_0 is random, however, it can be treated as such); (2) $D(c_n) = \ln c_n$; (3) $f(s_i) = s_i^m$ (m; constant); and (4) the (unstable) failure criterion is given by an expression

$$s_{cr} = k' c_{cr}^{-m_2} \tag{3}$$

where $k' > 0$ is the fracture coefficient, s_{cr} and c_{cr} denote the critical stress peak and the critical crack length, and m_2 denotes a positive constant. According to this criterion, failure (tearing) can occur to a specimen with a crack of any size, c_n, if the (random) stress peak, s_n, happens to exceed the critical value, s_{cr}, associated with c_n; $s_{cr} = k' c_n^{-m_2}$.

Figure 2 clearly indicates that the randomness in stress history alone cannot reproduce the wide dispersion of fatigue lives as observed in experiment. The

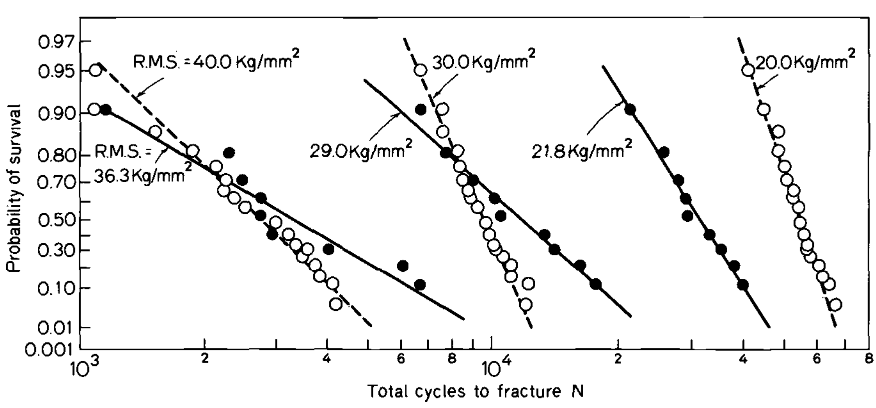

FIG. 2—*Distribution of fatigue life under random loading.*

present paper will show that the introduction of randomness into the propagation factor and the fracture coefficient indeed alleviates, if not completely eliminates, this difficulty. In fact, in what follows, the procedure of simulating $k(x)$, k', and s_i and reproducing crack growth and failure of a specimen is repeated over a sample of specimens, each subjected to an independent sequence of s_i until failure. The resulting sample of fatigue lives is compared with those obtained from experiments to see whether the assumptions and hypotheses used in the computation are to be accepted. It is in this sense that the words "Monte Carlo technique" are used here.

It is acknowledged that a variety of laws of crack growth are proposed and used by a number of researchers under various experimental conditions (for example, see comments by Paris and Erdogen in Ref *4*). The particular law used here is one of these, and is considered reasonable; it serves well for the purpose of demonstrating the Monte Carlo procedure to be pursued in the present study.

Statistical Characteristics of the Crack Propagation Factor and Stress History

The crack propagation factor in Eq 1 is a measure of the material resistance to fatigue crack propagation in the sense that the smaller the factor, the tougher the material. Since the propagation of a fatigue crack is highly dependent upon the property of material in the microscopic vicinity of the tip of the crack, this factor should reflect a sensitivity to the statistical variation of microscopic structure of the material (referred to as "structural sensitivity" in this paper) even though the analysis is performed in a macroscopic approximation using Eq 1.

Evidently, such statistical variation in the structural sensitivity will produce a statistical variation of the rate of crack propagation. In fact, given a law of crack propagation such as Eq 1, it is possible to derive an empirical distribution function of the crack propagation factor from the statistical scatter of the rate of crack growth measured at various values of the amplitude of stress-intensity factor. Caution should be exercised, since the measurements are usually made macroscopically taking the average growth rate over several hundred stress cycles. It should also be pointed out that the empirical distribution function thus obtained contains no information on the (strictly speaking, three dimensional) spacial correlation of the crack propagation factor. Some of the experimental studies involving measurements of microscopic crack propagation report that the fatigue crack propagates successively creating striations randomly spaced as shown in Fig. 3, and suggest that the spacing of such striations is somehow related to the rate of crack propagation. In some instances, the correspondence between individual striations and stress cycles has been identified [*5*]. The statistical dispersion of the spacing of striations observed in a wide area of a crack surface are reported in some papers[*6,7*] (Fig. 4[*7*]). Detailed examination of striation patterns, however, indicates an important fact:

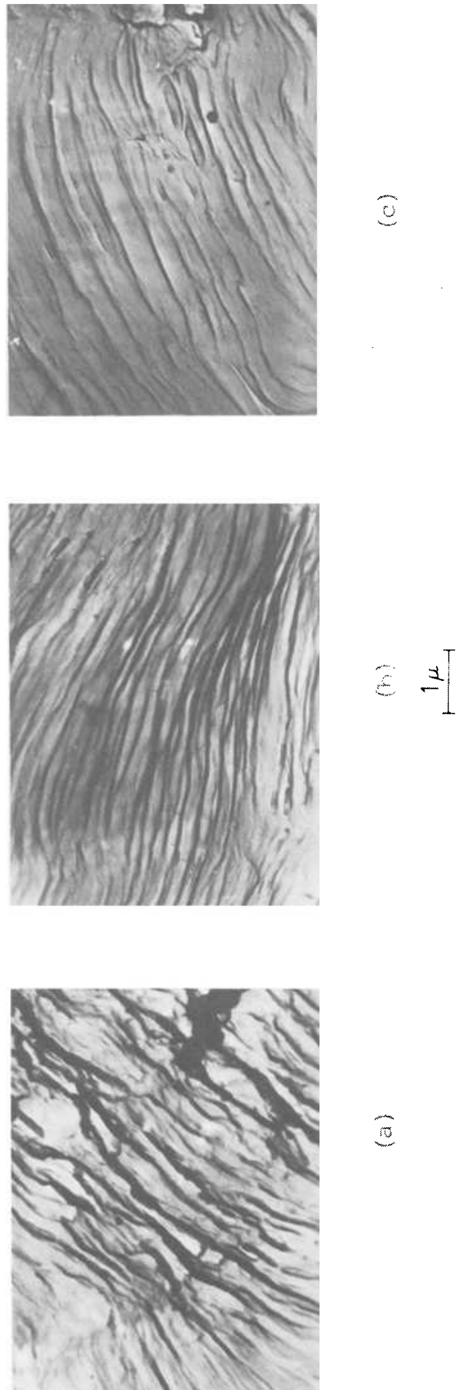

FIG. 3 —*Striation patterns.*

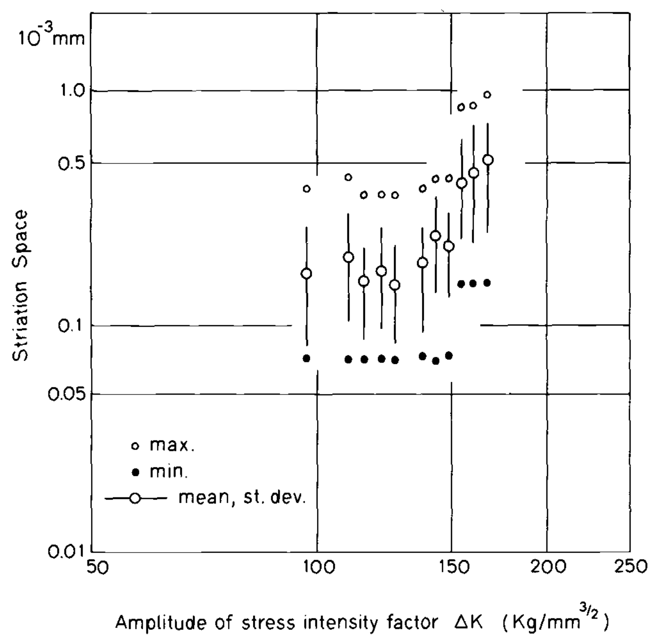

FIG. 4–*Dependence of striation space on amplitude of stress-intensity factor.*

the striation spacing is not independent but correlated as shown in Fig. 3. These photographs show three microscopic areas chosen arbitrarily from a 0.5-mm square on a fatigue crack surface produced in a mild steel specimen. Independent spacings would be characterized by a random mixture of spacings of all sizes, for example, a spacing of extremely small size is immediately followed by that of extremely large size, and so forth. This implies that the crack propagation factor may be represented by a random process of white characteristics. The three parts of Fig. 3, however, do not indicate such a trend. Rather, they exhibit a gradual change in size as the striation process proceeds, eventually producing notable differences in size at distant (microscopically) locations. This appears to substantiate at least qualitatively the hypothesis that the crack propagation factor, $k(x)$, is a random process in space with a nonzero spacial correlation, although more quantitative observations must obviously be made in a future study.

Since there is usually no reason to believe *a priori* that the statistical characteristics of a crack propagation factor at a particular location within a specimen differ from that at any other location, the process $k(x)$ is homogeneous. Also, the process $k(x)$ is assumed to be ergodic so that statistical characteristics are identical for all the realizations of the crack propagation factor.

Because of the lack of further information, it is assumed that the crack propagation factor $k(x)$ is represented by a process such that the logarithm $z(x)$ of $k(x)/\bar{k}(x)$ has the following forms of the autocorrelation $R_z(\xi)$, the mean square spectral density $S_z(\omega)$, and the distribution function $F(z)$;

$$R_z(\xi) = E[z(x)z(x+\xi)] = \sigma_z{}^2 e^{-\alpha|\xi|} \tag{4}$$

$$S_z(\omega) = \frac{1}{2\pi}\int_{-\infty}^{\infty} R_z(\xi)e^{-i\omega\xi}d\xi = \frac{\alpha\sigma_z{}^2}{\pi}\,(\alpha^2+\omega^2) \tag{5}$$

$$F(z) = \int_{-\infty}^{\infty} \frac{1}{\sqrt{2\pi}\sigma_z} \exp\left\{-\frac{(z-\mu_z)^2}{2\sigma_z{}^2}\right\} dz \tag{6}$$

where

$E[\ldots]$ = expectation
$z(x) = \ln k(x) - \overline{\ln k(x)}$
σ_z = standard deviation of $z(x)$
$1/\alpha$ = correlation length of $z(x)$

Although the validity of such assumptions should be tested in a future study, at least the hypothesis (Eq 6) implying that $k(x)$ has a log-normal distribution appears to be reasonable. In this connection, it is pointed out that the emphasis in the present study is placed on: (1) the analytical approach through which the crack propagation and the failure criteria (Eqs 1 and 3) can be numerically treated to account for the scatter of fatigue life; and (2) on the identification of the specific information such as the form of $R_z(\xi)$ which should be obtained in future experiments.

The well known relationship between the statistics of a log-normal variate and the corresponding normal variate indicates that

$$\mu_k = \exp\,(\mu_z + \tfrac{1}{2}\,\sigma_z{}^2) \tag{7}$$

$$\sigma_k \approx \mu_k\sigma_z \text{ for } \sigma_z{}^2 \ll 1 \tag{8}$$

where

$$\mu_k = E[k(x)]\,,\, \mu_z = E[z(x)] \tag{9}$$

$$\sigma_k{}^2 = E[k(x)-\mu_k]^2\,,\, \sigma_z{}^2 = E[z(x)-\mu_z]^2 \tag{10}$$

With the aid of the method developed in Ref *2*, the process $z(x)$ can be simulated in the form

$$z(x) = \sigma_z \left(\frac{2}{M}\right)^{1/2} \sum_{i=1}^{M} \cos(\omega_i x + \theta_i) \tag{11}$$

where

x = length along fracture path
θ_i = random variable distributed uniformly between 0 and 2π; independent of $\theta_j (i \neq j)$
ω_i = random variable identically and independently distributed with density function $g(\omega_i) = S(\omega_i)/\sigma_z^2$; independent of $\omega_j (i \neq j)$ and $\theta_j (j = 1,2, \ldots, M)$.

If a large positive integer is used for M, the central limit theorem asserts that $z(x)$ in Eq 11 is Gaussian. Furthermore, it can be shown that $z(x)$ in Eq 11 satisfies Eqs 4 and 5 and is ergodic and therefore so is $k(x)$. In passing, it is noted that a more efficient method of simulation [8] has recently been developed and can be used in place of Eq 11.

It is noted here that when Eq 11 is used together with Eq 2, x should be replaced by the crack length, c.

As to the random-stress history, the method developed in Ref 3 is employed to simulate the stress sequence since the experimental results, with which the present analysis is to be compared, are available under such a sequence. The method of simulation calls for digital generation of two independent Markovian sequences of Gaussian variables

$$a_1, a_2, \ldots$$
$$b_1, b_2, \ldots$$

The (conditional) probability of a_i depends only on the realization of a_{i-1} with the probability density

$$P\{u < a_i \leqslant u + du\} = \exp(-u^2/2) du/(2\pi)^{1/2} \tag{12}$$

and the conditional density of a_i given $a_{i-1} = v$

$$P\{u < a_i \leqslant u + du | a_{i-1} = v\}$$
$$= \exp\left\{-\frac{(u - \rho v)^2}{2(1-\rho^2)}\right\} du / \{2\pi(1-\rho^2)\}^{1/2} \tag{13}$$

where $P\{A\}$ denotes the probability of event A. The same probability densities apply to the sequence b_i.

The peak stress s_i is then constructed in terms of a_i and b_i in the form;

$$s_i = \sigma_s(a_i^2 + b_i^2)^{1/2}/(2)^{1/2} \tag{14}$$

where σ_s is the root mean square of s_i. It can be shown [3] that the probability density of s_i is that of the Rayleigh distribution

$$P\left\{u < s_i \leqslant u + du\right\} = \frac{2u}{\sigma_s} \exp\left(-\frac{u^2}{\sigma_s^2}\right) du \quad u \geqslant 0 \tag{15}$$

and the joint probability density of s_i and s_{i-1} is

$$P\left\{u < s_i \leqslant u + du,\, v < s_{i-1} \leqslant v + dv\right\}$$

$$= \frac{4uv}{\sigma_s^4(1-\rho^2)} \exp\left\{-\frac{u^2 + v^2}{\sigma_s^2(1-\rho^2)}\right\} I_0\left\{\frac{2\rho uv}{\sigma_s^2(1-\rho^2)}\right\} du dv \tag{16}$$

where $P\{A, B\}$ is the probability of joint occurrence of A and B and $I_0\{\ldots\}$ is the zero-order modified Bessel function of the first kind. It can also be shown, by comparing Eqs 1 and 3 of Ref *1* with Eqs 15 and 16, respectively, that the sequence s_i represents a point process consisting of peak and trough values of a narrow-band process with mean zero, central frequency, ω_o, and normalized autocorrelation functions, $r(\tau)$, such that $\rho = r(\pi/\omega_o)$. Such a narrow-band process can be obtained by filtering a white noise through a lightly damped oscillator (of single-degree of freedom) with natural frequency, ω_o. Obviously, it is this interpretation that makes the sequence, s_i, meaningful in engineering applications.

The digital simulation of both $k(x)$ and s_i therefore requires the generation of random variables such as ω_i, θ_i, a_i, and b_i with specified density of conditional density functions. Such generation of random variables is routine with the aid of a digital computer.

Numerical Example

The preceding procedure of predicting crack propagation is now mumerically carried out with the aid of Eq 1 or its equivalent. At the same time, Eq 3 is used to compute the critical value s_{cr} of the stress peak corresponding to the crack length, c, existing within a specimen immediately after the application of, say, s_{i-1}. If this critical value is exceeded by the stress peak, s_i, the fatigue failure occurs at the i^{th} application of stress peak. This failure criterion produces an *S-N* relationship when applied to a fatigue test performed under constant stress amplitude. For example, consider the result, as shown in Fig. 5, of a constant-stress-amplitude fatigue test [3,7] performed under rotating bending on

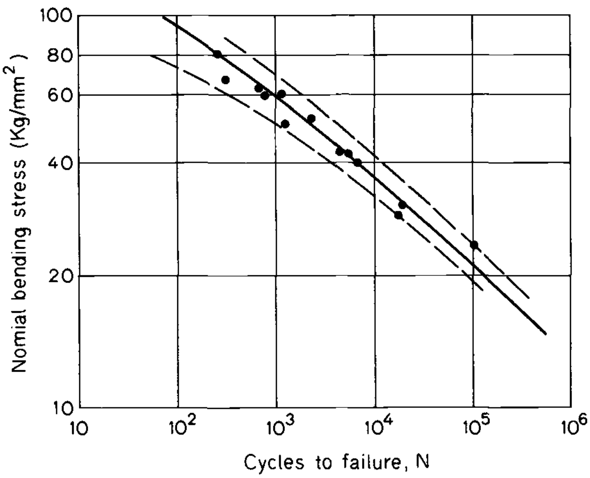

FIG. 5–S-N *diagram under constant-amplitude test.*

thirteen nominally identical notched specimens (Fig. 6) of mild steel. Then, a special form of Eq 1 (the difference equation is approximated by a differential equation with $k_1 = k_2 = \ldots = k$)

$$\frac{dc}{dn} = kcs^{4.2}(\text{mm/cycle}) \tag{17}$$

under the initial condition $c_0 = 3.5$ mm can be used with Eq 3 of the form

$$s_{cr} = k'c^{-3.5}(\text{kg/mm}^2) \tag{18}$$

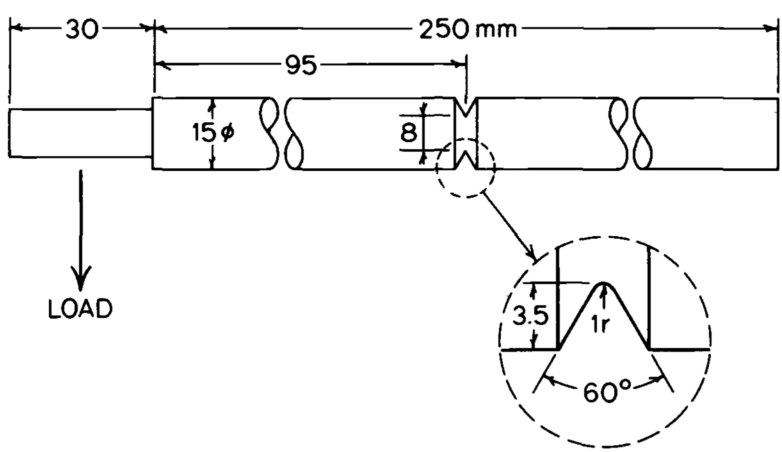

FIG. 6–*Notched specimen.*

to reproduce a central trend of the *S-N* relationship as indicated by the solid curve in Fig. 5, provided $k = 1.3 \times 10^{-11}$ and $k' = 1.45 \times 10^4$ are assumed.

In Ref *9* it is assumed that the scatter of thirteen fatigue lives (at various levels of stress amplitude) around this central trend is attributable solely to the statistical variation (from specimen to specimen) of the coefficient k' in Eq 18 and that the distribution is log-normal.

To estimate two parameters of this log-normal distribution, first Eqs 17 and 18 are used with $k = 1.3 \times 10^{-11}$ and $c_0 = 3.5$ mm (0.138 in.) to compute those values of k' which would exactly reproduce the thirteen fatigue lives at their respective stress levels. From this set of thirteen values of k', the median value $\breve{k}'$ (of k') = 1.45×10^4 and the standard deviation δ(of $\ln k'$) = 0.37 are then estimated. Note that $\ln \breve{k}'$ is the mean value of $\ln k'$. A pair of dashed curves in Fig. 5 (where the fatigue life is plotted on logarithmic scale) define a domain of $\pm 2\delta$ in which a fatigue life at any stress level will be found with an approximate probability 0.95. Inspecting Fig. 5, one can conclude that the statistical-mechanical model assumed above with $\breve{k}' = 1.45 \times 10^4$ and $\delta = 0.37$ appears to reflect correctly the extent of scatter as well as the central trend of the *S-N* relationship.

In Fig. 7, the value of the critical stress peak s_{cr} (that produces an immediate

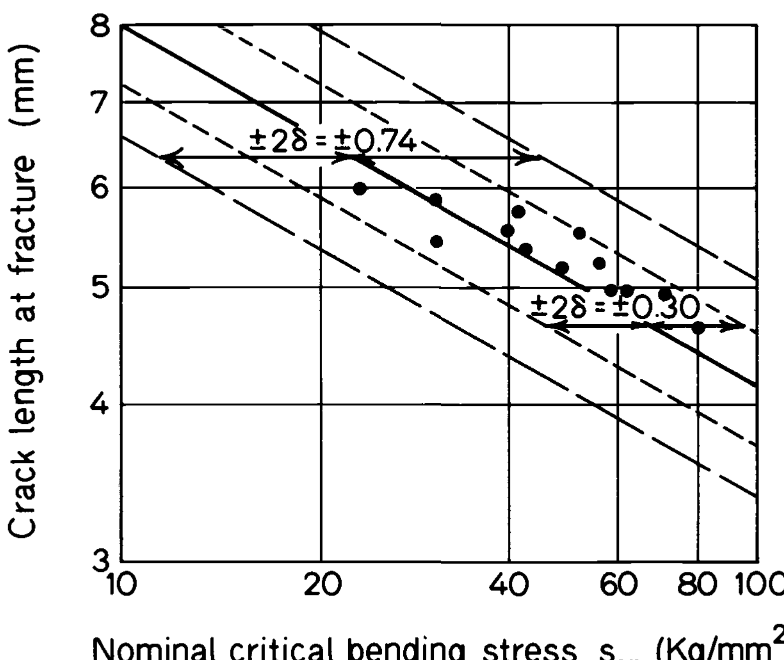

FIG. 7—*Crack length at fracture as a function of nominal critical stress.*

fracture to the specimen) is replotted from Ref 7 against the corresponding crack length (which existed at the time of application of the critical stress peak); such a crack length can be identified and measured by inspecting the fracture surface. In Fig. 7, the solid line represents Eq 18 with $\breve{k}' = 1.45 \times 10^4$ and a pair of dashed lines define a domain of $\pm 2\delta$ as in Fig. 5. This result reflects the fracture criterion given in Eq 18 and is independent of the crack propagation mechanism. Therefore, the hypothesis that the statistical variation in k' is solely responsible for the scatter of fatigue life, can be tested by checking whether the log-normal model for k' together with the estimated parameter values ($\breve{k}' = 1.45 \times 10^4$ and $\delta = 0.37$) reflects the extent of scatter of s_{cr} shown in Fig. 7 as reasonably well as it did for the *S-N* diagram in Fig. 5.

A close examination of Fig. 7 shows that the log-normal model of k' appears to overestimate the scatter of the critical stress; the domain of $\pm 2\delta$ in Fig. 7 is too wide to be a reasonable indication of the scatter, if the parameters involved in this log-normal model of k' are estimated from the observed *S-N* relationship as was done in this study. Obviously, it is expected that, if these parameters were estimated from the result given in Fig. 7, they would reproduce a much narrower dispersion in the *S-N* relationship than observed. The hypothesis that the coefficient k' is solely responsible for the scatter must therefore be discarded.

It is this conclusion that initially motivated the present study in which the modified hypothesis is used so that not only the randomness of k' but also the stochastic nature of k (as a random process) are introduced into the statistical-mechanical model of fatigue failure.

The following three different cases are considered for numerical computation (refer to Eqs 4-10).

Case A:	$\mu_k = 1.3 \times 10^{-11}$,	$\sigma_k = \sigma_z = 0$
	$\breve{k}' = 1.45 \times 10^4$,	$\delta = 0$
Case B:	$\mu_k = 1.3 \times 10^{-11}$,	$\sigma_k = \sigma_z = 0$
	$\breve{k}' = 1.45 \times 10^4$,	$\delta = 0.15$
Case C:	$\mu_k = 1.3 \times 10^{-11}$,	$\sigma_k = 0.5\, \mu_k$ or $\sigma_z \approx 0.5$
	$\breve{k}' = 1.45 \times 10^4$,	$\delta = 0.15$

Case A deals with no randomness in either $k(x)$ or k'. In Case B, however, the randomness of k' is introduced with $\delta = 0.15$, whereas in Case C, the randomness of both $k(x)$ and k' is taken into consideration. The value of $\delta = 0.15$ has been used in all cases since this value appears to be consistent with the amount of scatter observed in Fig. 7.

It is pointed out that, in Case C, an ad hoc assumption that the correlation length, $1/\alpha$, is equal to 1/8 mm has been used. A portion of a realization of $k(x)$ is plotted in Fig. 8 where the patterns of striations at three different points along the fracture path, x, are schematically shown. These patterns reflect the nonzero

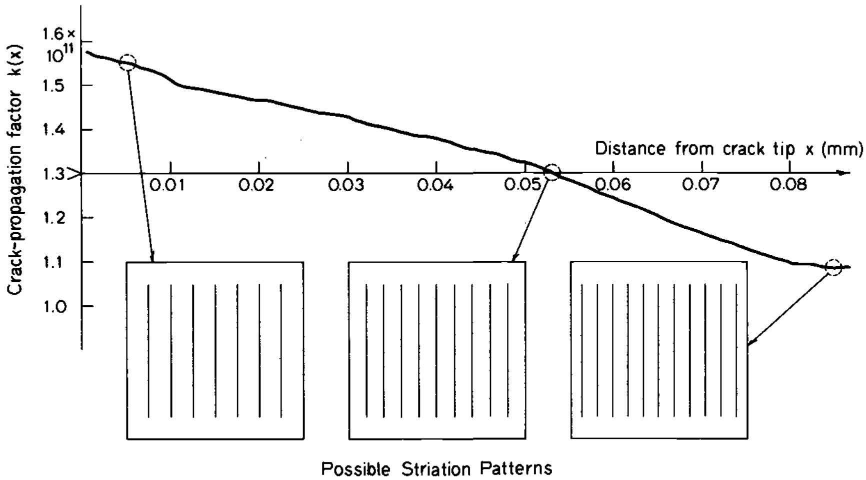

FIG. 8—*Sample of crack-propagation factor* k(x) *and possible striation patterns.*

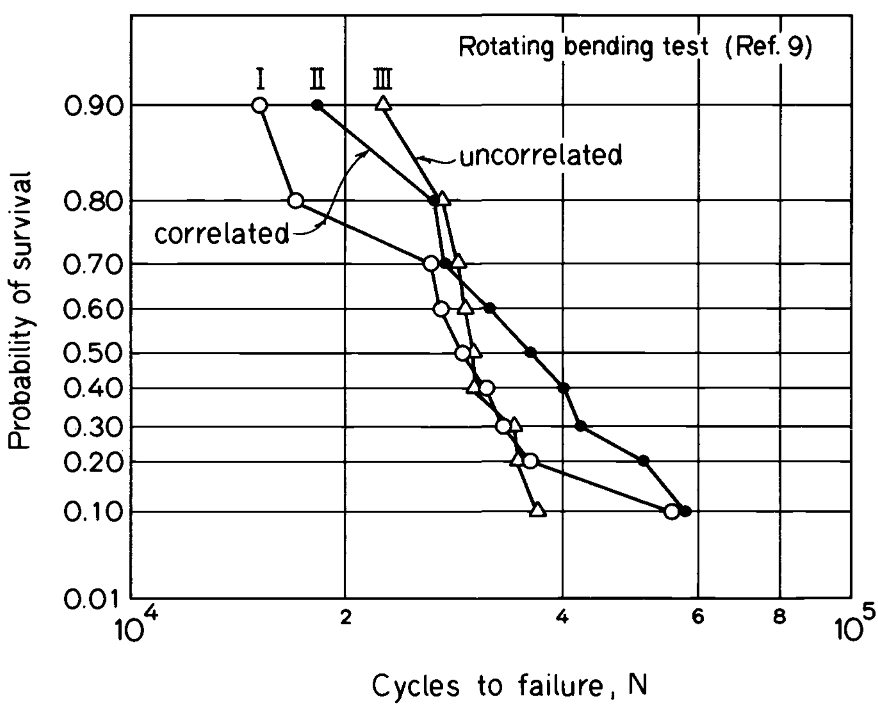

FIG. 9—*Distribution of fatigue life under rotating bending test.*

correlation introduced in the modified model and reproduce the gradual change of the size of striations observed in Fig. 3.

In all cases, the stress peak $s_i = |s(t_i)|$ with $\sigma_s = 21.8$ kg/mm^2 (31.0 ksi) is simulated by the method described in the preceding section. In Ref *9*, however, for experimental ease, a sequence of blocks of identical stress peaks (one block consists of 25 identical peaks) is applied to each specimen until failure; a block of 25 stress peaks of s_i is followed by a block of 25 stress peaks of s_{i+1} and so forth, where s_i, s_{i+1}, and so forth, are the sequence described above. Three sequences, I, II, and III, of stress peaks are considered, each with a different autocorrelation property. In fact, sequences I, II, and III are constructed using Eqs 12 and 13 with $\rho = 0.95$, 0.98, and 0, respectively. This implies [*3*] that the correlation coefficients, ρ_S, between s_i and s_{i+1} are 0.90, 0.95, and zero, respectively, for sequences I, II, and III. For each sequence, nine realizations are simulated and each of these realizations is applied to one of nominally identical specimens shown in Fig. 6. Hence, three sets of nine specimens are tested until failure. The result is plotted on extremal probability paper (Fig. 9) where I, II, and III indicate the corresponding sets of nine specimens, respectively.

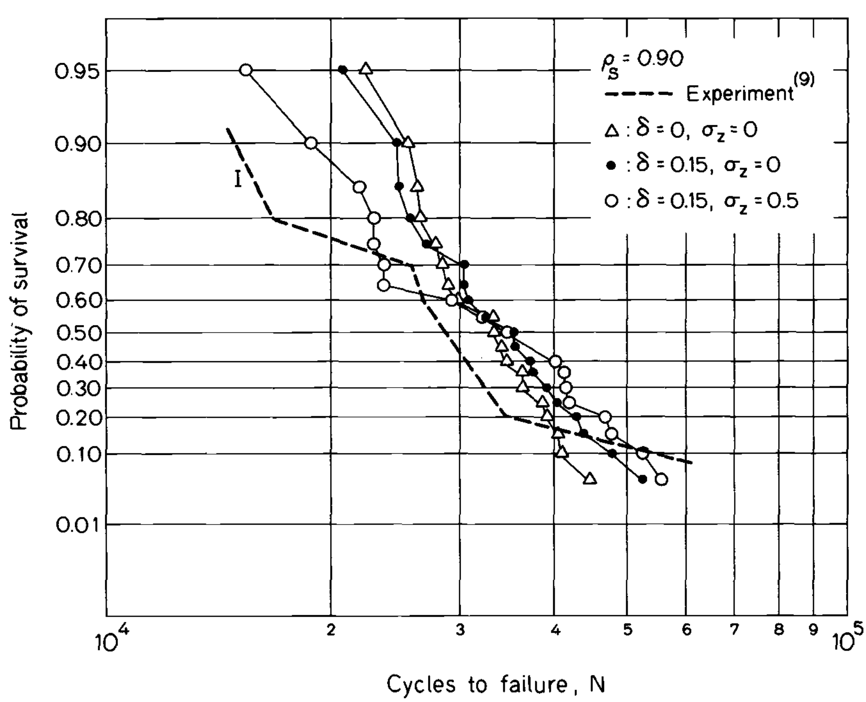

FIG. 10—*Analytically predicted distribution of fatigue life* (ρ_S = *0.90*).

To establish a meaningful comparison, therefore, a similar sequence consisting of blocks of 25 stress peaks is applied to each specimen (with a particular realization of $k(x)$) in the numerical analysis using Eqs 17 and 18. The results of such analyses performed on 57 (nominally identical) specimens (Fig. 6), 19 for each of Cases A, B, and C, are also plotted on extremal probability paper; using open triangles for A, solid circles for B, and open circles for C. Figures 10 to 12 show, respectively, the results under the stress sequences I, II, and III, each with the corresponding experimental result being replotted. Examination of these diagrams confirms the fact that only assumption C is capable of reproducing the extent of scatter actually observed without introducing unduly wide scatter to k' (recall Fig. 7).

Conclusion

This paper presents a Monte Carlo method by which the randomness of the material property as well as that of the applied load can be incorporated into a reasonable statistical-mechanical model of crack propagation process and failure criterion such as Eqs 1 and 3 or, equivalently, Eqs 17 and 18 to predict the statistical characteristics of fatigue life. In this Monte Carlo method, the crack propagation factor is treated as a stochastic process $k(x)$ and the combined

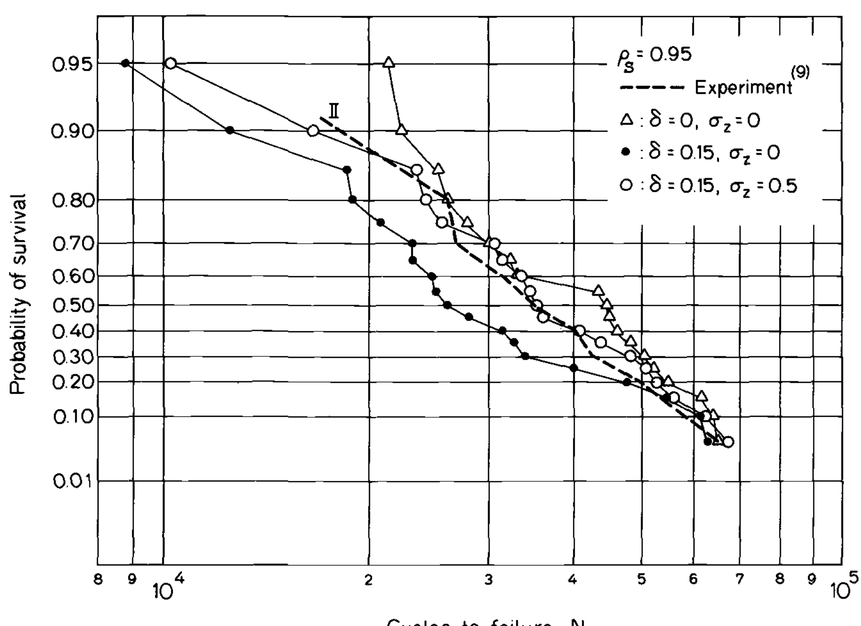

FIG. 11—*Analytically predicted distribution of fatigue life* (ρ_S = *0.95*).

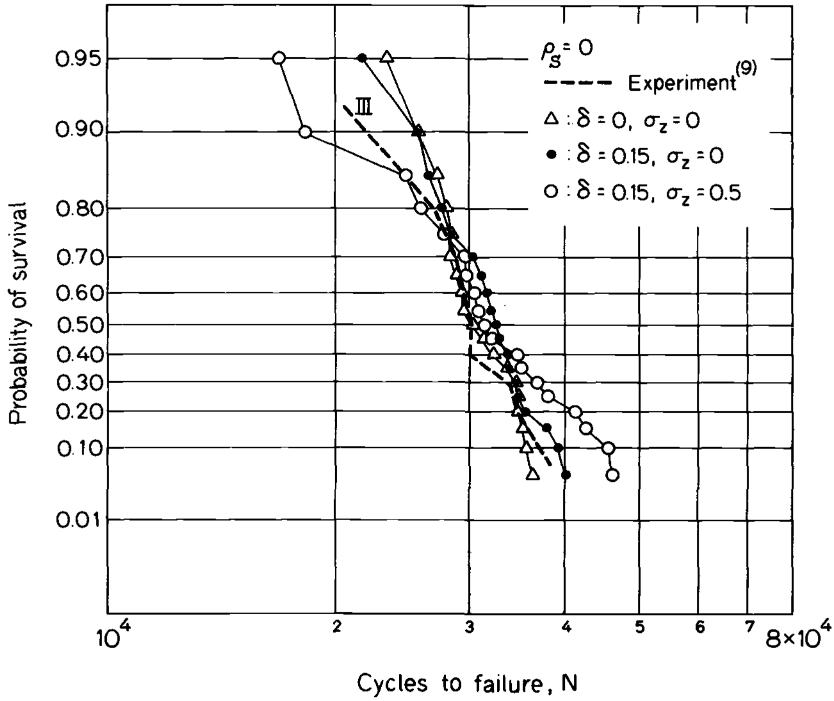

FIG. 12—*Analytically predicted distribution of fatigue life* (ρ_S = *0*).

effect of the randomness of $k(x)$, k' and the stress peak, s_i, on the statistical characteristics is predicted analytically with the aid of digital simulation techniques (in simulating $k(x)$, k', and s_i). The statistical characteristics are found to be in excellent agreement with those from the experimental results, indicating that the underlying assumptions and hypotheses are more than adequate. A number of quantities that have to be investigated in future experimental studies to improve the present method are identified.

Acknowledgment

This study is jointly supported by the Institute of Flight Structures, Department of Civil Engineering and Engineering Mechanics, Columbia University and the National Science Foundation under Grant GK 24925.

References

[*1*] Yang, J. N. and Shinozuka, M., *Journal of Applied Mechanics, Transactions of American Society of Mechanical Engineers,* JAMCA, Vol. 38, Series E, No. 4, Dec. 1971, pp. 1017-1022.

[2] Shinozuka, M., *Journal of Acoustical Society of America*, JASMA, Vol. 49, No. 1 (Part 2), 1971, pp. 357-367.
[3] Minami, Y., Itagaki, H., and Ogawa, T. in *Proceedings of the 13th Japanese Congress of Materials Research*, March 1970, pp. 248-253.
[4] Liu, H. W., *Journal of Basic Engineering, Transactions of the American Society of Mechanical Engineers*, JBAEA, Series D, Vol. 85, No. 1, 1963, pp. 116-122.
[5] *Fatigue Crack Propagation, ASTM STP 415*, American Society for Testing and Materials, 1966, pp. 131-242.
[6] Yokobori, T. and Nambu, M., *Report of Research Institute of Strength and Fracture of Materials*, Tohoku University, Vol. 3, No. 2, 1967, pp. 73-94.
[7] Y. Minami, a private communication. Professor, Department of Naval Architecture, Yokohama National University, Yokohama, Japan.
[8] Shinozuka, M., and Jan, C.-M., "Simulation of Multivariate and Multidimensional Processes II," Technical Report 12, NSF–GK 3858 and 24925, Department of Civil Engineering and Engineering Mechanics, Columbia University, April 1971.
[9] Minami, Y., Itagaki, H., and Ogawa, T., *Journal of the Society of Naval Architects of Japan*, ZOKYA, Vol. 128, 1970, pp. 311-316.

S. C. Saunders [1]

On the Probabilistic Determination of Scatter Factors using Miner's Rule in Fatigue Life Studies

REFERENCE: Saunders, S. C., "On the Probabilistic Determination of Scatter Factors using Miner's Rule in Fatigue Life Studies," *Probabilistic Aspects of Fatigue, ASTM STP 511,* American Society for Testing and Materials, 1972, pp. 185–203.

ABSTRACT: A particular two-parameter family of life-length distributions for fatigue life is assumed. This family, first formulated by Freudenthal and Shinozuka in 1961, was systematically examined by Birnbaum and Saunders in 1968 where it was derived, using considerations from renewal theory, for the number of cycles needed to force a fatigue-crack extension to exceed a critical value. By employing this new family, tolerance bounds are obtained for the population of life times until fatigue failure under a programmed load. This is accomplished by utilizing a generalization of Miner's rule which computes the mean life under the programmed load in terms of the mean lives under simpler programmed loads at stress levels for which data are available. Such bounds have never been obtained previously for any other life-length distribution and the confidence level exactly determined. This paper concludes with an application of these results to a set of real fatigue data.

KEY WORDS: probability theory, distribution theory, loading, fatigue(materials), fatigue life, fatigue limit, scattering, crack propagation

Miner's rule, which is well known in engineering practice, has long been used to predict the accumulated fatigue damage in metals. This result[*1*], is a deterministic formula which predicts the life until failure from fatigue under repetitions of a given cycle comprised of various fluctuations in load. This rule, in use, computes a weighted harmonic mean for the number of such cycles until failure, namely $[\Sigma n_i/\nu_i]^{-1}$, where n_i is the number of repetitions of the i^{th} load in each cycle and ν_i is the number of oscillations until failure if only the i^{th} load is repeated.

The fundamental premise, in what follows, is that the number of repetitions until failure of any fixed load is not a physical constant, identically the same for

[1] Department of Mathematics, Washington State University, Pullman, Wash.; formerly, Boeing Scientific Research Laboratories, Seattle, Wash.

each metallic specimen which can be measured exactly with a single test, but is, rather, a stochastic variable for which only knowledge of the distribution function should be employed in the prediction of the time until failure.

It is known empirically (see Refs *2, 3* and the bibliographies given there), that under many practical conditions Miner's rule may be used to estimate the mean life. However, even in those cases where sufficient data have been accumulated to verify that Miner's rule is correct on the average, that is, is a good estimate of the mean, there is still far too much scatter to use it by itself to predict fatigue life. (This would be comparable to using an estimate of the average age of death to derive contingency tables for a life insurance policy.)

By considering an appropriate generalization of Miner's rule as a function of the statistical estimates of the quantities ν_i and by obtaining confidence bounds on the true value, one might hope to ascribe a precise probability level to the safety factors used in design which are presently derived from the use of the rule. From such a study the determination of an appropriate scatter (or safety) factor might be possible so as to obtain the exact level of risk that can be tolerated. The important practical problem which is considered here is the determination of exact confidence levels for the probability of failure as a function of the stochastic variation away from the estimate of mean life obtained from Miner's rule. To date no rigorous statistical method has been developed to satisfy such a need.

That this does constitute a contribution to an acknowledged problem can be seen from a presently accepted method of calculating a combined lower tolerance bound, given in Ref *4* (p. 42). It is recalled that a tolerance bound is a bound before which, with a certain confidence, no more than a specified proportion of all future components subjected to the same stress history would fail.

The reference cited says that the first step is to reduce the data at each stress level by normalizing with an appropriate transformation, such as the logarithm. Making such assumptions on the distribution of the transformed data (usually that it is normal) that one may determine a tolerance bound at each stress level, the lower tolerance bounds at each stress level are combined and then the lower tolerance bounds at the same confidence level are combined throughout the various stress levels in the programmed load by using Miner's rule. Reference *4* states explicitly that the exact probability level of the combined estimate obtained in this manner is not known; one may add that it also requires some faith to believe that the answer is not far off.

Another method that has been advocated is to construct a *P-S-N* curve by fitting a particular distribution, usually a Weibull, to the available data at each stress level and computing an estimate of a specified percentile of that distribution. Then Miner's rule is used to combine these percentile estimates for the programmed load which contains the various stress levels. It is clear that this method does not take into account the confidence levels with which each percentile was established (that is, the sample sizes) and so the combined probability level is not known.

Programmed Loads and Cumulative Damage

Next, the basic ideas of this section will be described as clearly as possible, in terms of their physical meaning and some of the conceptual difficulties which are often encountered will be discussed. The formal mathematical presentation is deferred until Appendix I.

The nomenclature will be introduced first. A load function for a structural component is a function which at any time gives the stress imposed on that component. For such functions, λ or ω with or without affixes will be used. A load spectrum is a load function which assumes various values for a fixed duration of time d. (This includes as a special case constant-amplitude-load functions. A programmed load, which may be block loading or a loading with various stress values interspersed, is merely the repetition of a given spectrum of interest.)

The following is the fundamental assumption concerning load functions. It is assumed there exists a finite set of loading functions $\Omega = \{\omega_1, \ldots, \omega_m\}$, which are not necessarily of constant amplitude, and the mean life under the programmed load for each element of Ω is known. But further, an equivalence relation is known, in terms of cumulative fatigue damage (which might be interpreted as crack growth) between any spectrum, λ, and the elements of Ω. This relation makes possible the definition of the function $n_j(\lambda)$ which is equal to the number of load oscillations in the spectrum λ, occurring in their given order, which are equal in incremental damage to each repetition of ω_j for $j = 1, \ldots, m$.

According to statistical convention, E denotes the mathematical expectation of any random variable with which it is in juxtaposition. A result which follows under the above assumption and a very general condition on the distribution of incremental damage can be stated. It is intended that the validity of the result, as applied, need not be in question here, but the theorem is not true for every possible mathematical distribution of incremental damage. A formal discussion of this point, as well as the proof, are given in Ref 5.

Theorem 1: Let $T(\lambda)$ be the random life, which is measured in periods of the spectrum λ, under repetitions of the programmed load. Let ν_j be the expected number of such periods of cycles which can be repeated until failure under the programmed load corresponding to ω_j, that is,

$$\nu_j = ET(\omega_j) \text{ for } j = 1, \ldots, m$$

then the expected life, $ET(\lambda)$, is bounded by

$$\frac{1}{\sum_{j=1}^{m} \frac{n_j(\lambda)}{\nu_j}} - 1 \leqslant ET(\lambda) \leqslant \frac{1}{\sum_{j=1}^{m} \frac{n_j(\lambda)}{\nu_j + 1}}$$

Thus, it is the expected life that is bounded between two harmonic means, differing by at most unity, from an expression which is recognized as being equivalent to the original form of Miner's rule. The approximate equality, which will here be called "Miner's rule in expectation"

$$ET(\lambda) = \frac{1}{\sum_{j=1}^{m} \frac{n_j(\lambda)}{\nu_j}} \tag{1}$$

will be assumed as exact hereafter. A few calculations will show that for virtually all cases of practical interest these bounds are so close that the approximation is fully adequate.

Miner's rule in its original form was proved in Ref *1* under the most primitive and unrealistic of assumptions. In that derivation no stochastic variation was considered, so that all values were expected values in a sense. These unrealistic assumptions concerning linear and deterministic accumulation of damage account for its lack of acceptance. In fact it is known that damage, under various interpretations of that word, does not accumulate in that fashion nor is the failure time deterministic.

One of the implications of Miner's assumption was that the counting function $n_j(\lambda)$ consisted merely of the number of peak stresses in the spectrum, λ, equal in magnitude to those of the j^{th} element of Ω and each ω_j was of constant amplitude of different maximum stress for each $j = 1, \ldots, m$. The foregoing assumptions do not preclude a strong dependence upon the order of peak loads. In fact, *no assumption about the nature of* $n_j(\lambda)$ *is made* other than its being discrete-valued. Its exact nature is unspecified and only its existence is assumed. In particular, in the present formulation two spectra with the same number and value of peak stresses would not necessarily yield the same values of the function $n_j(\cdot)$ unless they occurred *in exactly the same order*. This is made clear in Appendix I.

In order to make a proper determination of $n_j(\lambda)$, one must take into account both the metallurgical and environmental considerations which are known (see, for example, Ref *6* and the entire volume given to this topic, Ref *7*). It is not the purpose to pursue this aspect of the problem further in this paper. The problem of formulating the statistical aspects of the question will be considered next.

Distribution of Fatigue Life

The problem of deciding which statistical law is the "true one" in fatigue studies has occupied investigators for many years. This is believed to be a fruitless pursuit and can never be actually decided, since the amount of data which can be collected is generally not sufficient to discriminate among any of the two-parameter families which are continuous, unimodal, and skewed to the right, using any of the usual statistical tests of goodness-of-fit. Fortunately this fact is now being realized and the construction of more powerful and appropriate tests is being undertaken [*8*]. At the present many models can be made to fit the extant data reasonably well within the area of central tendency of the distribution. This is not enough. What one wishes to accomplish is to make predictions about the percentage of failures which will occur before some service life which is determinable from the data at hand, at a prescribed confidence level. The reason for this is obvious.

In practical situations it is the earliest fatigue failures that are of primary concern and they are the only ones whose prediction is of interest. Clearly among mathematical models for fatigue, all of which fit the data equally well, the one that can be used to obtain exact confidence levels, and so be used with assurance in design problems, should be adopted for use. This is because it allows one to make a calculation of the safety of the component in service which can be checked subsequently. Moreover, using an alternative model for which the level of safety is unknown leaves one relying on fickle luck.

In an earlier publication, Birnbaum and Saunders [*9*] derived a distribution for life length based on the use of renewal theory to obtain the number of cycles for a fatigue crack to grow until it exceeds some critical value. The same authors also studied the estimation problem for this family of distributions [*10*].

The interconnection between this family of life lengths and the cumulative damage assumptions of the previous section will now be detailed. The set of programmed load functions which are admissible for the component within the use for which it was designed will be denoted by $\mathcal{L}$.

Assumption 1:

For any programmed load $\underset{\sim}{\lambda} \epsilon \mathcal{L}$ there exist positive parameters α and β, with α being constant but β depending upon $\underset{\sim}{\lambda}$, such that the fatigue life of a component subjected to $\underset{\sim}{\lambda}$ is a random variable T, expressed in units which are multiples of the period of $\underset{\sim}{\lambda}$ and

$$P\left[T \leqslant t\right] = \Phi\left[\frac{1}{\alpha}\xi(t/\beta)\right] \text{ for } t > 0 \tag{2}$$

where Φ is the standard normal distribution function and ξ is the function defined by

$$\xi(x) = \sqrt{x} - \frac{1}{\sqrt{x}} \text{ for } x > 0 \tag{3}$$

In Eq 2, the constant α is called the *shape parameter* while the constant β is a scale parameter called the *characteristic* (or median) *life.* The equality in distribution between the random variable T as defined in Eq 2 and its law is expressed as

$$T \sim \mathcal{F}(\alpha, \beta)$$

or what is equivalent, the expression in terms of a standardized normal distribution:

$$\frac{1}{\alpha}\xi(T/\beta) \sim \mathcal{N}(0, 1) \tag{4}$$

The adequacy of this two-dimensional family of life-length distributions to describe fatigue life has been demonstrated elsewhere. In Ref *10* it has been fitted to some fatigue data. It had been previously given by Freudenthal and Shinozuka[*11*] in a different parametric form and it is also implicit in the formula of Parzen [*12*].

Using the notation in Ref *9*, the function, Ψ is defined as

$$\Psi(x) = \xi^{-1}(2x) \quad \text{for all real } x \tag{5}$$

where ξ is given in Eq 3. It is also shown in Ref *9* that

$$\Psi(x) = [\rho(x)]^2 \tag{6}$$

where

$$\rho(x) = x + (x^2 + 1)^{1/2} \tag{7}$$

It follows from Theorem 1 (more correctly from the assumed exact equality of Eq 1) and Assumption 1 that under a loading spectrum, λ, the random life, T, has a distribution $\mathcal{F}(\alpha, \beta)$ where

$$\beta = \frac{1}{\sum_{i=1}^{m} \frac{n_i(\lambda)}{\beta_i}} \tag{8}$$

This result has been stated earlier in Ref *3*. It follows from the results of Ref *13* and the fact that

$$ET = \beta\left(1 + \frac{\alpha^2}{2}\right) \tag{9}$$

and the interpretation that $\nu_i = \beta_i \left(1 + \frac{\alpha^2}{2}\right)$ in Miner's rule. Now it is assumed that α and $n_i(\lambda)$, $[i = 1, \ldots, m]$ are known, but that the β_i are unknown and must be estimated from the data.

What is desired, of course, is an estimation procedure based on sparse data. It is presumed that one specimen only has been tested under each load spectrum, ω_i, and the random life observed as T_i. The observed life at each stress level is used to estimate the characteristic life and thus an estimate of β is formed in

$$\hat{\beta} = \frac{1}{\sum_{i=1}^{m} \frac{n_i(\lambda)}{T_i}} \tag{10}$$

where $T_i \sim \mathcal{F}(\alpha, \beta_i)$.

A service life, say T_0 is selected which is also a random variable, based on the estimated median life under repeated spectrum, λ, and a scatter factor κ is computed by the formula

$$T_0 = \hat{\beta}/\kappa \tag{11}$$

The scatter factor, κ, is to be selected so that the proportion of failures before T_0, each exposed to the repeated loading spectrum, λ, and hence with life distribution, $\mathcal{F}(\alpha, \beta)$, does not exceed ϵ. But further, this event is to occur with confidence exceeding $(1 - \delta)$ where both ϵ and δ are preassigned and small.

Succinctly, it is desired to find κ in Eq 11 so that for given ϵ, δ one should have

$$P\left[\Phi\left[\frac{1}{\alpha}\xi\left(\frac{T_0}{\beta}\right)\right] \leqslant \epsilon\right] \geqslant 1 - \delta \tag{12}$$

This expression is equivalent with

$$P[\xi(\hat{\beta}/\kappa\beta) \leqslant \alpha z_\epsilon] \geqslant 1 - \delta$$

where $z_\epsilon = \Phi^{-1}(\epsilon)$ will be the notation for the $100\epsilon^{th}$ percentile of the standard normal distribution. This, in turn, can be rewritten as

$$P[\hat{\beta}/\beta \geqslant u] \leqslant \delta \tag{13}$$

if

$$u = \kappa\psi\left(\frac{\alpha}{2} z_\epsilon\right) \tag{14}$$

It will be shown that u in Eq 13 can be determined independently of all unknown parameters β_i $i = 1, \ldots, m$ so that a precise tolerance bound at a specified confidence level can be found. Then using Eq 14, the scatter factor can be defined in terms of a precise probabilistic meaning. The principal result can be stated as follows (the proof is presented in Appendix II).

Theorem 2: If

$$\hat{\beta} = \left(\sum_{i=1}^{m} \frac{n_i(\lambda)}{T_i} \right)^{-1} \tag{15}$$

where $T_i \sim \mathcal{F}(\alpha, \beta_i)$ $i = 1, \ldots, m,$ is defined as an estimate for the true characteristic life

$$\beta = \left(\sum_{i=1}^{m} \frac{n_i(\lambda)}{\beta_i} \right)^{-1}$$

under the programmed spectrum λ, then with confidence at least $(1 - \delta)$ no more than a proportion ϵ of all future components subjected to repetitions of the spectrum, λ, will fail before the service life $\hat{\beta}/\kappa$, where κ is a scatter factor given by

$$\sqrt{\kappa} = \rho\left(-\frac{\alpha}{2} z_\delta\right) \rho\left(\frac{\alpha z_\epsilon}{2}\right) \tag{16}$$

with ρ defined in Eq 7.

As an illustration of the range of values resulting from the use of Eq 16, some typical values of α, δ, and ϵ are chosen and the resulting scatter factors, κ are calculated. These are presented below. Table 1.

α	δ	ϵ	κ
0.10	0.20	0.01	1.32
0.20	0.10	0.005	2.06
0.15	0.05	0.001	2.02
0.15	0.10	0.002	1.91

The chosen values are within the range of those which have been found from fatigue testing, for example, see the estimates of α given in Ref *10*. The choices of δ and ϵ are also usual.

Application

As a simple illustration of the preceding theory, all the calculations will be performed for a tolerance bound making use of some rather extensive data which have been previously reported [*11*] and are presented here in Table 1. These fatigue tests were performed on 6061-T6 aluminum coupons cut parallel to the direction of rolling at 18 cps.

Using the maximum likelihood estimation techniques for the shape and scale parameters which were developed in Ref *10* for this family of distributions, we obtain

Shape Parameter	Scale Parameter	Maximum Stress
$\alpha_1 = 0.170$	$\beta_1 = 131.8 \times 10^{-3}$	31×10^{-3}
$\alpha_2 = 0.161$	$\beta_2 = 392.7$	26
$\alpha_3 = 0.310$	$\beta_3 = 1336.4$	21

These six parameters are regarded as being known. The fit of the data to the distributions with the appropriate maximum likelihood estimate, shape, and scale parameters is shown in Figs. 1 to 3 and is offered as evidence of the reasonableness of the assumption.

It is assumed next that the characteristic lives at each stress β_1, β_2, or β_3, are not known and only one observation T_i for $i = 1, 2, 3$ will be made at each stress level. In order to concentrate on the statistical concepts, any load order interactions within this stress range will be disregarded and a spectrum containing n_1 oscillations at the lowest stress level, n_2 at the intermediate level and n_3 oscillations at the highest level will be constructed. The estimated median life would then be

$$\hat{\beta} = \left(\sum_{i=1}^{3} \frac{n_i}{T_i} \right)^{-1} \tag{17}$$

counted in terms of a cycle of duration $n_1 + n_2 + n_3$ oscillations. (Compensating for load-order interactions would change the values of n_i in Eq 17, but in any case they are presumed known.)

Clearly this is a statistic, being a function of the observations T_1, T_2, T_3, which will change with each sample. However the theory previously derived and to be applied here is ignorant of the fact that enough experimentation has been done in this case to calculate directly the distribution of life under repetitions of any spectrum with oscillations taken from these three stress levels.

TABLE 1—*Fatigue lifetimes in cycles* ($\times 10^{-3}$).

Sample Size = 101 at 31,000 psi maximum stress per cycle							
70	90	96	97	99	100	103	104
104	105	107	108	108	108	109	109
112	112	113	114	114	114	116	119
120	120	120	121	121	123	124	124
124	124	124	128	128	129	129	130
130	130	131	131	131	131	131	132
132	132	133	134	134	134	134	134
136	136	137	138	138	138	139	139
141	141	142	142	142	142	142	142
144	144	145	146	148	148	149	151
151	152	155	156	157	157	157	157
158	159	162	163	163	164	166	166
168	170	174	196	212			
Sample Size = 102 at 26,000 psi maximum stress per cycle							
233	258	268	276	290	310	312	315
318	321	321	329	335	336	338	338
342	342	342	344	349	350	350	351
351	352	352	356	358	358	360	362
363	366	367	370	370	372	372	374
375	376	379	379	380	382	389	389
395	396	400	400	400	403	404	406
408	408	410	412	414	416	416	416
420	422	423	426	428	432	432	433
433	437	438	439	439	443	445	445
452	456	456	460	464	466	468	470
470	473	474	476	476	486	488	489
490	491	503	517	540	560		
Sample Size = 101 at 21,000 psi maximum stress per cycle							
370	706	716	746	785	797	844	855
858	886	886	930	960	988	990	1000
1010	1016	1018	1020	1055	1085	1102	1102
1108	1115	1120	1134	1140	1199	1200	1200
1203	1222	1235	1238	1252	1258	1262	1269
1270	1290	1293	1300	1310	1313	1315	1330
1355	1390	1416	1419	1420	1420	1450	1452
1475	1478	1481	1485	1502	1505	1513	1522
1522	1530	1540	1560	1567	1578	1594	1602
1604	1608	1630	1642	1674	1730	1750	1750
1763	1768	1781	1782	1792	1820	1868	1881
1890	1892	1895	1910	1923	1940	1945	2023
2100	2130	2215	2268	2440			

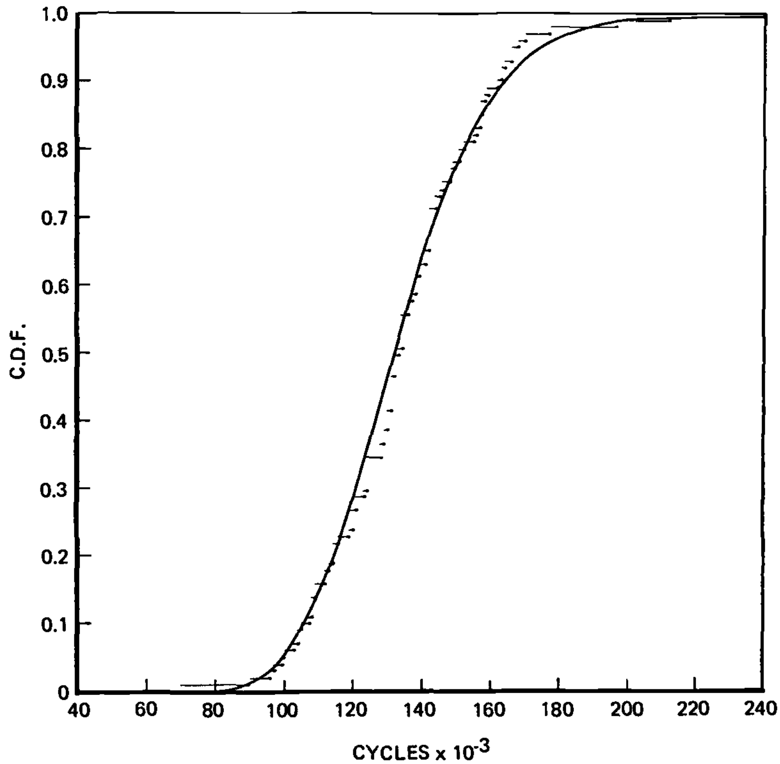

FIG. 1—*The empiric cumulative distribution* $\mathcal{F}(\alpha_1, \beta_1)$ *for fatigue life at a stress of 31,000 psi.*

The distribution of life until fatigue failure is taken as $\mathcal{F}(\alpha, \beta)$, where conservatively,

$$\alpha = \max(\alpha_1, \alpha_2, \alpha_3) \qquad \frac{1}{\beta} = \sum_{i=1}^{3} \frac{n_i}{\beta_i} \tag{18}$$

The true service time (population percentile) t_ϵ, at which only 100ϵ percent of all future components subjected to such a programmed spectrum will fail, is given by

$$t_\epsilon = \beta\, \psi\left(\frac{\alpha}{2}\, z_\epsilon\right) \tag{19}$$

where α and β are given in Eq 18.

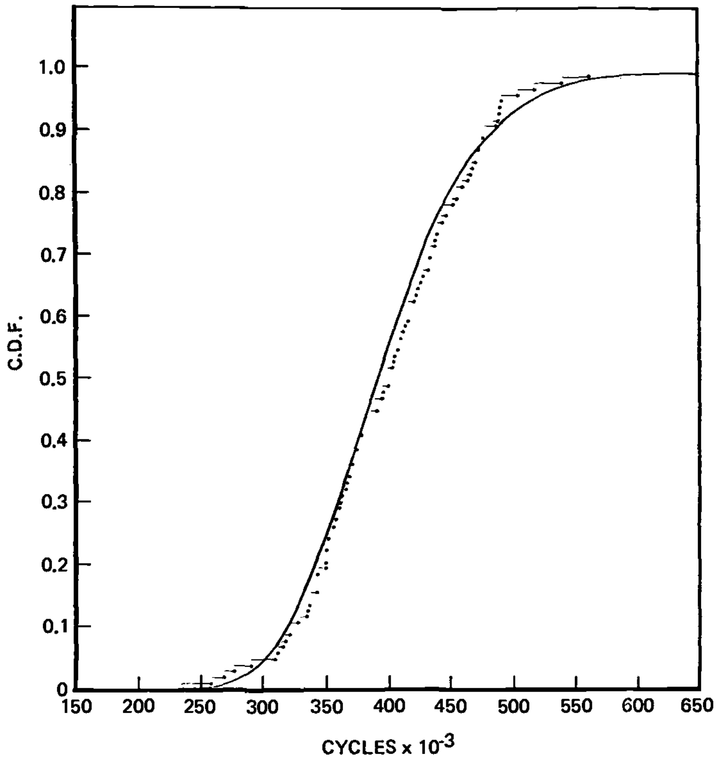

FIG. 2—*The empiric cumulative distribution* $\mathcal{F}(\alpha_2, \beta_2)$ *for fatigue life at a stress of 26,000 psi.*

Theorem 2 asserts that for given ϵ, δ one can pick a safety factor κ by Eq 16, namely

$$\sqrt{\kappa} = \rho\left(-\frac{\alpha}{2} z_\delta\right) \rho\left(-\frac{\alpha}{2} z_\epsilon\right)$$

where z_γ is the $100\gamma^{th}$ percentile of the standardized normal distribution for any value of γ and ρ is the function defined in Eq 7 by

$$\rho(x) = x + (1 + x^2)^{1/2} \tag{20}$$

and claim that with a statistical confidence of $100\,(1 - \delta)$ percent, no more than a proportion of ϵ of all future components subjected to that same spectrum will fail before the time (tolerance bound) $\hat{\beta}/\kappa$. This tolerance bound is compared with the time-population percentile t_ϵ as defined in Eq 19.

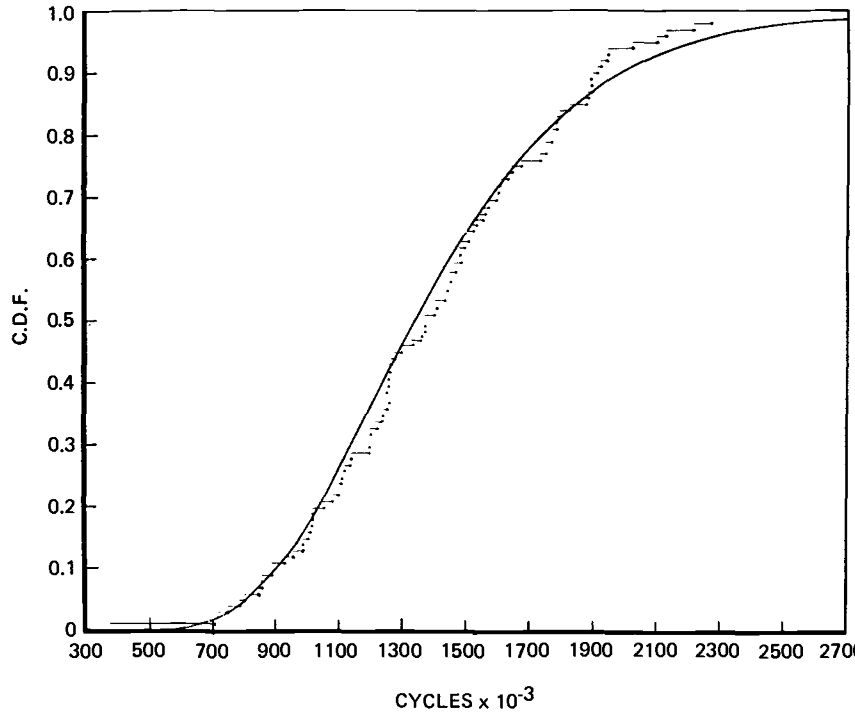

FIG. 3—*The empiric cumulative distribution* $\mathcal{F}$ (α_3, β_3) *for fatigue life at a stress of 21,000 psi.*

Let α and β be the parameters for the life distribution under a spectrum which contains two oscillations at the higher stress of 31,000 psi and 8 oscillations at the lower stress of 26,000 psi within each cycle. Thus disregarding any load-order interaction within this stress range, $n_1 = 2$ and $n_2 = 8$. Since $p_i = n_i/\beta_i$ (for $i = 1, 2$) $p_1 = 0.015$ and $p_2 = 0.020$ (see Table 3 for β_i).

$$\beta = \frac{1}{\sum p_i} = 28.1 \times 10^3$$

where β is counted in units of the period $d = 10$. A conservative value of the shape parameter, namely, $\alpha = 0.17$, will be used for the spectrum.

Using Eq 16 with $\delta = 0.10$ and $\epsilon = 0.002$, that is, 90 percent confidence of less than one failure in 500 (which is a selection of confidence levels specified in certain regulations), the requisite calculation is performed from which $\kappa = 2.02$

is obtained. Thus for $\alpha = 0.17$ the true service time, t_ϵ, at which less than a proportion $\epsilon = 0.002$ will fail is,

$$t_\epsilon = \beta\, \psi\left(\frac{\alpha}{2} z_\epsilon\right) = 17.3 \times 10^3$$

also being counted in units of $d = 10$; $\psi(x) = [\rho(x)]^2$ with ρ defined in Eq 20. Thus what the theory asserts is that 90 percent of the time the estimated median life, $\hat{\beta}$, divided by $\kappa = 2.02$ will not exceed the value t_ϵ. This follows from Eqs 13 and 14. This value certainly does not violate one's intuition, since it is seen that the ratio $\beta/t_\epsilon = 1.62$ which is 80 percent of κ.

Picking two numbers at random between 1 and 102 inclusive, the corresponding ordered observations were selected. In this case the 60th and 76th ordered observations, respectively, from the 26,000 psi and 31,000 psi data were used. Thus

$$T_1 = 138 \times 10^3,\ T_2 = 438 \times 10^3$$

and from Eq 17,

$$\hat{\beta} \times 10^{-3} = \left(\frac{2}{138} + \frac{8}{438}\right)^{-1} = 29.51$$

measured in cycles of length 10 from which $\hat{\beta}/\kappa = \dfrac{29.51}{2.02} = 14.61 \times 10^3$.

It is believed that if this procedure were repeated the resulting value would be less than 17.3×10^3 nine times out of ten on the average and in service only one in five hundred components will fail before 17.3×10^3 cycles of length 10.

Concluding Remarks

A few critical comments about this procedure for obtaining scatter factors are in order. It has been presumed throughout that the shape parameter is known and is the same for each distribution of fatigue life corresponding to any programmed spectrum from $\mathcal{L}$. If this assumption is not met and the shape parameter is different, but known, for each different spectrum in Ω, then either the conservative maximum value is used or more calculation is required. In particular it would be necessary (and perhaps difficult) to derive some method to compute the shape parameter under the programmed spectrum from the shape parameters of its constituent parts. However, there would seem to be little theoretical difficulty in obtaining a similar result to that of Theorem 2. On the other hand, if the shape parameters vary considerably with the ω_i's and these values are unknown, then the problem of simultaneously estimating both shape and scale parameters and combining these estimates into a single tolerance bound independent of all the actual shape and scale parameters, which are unknown, seems to be very difficult.

However, this does not appear to be the case if care is taken in insuring that the sample is from a single population. The inference that the shape parameter should vary considerably may be an unjustified extrapolation from experience with other two-parameter distributions. For example, the behavior of the standard deviation of the logarithmic life at different stress levels does not necessarily imply the same behavior for the shape parameter of the model presented here.

A usual inquiry in such circumstances as this is whether the apparent degree of mathematical sophistication in the model is justified in terms of more accurate predictions than simpler ones. However, in this case there are no other methods for which the confidence level is known or can be calculated and thus no direct comparisons are possible.

A further criticism of this approach is that it requires either an assumption about the shape parameter or an estimate of it from a rather large amount of data. This criticism applies *a fortiori* to any other two-parameter models of the distribution of fatigue life. However, in many instances the great expense of full-scale testing of structures insures that only one observation will be made. Since it is impossible to estimate two parameters with one observation, either an assumption or prior information about one of the parameters must be employed for any inference to be made at all.

In accord with the situation where the shape parameter is known and is constant and only the scale parameter varies with the choice of the spectrum in Ω, it has been presumed that only one observation of the fatigue life is made for each spectrum in Ω and can be used to estimate the characteristic life. This situation is often the case in full-scale testing. If more observations are made, it is yet to be shown how such information could be fully utilized to increase the confidence level of the tolerance bound. The property that has been exploited is that fatigue life random variables, which have the distribution postulated in Appendix I, suitably scaled, are distributed as their own reciprocals and that the transformation ψ is convex increasing. Clearly such properties may not apply to all estimates of the characteristic life formed from such random variables.

An immediate extension of the preceding result could be accomplished by developing a wide class of random variables, all elements of which possess the requisite symmetries and the convexity necessary to obtain a tolerance bound. Work is now proceeding on this development.

APPENDIX I

In this section the mathematical model for incremental damage and its relation to a programmed load will be formulated.

A load function is a continuous piecewise linear function defined on zero to infinity, the value of which at any time gives the stress imposed on the structural component by its deflection. Moreover the slope of the function changes sign exactly once at the midpoint of each unit interval $(j, j+1)$ for $j = 0, 1, \ldots$. *A load spectrum* is a load function which takes the value zero except on some interval of the form $(0, d)$ where the integer, d, is called the *duration*. *A programmed load*, $\underline{\lambda}$, is the repetition of a spectrum, λ, and $\underline{\lambda} = (\lambda_1, \lambda_2, \ldots)$ where λ_j is the j^{th} repetition of the spectrum, λ, defined for $j = 0, 1, \ldots$ by

$$\lambda_{j+1}(t) = \lambda(-jd + t) \text{ for } t > 0$$

and d is the duration of λ (and the period of $\underline{\lambda}$).

A load history (a partially completed spectrum) of length i, denoted by λ^i, is λ restricted in domain to the interval $(0, i)$. To denote equality in distribution between two random variables $\sim$ will be used.

Assumption 2: There exists a finite set of loading functions of simple structure, say $\Omega = \{\omega_1, \ldots, \omega_m\}$, such that for any admissible loading spectrum, λ, of duration, d, the random incremental damage, $Z(\lambda^i)$, for $i = 1, \ldots, d$ occurring during the i^{th} oscillation and due to the stress history, λ^i, is equal in distribution to the incremental damage due to the load oscillation in exactly one element of Ω, namely,

$$Z(\lambda^i) \sim \sum_{i=1}^{m} \{\lambda^i \equiv \omega_j\} Z(\omega_j) \tag{21}$$

where the relation $\equiv$ means equivalent in damage between partial spectra and $\{\lambda^i \equiv \omega_j\}$ is the indicator of the relation $\lambda^i \equiv \omega_j$ being 1 if true and zero otherwise.

This assumption and the concepts involved are a restatement of those made in Ref *3*. These have been detailed in order to make clear the generality of the approach. There follows from the equivalence relation $\equiv$, the counting function

$$n_j(\lambda) = \sum_{i=1}^{d} \{\lambda^i \equiv \omega_j\} \quad j = 1, \ldots, m \tag{22}$$

which represents the number of oscillations in the spectrum, λ, occurring in order which are equivalent in damage to each oscillation in ω_j. This formula takes into account both the acceleration or deceleration of crack growth resulting from load-order interactions within each repetition of the spectrum. It follows that the expected cumulative damage in one replication of the spectrum, λ, is

$$\sum_{i=1}^{d} EZ(\lambda^i) = \sum_{i=1}^{m} n_j(\lambda) EZ(\omega_j) \tag{23}$$

Here E denotes the mathematical expectation of any random variable which follows.

APPENDIX II

For convenience the relevant results from Ref *10* which will be used subsequently are summarized here in a lemma.

Lemma 1: If $T \sim \mathcal{G}(\alpha, \beta)$ then $\frac{1}{T} \sim \mathcal{G}\left(\alpha, \frac{1}{\beta}\right)$ and $aT \sim \mathcal{G}(\alpha, a\beta)$ for any $a > 0$.

Proving next

Lemma 2: The function, ψ, as defined in Eq 5 is nonnegative, convex and increasing and satisfies

$$\psi(-x) = \frac{1}{\psi(x)} \text{ for all real } x \tag{24}$$

Proof: It is trivial that ψ is nonnegative by Eq 6 and one sees that $\rho(-x) = \frac{1}{\rho(x)}$ would imply the similar property, as in Eq 24, for ψ. One may check this from Eq 7. It is sufficient to show that ρ^2 is convex increasing by Eq 6, for which it is sufficient that the first and second derivatives are positive

$$D(\rho^2) = 2\rho\rho' \quad D^2(\rho^2) = 2\rho\rho'' + 2(\rho')^2$$

Now by Eq 7,

$$\rho'(x) = 1 + \frac{x}{\sqrt{x^2 + 1}} = \rho(x)/\sqrt{x^2 + 1}$$

and

$$\rho''(x) = (1 + x^2)^{-3/2}$$

Clearly, $\rho, \rho', \rho'' > 0$ and therefore $\psi' > 0, \psi'' > 0$. ||

Next the proof of basic result Theorem 2 is presented.

Proof: Let X with or without affixes by $\mathcal{N}\left(0, \frac{\alpha^2}{4}\right)$ and set $p_i = n_i(\lambda)/\beta_i$ for $i = 1, \ldots, m$. Note that $\beta = 1/\Sigma p_i$. Now from Eq 15

$$\sum p_i \frac{\beta_i}{T_i} \sim \sum p_i \psi(X_i) \gtrsim \frac{1}{\beta}\psi(\beta \sum \rho_i X_i) \tag{25}$$

When $\gtrsim$ denotes stochastic inequality between two random variables, recalling for any random variable U, V that $U \lesssim V$ implies $P[U \geqslant u] \leqslant P[V \geqslant u]$ for all real u. Here use has been made of the property Eq 24 and the fact that X_i is symmetric (that is, $X_i \sim -X_i$) to see that

$$\frac{\beta}{T_i} \sim \frac{1}{\psi(X_i)} \sim \psi(X_i) \sim \mathcal{F}\ (\alpha, 1).$$

Then the convexity of ψ has been used to obtain the stochastic inequality in Eq 25. But it should be noted that since linear combinations of normal random variables are normal

$$\beta \ \sum p_i X_i \sim \mathcal{N}\left(0, \frac{\theta^2 \alpha^2}{4}\right)$$

where

$$\theta^2 = \beta^2 \sum p_i^2 \leqslant 1 \tag{26}$$

Thus the stochastic inequality of Eq 25 may be written as

$$\beta/\hat{\beta} \gtrsim \psi(\theta X)$$

Hence

$$P[\hat{\beta}/\beta \geqslant u] \leqslant P[\psi(\theta X) \geqslant u] = P[2\theta X \geqslant \xi(u)]$$

since ξ is an order preserving transformation. Now using the bound for θ in Eq 26 it is seen that for $u \geqslant 1$

$$P[2\theta X \geqslant \xi(u)] = \Phi\left[-\frac{\xi(u)}{\theta\alpha}\right] \leqslant \left[\Phi - \frac{\xi(u)}{\alpha}\right]$$

Equating the right-hand side of the inequality above to δ and solving for u shows $u = \psi\left(-\frac{\alpha z_\delta}{2}\right)$, which clearly exceeds unity for δ small since $\psi(x) > 1$ for $x > 0$. Thus (Eq 13) has been effected. Setting the u above equal to (Eq 14) and solving for κ yields the result. ||

References

[1] Miner, M. A., *Journal of Applied Mechanics*, JAMCA, Vol. 12, 1945, pp. A159-A164.

[2] Crichlow, W. J., "An Engineering Evaluation of Methods for Prediction of Fatigue Life in Airframe Structures," ASD-TR-61-434, Aeronautical Systems Div., Wright-Patterson AFB, Ohio, 1962.

[3] Saunders, S. C. in *Proceedings of the Air Force Conference on Fatigue and Fracture of Aircraft Structures and Materials*, Air Force Flight Dynamics Laboratory, TR-70-144, 1970.

[4] *A Guide for Fatigue Testing and the Statistical Analysis of Fatigue Data*, 2nd ed., *ASTM STP 91-A*, American Society for Testing and Materials, 1963.

[5] Saunders, S. C., *SIAM Journal of Applied Mathematics*, Society for Industrial and Applied Mathematics, SMJMA, Vol. 19, 1907, pp. 251-265.

[*6*] McMillan, J. C. and Pelloux, R. M. in *Fatigue Crack Propagation, ASTM STP 415*, American Society for Testing and Materials, 1967, pp. 505-532.
[*7*] *Effects of Environment and Complex Load History on Fatigue Life, ASTM STP 462*, American Society for Testing and Materials, 1970.
[*8*] Weibull, Wallodi, "Outline of a Theory of Powerful Selection of Distribution Functions," AFML-TR-71-52, Air Force Materials Laboratory, 1971.
[*9*] Birnbaum, Z. W. and Saunders, S. C., *Journal of Applied Probability*, JPRBA, Vol. 6, 1969, pp. 319-327.
[*10*] Birnbaum, Z. W. and Saunders, S. C., *Journal of Applied Probability*, JPRBA, Vol. 6, 1969, pp. 328-347.
[*11*] Freudenthal, A. M. and Shinozuka, M., "Structural Safety under Conditions of Ultimate Load Failure and Fatigue," Wright Air Development Document TR-6-177, 1961.
[*12*] Parzen, E. in *Time Series Analysis Paper*, Holden-Day, San Francisco, 1967.
[*13*] Birnbaum, Z. W. and Saunders, S. C., *SIAM Journal of Applied Mathematics*, Society for Industrial and Applied Mathematics, SMJMA, Vol. 16, 1968, pp. 637-652.